AD-A035 215 BOEING VERTOL CO PHILADELPHIA PA F/G 13/9
TRANSMISSION CONDITION ASSESSMENT.(U)
DEC 76 O L SANDORA DAAJ02-75-C-0021
UNCLASSIFIED D210-11067-1 USAAMRDL-TR-76-36 NL

1 OF 2
AD
A035215

USAAMRDL-TR-76-36

(12)

NW

TRANSMISSION CONDITION ASSESSMENT

Boeing Vertol Company
P. O. Box 16858
Philadelphia, Pa. 19142

December 1976

Final Report

Approved for public release; distribution unlimited.

Prepared for

EUSTIS DIRECTORATE
U. S. ARMY AIR MOBILITY RESEARCH AND DEVELOPMENT LABORATORY
Fort Eustis, Va. 23604

EUSTIS DIRECTORATE POSITION STATEMENT

This report establishes the feasibility of using high-frequency vibration signatures and/or oil filter debris for determining component condition. However, due to the limited size of the data base, the techniques used do not allow high level of confidence estimates for diagnosing component condition by either method.

The results of this program can serve as a basis for future work that will yield the level of confidence necessary for an accurate diagnosis of component condition.

The technical monitor for this contract was Mr. D. P. Lubrano, Military Operations Technology Division.

Unclassified

SECURITY CLASSIFICATION OF THIS PAGE (When Data Entered)

REPORT DOCUMENTATION PAGE — READ INSTRUCTIONS BEFORE COMPLETING FORM

1. REPORT NUMBER: 18 USAAMRDL TR-76-36 19
2. GOVT ACCESSION NO.
3. RECIPIENT'S CATALOG NUMBER: 9
4. TITLE (and Subtitle): 6 TRANSMISSION CONDITION ASSESSMENT.
5. TYPE OF REPORT & PERIOD COVERED: Final Report. 10
6. PERFORMING ORG. REPORT NUMBER: 14 D210-11067-1
7. AUTHOR(s): 10 O. L./Sandora
8. CONTRACT OR GRANT NUMBER(s): 15 DAAJ02-75-C-0021 new
9. PERFORMING ORGANIZATION NAME AND ADDRESS: Boeing Vertol Company, P. O. Box 16858, Philadelphia, Pa. 19142
10. PROGRAM ELEMENT, PROJECT, TASK AREA & WORK UNIT NUMBERS: 16 62209A 1F262209AH76 17 DD 042 EK
11. CONTROLLING OFFICE NAME AND ADDRESS: Eustis Directorate, U.S. Army Air Mobility Research & Development Laboratory, Fort Eustis, Va. 23604
12. REPORT DATE: 11 December 1976
13. NUMBER OF PAGES: 182 12 183p.
14. MONITORING AGENCY NAME & ADDRESS (if different from Controlling Office)
15. SECURITY CLASS. (of this report): Unclassified
15a. DECLASSIFICATION/DOWNGRADING SCHEDULE

16. DISTRIBUTION STATEMENT (of this Report)

Approved for public release; distribution unlimited.

17. DISTRIBUTION STATEMENT (of the abstract entered in Block 20, if different from Report)

18. SUPPLEMENTARY NOTES

19. KEY WORDS (Continue on reverse side if necessary and identify by block number)

Vibration Analysis
Debris Particle Size Distribution
ASOAP

20. ABSTRACT (Continue on reverse side if necessary and identify by block number)

This program was conducted to provide the correlation and analysis of vibration signatures, component condition and oil-borne debris from 38 CH-47C rotor transmissions tested under a spectrum of load conditions. The transmission tested included new, postoverhaul, and preoverhaul scheduled and unscheduled removals. The analysis of data shows the relative diagnostic accuracies of transmission condition assessment by analysis of

DD FORM 1 JAN 73 1473 EDITION OF 1 NOV 65 IS OBSOLETE

Unclassified 403 682

SECURITY CLASSIFICATION OF THIS PAGE (When Data Entered)

bpg

Block 20. Continued

particulate debris from filters and by spectral analysis of demodulated high-frequency vibration.

PREFACE

This report presents the results obtained from the debris and vibration analysis performed on new and preoverhauled CH-47C forward and aft transmissions.

The study was conducted under Contract DAAJ02-75-C-0021 for the Eustis Directorate, U. S. Army Air Mobility Research and Development Laboratory, Fort Eustis, Virginia.

USAAMRDL technical direction was provided by Mr. D. Lubrano.

The Project Engineer for the Boeing Vertol Company was Mr. O. L. Sandora of Product Assurance Research and Development. Program management and technical direction were provided by Mr. D. B. Board, Diagnostics Technology Manager of Product Assurance. Assistance was provided by Messrs. J. Sramek, H. Ardinger, R. B. Aronson, and H. Baker.

The author gratefully acknowledges the assistance received from Mr. R. Lee of ARADMAC, and Captain J. Coyle, USN Retired, of Villanova University. Mr. R. Lee provided the ASOAP analysis on the oil samples removed from the transmissions used in this program. Captain J. Coyle and members of his staff provided the analysis on the debris removed from the oil filters.

TABLE OF CONTENTS

Page

LIST OF ILLUSTRATIONS

Figure		Page

LIST OF TABLES

INTRODUCTION

Helicopter transmission failure prognostic and diagnostic systems, when properly conceived and designed, can significantly increase aircraft flight safety, mission reliability and availability. At the same time they can reduce aircraft downtime for troubleshooting, erroneous maintenance, erroneous or unnecessary part removals and aircraft life-cycle cost.

The objective of this program was to collect and analyze debris and vibration data from CH-47C transmissions, and to correlate this information with component condition.

The types of debris data collected were ASOAP results and oil filter contents. The tape recorded vibration data consisted of "raw" accelerometer signals and demodulated high frequency data.

Data samples were collected from 38 rotor transmissions. Twenty of them were either newly manufactured (referred to as "new" transmissions) or recently overhauled (referred to as "postoverhaul" transmissions). The data samples for these transmissions were taken during their green runs. The remaining 18 transmissions had been returned to Boeing Vertol for overhaul (referred to as "preoverhaul" transmissions). The data samples for these transmissions were collected during special test runs prior to overhaul. The debris and high-frequency vibration data collected from these transmissions was correlated with the findings of the subsequent transmission teardown inspection. These data were also compared with the data taken from the new/postoverhaul group.

The flow diagram of Figure 1 illustrates the operational sequence and data collection activity in each stage of the Transmission Condition Assessment program. All transmission testing was conducted in Boeing Vertol's production test cells.

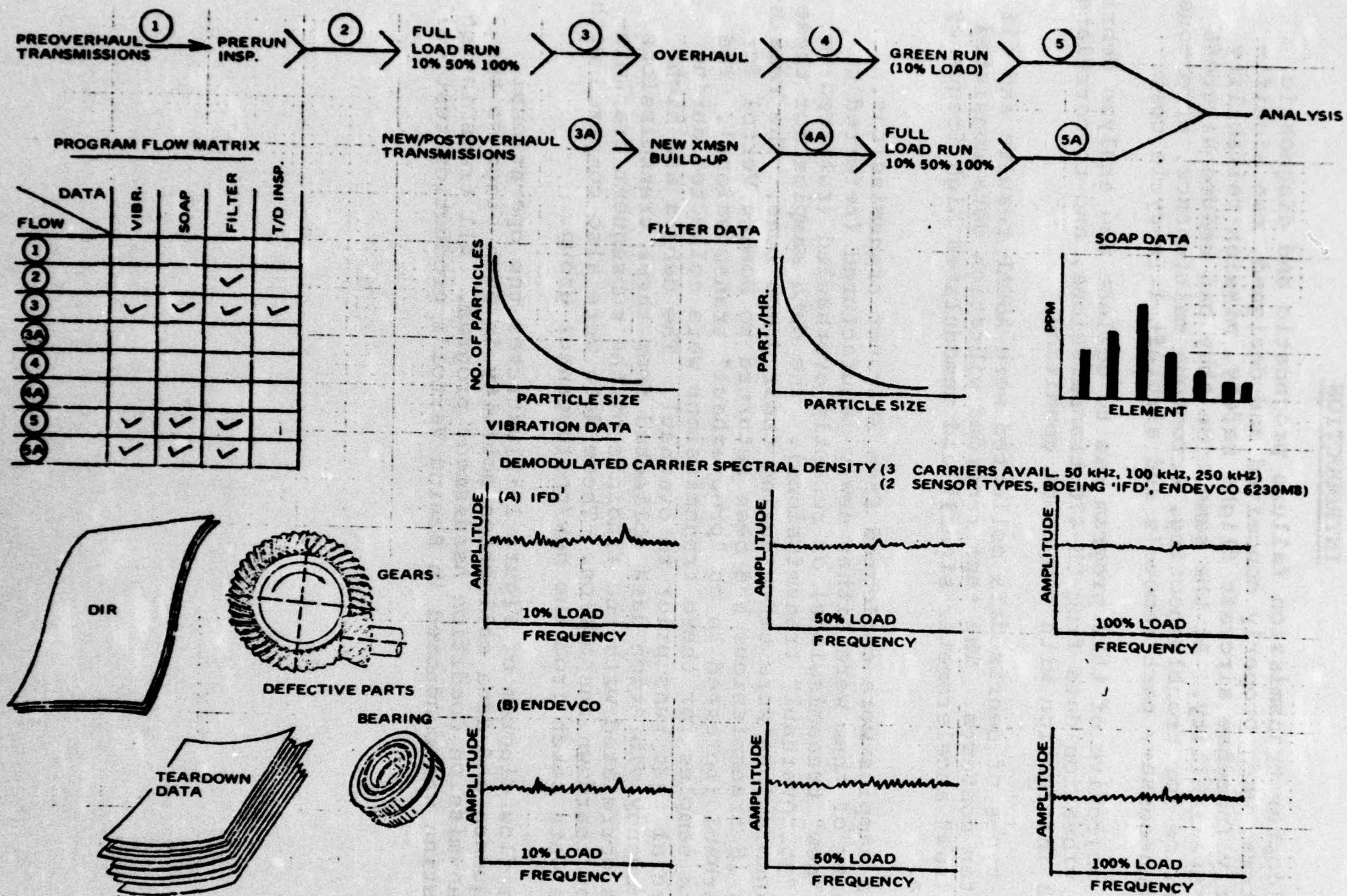

Figure 1. Transmission Condition Assessment Program Flow Diagram.

DATA COLLECTION PROCEDURE

TRANSMISSION HISTORY

Each of the CH-47C transmissions received for overhaul had a log which contained most of the relevant data necessary for the performance of this program. Included in this data were items such as transmission serial number, part number, total time, time since new or a previous overhaul, reason for removal, agency or using activity, aircraft removed from, date removed from aircraft, and transmission condition as received at Boeing Vertol. Table 1 provides a detailed description of the format and the collected data for each preoverhaul transmission.

The historical data required for the new CH-47C transmissions was not as extensive as that required for the preoverhaul transmissions. The logs contained only the serial numbers and part numbers of the transmissions involved. Table 2 is a listing of the new transmissions monitored in this program and 1 postoverhaul transmission.

VIBRATION ANALYSIS

High-Frequency Vibration Analysis

The terms "low" and "high" frequencies, when referring to vibration analysis, are the portions of the vibration spectrum that are monitored. Low-frequency vibration analysis for rotating machinery will always include that portion of the transducer signal which contains the unfiltered dynamic event frequencies of the machinery (the "raw" 0 to 10 kHz band). Some sort of processing such as spectrum analysis may be performed on the low frequency signal, but the processing technique will deal specifically with the amplitudes of bands that include the dynamic event frequencies and their lower harmonic orders. High-frequency vibration analysis, on the other hand, utilizes the transducer output signal frequencies several orders of magnitude above the dynamic event frequencies of the machinery.

Demodulated High-Frequency Vibration Analysis

The basic premise of high frequency vibration monitoring is that dynamic events related to the presence of a defect in a machine will cause amplitude modulation in the time domain across a relatively broad frequency spectrum. Thus, for example, each time a bearing's rolling element impacts a spall on the bearing's outer race it will result in amplitude modulations across a broad frequency spectrum, including frequencies well above the machine's fundamental and lower harmonic frequencies.

TABLE 1. PREOVERHAUL TRANSMISSION HISTORICAL DATA

SERIAL NUMBER	PART NUMBER	TOTAL TIME	TIME SINCE O/H	DATE REMOVED	AIRCRAFT	ACTIVITY	REASON FOR REMOVAL	COMPONENT CONDITION AS RECEIVED
A7-827	114D1200-5	1274	292	4190	67-18549	N.C.A.D.	EXCESSIVE VIBRATION	ACCEPTABLE
A7-878	114D1200-5	1420	525	4088	70-15011	FORT RUCKER	HIGH METAL ON FILTER	ACCEPTABLE
A7-896	114D1200-5	610	6	UNK.	66-104	IROAN AIRCRAFT, BOEING VERTOL	PITTING ON SHAFT SPLINES	ACCEPTABLE
A7-1040	114D1200-5	485	NEW	UNK.	65-7980	271ST AVN. CO.	THREADS STRIPPED	ACCEPTABLE
A9-724	114D2200-7	2149	949	4142	68-15828	N.C.A.D.	METAL CONTAMINATION	ACCEPTABLE
A9-734	114D2200-7	1584	377	4132	67-18504	147TH AVN. CO.	HIGH METAL IN OIL	ACCEPTABLE
A9-728	114D2200-5	1499	299	4017	66-19044	582ND T.C.	METAL ON MAG PLUG	ACCEPTABLE
A9-748	114D2200-7	1205	133	4092	69-17110	147TH AVN. CO.	INTERNAL FAILURE	ACCEPTABLE
A9-856	114D2200-7	856	272	UNK.	67-18503	FORT SILL	INTERNAL FAILURE	TWO STUDS PULLED OUT OF ACCESSORY HOUSING
A9-871	114D2200-7	1212	NEW	UNK.	67-18526	UNKNOWN	TIME CHANGE	ACCEPTABLE
A9-918	114D2200-7	1510	306	5038	68-16002	205TH AVN. CO.	HIGH METAL IN OIL	ACCEPTABLE
A9-962	114D2200-8	304	204	4126	68-16004	FORT RUCKER	HIGH METAL ON FILTER	ACCEPTABLE
A9-971	114D2200-7	463	88	4120	64-13160	N.C.A.D.	LEAKING	ACCEPTABLE
A9-984*	114D2200-7	1221	742	UNK.	68-15864	AIR AMERICA	METAL CONTAMINATION	TRANSMISSION REC'D IN A DISASSEMBLED CONDITION*
A9-1035	114D2200-7	508	108	4032	68-15836	N.C.A.D.	METAL ON MAG PLUG	ACCEPTABLE
A9-1082	114D2200-5	528	NEW	0309	64-13111	N.C.A.D.	EXCESSIVE BACKLASH	BLOWER DRIVE SECTION OF XMSN REMOVED
A9-1083	114D2200-5	396	NEW	1040	66-19068	N.C.A.D.	EXCESSIVE BACKLASH	BLOWER DRIVE SECTION OF XMSN REMOVED
A9-1133	114D2200-7	1249	849	4236	66-19124	IROAN AIRCRAFT, BOEING VERTOL	SCUFFED PINION & RING GEARS	ACCEPTABLE
A9-1221*	114D2200-7	22	NEW	UNK.	70-15016	196TH AVN. CO.	GEN. SHAFT SHEARED	4 STUDS PULLED FROM UPPER HSG. - XMSN PARTLY DISASSEMBLED*
A9-1245	114D2200-7	447	NEW	5092	70-15030	205TH AVN. CO.	PLUG LOOSE IN INPUT HOUSING	114D2134 INPUT GEAR PLUG LOOSE.

* TRANSMISSION NOT USED FOR THIS PROGRAM

TABLE 2. NEW/POSTOVERHAUL TRANSMISSION HISTORICAL DATA

	SERIAL NUMBER	PART NUMBER
	A7-987	114D1200-7**
	A7-1408	114D1200-8
	A7-1417	114D1200-7
FORWARD	A7-1418	114D1200-7
TRANSMISSION	A7-1421	114D1200-8
	A7-1422	114D1200-8
	A7-1423	114D1200-8
	A9-1330	114D2200-7
	A9-1337	114D2200-9
	A9-1339	114D2200-10
	A9-1341	114D2200-9
	A9-1342	114D2200-9
AFT	A9-1343	114D2200-9*
TRANSMISSION	A9-1348	114D2200-9
	A9-1349	114D2200-9
	A9-1355	114D2200-9
	A9-1367	114D2200-9
	A9-1368	114D2200-9
	A9-1373	114D2200-9
	A9-1376	114D2200-9

* 10% TORQUE LEVEL ONLY
** POSTOVERHAUL TRANSMISSION - 10% TORQUE LEVEL

ALL OTHER TRANSMISSIONS COMPLETED FULL LOAD RUNS OF 10%, 50%, AND 100%.

A bandpass filter can detect the energy in a relatively narrow band centered on a selected carrier frequency and monitor the amplitude modulations of the carrier frequency as a function of time (Figure 2A). The time-varying carrier frequency will be modulated by the impact each time a rolling element impacts the spall. The impacts will occur at the ball-pass frequency over the spall, and the ring-down frequency will be a function of the mounted resonance of the spalled race. Since the race-mounted resonant frequency is difficult to predict, and not as easily measurable or clearly characteristic of a particular bearing and defect as the ball-pass frequency, the bandpass-filtered carrier frequency is demodulated (envelope-detected). This converts it to a relatively low-frequency signal whose frequency is equal to the ball-pass frequency of the outer race of the particular spalled bearing (Figure 2B). Therefore, the envelope-detected signal can be spectrum analyzed or band-pass-filtered at the ball-pass frequency, and the limit exceedance can be monitored, to detect bearing surface defects (Figure 2C).

A good high frequency transducer is mandatory for the demodulation signal processing technique. Engineers working on this program have recorded vibration data from two different sensors: Endevco Model 6230M8 and Boeing Model 253. The Endevco and the Boeing sensors have essentially the same response: flat from 0-10 kHz, a resonance peak around 30 kHz, and a gradual signal drop-off with several resonances out to 200 kHz. Figures 3 through 5 provide the general description and performance specifications for the Endevco and IFD transducers. Figures 6 through 9 are typical calibration curves for both transducer types.

The Boeing Vertol Company utilizes three demodulated high frequency data processing systems. There are two 4-channel data processors. One is operated in conjunction with four Krohn-Hite Model 3202 bandpass filters. The other 4-channel processor contains built-in bandpass filters, thus allowing it to be extremely versatile and portable. In addition, Boeing Vertol has a 13-channel processor for data collection efforts. It requires simultaneous recording of demodulated vibration data from multiple (more than four) sensor locations. From the analysis of CH-47 demodulated high frequency data performed under this contract, a good correlation of processed data has been obtained from all three systems.

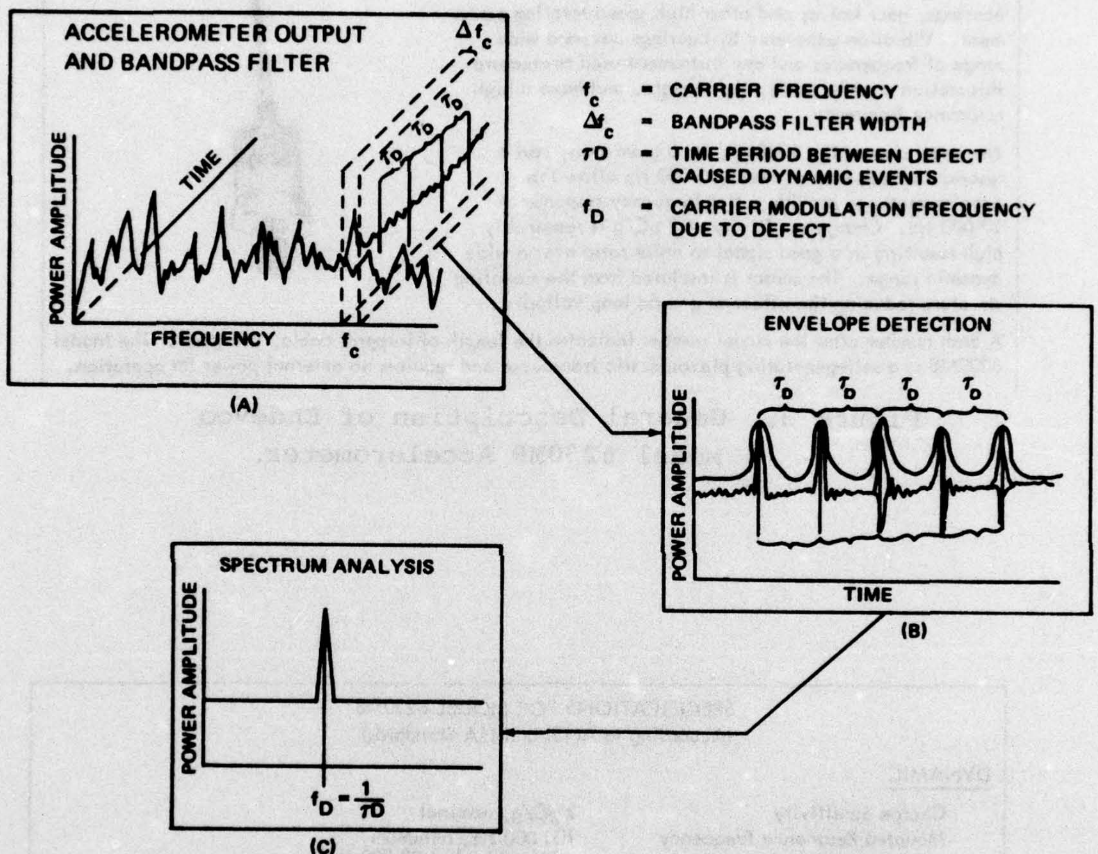

A) A CARRIER FREQUENCY IS SELECTED AT A SUFFICIENTLY HIGH VALUE (> 25 kHz) THAT IT IS NOT AFFECTED BY NORMAL TRANSMISSION NOISE, BUT AT A LOW ENOUGH VALUE (< 500 kHz) THAT IT IS AMPLITUDE MODULATED BY PERIODIC DEFECTS.

B) THE BANDPASS-FILTERED CARRIER FREQUENCY SIGNAL IS AMPLITUDE DEMODULATED (ENVELOPE-DETECTED) BACK INTO A LOW FREQUENCY (0-20 kHz) SIGNAL.

C) THE DEMODULATED CARRIER IS SPECTRUM ANALYZED AND THE LIMIT EXCEEDANCE IS MONITORED TO DETECT AND ISOLATE THE DEFECT (VIA ITS CHARACTERISTIC FREQUENCY IN THE MACHINE).

Figure 2. "Demodulated Carrier" High-Frequency Vibration Analysis.

GENERAL DESCRIPTION

The Endevco® Model 6230M8 Accelerometer is designed to sense high frequency vibrations caused by defects in bearings, gear trains, and other high speed rotating equipment. Vibration generated by bearings covers a wide range of frequencies and any instrument used to measure this motion must be small, lightweight, and have a high resonance frequency.

The small size of the 6230M8, its 5 gram mass, and a resonance frequency of over 100 000 Hz allow this accelerometer to provide a flat frequency response to 20 000 Hz. Charge sensitivity of 2 pC/g is reasonably high resulting in a good signal to noise ratio over a wide dynamic range. The sensor is insulated from the mounting structure reducing the effect of ground loop voltages.

A dash number after the model number indicates the length of integral cable, in inches. The Model 6230M8 is a self-generating piezoelectric transducer and requires no external power for operation.

Figure 3. General Description of Endevco Model 6230M8 Accelerometer.

SPECIFICATIONS FOR MODEL 6230M8
(According to ANSI and ISA Standards)

DYNAMIC

Charge Sensitivity	2 pC/g, nominal
Mounted Resonance Frequency	100 000 Hz, minimum
Frequency Response[1]	+5% typical at 20 000 Hz, reference 100 Hz
Transverse Sensitivity	Designed for 5% maximum
Amplitude Linearity, Range	Sensitivity increases approximately 1% per 500 g, 0 to 500 g.

ELECTRICAL

Transducer Capacitance	1400 pF nominal, with six inch cable
Transducer Resistance (70°F)	1000 MΩ minimum
Insulation	Signal return insulated from case.

Page 1 of 2
1/75

Figure 4. Specifications for Endevco Model 6230M8 Accelerometer (Sheet 1 of 2).

Specifications for Model 6230M8 (Continued)

Tolerances: .XX(X.X) = ± 0.03 (±0.8) Dimensions in inches and (millimetres)
.XXX (X.XX) = ±0.010 (±0.25)

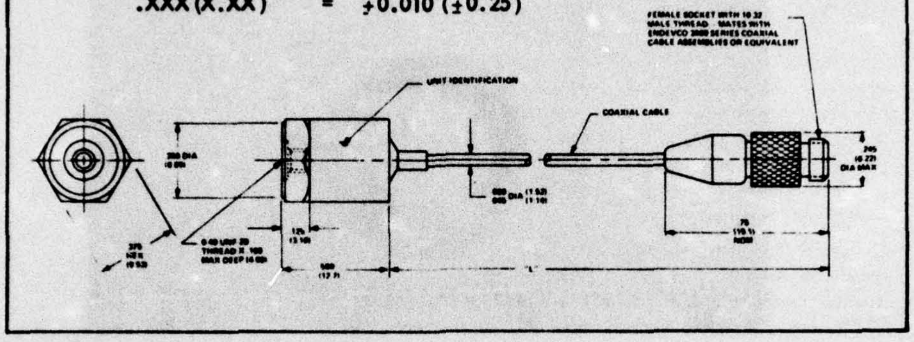

PHYSICAL

Design	Single-ended Compression
Weight	5 grams
Crystal Material	Piezite® Element Type P-8
Case Material	Corrosion resistant steel
Integral Cable	Coaxial, 6 inch (15 cm), Teflon dielectric and jacket, low-noise treated, terminated with 10-32 coaxial receptacle (EP 189).
Mounting	Hole for 6-40 x 1/8 inch stud. Recommended mounting torque: 7 lbf-in (0.8 Nm).
Accessory Supplied	Model 2984-4 Mounting Stud, adapts 6-40 to 10-32 threads.
Accessories Available	Model 3090A or 3090B Low-Noise Coaxial Cable Assemblies

ENVIRONMENTAL

Acceleration Limit	500 g peak
Temperature	-40°F to 500°F (-40°C to 260°C)
Altitude	Not affected
Seal	Epoxy sealed

Continued product improvement necessitates that Endevco reserve the right to modify these specifications without notice.

CALIBRATION: Each accelerometer is calibrated at room temperature for charge sensitivity, capacitance (including integral cable), and charge frequency response from 25 Hz to 10 000 Hz. Temperature response at room temperature, 300°F (150°C), and 500°F (260°C), and other calibrations are available on special order. See Calibration Service Bulletin 301.

Note: [1] Base strain sensitivity may limit the use of this transducer on flexible structures at frequencies below 100 Hz. Cable must be tied down as close as possible to accelerometer, with one inch diameter service loop, minimum, to reduce the effects of cable motion.

Cable strain, pyroelectric output, and minor resonances in test shaker limit our capability for accurately measuring frequency response to no better than ±10% from 25 Hz to 10 kHz.

Page 2
1/75

Figure 4. Specifications for Endevco Model 6230M8 Accelerometer (Sheet 2 of 2).

IFD MODEL 253 TRANSDUCER

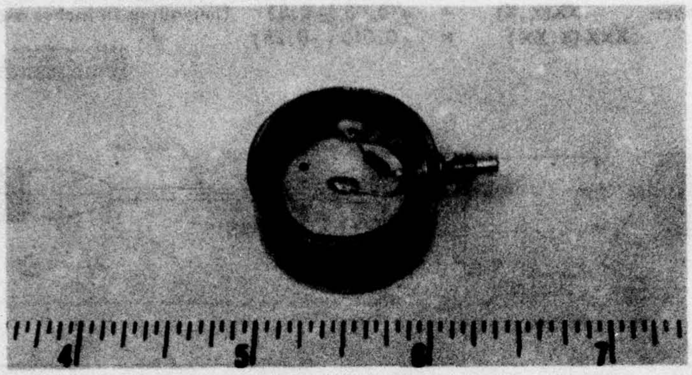

INTERNAL STRUCTURE (SHOWN BEFORE POTTING)

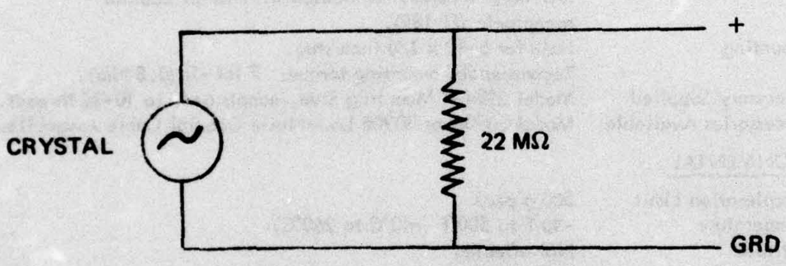

TRANSDUCER SCHEMATIC

Charge Sensitivity: $\approx$ 55 pC/g
Frequency Response: $\pm$ 1 db from 100 Hz to 10 kHz, + 1 db @ 20 kHz (Ref. 100 Hz)
Mounted Resonant Frequency: 1st Resonance @ $\approx$ 30 KHz, numerous additional resonant frequencies up to 1 MHz
Transducer Capacitance: 650 pF nominal, without cable
Transducer Resistance: $>$10 M Ω
Temperature Limitation: 300^{o}F
Transducer Weight: 38 gm

Figure 5. IFD Accelerometer and Schematic.

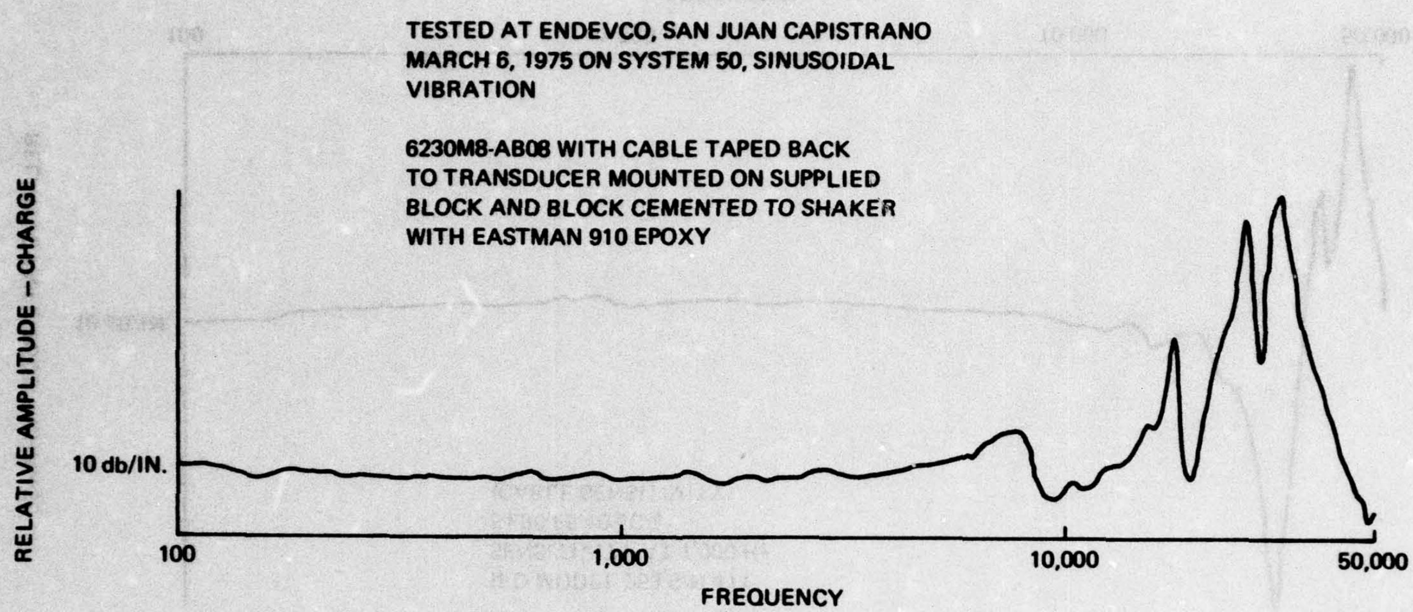

Figure 6. Response of Endevco Accelerometer Model 6230M8 Serial No. AB08--Mounting Block Secured with Epoxy Cement.

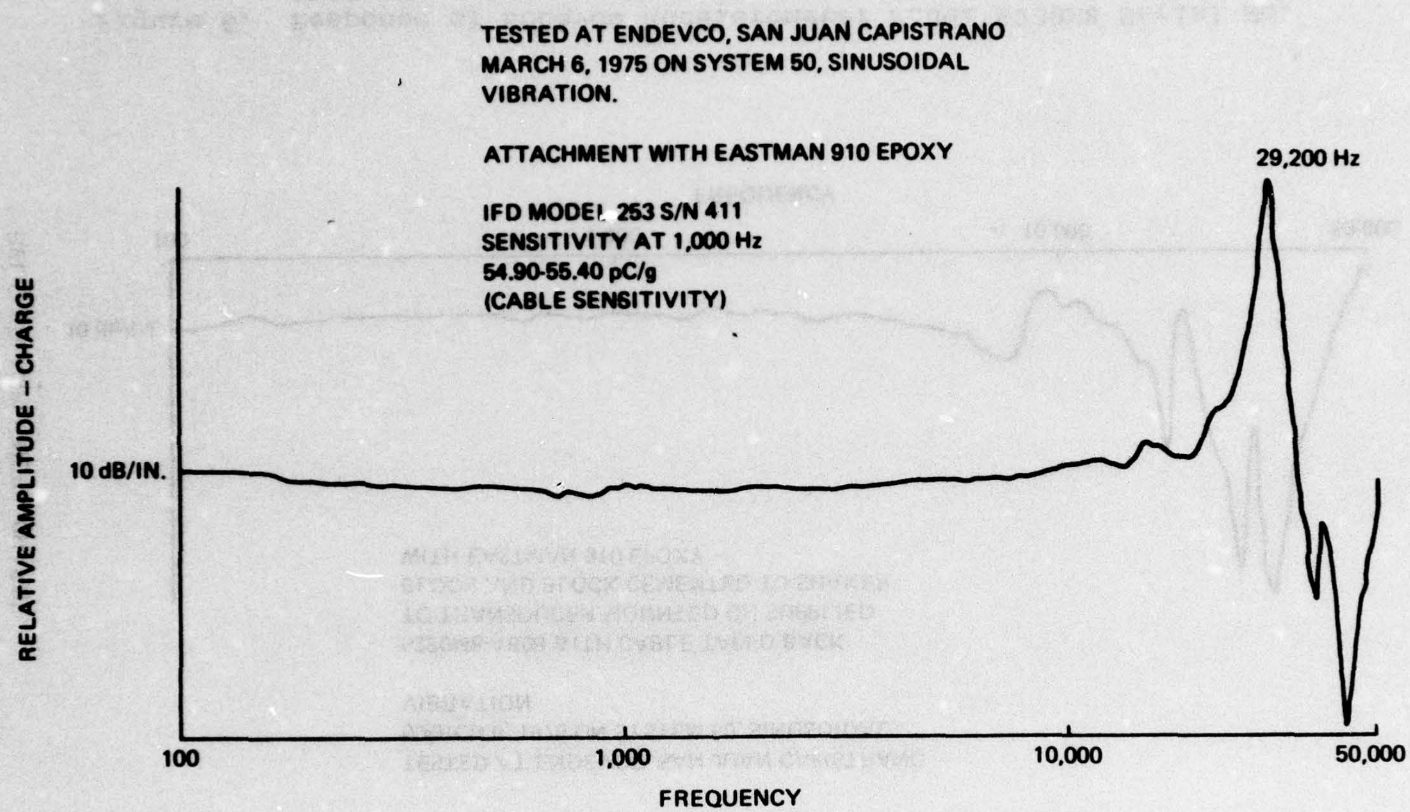

Figure 7. Response of Boeing Accelerometer Model 253, Serial No. 411--Attached Directly to Shaker with Epoxy Cement.

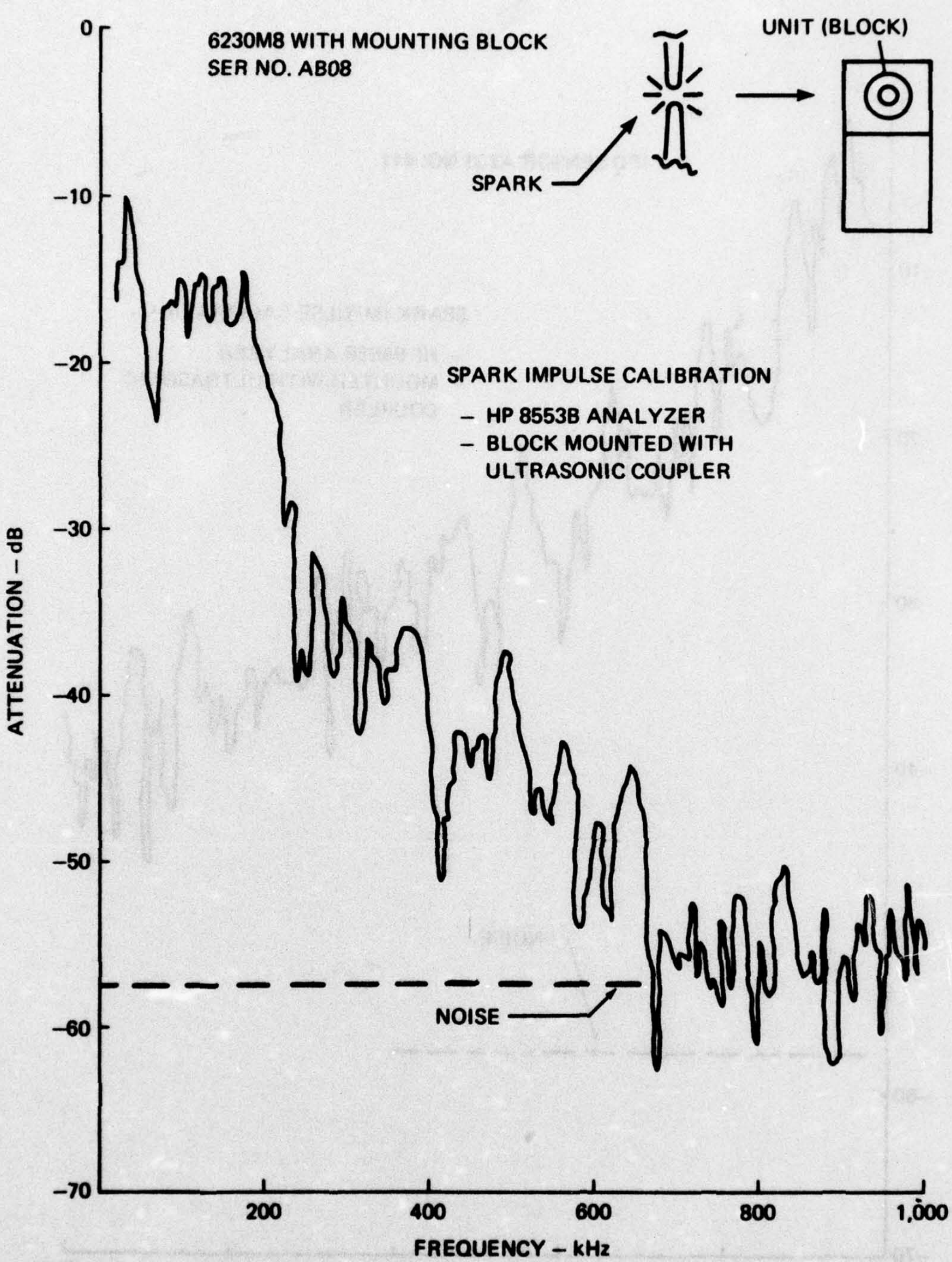

Figure 8. Response of Endevco Accelerometer Model 6230M8, Serial Number AB08--Mounting Block Secured with Ultrasonic Compliant.

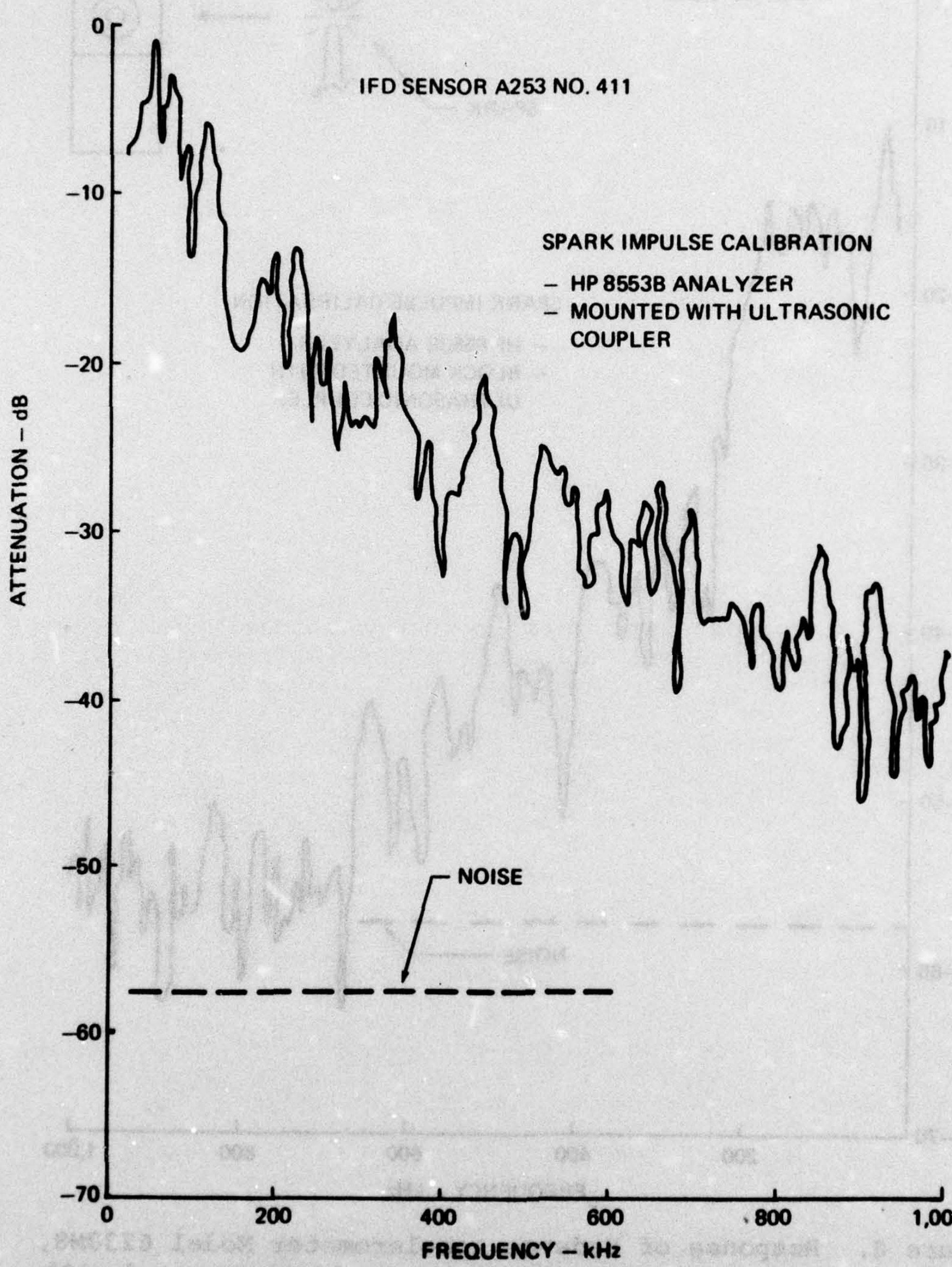

Figure 9. Response of Boeing Accelerometer Model 253, Serial No. 411--No Mounting Block - Ultrasonic-Compliant Bonded.

We have found there is good correlation between "raw" data processed off magnetic tape, within the recorded electronic frequency limits, and data that is bandpass-filtered and demodulated before taping. Demodulated data from higher carrier frequencies (100 kHz and higher) was processed before recording due to tape recorder electronic constraints.

Low-Frequency Vibration Analysis

Low-frequency vibration analysis is performed by spectrum analyzing the output of an accelerometer over a frequency range that includes the fundamental and lower harmonic frequencies characteristic of a machine in normal operation. (These frequencies include rolling element pass frequencies over points on bearing races, gear mesh frequencies, and rotational frequencies of gearshafts, bearing cages, planetary gear carriers, etc. Thus for low frequency vibration analysis, accelerometer data above 10 kHz in the frequency spectrum is ignored.) Diagnosis is based upon pattern changes. A baseline spectrum is recorded for a good transmission and subsequent spectra are then compared to the baseline for significant deviations that can be considered indicative of component deterioration. The problems that arise with this technique are:

1. How to implement simple field recording and storage of custom baseline data in such a manner that frequent rebaselining does not occur after fault indication (similar to cleaning and reinstalling a chip detector)

2. Calibration and maintenance of flat-response accelerometers in a field environment.

Since low-frequency vibration analysis has been performed for a number of years with few conclusive results, Boeing has little confidence of accurate fault detection in this portion of the transducer frequency spectrum.

EQUIPMENT INSTALLATION AND DATA RECORDING PROCEDURES

Whenever high-frequency vibration data has been obtained in the Boeing Vertol test cells, Endevco Model 6230M8 vibration data has been recorded from 0-75 kHz. This data can be analyzed by the demodulated high frequency technique by processing the signal from the magnetic tape for carrier frequencies through 50 kHz.

Eighteen preoverhaul and 18 new/postoverhaul transmissions were instrumented and then monitored during the duration of the load runs. Endevco Model 6230M8 and IFD Model A253 accelerometers were installed on the exterior surfaces of the transmissions as indicated in Figures 10, 11, 12 and 13. As noted in these figures, two configurations were utilized for both the forward and aft transmissions. The transmissions used for each configuration are recorded by serial number under the applicable configuration. The discussion pertaining to the configuration change is noted in the latter section of the report.

Various epoxy compounds were tested in an effort to determine which would be the most suited as an agent to bond transducers to the transmission surfaces. Dental cement was found to be the most suitable bonding agent for all the transmission surfaces, except the stationary ring gear, in that it provided acceptable adherence qualities and signal transmission ability, ease of use, and fast curing time. On the significantly smoother stationary ring gear surface, a five-minute epoxy provided better adherence characteristics but reduced temperature capabilities. Dental cement in this application did not provide the adherence qualities desired.

IFD accelerometers were bonded directly to the transmission surfaces. Endevco accelerometers were stud mounted to 3/4-inch aluminum cubes which were bonded to the transmission surfaces. This procedure was necessary for two reasons:

1. It was not feasible to drill and tap the CH-47C transmission housings to accomodate the Endevco transducer studs

2. The much smaller Endevco transducers were too delicate to be removed (if glued directly onto the transmission housing) by a sharp blow with a hammer and drift (as were the larger IFD sensors).

The Boeing IFD Model 253 high frequency vibration sensors were used extensively because they have a very high signal output (nominally 55 pC/g) which eliminates the need for charge amplifiers. They also have a resonant frequency range which allows the routine use of carrier frequencies up to 500 kHz.

The bandpass-filtered and envelope-detected output of the IFD signal conditioning equipment is essentially 0 to 15 kHz and hence is satisfactory for recording on FM channels at 15 inches per second. In addition, on several IFD transducers, "Broad Band" data (amplified but not bandpass-filtered or envelope-detected) was recorded on "Direct" channels (150 Hz to 75 kHz response) at 15 inches per second. Endevco signals were not bandpass-filtered or envelope-detected prior to recording, and

were always recorded on "Broad Band". Each Endevco pickup signal was fed to a direct channel to cover the frequency range from 0 Hz to 20 kHz. The results was 0 Hz to 75 kHz coverage for the Endevco accelerometers. Direct tape channels were capable of handling in excess of 5 volts RMS, while FM tape channels would saturate for voltages in excess of 1 volt RMS.

Accordingly, Endevco charge amplifiers were adjusted to prevent voltages in excess of 1 volt RMS from being applied to the tape. Similarly, the variable amplification in the Boeing IFD signal conditioning equipment was adjusted to keep the envelope-detected signal voltages below 1 volt RMS to avoid FM tape saturation. Broad band IFD signal voltages recorded on direct tracks were maintained below 5 volts RMS.

For each of the 3 torque levels encountered (10%, 50%, 100%), the IFD bandpass filters for each IFD transducer were adjusted to 50 kHz, 100 kHz, and 250 kHz center frequency respectively. Due to tape track limitations, data was recorded from two groups of accelerometers in sequence. For the early configuration:

- Bank 1 comprised IFD transducers 1, 2, 3, and 4
- Bank 2 comprised IFD transducers 4, 5, 6, and 7.

For the later configration:

- Bank 1 comprised IFD transducers 1, 2, 3, and 4
- Bank 2 comprised IFD transducer 1 and the combined voltages (on 1 tape track) from transducers 2, 3, and 4.

Endevco accelerometers were not banked and their signal conditioning remained constant for a particular level of torque, since bandpass filtering was not involved.

Table 3, Magnetic Tape Index, tabulates the Boeing Vertol Diagnostic Test Number (BVD) and the tape reel assigned to each transmission.

TRANSMISSION TESTING

The vibration and debris data collected in this program were obtained from the load runs performed on new and preoverhaul CH-47C forward and aft transmissions. Figure 14 depicts the components used for collecting the vibration data.

Preoverhaul Transmissions

Twenty CH-47C transmissions being inducted into the overhaul program at Boeing Vertol under an AVSCOM Contract were selected for vibration analysis. The project involved 16 aft (114D2200) and 4 forward (114D1200) transmissions.

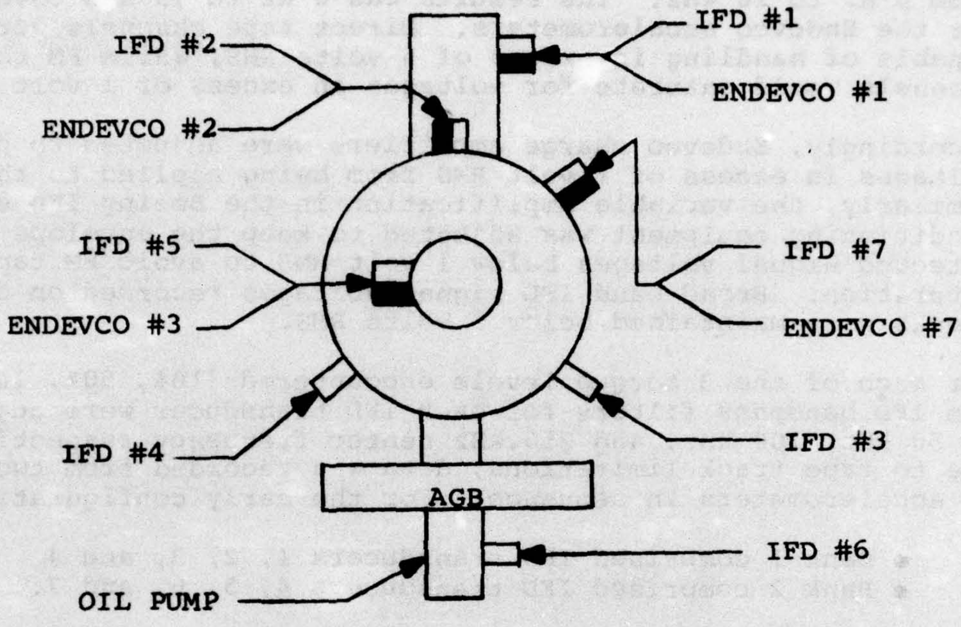

TRANSDUCER LOCATIONS (7)	TRANSDUCER NUMBER
Stationary Ring Gear	IFD #2, #3, #4, Endevco #2
Lower Housing	IFD #7, Endevco #4
Oil Pump	IFD #6
Input Pinion	IFD #1, Endevco #1
Upper Housing	IFD #5, Endevco #3

TRANSMISSIONS UTILIZING THIS CONFIGURATION

PREOVERHAUL TRANSMISSIONS	NEW TRANSMISSIONS
S/N A9-728	S/N A9-1330
S/N A9-962	S/N A9-1337
S/N A9-734	S/N A9-1339
S/N A9-1133	S/N A9-1341
S/N A9-871	S/N A9-1342
	S/N A9-1343*

* IFD & ENDEVCO #1 & #7 ONLY

Figure 10. First Configuration of Transducer Locations on CH-47C Aft Transmissions.

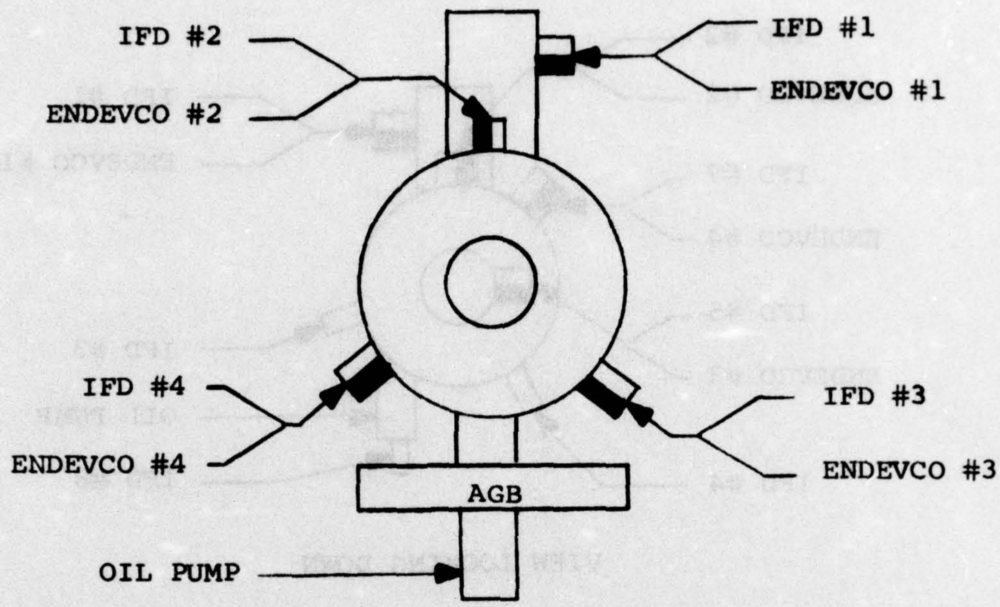

VIEW LOOKING DOWN

TRANSDUCER LOCATIONS (4)	TRANSDUCER NUMBER
Input Pinion	IFD & Endevco #1
Stationary Ring Gear	IFD & Endevco #2, #3, #4

TRANSMISSIONS UTILIZING THIS CONFIGURATION

PREOVERHAUL TRANSMISSIONS	NEW TRANSMISSIONS
S/N A9-971	S/N A9-1348
S/N A9-748	S/N A9-1349
S/N A9-1035	S/N A9-1355
S/N A9-724	S/N A9-1367
S/N A9-856	S/N A9-1368
S/N A9-1082	
S/N A9-1083	
S/N A9-918	
S/N A9-1245	

Figure 11. Second Configuration of Transducer Locations on CH-47C Aft Transmissions.

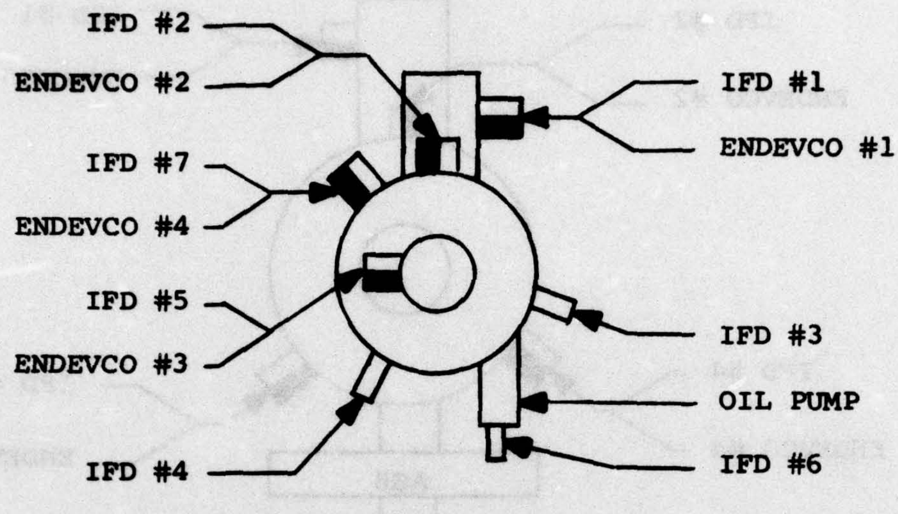

VIEW LOOKING DOWN

TRANSDUCER LOCATIONS (7)	TRANSDUCER NUMBER
Input Pinion	IFD & Endevco #1
Stationary Ring Gear	IFD #2, #3, #4, Endevco #2
Lower Housing	IFD #7, Endevco #4
Upper Housing	IFD #5, Endevco #3
Oil Pump	IFD #6

TRANSMISSIONS UTILIZING THIS CONFIGURATION

PREOVERHAUL TRANSMISSIONS	NEW TRANSMISSIONS
S/N A7-1040*	S/N A7-987**
S/N A7-896*	S/N A7-1408
S/N A7-878*	S/N A7-1417
S/N A7-827	

* THIS INSTALLATION DID NOT UTILIZE ENDEVCO TRANSDUCERS
** POSTOVERHAUL TRANSMISSION

Figure 12. First Configuration of Transducer Locations on CH-47C Forward Transmissions.

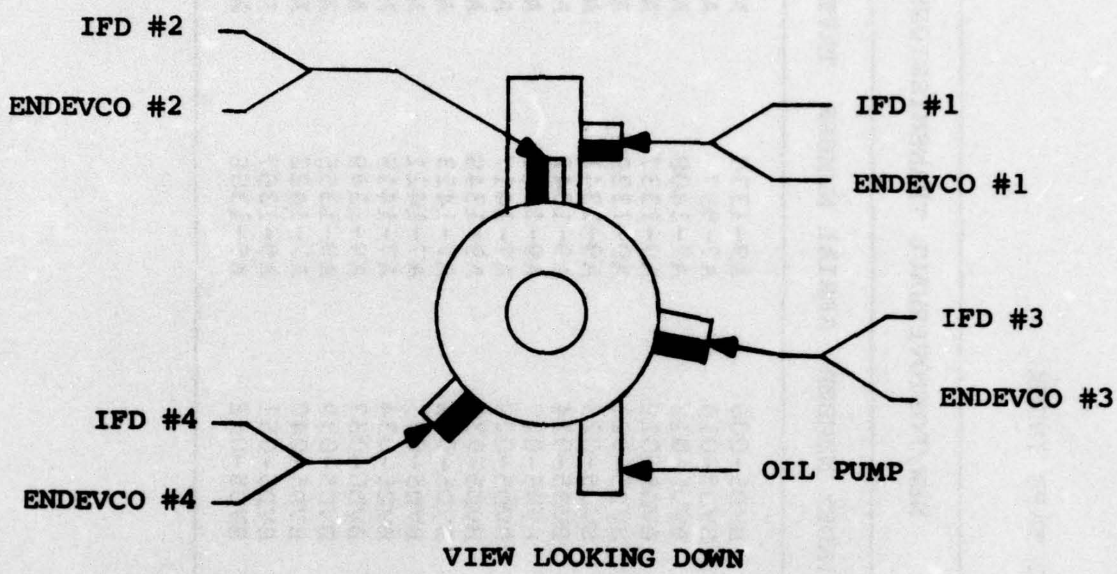

<u>TRANSDUCER LOCATIONS (4)</u>	<u>TRANSDUCER NUMBER</u>
Input Pinion	IFD & Endevco #1
Stationary Ring Gear	IFD & Endevco #2, #3, #4

<u>TRANSMISSIONS UTILIZING THIS CONFIGURATION</u>

<u>NEW TRANSMISSIONS</u>

S/N A7-1423
S/N A7-1421
S/N A7-1418
S/N A7-1422

Figure 13. Second Configuration of Transducer Locations on CH-47C Forward Transmissions.

TABLE 3. MAGNETIC TAPE INDEX

PREOVERHAUL TRANSMISSIONS			NEW/POSTOVERHAUL TRANSMISSIONS		
INDEX NUMBER	SERIAL NUMBER	TAPE REEL	INDEX NUMBER	SERIAL NUMBER	TAPE REEL
BVD4-004	A7-1040	H	BVD5-006	A9-1330	AI
BVD4-006	A7-896	C	BVD5-016	A7-987	AI
BVD4-009	A7-878	M	BVD5-018	A7-1408	AI
BVD5-008	A7-827	AI	BVD5-019	A9-1337	AM
BVD5-013	A9-728	AI	BVD5-021	A9-1339	AM
BVD5-014	A9-962	AI	BVD5-023	A9-1341	AM
BVD5-020	A9-734	AQ	BVD5-024	A9-1342	AM
BVD5-022	A9-1133	AM	BVD5-027	A9-1343	AM
BVD5-028	A9-871	AM	BVD5-029	A7-1417	AQ
BVD4-035	A9-971	AS	BVD5-031	A9-1348	AQ
BVD5-036	A9-748	AS	BVD5-032	A7-1423	AQ
BVD5-038	A9-1035	AS	BVD5-033	A7-1421	AQ
BVD5-042	A9-724	AT	BVD5-034	A7-1418	AQ
BVD5-043	A9-856	AT	BVD5-037	A9-1349	AS
BVD5-044	A9-1082	AS	BVD5-039	A9-1355	AS
BVD5-045	A9-1083	AT	BVD5-040	A7-1422	AT
BVD5-046	A9-918	AT	BVD5-051	A9-1367	AY
BVD5-047	A9-1245	AT	BVD5-052	A9-1368	AY

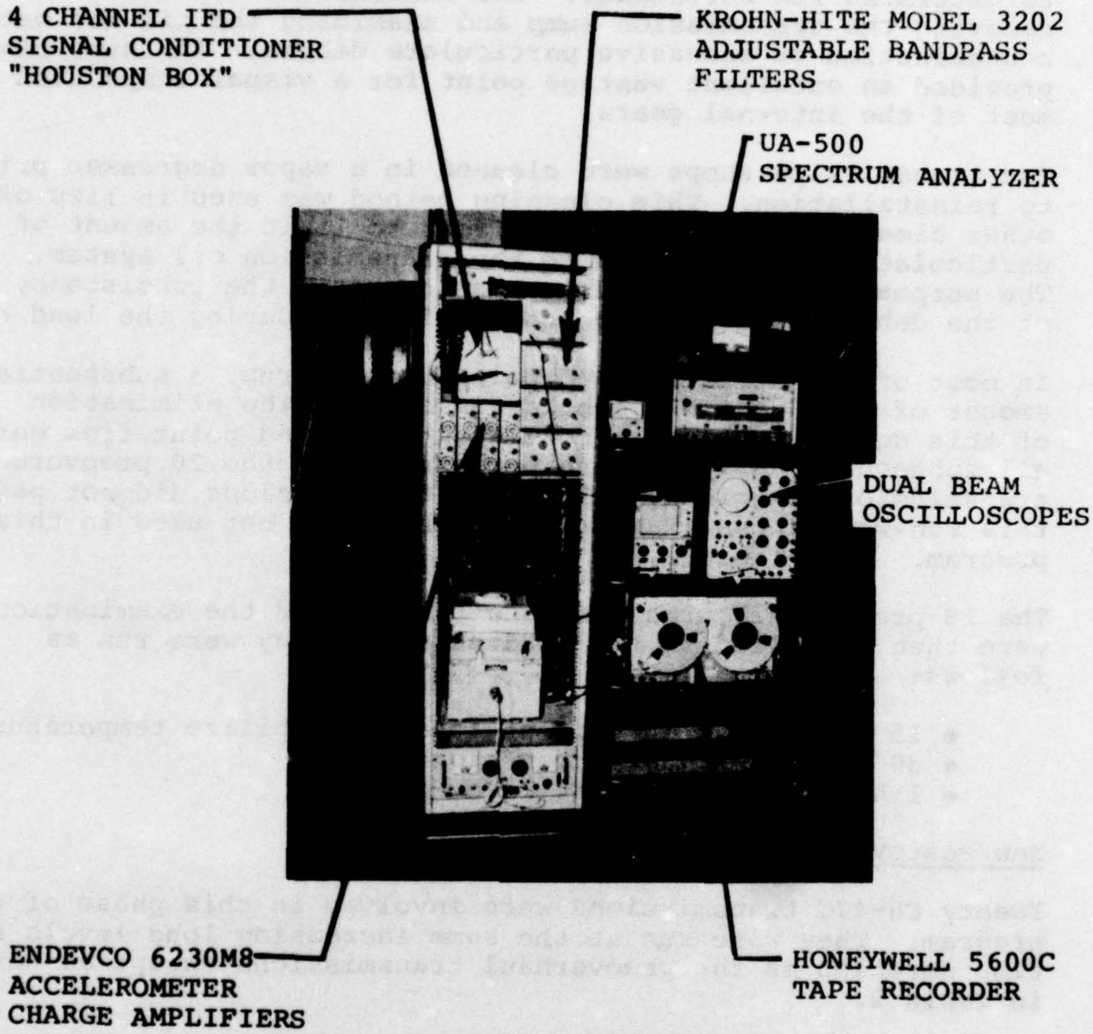

Figure 14. Components Used for Vibration Data Collection.

Load runs were performed on the preoverhaul transmissions in the condition they were received at Boeing Vertol. Prior to installation in the test cell, each transmission was examined to determine run worthiness. The examination consisted of removing the transmission sump and examining the oil for water contamination or excessive particulate debris. The sump removal provided an excellent vantage point for a visual inspection of most of the internal gears.

The transmission sumps were cleaned in a vapor degreaser prior to reinstallation. This cleaning method was used in lieu of other cleaning solvents in an effort to limit the amount of particulate debris exposed to the transmission oil system. The purpose of this procedure was to assure the consistency of the debris collected in the oil filters during the load runs.

In most of the sumps removed prior to load run, a substantial amount of residue field debris was found. The elimination of this debris provided a consistent starting point from which all subsequent analyses were performed. Of the 20 preoverhaul transmissions examined, only 2 aft transmissions did not pass this run-worthiness examination. They were not used in this program. (See Table 1.)

The 18 preoverhaul transmissions that passed the examination were then installed in the load stands. They were run as follows:

- 15 minutes at 10 percent load to stabilize temperatures
- 30 minutes at 50 percent load
- 1 hour at 100 percent load

New/Postoverhaul Transmissions

Twenty CH-47C transmissions were involved in this phase of the program. They were run at the same increasing load levels and time duration as the preoverhaul transmissions except as noted in Table 2.

Associated Information Related to Data Collection

The forward and the aft test stands used in this project are of closed-loop configuration. Figure 15 shows a typical installation. In this type of stand the torque is locked within the closed loop, which provides the capability of running high horsepower within the loop without using high applied horsepower.

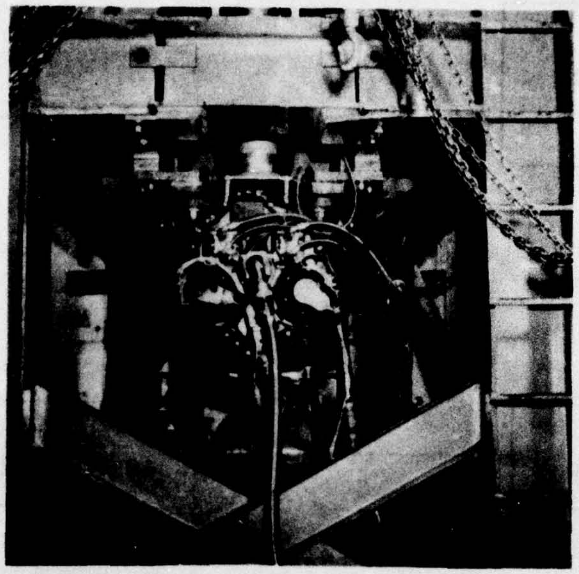

Figure 15 Typical Test Stand Installation.

Test data such as transmission oil pressure, temperature, and oil flow were monitored and documented during each load run.

Every transmission utilized for this program successfully completed the load runs within the required specifications.

New or recycled MIL-L-23699 oil was used in all of the transmissions tested. The recycled oil was filtered through a liquid control system which has 10-micron filtration and water removal capabilities.

The transmission oil was cooled by heat exchangers installed on the test stands. To prevent any debris associated with the cooling system from entering the transmission, a 40-micron absolute filter was installed in the transmission oil return line on the test cell. In addition, each transmission was protected by its own filter with a 40-micron nominal and a 64-micron absolute rating. These filters were a stacked, wafer-type construction capable of being cleaned.

Figure 16 illustrates the transmission lubrication system involved in testing the CH-47C forward and aft transmissions.

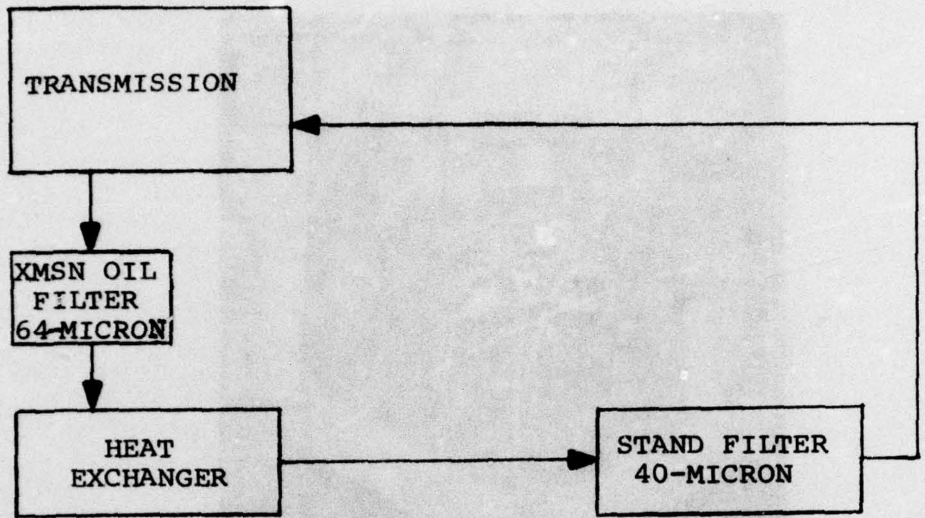

Figure 16. CH-47C Forward and Aft Transmission Lubrication System.

The test stand lubrication system is independent of the transmission lubrication system. Test stand lubrication is provided from a separate oil reservoir which lubricates the stand's drive components.

TRANSMISSION OIL FILTER REMOVAL AND CLEANING

Preoverhaul Transmission Oil Filters

Prior to the load run of each CH-47C preoverhaul transmission, the oil filter was removed from the housing and stored in a sterilized plastic bag. The debris retained on these oil filters was the debris the transmissions generated prior to removal from the aircraft. A cleaned oil filter was installed in place of the one removed. At the completion of the load run, the oil filter was once again removed in the same manner as stated above. The debris retained on these oil filters was the debris generated during the preoverhaul load run.

Thirty-four preoverhaul transmission oil filters were removed and retained for cleaning and analysis.

New Transmission Oil Filters

The only requirement for oil filter removal on the new CH-47C transmissions was after the load run. The oil filter removal procedure was the same as stated above for the preoverhaul transmissions.

Since new transmissions initially generate an abnormal quantity of debris, which is caused by normal cleanup, an effort was made to determine what the normal debris generation would be after cleanup. This was accomplished by using two oil filters instead of one during the load run. The first filter was removed at the conclusion of the 50% load (approximately 45 minutes of run time) and replaced with a cleaned oil filter, which was removed at the conclusion of the 1-hour, 100% load cycle. Four new aft transmissions were used for this effort. The first 45 minutes provided the required cleanup and the last hour provided the normal debris generation level.

Twenty-three new transmission oil filters were removed (15 under normal conditions and 8 from the dual filter installation) and retained for cleaning and analysis.

Oil Filter Cleaning Procedure

The removed CH-47C transmission oil filters were all cleaned manually by the following procedure.

1. The oil filter assembly was disassembled in order to remove each oil filter wafer.

2. These wafers were then individually cleaned by using a stiff bristled brush and isopropyl alcohol (anhydrous 99%). The brush was cleaned in isopropyl alcohol prior to use.

   To assure maximum cleanliness, the isopropyl alcohol agent was filtered through a 5-micron millipore paper prior to the cleaning process. Since the outer surfaces of the wafers retained the collected debris, only these surfaces were cleaned. A brushing action was applied to these surfaces using the precleaned brush and filtered alcohol until the desired cleanliness was obtained. The debris was brushed into a beaker containing approximately 400-milliliters of filtered alcohol. At the conclusion of the cleaning process, each wafer was viewed under a microscope to assure cleanliness. If acceptable, the brush was cleaned into the same solution by using a hand pressure laboratory fluid dispensing bottle.

3. The fluid was then transferred into a precleaned sample bottle and retained for particle size distribution. Each sample bottle was labeled with the pertinent transmission and filter removal data.

4. The oil filter was then sonically cleaned, reassembled, and retained for future use.

5. Each oil filter used in this program was cleaned by the same engineer in an effort to eliminate a variable that could exist between individuals.

ASOAP SAMPLES

Two 120-milliliter ASOAP samples were taken at the conclusion of each load run. Samples were taken in accordance with TB55-6650-300-15, Section III, Paragraph (c) (Drain Samples). The drain plug was opened and a pint of oil was permitted to drain. The samples were taken without flow interruption after the pint of oil was drained.

Each of the oil samples was taken within 5 minutes of shutdown.

The sample bottles were labeled with the transmission serial number, part number, when taken, and sequence taken. The samples were then sent to ARADMAC via USAAMRDL. The ASOAP results obtained from ARADMAC were then tabulated and retained for analysis.

All ASOAP samples were taken by the same engineer who was present during each load run.

TRANSMISSION DISASSEMBLY

At the completion of the load run, each transmission was forwarded to the disassembly area. If during disassembly a discrepancy was encountered, the author was immediately notified. This procedure assisted in evaluating the specific mechanism of the failure mode detected. Each transmission was completely disassembled with each component identified to denote the transmission from which it was removed.

These components were then cleaned and forwarded to the Quality Control area. Each component of the transmission was inspected in accordance with Work Requirements 55-1615-116 and -117 with one exception; i.e., the life-limited components which are normally rejected with only superficial inspection were examined thoroughly (visually and dimensionally) to obtain the detail data required for this program. All of the data recorded by Quality Control in this process was collected and categorized by transmission.

A Boeing Vertol overhaul discrepancy tag was affixed to all rejected components, reworkable and scrap. The basic information included on this tag was:

1. Part Number.

2. Part Name.

3. Part Serial Number (if applicable).

4. Part Total Time/Time Since Overhaul.

5. Transmission Removed From.

6. Transmission Total Time/Time Since Overhaul.

7. Part Discrepancy.

8. Part Disposition.

Copies of all the overhaul discrepancy tags were collected and catalogued according to the transmission from which they were removed.

The reworkable, rejected components were reviewed by the author. In the event any of these components were of potential value to the data analysis, the noted discrepant part was photographed prior to rework. The photographs were then retained and catalogued by transmission.

The scrap components removed from the transmissions were retained by the author and photographed as necessary. These scrap components are secured in a bonded area and are available for review. Photographic documentation was compiled only on the scrapped components, along with a notation about defects of potential value to the analysis.

DATA ANALYSIS AND CORRELATION

COMPONENT CONDITION AFTER DISASSEMBLY

The individual component discrepancies as noted on the overhaul discrepancy tags were catalogued by transmission serial number. These tags indicate the noteworthy discrepancies detected during visual, dimensional, magnaflux, and zyglo inspection. Photographic documentation of the major discrepancies found is provided and noted with the applicable transmission. Table 4 is a listing, by transmission serial number, of the discrepancies found during inspection. Figures 17 through 29 are photographs of the failed components referenced in Table 4.

DATA REDUCTION OF VIBRATION SIGNATURES

Data Reduction

Data reduction was accomplished by using a UA500 Spectrum Analyzer and a Model 131E X-Y Plotter. Magnetic tape was played back at 15 inches per second using the same equipment that had been used earlier to record the signals.

Power Spectral Density (PSD) plots were made of the signal amplitude displayed logarithmically (db scale) versus a selected frequency range of 0 to X Hz displayed linearly. For this program, the most used spectral frequency ranges were 0 to 200 Hz, 0 to 500 Hz, and 0 to 5,000 Hz. As a general rule, selection of PSD spectral range represented a trade-off involving maximum frequency content versus required degree of resolution to allow precise identification of spike frequencies. It should be recognized that in the absence of a range translation unit, the same degree of resolution is not available over the entire frequency range. For example, the 0- to 200-Hz scale provides resolution to 0.4 Hz, while the 0- to 500-Hz scale provides resolution to 1.0 Hz. With the current equipment, there is no way of obtaining 0.4 Hz resolution between 200 Hz and 500 Hz.

Data Analysis

Essential to the recognition of part degradation is the ability to identify the characteristic frequencies associated with the various rotating elements in the transmissions. Table 5 lists the excitation frequencies associated with the various gear, shaft and bearing rotating elements of the CH-47C forward transmission while operating at its test speed of 223.7 rotor shaft rpm. Table 6 lists the excitation frequencies associated with the CH-47C aft transmission at its operating test speed of 217.7 rotor shaft rpm.

TABLE 4. SUMMARIZATION OF MAJOR TRANSMISSION DISCREPANCIES

TRANSMISSION SERIAL NUMBER	CAUSE OF REMOVAL	TOTAL TIME/ TSO	DISCREPANCIES FOUND	PART CAUSING REMOVAL	REMARKS
AFT A9-856	INTERNAL FAILURE	855/272	114D2180 - HOUSING - LINER WORN, SCORING ON SCAVENGE PUMP FACE. 114DS251 - BEARING - EXCESSIVE SPALLING ON INNER RACE, OUTER RACE AND ROLLING ELEMENTS. CAGE SEVERELY WORN AND DISTORTED (FIGURE 25) 114D2071 - CARRIER - (2) POSTS WORN 114D2089 - RETAINER - EXCESSIVE WEAR ON FACE 114D2184 - RETAINER (4) - FACES EXCESSIVELY WORN. PIECES BROKEN OFF AT FACES (FIGURE 22))	114DS251 BEARING	SEE FIGURES 22 AND 25
AFT A9-971	LEAKING	463/88	114D2168 - RETAINER (5) - FLANGES CRACKED 114DS249 - BEARING - CAGE DISTORTED 114D2167 - HOUSING - TRANSFER TUBE PORT WORN .006-IN.	ASSUMED TO BE A SEAL	SEALS ARE 100% REPLACEMENT ITEMS AT DISASSEMBLY. THE SEALS ARE DISCARDED AT DISASSEMBLY AND REQUIRE NO INSPECTION.
AFT A9-748	INTERNAL FAILURE	1205/133	114DS247 - BEARING - WEAR ON EDGE OF CAGE. 114D2167 - HOUSING - TRANSFER TUBE PORT WORN .006-IN. 114DS273 - PUMP - SPLINES WORN .005-IN. 114DS259 - PUMP - SEVERELY SCORED ON GEROTOR 114D2194 - SUPPORT - LINER WORN .002-IN. 114D2139 - HOUSING (46B) - .006 - .010-IN. WEAR STEP ON BEARING SHOULDER 114DS256 - BEARING - CAGE SEVERELY WORN. SPALLING ON INNER AND OUTER RACES. SEVERE DAMAGE AND DETERIORATION OF ROLLING ELEMENTS (FIGURE 21) 114D2107/ 2132 - ACCESSORY GEARS - SPLINES WORN	114DS256 BEARING	SEE FIGURE 21
AFT A9-1035	METAL ON MAG PLUG	508/108	114D1080 - RETAINER - GOUGED AND SCORED ON MOUNTING SURFACE 114DS262 - BEARING - ABRASIVE WEAR ON OUTER DIAMETER OF INNER RACE, OUTER DIAMETER OF ROLLERS 114DS281 - PLANET - SMALL SPALL ON (1) GEAR TOOTH 114D2254 - RING GEAR - TEETH SCUFFED 114DS281 - PLANET - WEAR ON INNER DIAMETER OF CAGE 114D2093 - SHAFT - CLUTCH JOURNAL WORN 114D2045 - PINION - TEETH SCUFFED 114D2184 - RETAINER (4) - FLANGES WORN	UNKNOWN	°THE SCUFFING DETECTED ON THE RING AND PINION GEARS WAS MINIMAL AND REWORKABLE. °THE SMALL PLANET GEAR SPALL WAS VERY MINOR IN THAT A VERY CLOSE EXAMINATION WAS REQUIRED TO DISTINGUISH THIS DEFECT FROM CORROSIVE PITTING. THE SPALL WAS APPROXIMATELY 1/64-IN. DIA. °THE REMAINDER OF THE NOTED DISCREPANCIES WERE CAPABLE OF CREATING SUFFICIENT DEBRIS ON THE CHIP DETECTOR TO CAUSE THE XMSNS REMOVAL; HOWEVER, THE DEGRADATION LEVEL DID NOT WARRANT THE REMOVAL

TABLE 4. SUMMARIZATION OF MAJOR TRANSMISSION DISCREPANCIES - CONTINUED

TRANSMISSION SERIAL NUMBER	CAUSE OF REMOVAL	TOTAL TIME/ TSO	DISCREPANCIES FOUND	PART CAUSING REMOVAL	REMARKS
AFT A9-724	METAL CONTAMINATION	2149/949	114D2107 - GEAR - SPLINES WORN 114DS282 - PLANET BEARING - EXCESSIVE SPALLING ON OUTER DIAMETER OF INNER RACE (FIGURE 17) 114D2184 - RETAINER (4) - EXCESSIVE WEAR ON FLANGES 114D2089 - RETAINER - EXCESSIVE WEAR ON RETAINING FACE 114D2110 - GEAR - SPLINES WORN 114D2093 - GEAR - SPLINES WORN 114D2088 - HOUSING - WEAR STEP ON BEARING RETAINING FACE	114DS282 PLANET BRG.	SEE FIGURE 17
AFT A9-1245	PLUG LOOSE IN INPUT HOUSING	447/NEW	114D2119 - RETAINER - .065-IN. WEAR STEP ON RETAINING FACE (FIGURE 24) 114D2184 - RETAINER (4) - EXCESSIVE WEAR ON FACE 114D2100 - SLINGER - END FACE WORN .014-IN. 114D2056/ 2169 - GEARS - TEETH SEVERELY SPALLED DRIVE AND COAST SIDES (FIGURES 28 AND 29) 114DS257 - BEARING - LIGHT SPALLING AND DEBRIS DENTS ON INNER DIAMETER OF OUTER RACE	INPUT HOUSING PLUG FOUND DAMAGED UPON RECEIPT OF XMSN	THE NOTED REASON FOR REMOVAL WAS NOT A JUSTIFIABLE CAUSE TO REMOVE THE TRANSMISSION; HOWEVER, THE FOLLOWING DISCREPANCIES WOULD JUSTIFY REMOVAL: 114D2119 - RETAINER, 114D2056, 114D2169 - BLOWER DRIVE/DRIVEN GEARS (SEE FIGURES 24, 28 and 29). THE EXCESSIVE WEAR STEP (.065) ON THE 114D2119 RETAINERS WAS APPARENTLY CAUSED BY THE SPINNING OF THE ADJACENT BEARING'S OUTER RACE. THIS PERMITTED THE DRIVE SECTION OF THE ASSEMBLY TO MOVE INWARD, REDUCING THE BACKLASH BETWEEN THE MATING GEARS. THE RESULTANT SPALLING DUE TO POOR CONTACT PATTERN IS NOTED IN THE DISCREPANCIES ASSOCIATED WITH THE 114D2056/2169 GEARS.
AFT A9-1083	EXCESSIVE BACKLASH	396/NEW	114D2184 - RETAINER (4) - FLANGES CRACKED AND WORN 114D2089 - RETAINER - EXCESSIVE WEAR ON RETAINING FACE	SEE REMARKS	BLOWER ASSEMBLY WAS DISASSEMBLED FROM TRANSMISSION PRIOR TO RECEIPT. WHEN REASSEMBLED, THE BACKLASH WAS FOUND TO BE SLIGHTLY OVER SPECIFICATIONS. INTERNAL CONDITION OF THE TRANSMISSION WAS ACCEPTABLE.
AFT A9-1082	EXCESSIVE BACKLASH	528/NEW	114D2184 - RETAINER - FLANGES CRACKED AND WORN 114D2139 - HOUSING (AGB) - .006-IN. WEAR STEP ON BEARING SHOULDER.	SEE REMARKS	SAME AS ABOVE FOR A9-1083

TABLE 4. SUMMARIZATION OF MAJOR TRANSMISSION DISCREPANCIES - CONTINUED

TRANSMISSION SERIAL NUMBER	CAUSE OF REMOVAL	TOTAL TIME/ TSO	DISCREPANCIES FOUND	PART CAUSING REMOVAL	REMARKS
AFT A9-918	FAILURE INDICATED BY SOAP	1510/306	114D2254 - GEAR - TEETH SCUFFED 114D2184 - RETAINER (4) - EXCESSIVE WEAR ON FACE 114D2089 - RETAINER - .003-.015 IN. WEAR STEP ON FACE 114D2119 - RETAINER - .010 IN. WEAR STEP ON FACE 114D2147 - RETAINER - 0-.005 IN. WEAR STEP ON FACE 114D2045 - PINION - SCUFFED TEETH 114D2093 - SHAFT - CLUTCH JOURNAL WORN 114DS281 - PLANET BEARING - ABRASIVE WEAR ON INNER DIAMETER OF GEAR	SEE REMARKS	THE SCUFFING ON THE RING AND PINION GEARS WAS MINIMAL AND REWORKABLE THE NOTED WEAR ASSOCIATED WITH THE NOTED PARTS WAS NOT SIGNIFICANT ENOUGH TO WARRANT THE TRANSMISSIONS REMOVAL ALTHOUGH THEY WERE CAPABLE OF GENERATING A SOAP INDICATION.
AFT A9-1133	SCUFFED PINION AND RING GEARS	1249/849	114D2139 - HOUSING (AGB) - .008-.010 IN. WEAR STEP ON BEARING SHOULDER 114D2192 - LUBRICATOR - SCORING ON BOSSES 114D2073 - RETAINER (4) - .005/.010 IN. WEAR STEP ON FACE 114D2045 - PINION - SCUFFED 114DS281 - PLANET BEARING - SMALL CRACK ON ONE GEAR TOOTH 114D2170 - SUPPORT - LINER WORN .0043 IN. 114D2089 - RETAINER - .006 IN. WEAR STEP ON FACE 114DS265 - BEARING - CAGE DISTORTED 114D2069 - SUPPORT - BEARING SHOULDER WORN .007 IN. 114D2184 - RETAINER (4) - FACES EXCESSIVELY WORN. PIECES BROKEN OFF AT FACE (FIGURE 22) 114D2254 - RING GEAR - SCUFFED 114D2107 - GEAR - .015 IN. WEAR STEP ON SPLINE 114D2167 - HOUSING - OIL TRANSFER PORT WORN .007 IN. 114D2180 - HOUSING - .003 IN. WEAR STEP ON BEARING SHOULDER	114D2045 AND 114D2254 RING AND PINION GEARS	°THIS XMSN WAS REMOVED FROM 1 OF THE IROAN A/C. THE SCUFFED RING AND PINION GEARS WERE DETECTED DURING THE ROUTINE VISUAL INSPECTION WHEN THE INPUT PINION WAS REMOVED FOR GEAR INSPECTION. THE NOTED SCUFFING WAS REWORKABLE. °THE BEARING CAGE DISTORTION WAS CAUSED BY DISASSEMBLY DAMAGE. °THE SMALL CRACK ON THE PLANET GEAR TOOTH WAS APPROX. 1/16 IN. LONG AND APPEARED TO BE A SUPERFICIAL CRACK °THE WEAR NOTED ON REMAINING PARTS WAS ABOVE WHAT IS CONSIDERED TO BE NORMAL. SEE FIGURE 22
AFT A9-871	TIME CHANGE	1212/NEW	114D2045 - PINION - SCUFFED 114D2180 - HOUSING - LINER SCORED 114D2254 - RING GEAR - SCUFFED 114D2184 - RETAINER (4) - WEAR STEP ON FACE 114D2119 - RETAINER - GROOVED ON END FACE	NONE	THE SCUFFING NOTED WAS NOT SEVERE AND WAS REWORKABLE

TABLE 4. SUMMARIZATION OF MAJOR TRANSMISSION DISCREPANCIES - CONTINUED

TRANSMISSION SERIAL NUMBER	CAUSE OF REMOVAL	TOTAL TIME/ TSO	DISCREPANCIES FOUND	PART CAUSING REMOVAL	REMARKS
AFT A9-734	HIGH METAL CONTENT IN OIL	1584/377	114D2139 - HOUSING (AGB) - BEARING SEAT .006 IN. WEAR STEP 114DS274 - BEARING - SPALLED ON INNER AND OUTER RACES (FIGURE 20) 114D2170 - SUPPORT - LINER WORN .004 IN. 114D2184 - RETAINER (4) - EXCESSIVE WEAR ON FACE 114D2113 - TUBE - .010 IN. WEAR STEP ON OUTER DIAMETER	114DS274 BEARING	SEE FIGURE 20
AFT A9-962	EXCESSIVE METAL ON FILTER	304/204	114DS282 - PLANET BEARING - ABRASIVE WEAR ON OUTER DIAMETER OF INNER RACE (1) ROLLER SCORED 114DS281 - PLANET BEARING - SPALLING ON OUTER DIAMETER OF INNER RACE (FIGURE 19) 114D2107 - GEAR - .012-IN. WEAR STEP ON SPLINE 114D2166 - HOUSING - .002 .005 IN. WEAR STEP ON BEARING SEAT 114D2139 - HOUSING (AGB) - .007 IN. WEAR STEP ON BEARING SEAT 114D2089 - RETAINER - .003 IN. WEAR STEP ON FACE	114DS281 BEARING	SEE FIGURE 19
AFT A9-728	METAL ON MAGNETIC PLUG	1499/299	114DS247 - BEARING - CAGE DISTORTED 114D2094 - SUPPORT - DEEP SCORING ON LINERS 114D2091 - GEAR - TEETH GOUGED .025 IN DEEP (FIGURE 27) 114D2063 - GEAR - DEEP GOUGES AND CHIPPING ON GEAR TEETH (FIGURE 26) 114D2089 - RETAINER - .007 IN. WEAR STEP ON FACE 114D2184 - RETAINER (4) - EXCESSIVE WEAR ON FLANGE FACE 114D2180 - HOUSING - .011 IN. WEAR STEP ON BEARING SEAT 114D2147 - RETAINER - .006 IN. WEAR STEP ON FACE 114D2101 - RETAINER - INNER DIAMETER & FACE SEVERELY GOUGED (FIGURE 23)	114D2063 AND 114D2091 GEARS 114D2091 RETAINER	SEE FIGURES 23, 26 AND 27 CAGE DISTORTION WAS CAUSED BY DIS-ASSEMBLY DAMAGE. DISASSEMBLY IN-SPECTION REVEALED THAT THE NUTS THAT RETAINED THE 114D2101 RETAIN-ER WORKED LOOSE AND FELL INTO THE SUMP. THIS PERMITTED THE RETAINER TO EVENTUALLY VIBRATE AWAY FROM THE RETAINING STUDS AND FALL ONTO THE AGB QUILL SHAFT. THE DRIVE SECTION OF THE ASSEMBLY COULD THEN MOVE OUTWARD, CAUSING THE NOTED DAMAGE TO THE 114D2091/2063 GEARS DUE TO INADEQUATE CONTACT PATTERN.
FORWARD A7-896	PITTING - LOWER SPLINES OF SHAFT	610/6	114D1089 - HOUSING - .006 IN. WEAR STEP ON BEARING SEAT 114D2071 - CARRIER - INNER DIA. WORN .004 IN. 114D1088 - HOUSING .008 IN. WEAR STEP ON BEARING SEAT 114D1245 - ROTOR SHAFT - PITTING ON SPLINES	114D1245 ROTOR SHAFT	THE SPLINE PITTING DISCREPANCY ON THE ROTOR SHAFT WAS REPAIRED BY POLISHING. HOWEVER, THE CENTER SPLINES DID EXHIBIT AN EXCESSIVE DEGREE OF CORROSION.

TABLE 4. SUMMARIZATION OF MAJOR TRANSMISSION DISCREPANCIES - CONTINUED

TRANSMISSION SERIAL NUMBER	CAUSE OF REMOVAL	TOTAL TIME/ TSO	DISCREPANCIES FOUND	PART CAUSING REMOVAL	REMARKS
FORWARD A7-878	EXCESSIVE METAL ON FILTER	1420/525	114DS282 - PLANET BEARING - SPALLED ON OUTER DIAMETER OF INNER RACE (FIGURE 18) 114D1064 - RETAINER - .003-.005 IN. WEAR STEP ON FACE. 114DS240 - BEARING - .002 IN. WEAR STEP ON FACE OF INNER RACE 114D1088 - HOUSING - .002 IN. WEAR STEP ON BEARING SHOULDER	114DS282 PLANET BEARING	SEE FIGURE 18
FORWARD A7-827	EXCESSIVE VIBRATION	1274/292	114DS240 - BEARING - .0025 IN. WEAR STEP ON FACE OF INNER RACE 114D1113 - LUBRICATOR - END FACE WORN - .012-.020 IN. 114DS282 - PLANET BEARING - SMALL CHIP ON ONE TOOTH	UNKNOWN	THE SMALL CHIP ON THE PLANET GEAR TOOTH WAS CAUSED BY HANDLING DAMAGE
FORWARD A7-1040	THREADS STRIPPED ON SHAFT CORROSIVE PITTING THROUGHOUT INTERNAL PARTS	485/NEW	114D1113 - LUBRICATOR - FACE WORN .006 IN. 114DS282 - PLANET BEARING - CORROSIVE PITTING ON OUTER DIAMETER OF INNER RACE 114DS281 - PLANET BEARING - CORROSIVE PITTING ON OUTER DIAMETER OF INNER RACE 114D1088 - HOUSING - .004 IN. WEAR STEP ON BEARING SEAT 114D1245 - ROTOR SHAFT - THREAD STRIPPED	114D1245 ROTOR SHAFT	THE ROTOR SHAFT WAS RESTORED TO AN ACCEPTABLE CONDITION BY REWORK OF THE STRIPPED THREADS

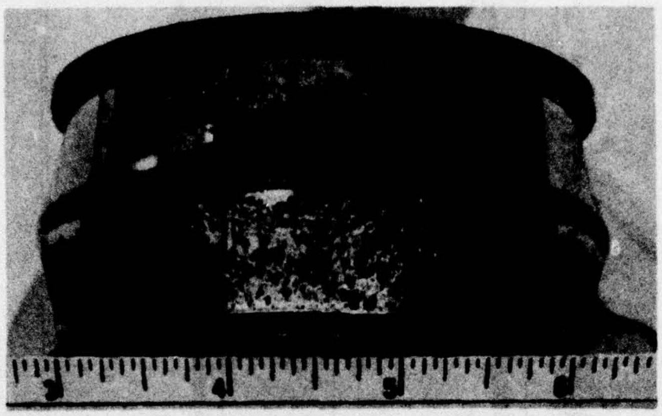

Figure 17. Spalled Inner Race of the 114DS282 Planet Assembly.

Figure 18. Spalled Inner Race of the 114DS282 Planet Assembly.

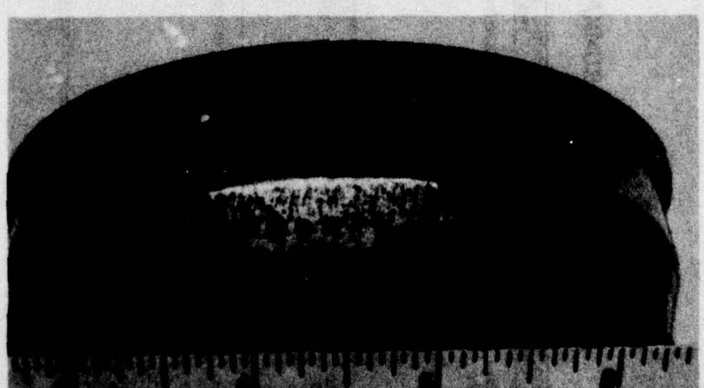

Figure 19. Spalled Inner Race of the 114DS281 Planet Assembly.

SPALLED INNER RACE

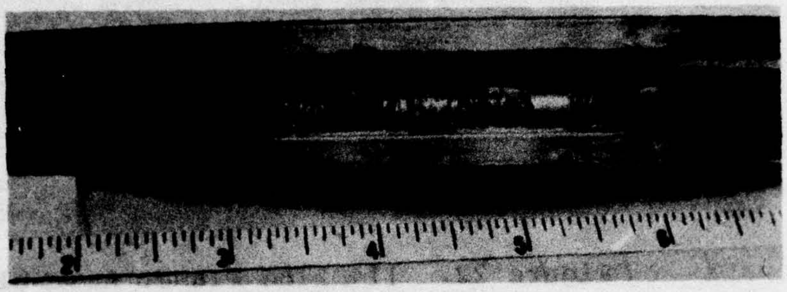

SPALLED OUTER RACE

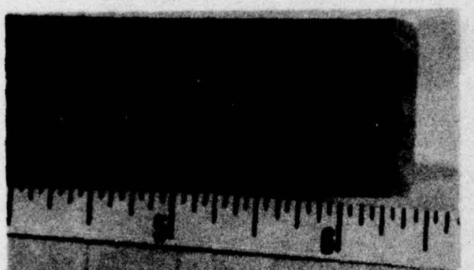

ASSEMBLY

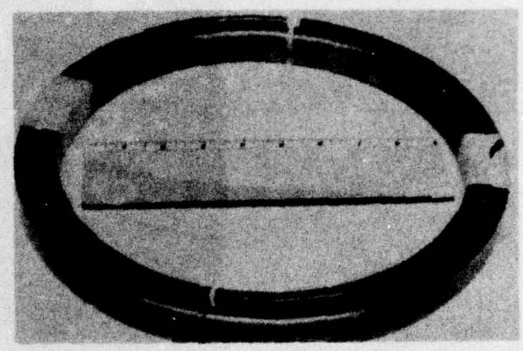

Figure 20. 114DS274 Bearing.

Figure 21. 114DS256 AGB Bearing.

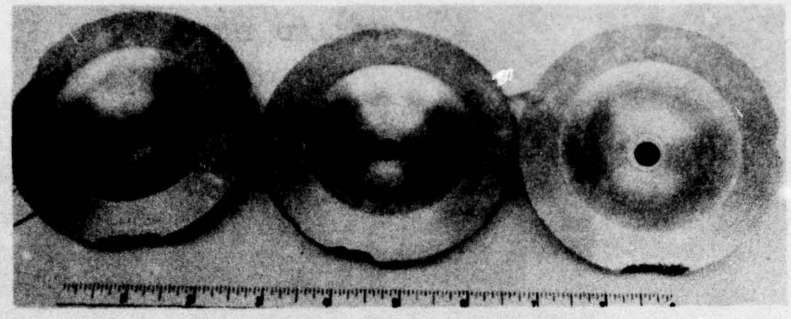

Figure 22. 114D2184 Planet Assembly Retainers.

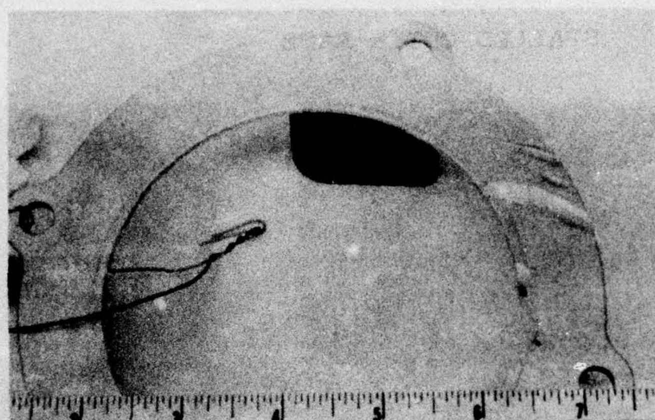

Figure 23. 114D2101 Retainer.

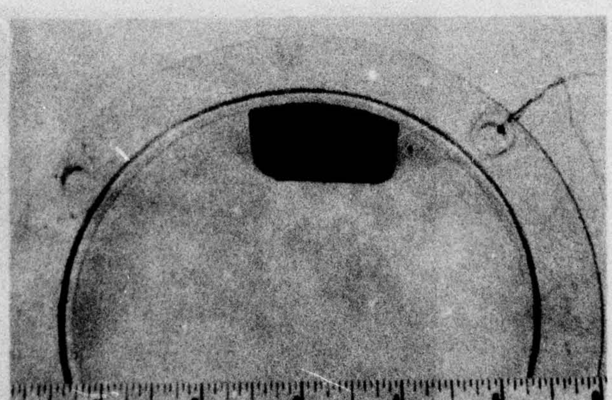

Figure 24. 114D2119 Retainer.

SPALLED INNER RACE

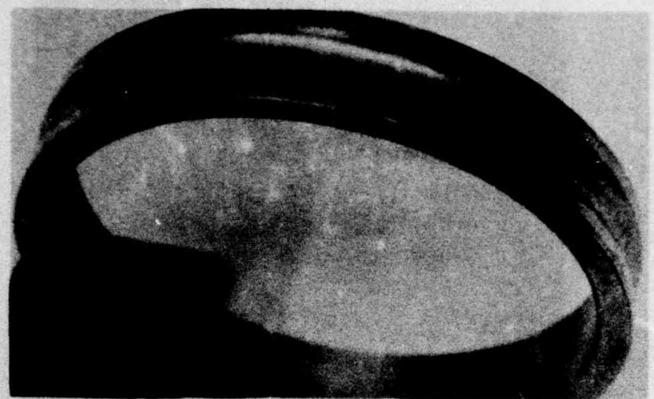

ASSEMBLY

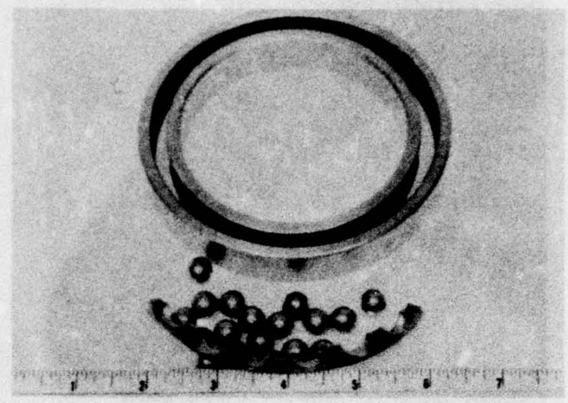

WORN/DISTORTED CAGE
SPALLED ROLLING ELEMENTS

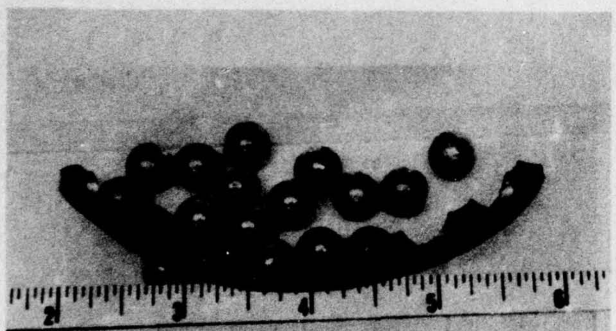

SPALLED OUTER RACE

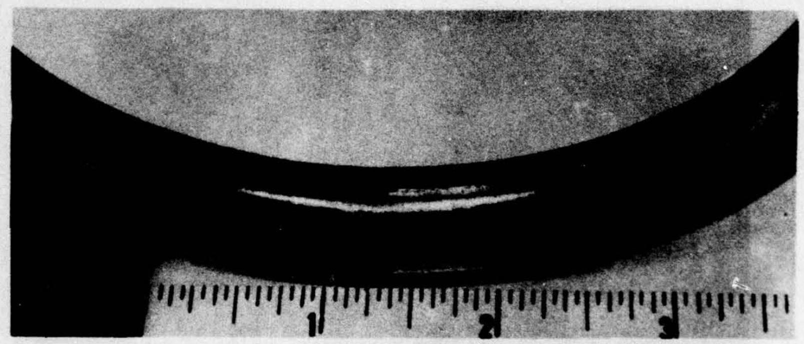

Figure 25. 114DS251 Bearing.

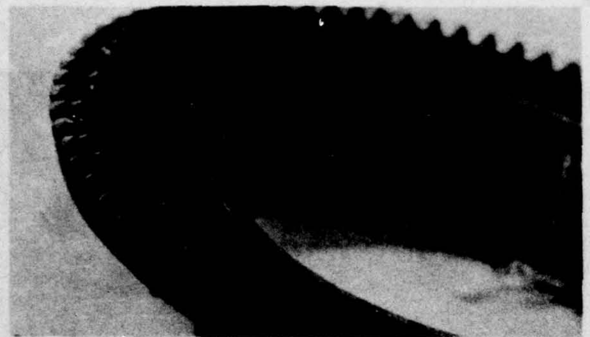

Figure 26. 114D2063 Gear Teeth Damage.

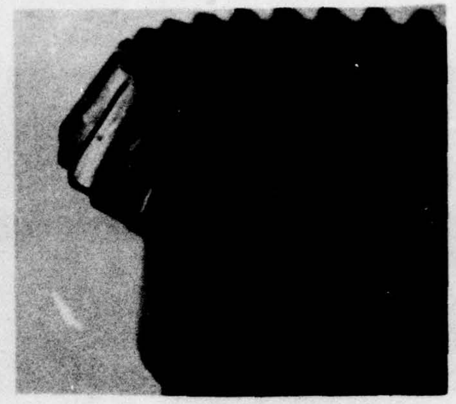

Figure 27. 114D2091 Gear Teeth Damage.

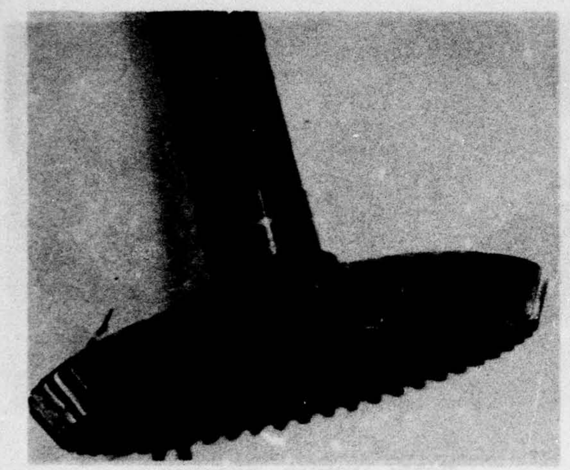

Figure 28. 114D2169 Gear Teeth Spalled.

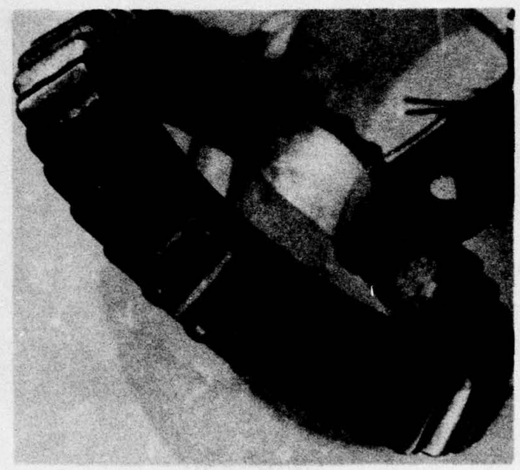

Figure 29. 114D2056 Gear Teeth Spalled.

TABLE 5. CH-47C FORWARD TRANSMISSION BEARING AND GEAR FREQUENCY SPECIFICATIONS

(ROTOR RPM - 223.7)

Bearing Frequency Specifications

PART NUMBER	LOCATION	CAGE f RELATIVE TO INNER RACE	INNER RACE BALL PASS f	BALL SPIN f	BALL DEFECT f	SPHERICAL ROLLER BEARING	CAGE f RELATIVE TO OUTER RACE	OUTER RACE BALL PASS f
114DS160	1ST-STAGE SUN GEAR	37.6	563.7	186.3	372.7	-	27.5	412.8
114DS161	ROTOR SHAFT	2.1	36.5	10.7	21.4	-	1.6	26.9
114DS240	INPUT PINION	66.0	1056.2	362.5	725.0	-	48.4	774.2
114DS262	INPUT PINION	65.0	1299.2	413.7	827.5	-	49.4	988.7
114DS275	2ND-STAGE SUN GEAR	5.4	97.3	51.3	102.6	-	4.5	80.3
114DS281	1ST-STAGE PLANET	20.9	376.9	135.7	271.4	4.7	16.0	288.8
114DS282	2ND-STAGE PLANET	7.0	98.6	32.4	64.8	4.5	4.9	68.9
114DS283	1ST-STAGE SUN GEAR	35.4	1063.2	363.9	727.7	-	29.7	889.8
.14DS284	INPUT, SMALLER DUPLEX	63.7	1400.6	452.7	905.3	-	50.7	1116.2
114DS284	INPUT, LARGER DUPLEX	66.8	934.6	301.4	602.8	-	47.6	667.0

Gear Frequency Specifications

PART NAME	ROTATIONAL SPEED	GEAR MESH f	SWEEP f
INPUT PINION	114.4	3318	-
RING GEAR	65.1	3318	-
1ST-STAGE SUN GEAR	65.1	1442	-
1ST-STAGE PLANET	23.3/37.0	1442	54.4
2ND-STAGE SUN GEAR	13.6/9.86	394	-
2ND-STAGE PLANET	8.24/11.96	394	22.38
2ND-STAGE CARRIER	3.73	-	-

TABLE 6. CH-47C AFT TRANSMISSION BEARING AND GEAR FREQUENCY SPECIFICATIONS

(ROTOR RPM - 217.7)

Bearing Frequency Specifications

PART NUMBER	LOCATION	CAGE f RELATIVE TO INNER RACE	INNER RACE BALL PASS f	BALL SPIN f	BALL DEFECT f	SPHERICAL ROLLER BEARING	CAGE f RELATIVE TO OUTER RACE	OUTER RACE BALL PASS f
114DS240	INPUT PINION	64.2	1027.9	352.8	705.5	-	47.1	753.5
114DS251	INPUT, BLOWER DRIVE	61.0	1098.1	575.0	1149.9	-	50.3	905.9
114DS251	INPUT, BLOWER DRIVE (Contact Angle = 10°)	60.9	1096.7	575.1	1150.2	-	50.4	907.3
114DS252	BLOWER DRIVEN	46.6	419.2	178.3	356.7	-	30.6	275.3
114DS252	BLOWER DRIVEN (Contact Angle = 10°)	46.5	418.1	178.6	357.2	-	30.7	276.4
114DS253	BLOWER DRIVEN	45.3	634.1	215.1	430.2	-	31.9	446.2
114DS256	ACC. GEAR 114D2109	69.6	695.8	303.5	607.0	-	47.7	477.0
114DS256	ACC. GEAR 114D2178/114D2110	40.7	407.0	177.5	355.0	-	27.9	279.0
114DS256	ACC. GEAR 114D2108	60.0	599.2	261.4	522.7	-	41.1	410.8
114DS256	ACC. GEAR 114D2132	34.8	347.9	151.8	303.6	-	23.9	238.6
114DS257	INPUT, BLOWER DRIVE	62.1	1366.9	472.9	945.8	-	49.2	1082.5
114DS262	INPUT PINION	63.2	1264.4	402.6	805.3	-	48.1	962.2
114DS274	2ND-STAGE CARRIER	1.9	59.2	34.9	69.7	-	1.7	53.3
114DS275	SUN GEAR	5.3	94.6	49.9	99.8	-	4.3	78.2
114DS280	1ST-STAGE SUN GEAR	35.1	737.3	252.6	505.2	-	28.2	593.1
114DS281	1ST-STAGE PLANET	20.4	366.7	132.0	264.0	4.7	15.6	281.0
114DS282	2ND-STAGE PLANET	6.8	95.9	31.5	62.9	4.5	4.8	67.0
114DS283	1ST-STAGE SUN GEAR	34.5	1034.6	354.1	708.1	-	28.9	865.9
114DS284	INPUT, SMALLER DUPLEX	62.0	1363.1	440.5	881.0	-	49.4	1086.2
114DS284	INPUT, LARGER DUPLEX	65.0	909.6	293.3	586.6	-	46.4	649.1

Gear Frequency Specifications

PART NAME	ROTATIONAL SPEED	GEAR MESH f	SWEEP f
INPUT PINION	111.3	3228	-
RING GEAR	63.3	3228	-
1ST-STAGE SUN	63.3	1403	-
1ST-STAGE PLANET	22.7/36.0	1403	52.80
2ND-STAGE SUN	13.2/9.6	384	-
2ND-STAGE PLANET	8.02/11.64	384	21.72
2ND-STAGE CARRIER	3.62	-	-
BLOWER DRIVE	111.3	4006.8	-
BLOWER DRIVEN	77.05	4006.8	-
ZEROL, DRIVE	63.4	4689	-
ZEROL, DRIVEN	130.3	4689	-
GEAR AGB (114D2132)	58.8	3647	-
GEAR AGB (114D2109)	117.6	3647	-
GEAR AGB (114D2190)	130.3	3647	-
GEAR AGB (114D2110)	68.9	3647	-
GEAR AGB (114D2178)	68.9	3647	-
GEAR AGB (114D2108)	101.3	3647	-

The analysis process essentially consisted of the following three approaches (given prior data reduction to produce the appropriate PSD plots described above):

1. Comparison of spectra from various acceptable transmissions to determine commonalities and differences (i.e., establishment of the degree of commonality in baseline signatures).

2. Searching for significant spikes at the frequency characteristic of the rotating elements found to be discrepant from the results of the transmission teardown analyses (i.e., inner race ball-pass frequency for a bearing with a spalled inner race or a shaft rotational-speed frequency and harmonics for a gear with spalled teeth).

3. Comparison of signatures obtained with IFD and Endevco accelerometers (subsequenly bandpass-filtered and envelope-detected) to ascertain the degree to which the Endevco accelerometers could detect encountered faults.

DATA REDUCTION OF DEBRIS SIGNATURES

Particle counts on the debris extracted from the oil filters were made at the following levels: 10, 25, 50, 100, 150, 250, 375, 500, 750, 1,000, 1,500, and 2,000 microns. The range from 10 to 150 microns was measured and counted with the millipore PI MC particle measurement computer system (see Figure 30). Particles from 250 to 2,000 microns were visually measured and counted with a microscope.

PI MC Particle Counting Procedure - Particles < 150 Microns

Particles smaller than 150 microns were counted by the following procedure:

1. The total volume of the sample's fluid was measured.

2. The fluid was then hand agitated for a minimum of 1 minute.

3. Three samples were drawn from the fluid with a burett. The volume of the sample extracted was determined by the cleanliness of the fluid. Sample volumes ranged from 10 milliliters for a clean sample to 5 milliliters for a dirty sample. Smaller volumes had to be used with the dirtiest samples to prevent too much debris from being deposited on the millipore filter paper. If this were to occur, the PI MC particle counter would be unable to distinguish between overlapping particles.

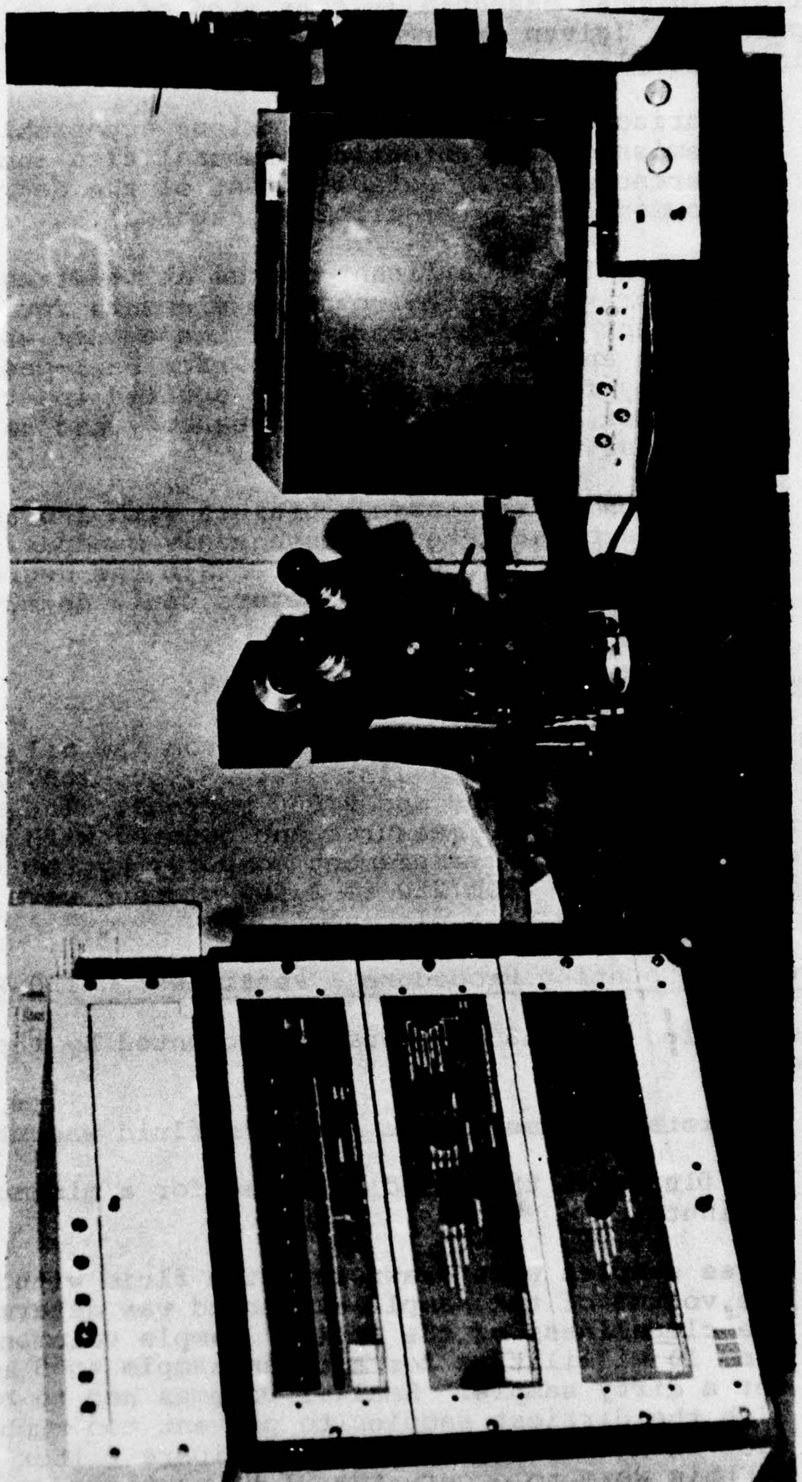

Figure 30. πMC Particle Measurement Computer System.

4. The manufacturer's recommended procedure for the extracted sample's preparation and use with the PI MC counter is listed in Appendix B.

5. Twenty-five fields from each of the three extracted samples were counted. The average of the three samples was used for particle count in each size range.

The filtration area of the millipore filter on which the extracted sample was placed is 9.6×10^8 square micrometers. Since the volume counted, total volume, and measured field areas counted were known, the total particle count could then be derived from the formula:

$$\text{TOTAL PARTICLE COUNT} = \frac{9.6 \times 10^8}{25 \times \text{MEASURED FIELD AREA}} \times \frac{\text{TOTAL VOLUME}}{\text{SAMPLE VOLUME}} \times \text{PI MC COUNT}$$

The millipore PI MC particle measurement computer system utilizes a TV microscope, from which the output from the TV is transmitted to a TV monitor and to a computer that automatically counts and sizes particles in the range selected. The microscope was equipped with a 40X power which magnified the particles projected on the TV monitor. Since a TV monitor can only scan horizontally, the particles were counted by their longest horizontal dimension. The maximum effective size range of this apparatus is 250 microns. Particles greater than 250 microns when magnified and projected onto the TV monitor saturate the field of vision. Another inherent problem with larger particles is that they tend to cover smaller particles which consequently would not be counted and could jeopardize the integrity of the particle counts.

Note: Particles larger than 150 microns were too large to be accurately counted by this statistical technique, and such large particles covered so many smaller particles that small particle counts would have been distorted by the particles larger than 150 microns.

<u>Large Particle Counts (Particles 100 Microns and Greater)</u>

Particles larger than 100 microns were filtered through a sieve. These particles were then placed on a 5-micron millipore filter and weighed. Following the weighing, the millipore filter was placed under a microscope and the particles counted manually. The gravimetric weight and particle counts were individually recorded and logged by transmission serial number. The large particle counts were made in accordance with ARP598; that is, particle size was determined by the longest dimension. (ARP598 describes "A Gravimetric Sampling Procedure for Making a Statistical Particle Count Using A Millipore Filtering System".)

Exceptionally dirty filters which did not provide a homogeneous distribution on the millipore filter were counted by the representative sample procedure described in ARP598. Approximately 20% of the filters analyzed in this program required the representative sample procedure. All particles were counted (i.e., metal, dirt, etc.) in all particle size ranges primarily because the millipore PI MC counter was unable to discriminate particle structure during the counting process.

Problems Encountered

Lint

The presence of lint inhibits automatic or manual counting because metallic particles can be hidden and retained by the lint.

Static Electricity

The movement of fluid has a tendency to create a charge of static electricity, which causes metallic particles to cling together. This problem is realistic in that automatic particle counters cannot distinguish the difference between a single particle and particles that have been grouped together. Manual counting is also inhibited since it is a very difficult task to disperse the particles that have grouped together.

Magnetic Particles

The same condition exists with magnetic particles as is noted above for static electricity.

Problem Impact on Results

Lint

Although lint particles were present in several particle size ranges above 750 microns, visual examination of the debris indicates that the lint particles represent a significant percentage (30% or more) of total counts for particles larger than 2,000 microns. Thus, counts for particles over 2,000 microns could be significantly reduced if lint could be eliminated. However, since lint particles would be "seen" by optical particle counters, and since many small metallic particles tend to adhere to the lint (making it detectable by magnetic chip detectors and indicating screens), the large lint particles may well be indistinguishable from metallic particles through conventional debris monitoring devices.

Particle Conglomerations

Particle conglomerations were minimized by sample agitation prior to making a particle count. However, since conglomeration of particles occurs naturally in a machine, these conglomerates would also be sensed by debris-monitoring devices as single large particles.

ANALYSIS OF ASOAP DATA

The ASOAP analysis performed on the samples taken from the CH-47C transmissions was accomplished at ARADMAC with the Baird Atomic Emission Spectrograph. The results of these analyses were forwarded to Boeing Vertol. A comparison was then made between the ASOAP data and the transmission disassembly data. The results of this comparison are noted in the following section. Twenty elements of the oil samples were analyzed and recorded, by transmission, on the standard oil analysis record D.D EOAPA Form SF-1 (4-71).

RESULTS AND SUMMARY

PHYSICAL TEARDOWN INSPECTION

Based on the results obtained from the teardown inspection, the overhaul transmissions were categorized as either acceptable or unacceptable. Acceptable meant the discrepancies found were minor and that the transmission would be flightworthy for at least 100 additional flight hours, or the failure was of a nature which would not produce debris (such as external leakage or stripped external threads). Unacceptable meant the deterioration found on one or more of the transmission's internal components warranted sufficient consideration to doubt the integrity of the transmission withstanding an additional 100 flight hours.

Based on the data provided in Table 4, the CH-47C transmissions were categorized as either acceptable or unacceptable. Table 7 lists the transmissions by serial number in their appropriate category.

An unacceptable transmission is exemplified in the photographic documentation provided in Figures 17 through 29 in the preceding section. The unacceptable category is not an indication of a catastrophic state, but is only an indication of a failure that should be detected. The acceptable/unacceptable categories were arbitrarily selected as a means of discrimination for the purposes of this program. Admittedly, there will be differences of opinion in what could be called acceptable or unacceptable.

The following conclusions are evident from Table 7:

1. All unacceptable (from a debris-related standpoint) units were detected with the existing diagnostic systems.

2. Of the acceptable units removed for debris-related symptoms (A9-918 for SOAP and A9-1035 for metal on the magnetic plug), both must be considered erroneous removals.

3. Of the acceptable units removed for non-debris reasons, all were considered to be valid removals except for A7-827, which was removed for a vibration symptom.

Of the transmissions itemized in Table 7, there are three debris and vibration data points missing from two CH-47C overhaul transmissions. Forward transmission A7-1040 was incapable of running at loads in excess of 10% because the rotor shaft threads which secure to the torquing mechanism were stripped. Hence, the particle counts derived from this test run were not comparable

TABLE 7. OVERHAUL TRANSMISSION CATEGORIZATION

ACCEPTABLE					UNACCEPTABLE				
TYPE	SERIAL NUMBER	SCHEDULED OR UNSCHEDULED	DEBRIS RELATED	FIELD SYMPTOM	TYPE	SERIAL NUMBER	SCHEDULED OR UNSCHEDULED	DEBRIS RELATED	FIELD SYMPTOM
AFT	A9-871	SCHEDULED			AFT	A9-724	UNSCHEDULED	YES	METAL CONTAM.
AFT	A9-918	UNSCHEDULED	YES	SOAP	AFT	A9-734	UNSCHEDULED	YES	SOAP
AFT	A9-971	UNSCHEDULED	NO	LEAK	AFT	A9-748	UNSCHEDULED	YES	INT. FAILURE
AFT	A9-1035	UNSCHEDULED	YES	MAG PLUG CONTAM.	AFT	A9-856	UNSCHEDULED	YES	INT. FAILURE
AFT	A9-1082	UNSCHEDULED	NO	BACKLASH	AFT	A9-962	UNSCHEDULED	YES	FILTER CONTAM.
AFT	A9-1083	UNSCHEDULED	NO	BACKLASH	AFT	A9-1133	UNSCHEDULED	YES	VISUAL INSP.
FWD	A7-827	UNSCHEDULED	NO	VIBRATION	AFT	A9-1245	UNSCHEDULED	YES	VISUAL-PLAY
FWD	A7-896	UNSCHEDULED	NO	SPLINE PITTING	AFT	A9-728.	UNSCHEDULED	YES	METAL CONTAM.
FWD	A7-1040	UNSCHEDULED	NO	THREADS STRIPPED	FWD	A7-878	UNSCHEDULED	YES	FILTER CONTAM.

with those obtained from the other transmissions. On this same transmission, the sample bottle containing the particles removed from the oil filter prior to the load run was accidentally broken; therefore, this data is not available. Forward transmission A7-896 was found to have water contamination in the sump oil during the examination prior to the load run. The transmission's oil system was flushed prior to the load run. It soon became evident from the excessively high particle counts obtained from the oil filter after this run that the flushing procedure had not been adequate.

DEBRIS RESULTS

Particulate

Total particle counts in the various size ranges noted were made and tabulated by transmission serial number. The results of these particle counts are listed in Table 8 for the unacceptable preoverhaul transmissions and in Table 9 for the acceptable preoverhaul transmissions. The results listed in Tables 8 and 9 were derived from those filters removed after the load runs. Likewise, the results of the particle counts derived from the new transmissions after the load run are tabulated in Table 10. In Tables 8 through 10, all particle counts are from the 1-hour and 45-minute run.

As previously noted, there were four new aft transmissions that utilized two oil filters during the load run. The results of the particle counts after the first 45 minutes and the last hour are listed in Table 11. The particle count results of the oil filters removed from the CH-47C preoverhaul transmission prior to load run (as received from the field) are tabulated in Table 12.

At the beginning of this program it was assumed that 750 microns would be the maximum limit of particle-size analysis. After the first particle counts were received, it became apparent (because of the large number of particles encountered) that the maximum size to be analyzed would have to be increased. Particle counts were then increased to the 2000-micron level. Those transmissions which do not have any particle counts above 750 microns fell into this "early data" category. At approximately the same time that the larger particle size ranges were added, the 200-micron count was dropped to balance the particle counting workload; due to the apparently low significance of this particular analysis point.

TABLE 8. UNACCEPTABLE PREOVERHAUL TRANSMISSION PARTICLE COUNTS AFTER LOAD RUN

TRANSMISSION SERIAL NUMBER	PARTICLE SIZE IN MICROMETERS													WEIGHT (mg)
	10	25	50	100	150	200	250	375	500	750	1000	1500	2000	
A9-856	3.931×10^{6}	1.986×10^{6}	804026	201206	68985	--	8412	3550	1075	376	112	25	0	69
A9-734	3.643×10^{6}	1.412×10^{6}	363524	89124	27860	8400	529	314	124	54	30	24	21	21
A9-1133	6.815×10^{6}	2.033×10^{6}	681822	163939	56691	24264	1039	503	268	80	46	37	31	39
A9-962	1.827×10^{6}	711678	199890	49003	22140	8315	454	152	64	30	24	15	9	11
A7-878	3.742×10^{6}	1.272×10^{6}	319411	95172	34862	4681	422	124	79	43	26	20	17	34
A9-728	3.792×10^{6}	$.804\times10^{6}$	$.16\times10^{6}$	31023	12662	1915	112	42	29	17	- - NOT AVAILABLE - -			18
A9-748	1.473×10^{6}	507694	94356	20458	6223	--	1030	500	388	135	63	9	6	34
A9-1245	2.754×10^{6}	941387	373067	98539	32846	--	1535	1110	337	109	59	25	6	19
A9-724	2.587×10^{6}	1.222×10^{6}	246889	43801	13938	--	1440	815	489	239	158	39	22	155.0

TABLE 9. ACCEPTABLE PREOVERHAUL TRANSMISSION PARTICLE COUNTS AFTER LOAD RUN

TRANSMISSION SERIAL NUMBER	PARTICLE SIZE IN MICROMETERS													WEIGHT (mg)
	10	25	50	100	150	200	250	375	500	750	1000	1500	2000	
A9-971	2.184×10^{6}	850199	244890	69395	23882	--	1911	754	163	66	45	18	5	16.0
A9-1082	$.967\times10^{6}$	446960	62574	21551	10251	--	8008	3595	1131	389	113	18	0	176.0
A9-1035	3.494×10^{6}	1.337×10^{6}	243488	47515	12031	--	1900	804	302	146	46	18	12	27.0
A9-871	1.378×10^{6}	595705	176842	43632	13076	--	574	239	116	42	25	13	9	15.0
A7-827	18.880×10^{6}	6.109×10^{6}	1.922×10^{6}	553500	198414	67650	1097	796	376	206	- - - - - NOT AVAILABLE			78.0
A9-1083	1.288×10^{6}	475752	150317	41871	17267	--	394	191	130	65	22	12	8	10.0
A9-918	1.620×10^{6}	502813	171968	35128	10122	--	755	390	158	45	20	8	3	8.0

TABLE 10. NEW TRANSMISSION PARTICLE COUNTS AFTER LOAD RUN

TRANSMISSION SERIAL NUMBER	PARTICLE SIZE IN MICROMETERS													WEIGHT (mg)
	10	25	50	100	150	200	250	375	500	750	1000	1500	2000	
A9-1367	2.060×10^6	1.180×10^6	$.385 \times 10^6$	102684	38302	--	590	354	170	73	44	8	5	47.0
A7-1422	9.793×10^6	4.305×10^6	1.145×10^6	304636	121581	--	2175	1200	586	196	81	48	24	23
A7-1421	6.447×10^6	2.525×10^6	$.804 \times 10^6$	215968	78010	--	2006	1242	288	90	60	15	1	26
A7-1417	10.143×10^6	4.675×10^6	1.296×10^6	330960	93099	44708	718	334	238	112	68	31	19	48
A9-1330	18.000×10^6	4.493×10^6	$.842 \times 10^6$	143280	39150	23400	591	238	185	129		-- NOT AVAILABLE --		35
A9-1337	22.558×10^6	5.011×10^6	1.506×10^6	195690	78934	20755	408	161	130	66		-- NOT AVAILABLE --		41
A9-1339	15.733×10^6	3.601×10^6	1.050×10^6	361590	136660	57120	1185	478	319	210		-- NOT AVAILABLE --		42
A9-1342	6.412×10^6	1.471×10^6	$.518 \times 10^6$	204516	105329	35568	421	196	158	65		-- NOT AVAILABLE --		29
A7-1408	12.476×10^6	3.055×10^6	1.219×10^6	330809	125463	67298	2379	891	397	205		-- NOT AVAILABLE --		73
A7-1418	7.570×10^6	4.869×10^6	1.957×10^6	512384	182922	--	3600	1204	502	191	92	31	3	58
A9-1349	4.962×10^6	3.171×10^6	1.256×10^6	287721	70600	--	2390	858	514	241	130	55	23	51
A9-1340	8.440×10^6	5.095×10^6	1.958×10^6	744978	347522	--	7518	1624	455	65	0	0	0	130
A9-1341	5.336×10^6	2.695×10^6	$.790 \times 10^6$	250093	91943	--	2040	800	496	188	75	37	7	45
A7-1423	7.246×10^6	2.830×10^6	$.910 \times 10^6$	252890	96054	--	2270	1625	489	167	57	35	4	25

TABLE 11. NEW TRANSMISSION PARTICLE COUNTS AFTER LOAD RUN (DUAL FILTER INSTALLATION)

TRANSMISSION SERIAL NUMBER	PARTICLE SIZE IN MICROMETERS													WEIGHT (mg)
	10	25	50	100	150	200	250	375	500	750	1000	1500	2000	
A9-1373	5.416×10^6	2.857×10^6	$.786 \times 10^6$	190498	66030	--	802	408	145	58	23	3	1	20
A9-1368	3.636×10^6	1.822×10^6	$.523 \times 10^6$	170102	69911	--	696	373	179	75	30	3	0	11
A9-1355	4.659×10^6	1.718×10^6	$.648 \times 10^6$	221941	95454	--	1510	537	262	157	62	18	10	29
A9-1376	8.814×10^6	3.921×10^6	$.848 \times 10^6$	166209	54588	--	2772	1152	637	180	80	25	15	50
PARTICLE COUNTS AFTER FIRST 0:45 MINUTES OF LOAD RUN														
A9-1373	1.960×10^6	693314	103957	26997	12296	--	130	73	44	22	5	1	1	11
A9-1368	1.606×10^6	541779	66104	12578	4774	--	115	66	39	16	5	2	1	1
A9-1355	1.169×10^6	326826	77172	19142	7052	--	837	288	150	46	30	11	9	6
A9-1376	1.656×10^6	581622	69164	16135	6405	--	95	29	19	5	1	0	0	3
PARTICLE COUNTS AFTER LAST HOUR OF LOAD RUN														

TABLE 12. PREOVERHAUL TRANSMISSION PARTICLE COUNTS PRIOR TO LOAD RUN

TRANSMISSION SERIAL NUMBER	PARTICLE SIZE IN MICROMETERS 10	25	50	100	150	200	250	375	500	750	1000	1500	2000	WEIGHT (mg)
							UNACCEPTABLE TRANSMISSIONS							
A9-856	$3.942x10^6$	$2.957x10^6$	$1.353x10^6$	418775	120089	--	743	407	272	170	78	13	6	288
A9-734	$27.984x10^6$	$8.031x10^6$	$2.430x10^6$	218120	24096	17340	394	158	92	47	-- NOT	AVAILABLE	--	49
A9-1133	$1.698x10^6$	726246	204840	64454	27292	--	1230	365	148	59	37	6	3	10
A9-962	$2.392x10^6$	646944	106398	31510	10810	4554	108	43	26	10	7	6	5	5
A7-878	$2.763x10^6$	578435	75660	12186	4498	2023	407	92	27	14	9	7	6	8
A9-728	$1.737x10^6$	500956	99425	28566	1125	5383	388	86	37	13	9	6	4	5
A9-748	$4.857x10^6$	$2.208x10^6$	841065	253485	108340	--	5750	2855	915	154	45	17	4	165
A9-1245	$4.018x10^6$	$1.836x10^6$	439033	85104	35340	--	2270	1172	590	193	82	45	18	76
A9-724	473804	112961	36999	11233	2885	--	231	144	99	50	31	14	6	23
							ACCEPTABLE TRANSMISSIONS							
A9-971	$5.645x10^6$	$3.822x10^6$	$1.625x10^6$	511232	201364	--	22715	11357	4180	1686	825	421	146	385
A9-1082	$3.181x10^6$	953502	153294	16276	7102	--	1876	531	132	64	39	26	10	19.0
A9-1035	$14.797x10^6$	$10.138x10^6$	$3.712x10^6$	620380	106890	--	14270	5310	3260	520	150	50	10	230.0
A9-871	$2.342x10^6$	699138	156384	42768	11124	2808	361	129	48	21	11	8	6	6
A7-827	$1.117x10^6$	563440	189923	50964	17631	10480	521	315	168	70	47	29	21	51
A7-896	$2.041x10^6$	$1.199x10^6$	517229	109053	35106	--	1192	498	220	105	67	20	0	36
A9-1083	63997	33479	21299	6542	2862	--	731	280	133	40	33	15	9	5.0
A9-918	$3.756x10^6$	$1.649x10^6$	35111	87032	30998	--	2985	2238	507	207	106	59	29	26

DEBRIS SUMMARY

From the debris data in Table 8 and 9, a comparison was made to establish the difference between an acceptable versus an unacceptable transmission. This comparison was accomplished by plotting the relationship between the size of the particles and the number of particles. Figures 31 through 34 illustrate the plots made using basic least-squares regression. Figures 31 and 33 are the regression plots from 10 to 250 micrometers and Figures 32 and 34 are the regression plots from 250 to 2,000 micrometers. Overlays of these regression plots are illustrated in Figures 35 and 36. In Figure 35 (10-250 micrometers) it is evident that the difference between an acceptable and an unacceptable transmission is impossible to distinguish since the two lines almost overlap. However, in Figure 36 (250-2000 micrometers) there is a significant difference between acceptable and unacceptable transmissions starting at approximately 700 micrometers, with the difference increasing up to the 2000-micrometer range.

Least-squares regression plots, Figures 37 and 38, were made for the new transmissions from the debris data noted in Table 10. Figure 37 plots the 10- to 250-micrometer range and Figure 38 the 250- to 2000-micrometer range. These plots are also illustrated in Figures 35 and 36, together with the acceptable and unacceptable preoverhaul regression plots. It should be noted that the new transmission particle counts in the size ranges below 250 micrometers are significantly higher than those of the preoverhaul transmissions. This is primarily attributable to the normal wear-in associated with new transmissions. The particle counts from the larger size ranges, greater than 250 micrometers, are relatively consistent with those of the preoverhaul transmissions; however, it is expected that these counts will also drop after wear-in has occurred. This assumption is based on the particle counts derived from the dual filter installation on new transmissions (Table 11). The particle counts after the last hour of the load run were significantly lower than those collected after the first 45 minutes of the load run. The exact position of the new transmissions regression line after cleanup cannot be defined due to dissimilar durations and load settings. It is expected to fall below the line for acceptable preoverhaul transmissions. An extension to the load run time of the new transmission would have been desirable; however, scheduling, cost limitations, and contractual authority restricted any additional running time or filter replacements.

Unfortunately, the historical field data associated with oil filters removed from the preoverhaul transmissions prior to load run was not available. The number of particles per the interval could not be established. Therefore, any comparisons or conclusions that could be derived from the debris from these filters

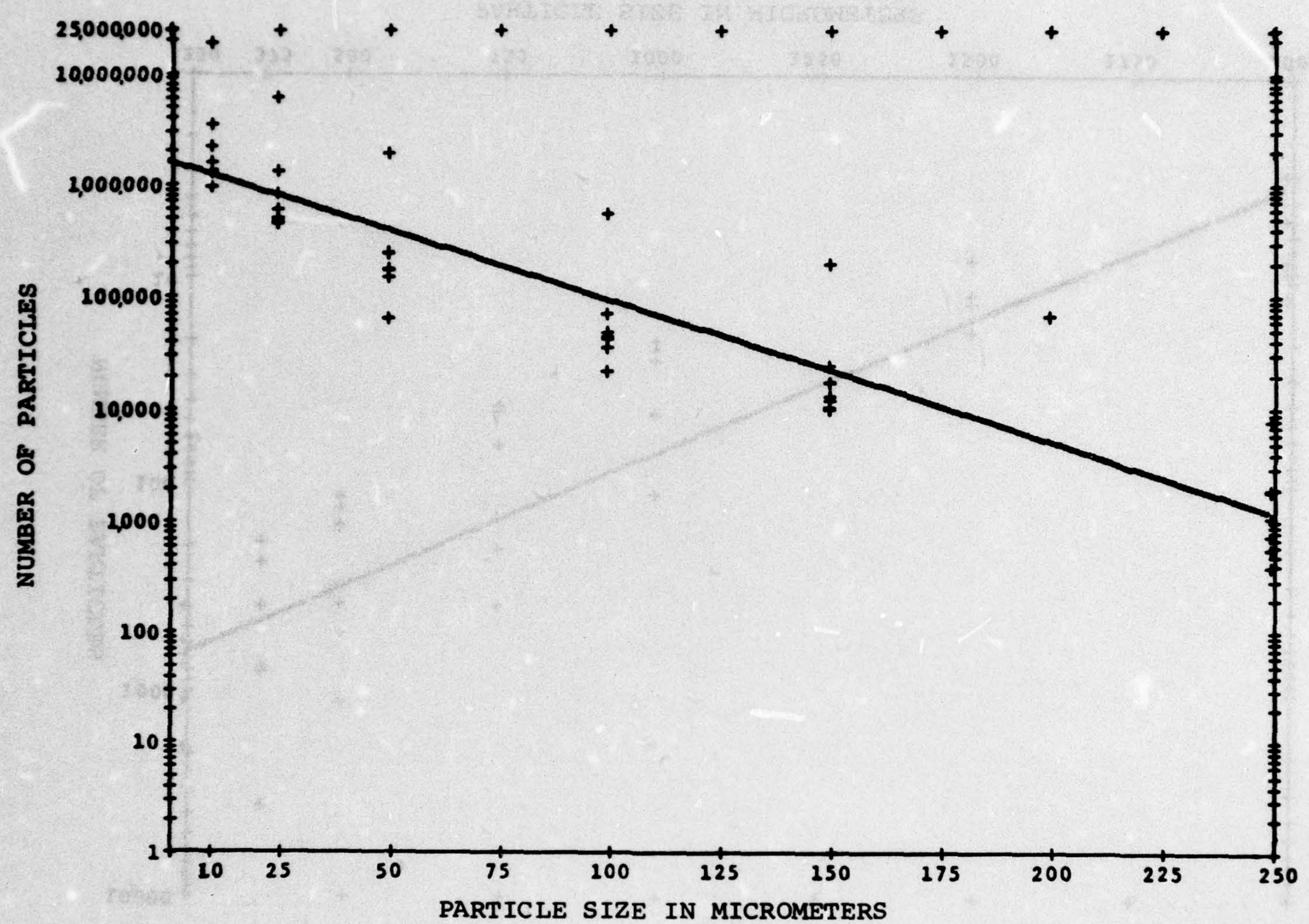

Figure 31. 10- to 250-Micrometer Least-Squares Regression Plot for Acceptable Preoverhaul Transmissions.

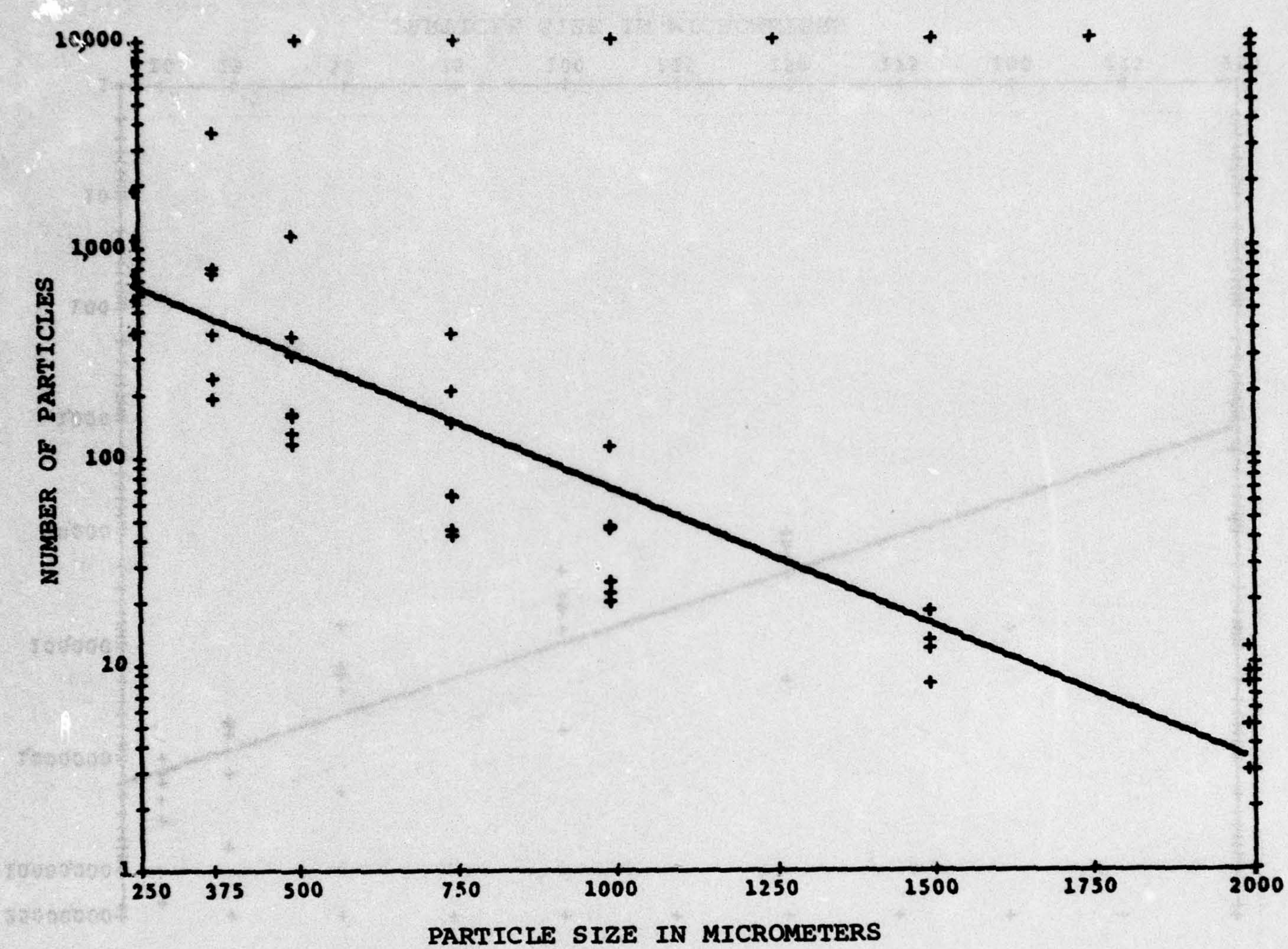

Figure 32. 250- to 2000-Micrometer Least-Squares Regression Plot for Acceptable Preoverhaul Transmissions.

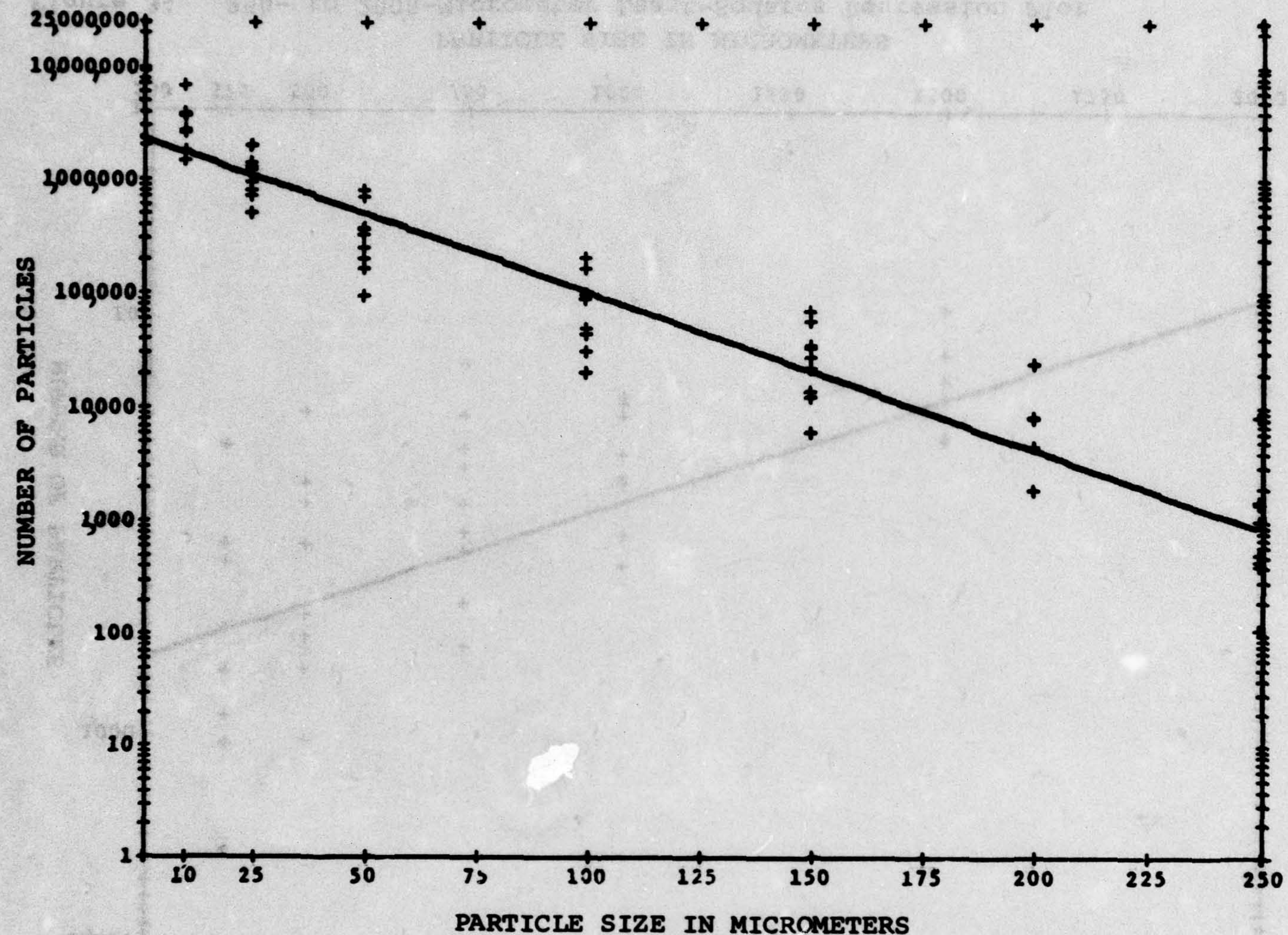

Figure 33. 10- to 250-Micrometer Least-Squares Regression Plot for Unacceptable Preoverhaul Transmissions.

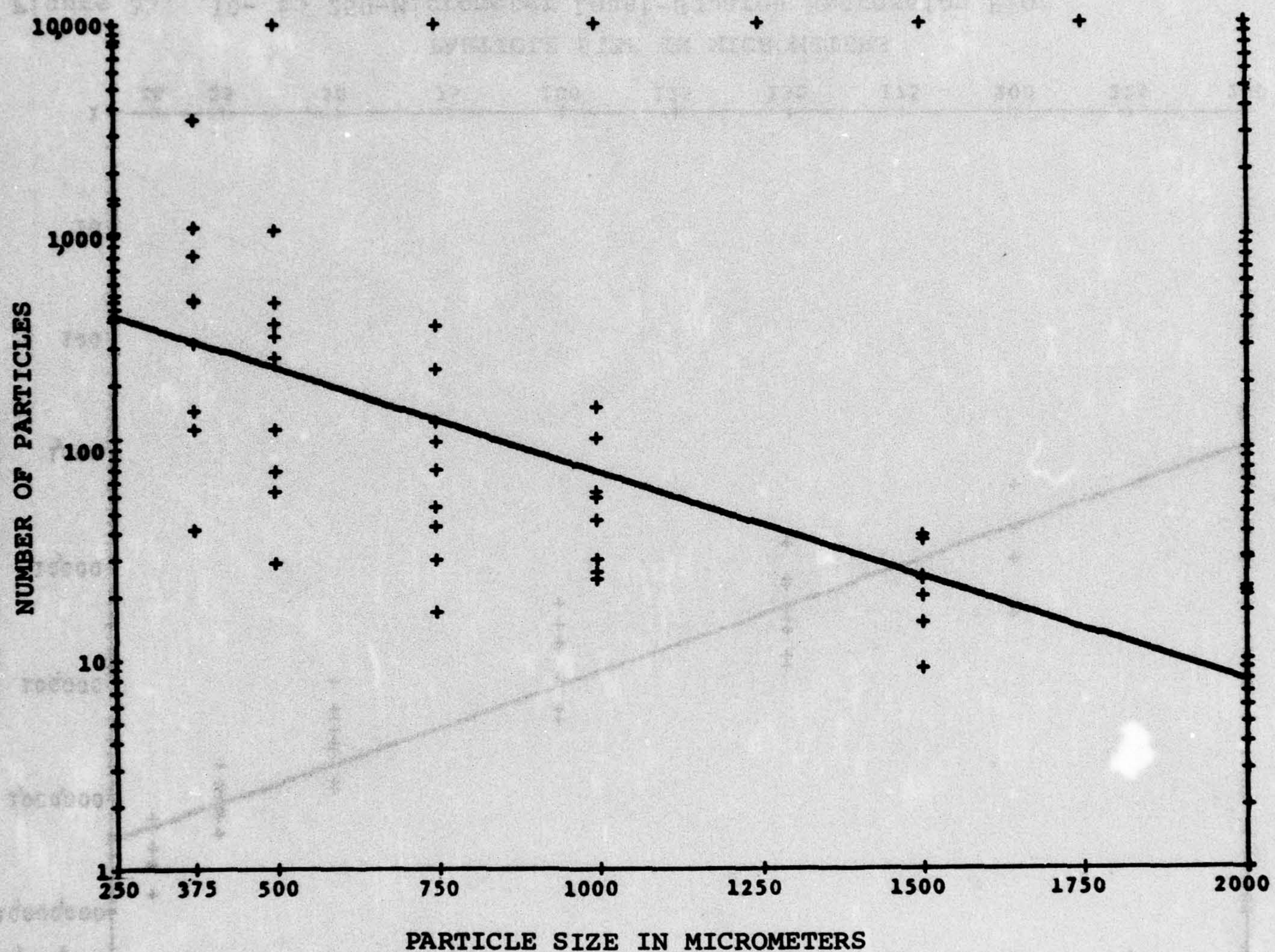

Figure 34. 250- to 2000-Micrometer Least-Squares Regression Plot for Unacceptable Preoverhaul Transmissions.

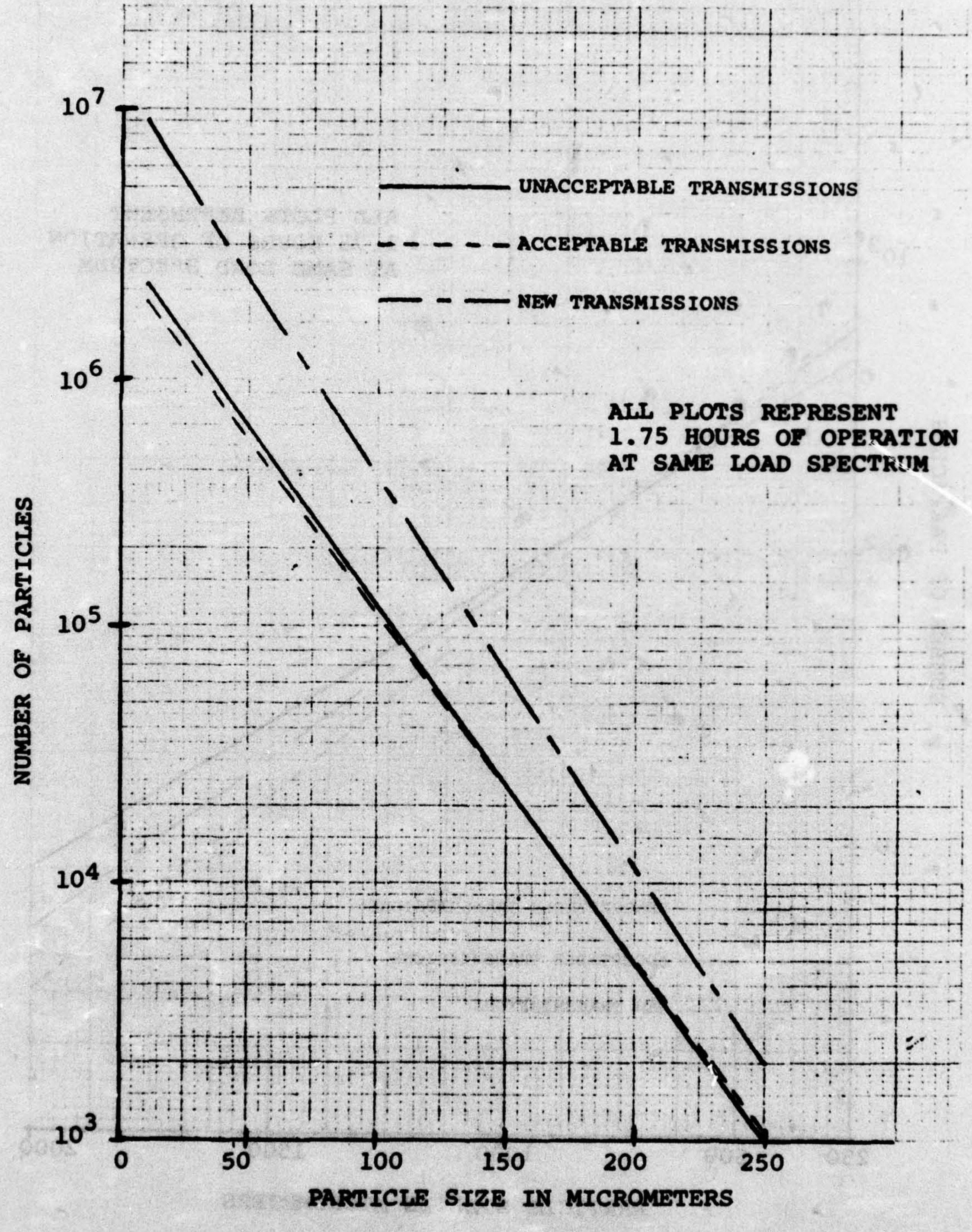

Figure 35. 10- to 250-Micrometer Overlay of Regression Plots.

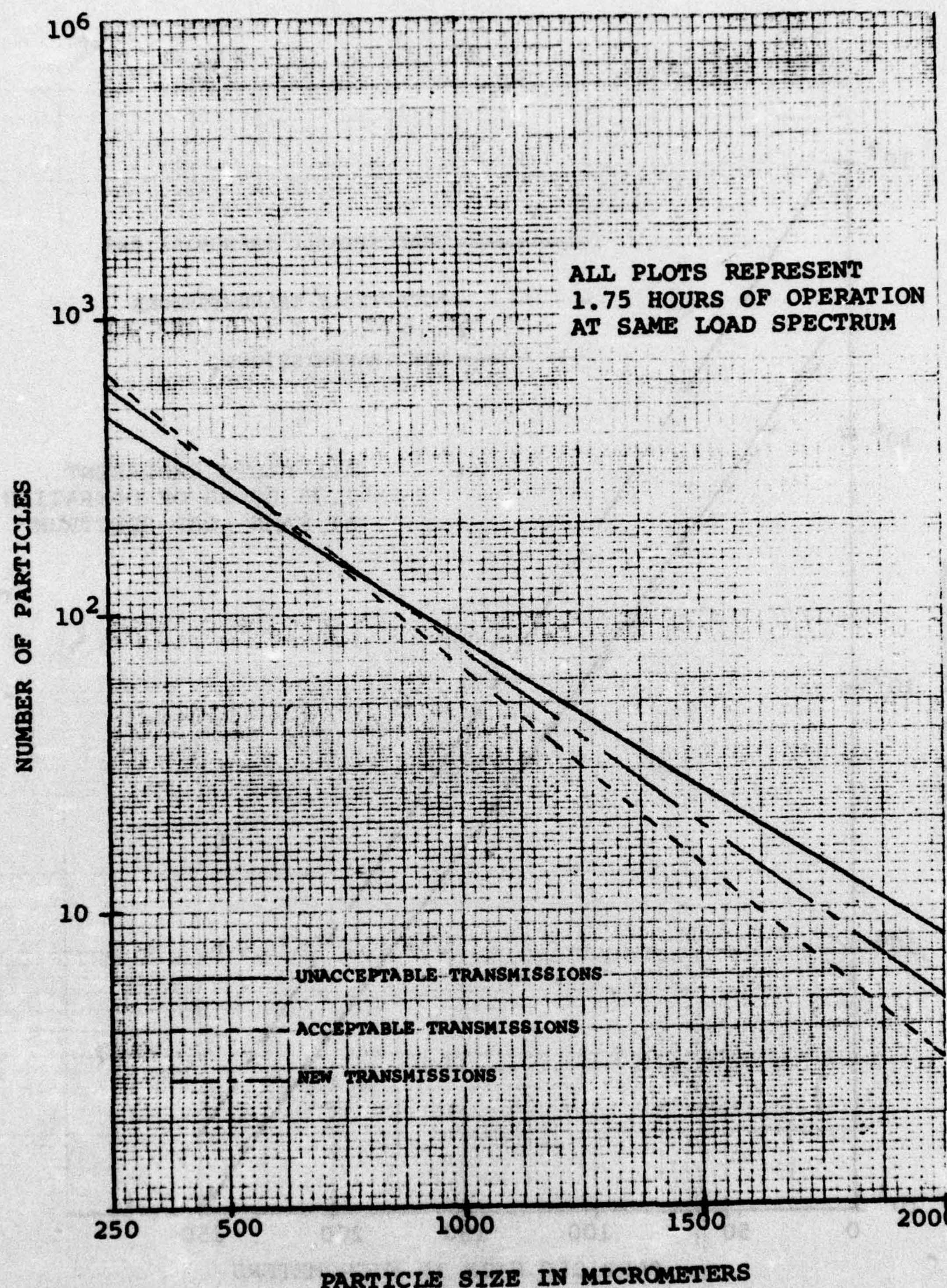

Figure 36. 250- to 2000-Micrometer Overlay of Regression Plots.

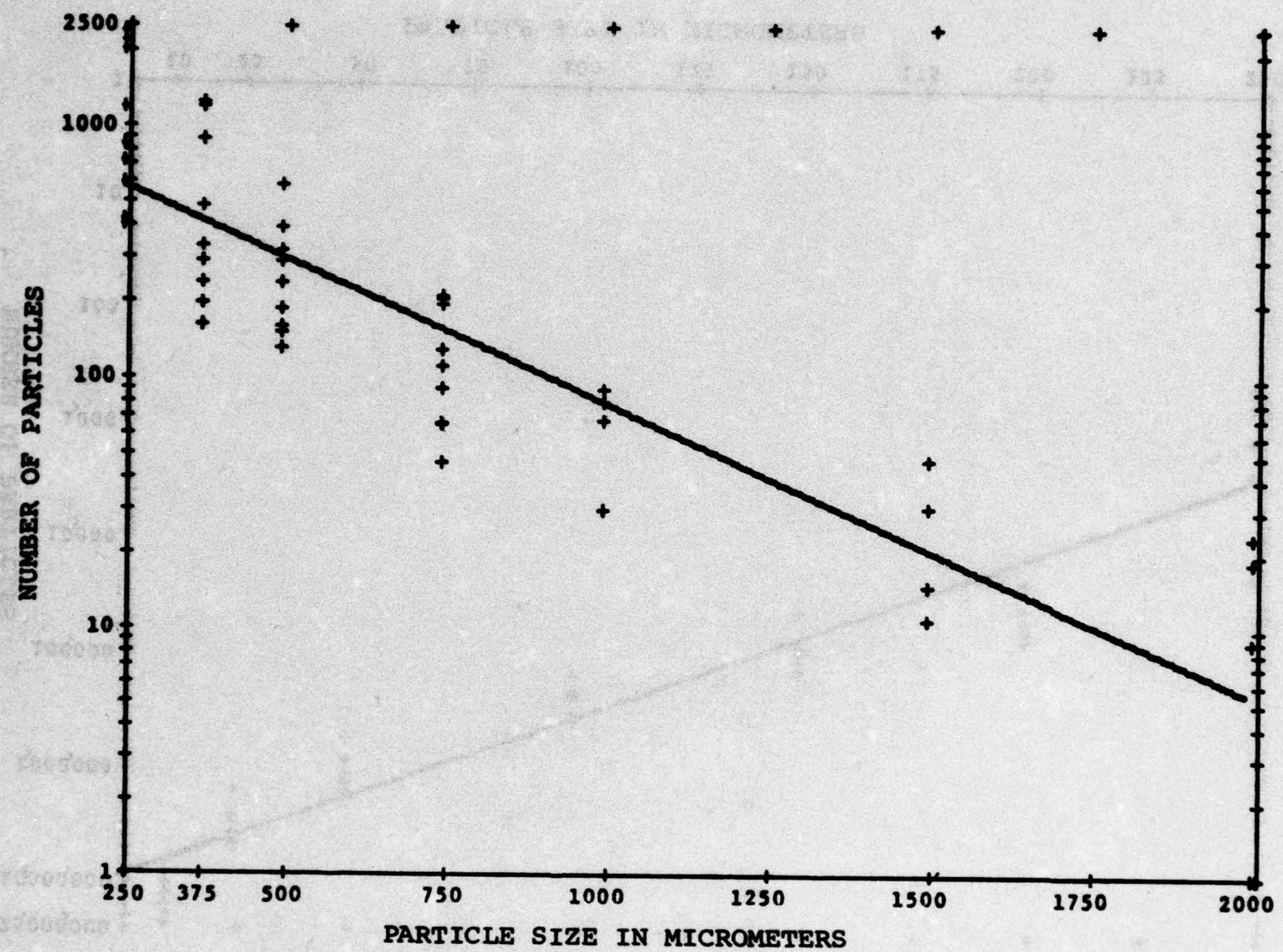

Figure 37. 250- to 2000-Micrometer Least-Squares Regression Plot for New Transmissions

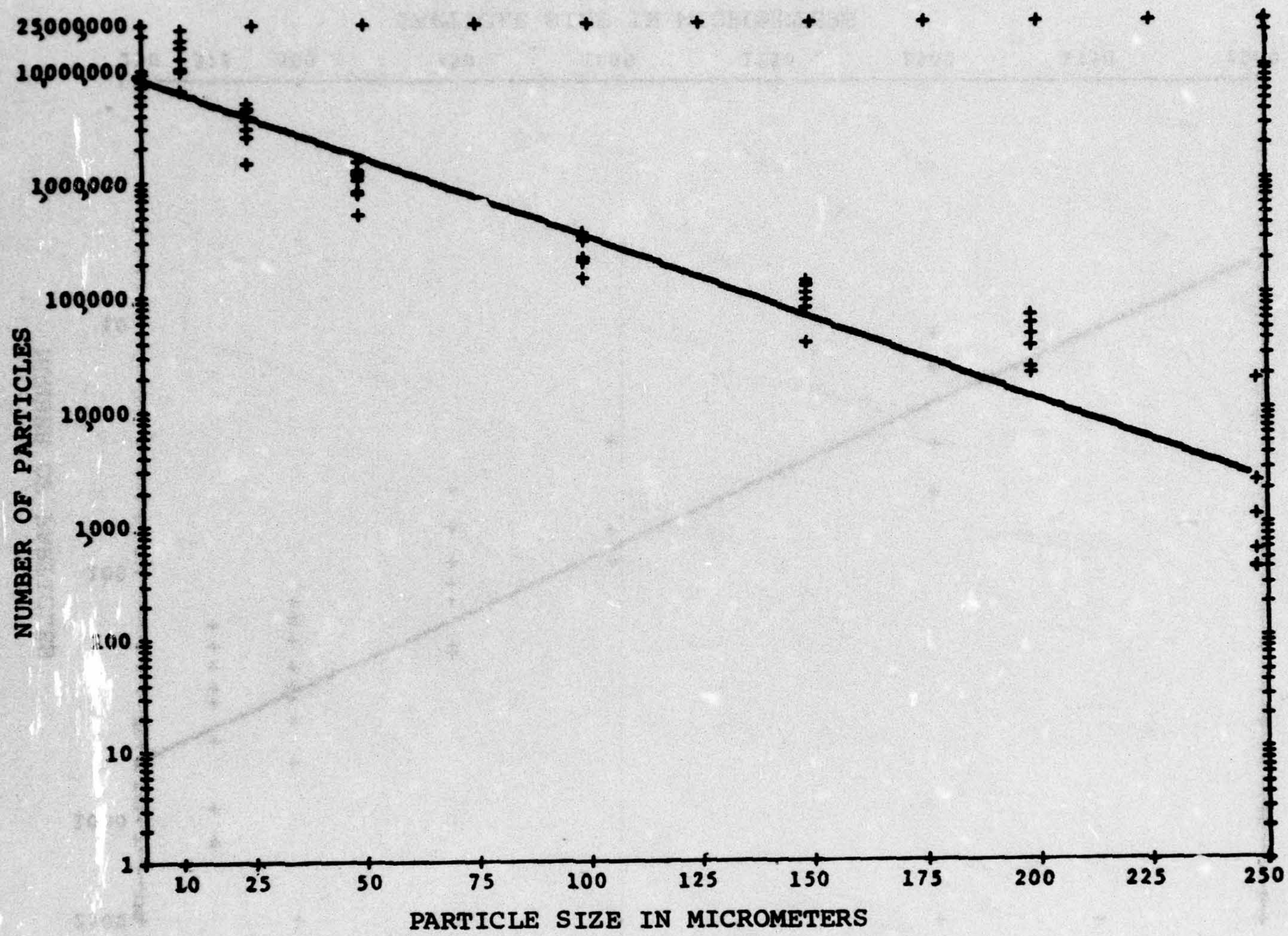

Figure 38. 10- to 250-Micrometer Least-Squares Regression Plot for New Transmissions.

cannot be accomplished at this time. In the event this data becomes available, it can readily be utilized with the particle counts listed in Table 12 for an additional, and perhaps more meaningful, analysis.

Figure 39 is a standard deviation plot indicating the ±1-sigma distributions from 750 to 2,000 micrometers for the acceptable and unacceptable transmissions. The 1,500-micrometer range has the minimum overlap and would provide the highest confidence point in predicting a transmission's acceptability or unacceptability. The ±1-sigma calculations in addition to the mean for the 1,500-micrometer range are listed in Table 13.

TABLE 13. 1,500-MICROMETER RANGE STANDARD DEVIATION CALCULATIONS FOR ACCEPTABLE/UNACCEPTABLE PREOVERHAUL TRANSMISSIONS

	NUMBER OF PARTICLES IN 1.75-HOUR EXPOSURE			
TRANSMISSION CONDITION	MEAN	+1-SIGMA	-1-SIGMA	STANDARD DEVIATION
ACCEPTABLE	14.50	18.68	10.32	4.18
UNACCEPTABLE	24.25	34.37	14.13	10.12

Based on the calculations from Table 13, the cumulative normal distribution lines for the acceptable and unacceptable transmissions were plotted (Figure 40). The intention of the cumulative normal distribution line is to provide some insight into the selection of a particle count threshold and the associated confidence level with which this selection would discriminate between good and bad transmissions. This curve then can be used on a selected particle count threshold to determine the probability that an acceptable transmission would be called acceptable and an unacceptable transmission would be called unacceptable. The compliment or probability of calling an acceptable transmission unacceptable and vice versa can also be determined from this plot. The cumulative normal distribution views the entire CH-47C transmission population based on the available data. Figure 40 can be used as follows:

1. Assuming 18 particles to be the particle count threshold, then

2. The probability of calling an unacceptable transmission unacceptable is 73%, and 27% for calling this transmission acceptable.

3. The probability of calling an acceptable transmission acceptable is 78%, and 22% for calling this transmission unacceptable.

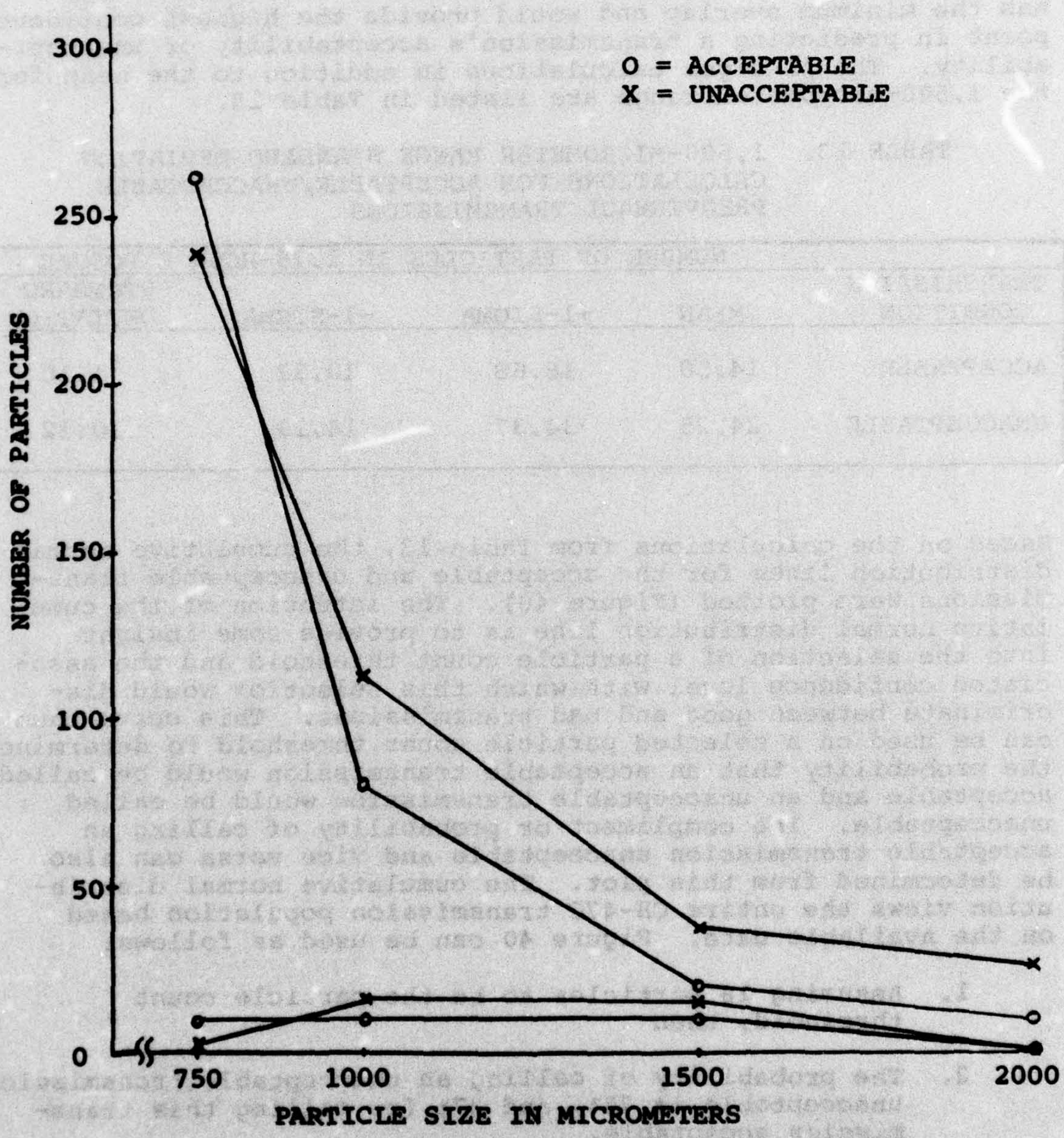

Figure 39. Standard Deviation 1-Sigma Plots for Acceptable and Unacceptable Preoverhaul Transmissions.

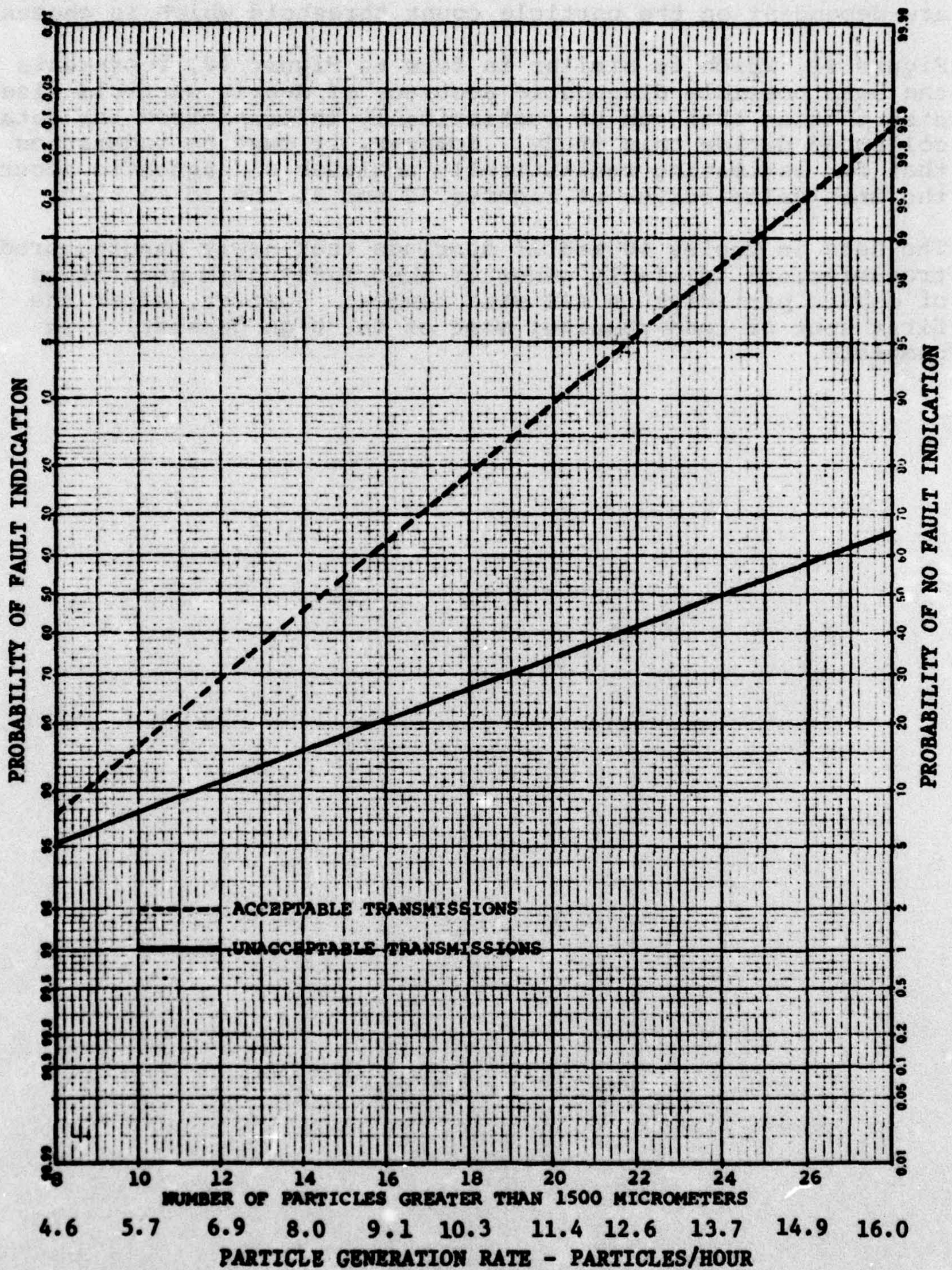

Figure 40. Cumulative Normal Distribution.

Hence, the confidence levels for each of the variables involved are dependent on the particle count threshold which is chosen.

Figure 41, which is similar in form to Figure 40, represents the best possible diagnostic accuracy of debris particle size distribution that can be statistically inferred from the data collected during this study. However, it must be understood that for estimating realistically achievable diagnostic accuracy, the mean value curves of Figures 40 and 41 should be used.

The data in Tables 10 and 11 conclude that newly manufactured transmissions initially generate abnormally high quantities of debris particles in all size ranges. However, after the first hour of load running, most of the high generation is complete.

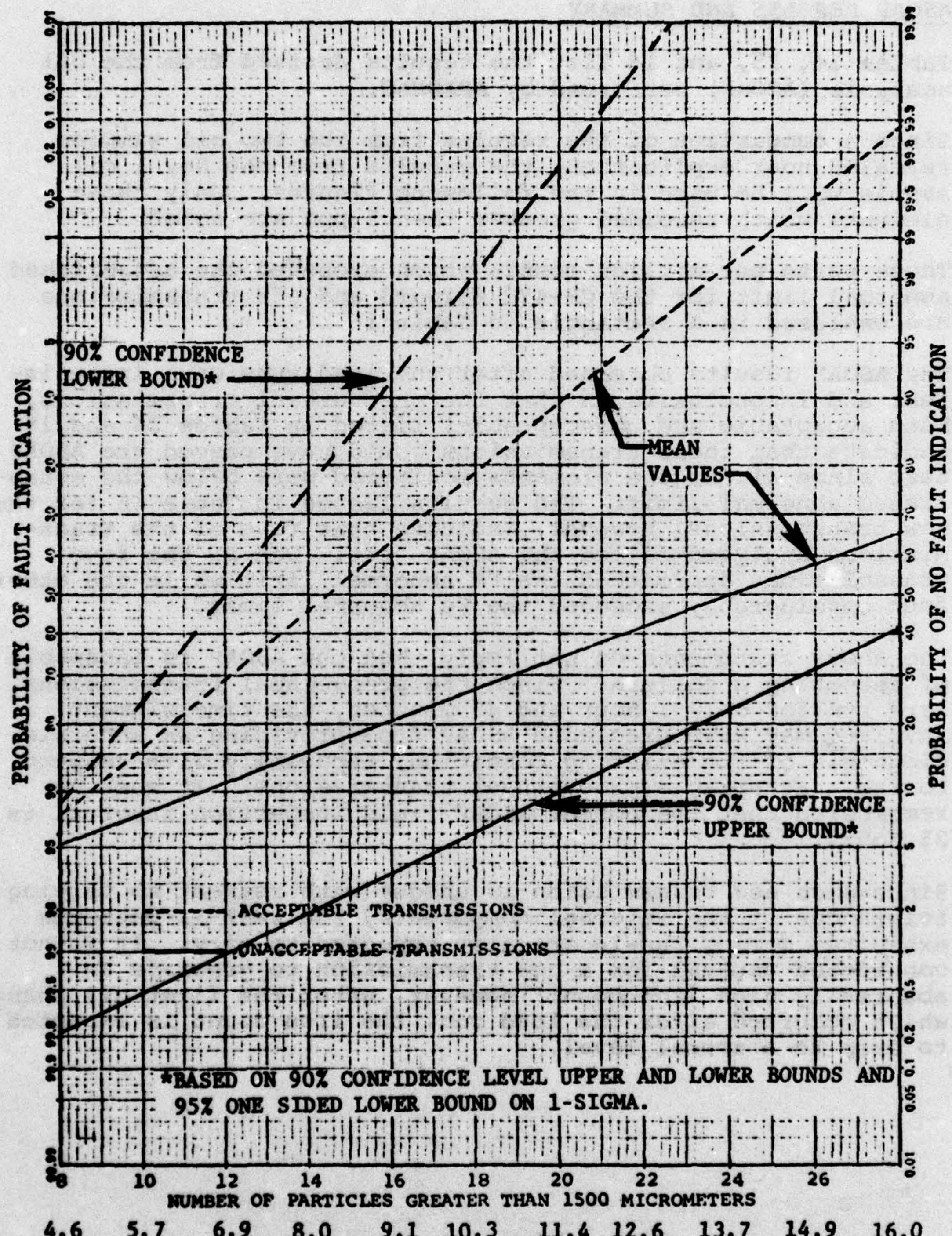

Figure 41. Cumulative Normal Distribution.

ASOAP RESULTS AND SUMMARY

Tables 14, 15, and 16 list the results derived from the oil analysis (ASOAP) performed by ARADMAC.

Since a comparison of the results from the two oil samples revealed near duplication, the results from the No. 1 oil sample will be used in the following figures. Only those elements which recorded greater than 5 ppm are noted.

Those parts per million counts which exceeded the established abnormal limit for the CH-47C forward and aft transmissions are enclosed in a rectangle in Table 16.

The ASOAP results obtained after the load runs were inconsistent and inconclusive in that the preoverhaul transmissions, both acceptable and unacceptable, listed in Tables 14 and 15 indicate that these transmissions would have passed the ASOAP test since all of the elements monitored were below the established abnormal limit. The results listed in Table 16 for the new transmissions, however, indicate that five of the transmissions analyzed failed the ASOAP test. One of the five transmissions approached the Fe abnormal limit while the other four considerably exceeded the Fe abnormal limit.

The above statements do not imply that the ASOAP is incapable of detecting a failure. Since the preoverhaul transmissions were run for only 1 hour and 45 minutes, the time element involved may have precluded ASOAP from providing an accurate diagnosis of the existing condition, especially with respect to the unacceptable preoverhaul transmissions. It must be remembered that the normal ASOAP field inspection interval is 25 hours.

Since each new transmission is unique with respect to varying tolerances of the internal components, the wear-in patterns exhibited during run-in are also expected to vary. It is not considered unusual for a new transmission to generate an abnormally high iron count; however, after the first oil change, which occurred after the load run, the iron count is expected to drop to a normal level.

TABLE 14. UNACCEPTABLE PREOVERHAUL TRANSMISSIONS ASOAP RESULTS

TRANSMISSION SERIAL NUMBER	ABNORMAL=106 Fe ppm	ABNORMAL=16 Ag ppm	ABNORMAL=58 Mg ppm	ABNORMAL=31 Si ppm	ABNORMAL=UNK Sn ppm
A9-856	26	2	0	4	5
A9-734	35	2	0	7	12
A9-1133	51	5	2	4	10
A9-962	27	3	0	3	13
A7-878	69	9	5	11	9
A9-728	25	3	0	3	11
A9-748	20	2	1	3	5
A9-1245	36	3	1	7	6
A9-724	29	3	0	5	7
AVERAGE	35	4	1	5	9

TABLE 15. ACCEPTABLE PREOVERHAUL TRANSMISSIONS ASOAP RESULTS

TRANSMISSION SERIAL NUMBER	ABNORMAL=106 Fe ppm	ABNORMAL 16 Ag ppm	ABNORMAL=58 Mg ppm	ABNORMAL=31 Si ppm	ABNORMAL=UNK Sn ppm
A9-971	30	2	1	6	7
A9-1082	16	0	0	4	7
A9-1035	46	4	0	5	7
A9-871	60	5	2	6	6
A7-827	43	4	4	3	8
A7-896	99	11	7	5	11
A9-1083	16	0	0	3	7
A9-918	24	1	0	3	6
A7-1040	76	6	2	3	10
AVERAGE	45	4	2	4	8

TABLE 16. NEW TRANSMISSIONS ASOAP RESULTS

TRANSMISSION SERIAL NUMBER	ABNORMAL=106 Fe ppm	ABNORMAL=16 Ag ppm	ABNORMAL=58 Mg ppm	ABNORMAL=31 Si ppm	ABNORMAL=UNK Sn ppm
A9-1367	54	5	1	4	0
A7-1422	$\boxed{105}$	11	2	10	7
A7-1421	$\boxed{137}$	13	3	7	7
A7-1417	91	10	2	6	5
A9-1330	36	2	0	4	11
A9-1337	70	7	0	7	10
A9-1339	80	6	1	4	8
A9-1342	79	6	2	5	7
A7-1408	$\boxed{137}$	13	2	7	10
A7-1418	$\boxed{141}$	12	3	7	7
A9-1349	67	5	1	11	6
A9-1348	78	8	2	6	6
A9-1341	79	7	2	14	11
A9-1423	$\boxed{118}$	12	3	7	6
A9-1373*	47	4	1	4	0
A9-1368*	60	4	2	5	0
A9-1355*	63	5	1	5	6
A9-1376*	52	5	0	6	11

$\boxed{}$ - Indicates that the transmission ppm count approached or exceeded the abnormal limit.

* - Sample taken during 2nd hour or running after filter replacement (dual filter installation).

VIBRATION ANALYSIS RESULTS

As previously mentioned in the section covering data reduction of vibration signatures, the analysis of vibration data was structured towards resolving three issues:

1. Baseline Commonality
2. Fault Detection Capability
3. Endevco and IFD Sensor Comparison

During the course of this program, vibration data was acquired from 24 aft transmissions, but only 10 forward transmissions. Therefore, the detailed vibration analysis was restricted to the aft transmissions.

Baseline Commonality Analysis

Baseline vibration data was recorded broad-band and at three carrier frequencies for each of three load conditions on each of the ten new aft transmissions. To keep the scope of the baseline analysis within program cost constraints, it was necessary to consider only the 100% torque load condition and the input pinion sensor location.

Figure 42 is the Power Spectral Density (PSD) envelope which contains all the baseline data at all the carrier frequencies of all ten new aft transmissions. Figure 42 was constructed by superimposing the individual PSD plots for each of the three carrier frequencies for each of the ten new aft transmissions, and tracing the envelope of the maximum observed amplitude at each frequency. The individual plots for the ten transmissions are presented in Appendix C (Figures C1 through C10). Detailed examination of these thirty PSD plots shows that the 250-kHz carrier frequency consistently contains the highest peaks.

The envelope of Figure 42 constitutes the "Generic Baseline" (a common baseline for all LRU's of the same part number). It is used as a comparison reference for the defect cases studied.

It is important to note that for all carrier frequencies on all new transmissions, all the significant peaks (those more than 15 db above the baseline reference) occur at the same machine frequencies. Closer analysis of this data reveals that all these peaks are related to the first-stage planet carrier of the two-stage planetary gear systems in this transmission. The predominant planet carrier frequency is the 2/rev and its harmonics, with the 1/rev and the four associated sidebands showing up in only one of ten new aft transmissions (A9-1368). Figures 43, 44, and 45 are 50-kHz, 100-kHz, and 250-kHz PSDs

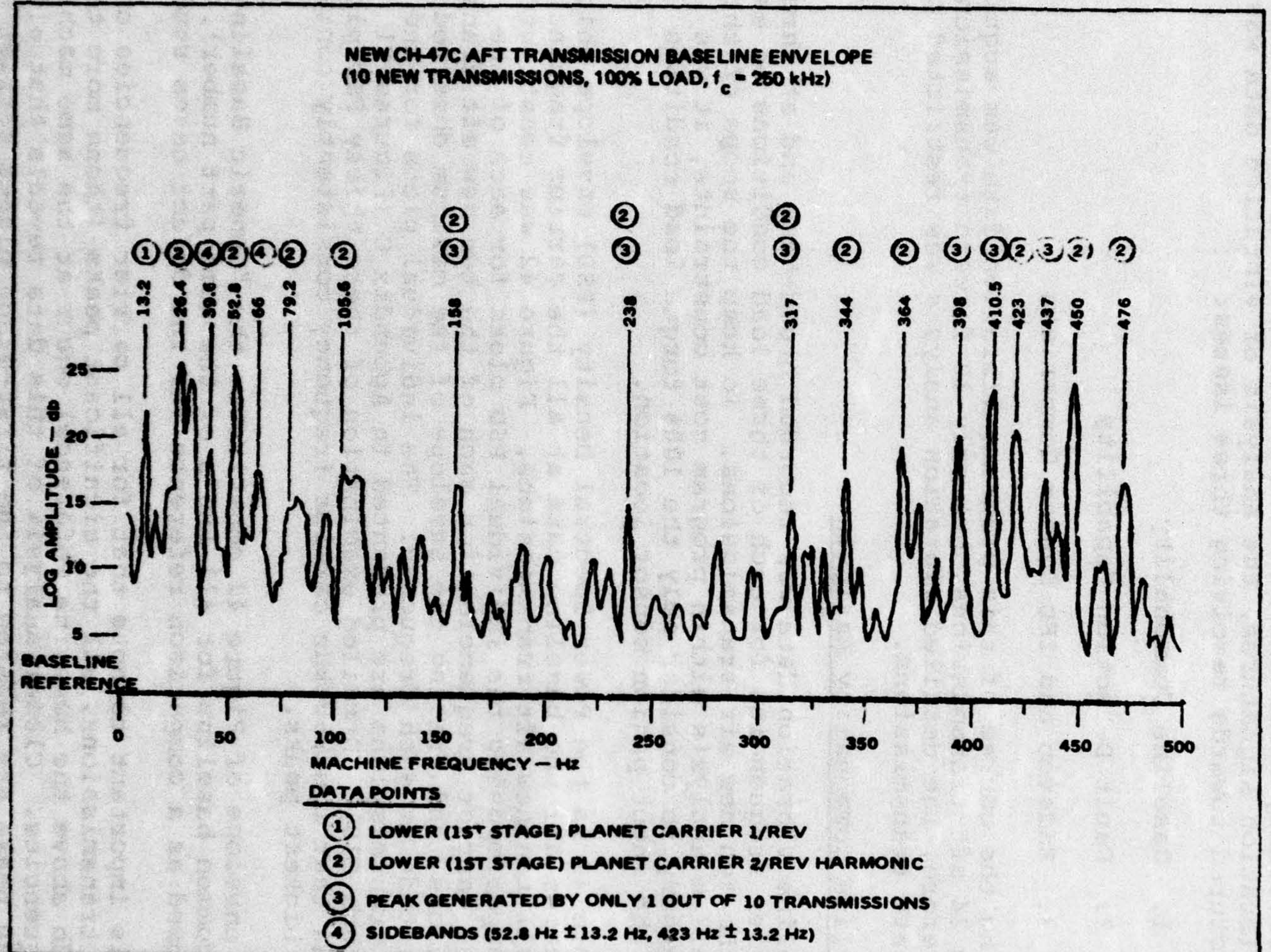

Figure 42. PSD Generic Baseline, 10 New Aft Transmissions.

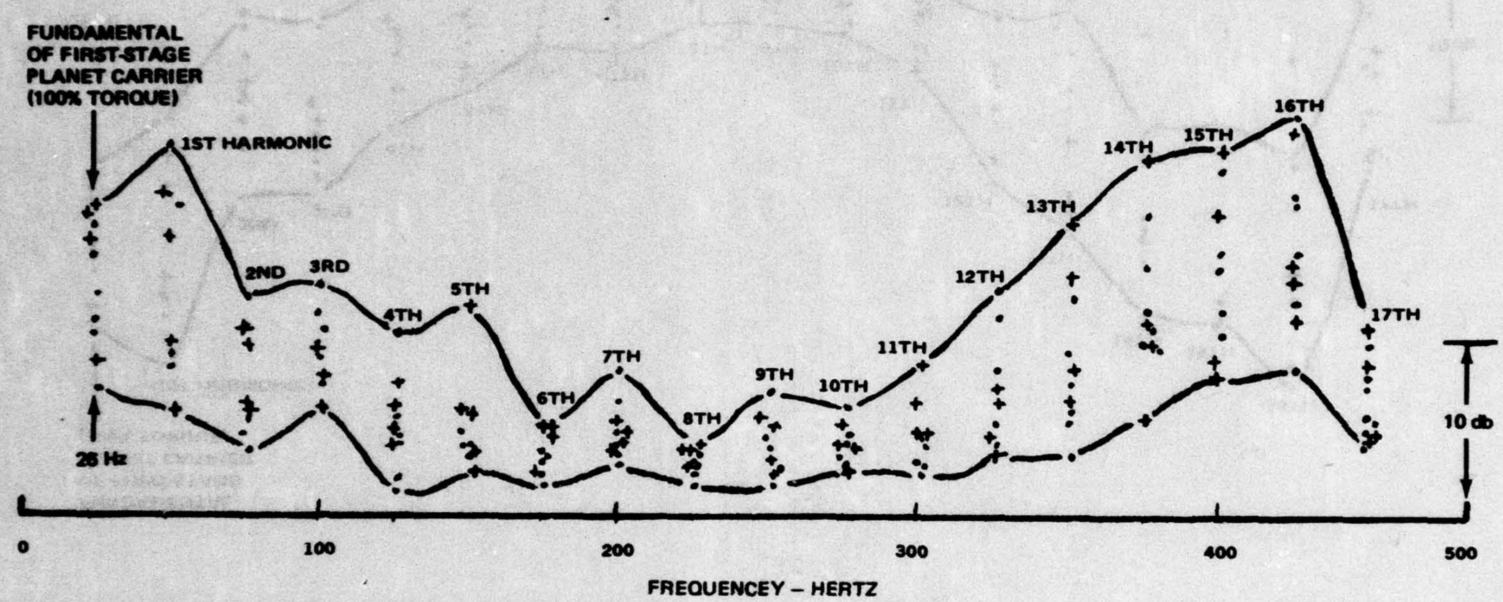

Figure 43. Composite of Planet Carrier Excitations, 10 New Aft Transmissions, 50 kHz Carrier.

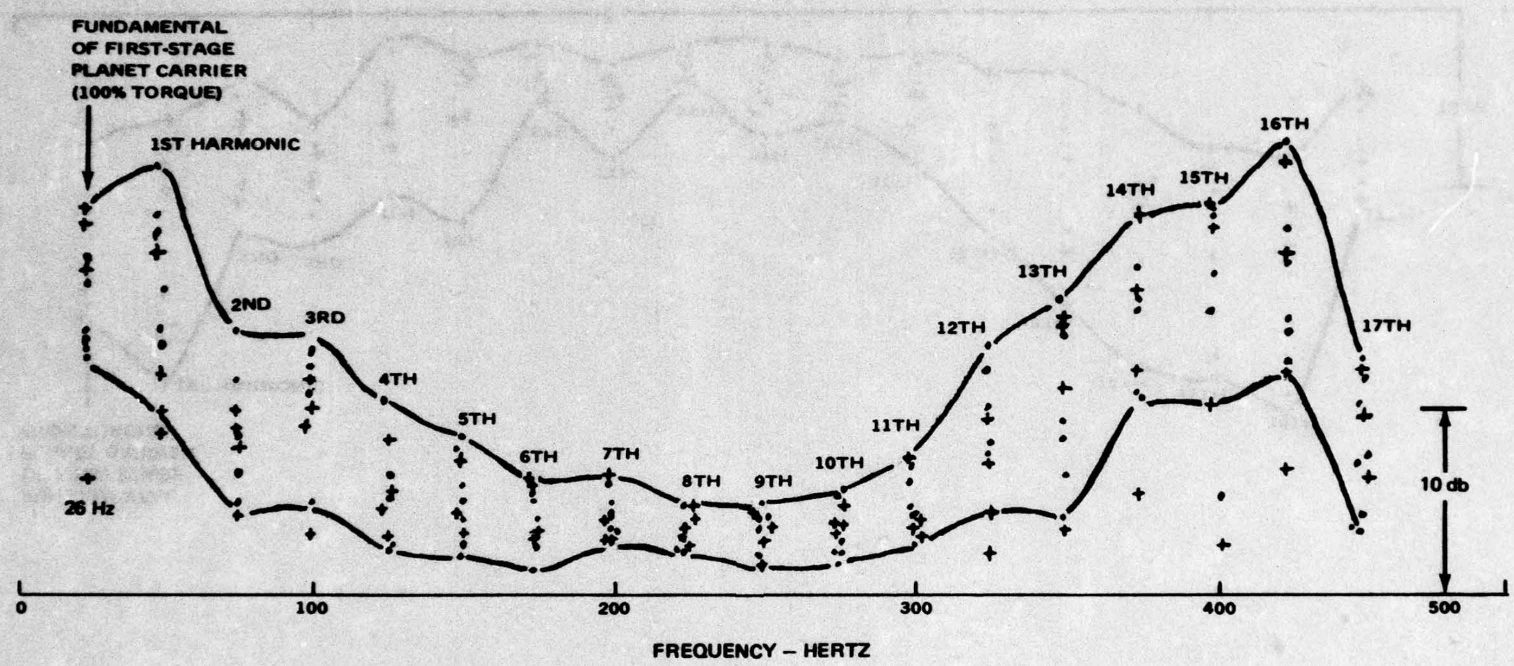

Figure 44. Composite of Planet Carrier Excitations, 10 New Aft Transmission, 100 kHz Carrier.

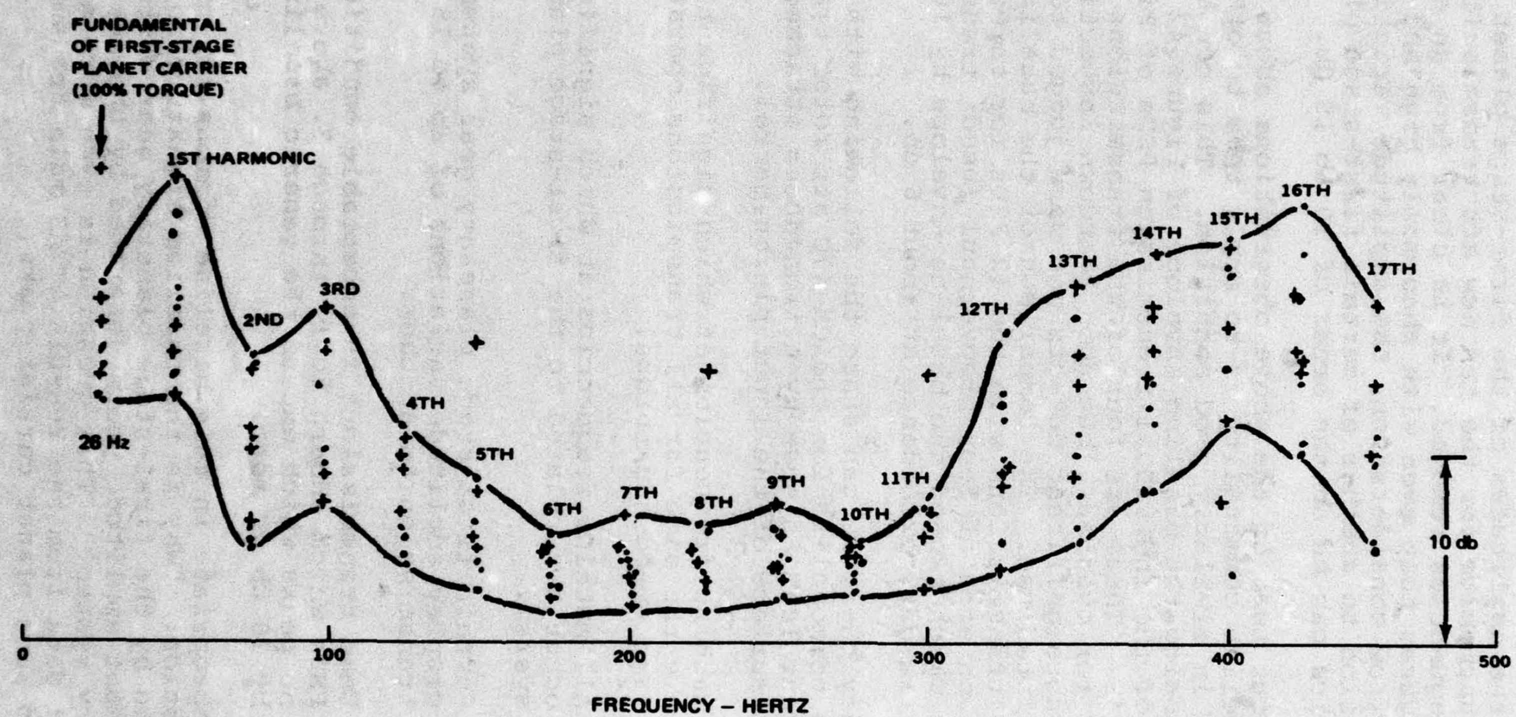

Figure 45. Composite of Planet Carrier Excitations, 10 New Aft Transmissions, 250 kHz Carrier

showing the amplitudes of the first-stage planet carrier 2/rev and its harmonics for the ten new aft transmissions with all other frequencies removed. It is clear from an examination of these figures that even with abnormally high and low data points removed from consideration, the amplitude variation from one transmission to another of certain first-stage planet carrier frequencies can be on the order of 10 to 15 db.

The obvious test of the above observations about new transmission baseline commonality is to apply them to other aft transmissions in similarly good condition. This can be done by superimposing the baseline envelope of Figure 42 on the PSDs of each of the individual transmission PSDs of Figures 46 through 49. These are four of the transmissions which were returned for overhaul, but upon teardown inspection were found to have no significant defects and were judged to be acceptable for continued use. The comparison of the baseline envelope from new transmissions with the 12 PSDs for three carrier frequencies on each of four preoverhaul (used) transmissions shows no peaks which exceed the baseline envelope by 10 db or more, with the largest exceedance at about 6 db.

In summary then, we can state the following with regard to baseline commonality for the CH-47C aft rotor transmission at 100 percent load as seen by a transducer attached to the external surface of the input pinion barrel.

1. Machine frequencies at which significant peaks occur are the same for all transmissions operating at the same speed and torque.

2. All machine frequencies at which significant peaks occur are related to the first-stage planetary gear system.

3. Certain first-stage planetary gear system peaks can display amplitude variations of up to 15 db from one transmission to another.

4. Used transmissions in acceptable condition generate PSDs which adhere to 1. through 3. above and display no peaks which exceed the generic baseline envelope by 10 db or more.

It is appropriate in this baseline commonality analysis to ask the question: "Why is the baseline signature so completely dominated by the first-stage planetary gear system, with no significant amplitude peaks generated by the second-stage planetary system?" This question is even more appropriate in light of data from the YUH-61A UTTAS main transmission which shows no such planet carrier peaks.

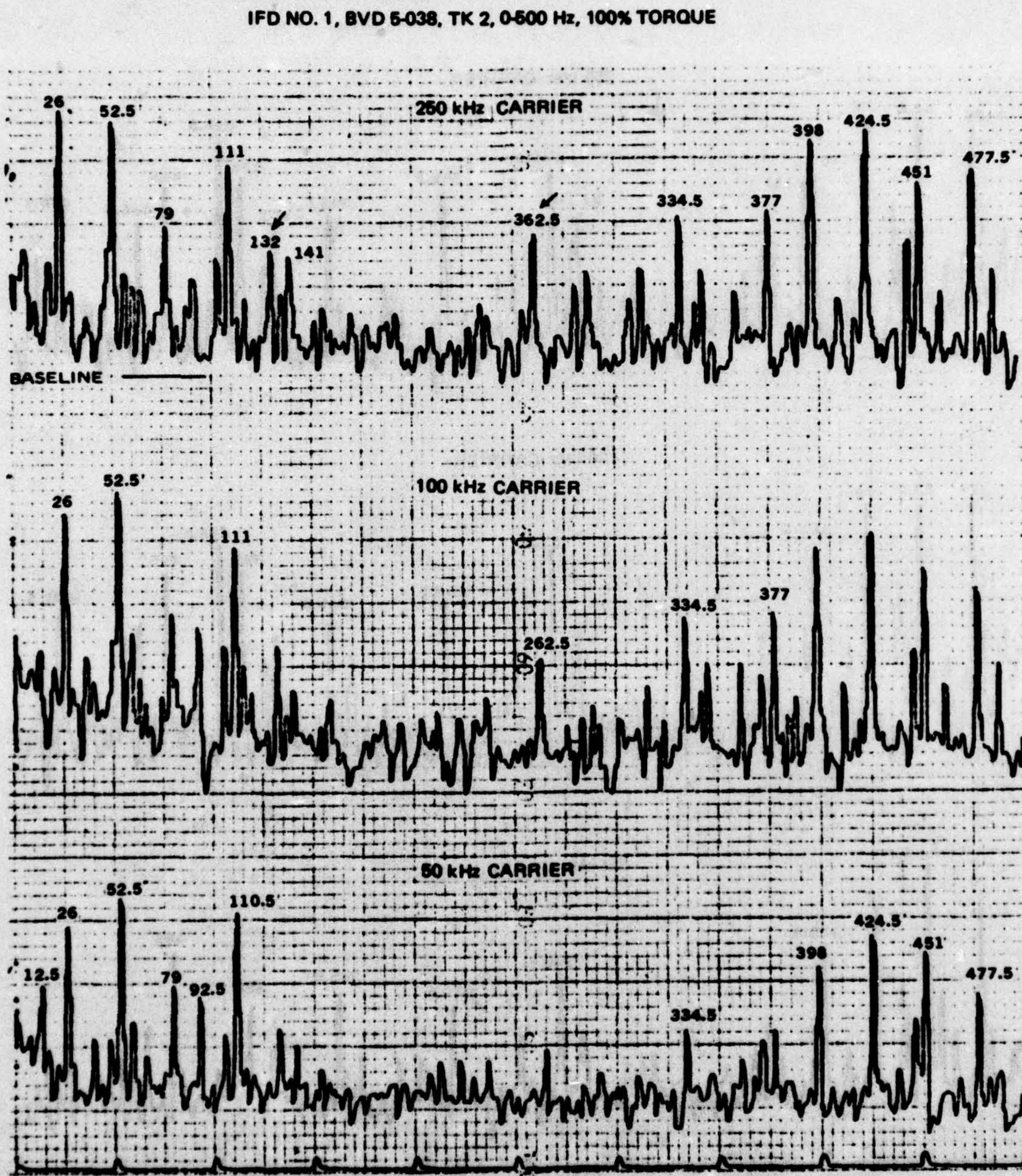

Figure 46. PSD Plot, No Defect, High Time Aft Transmission A9-1035.

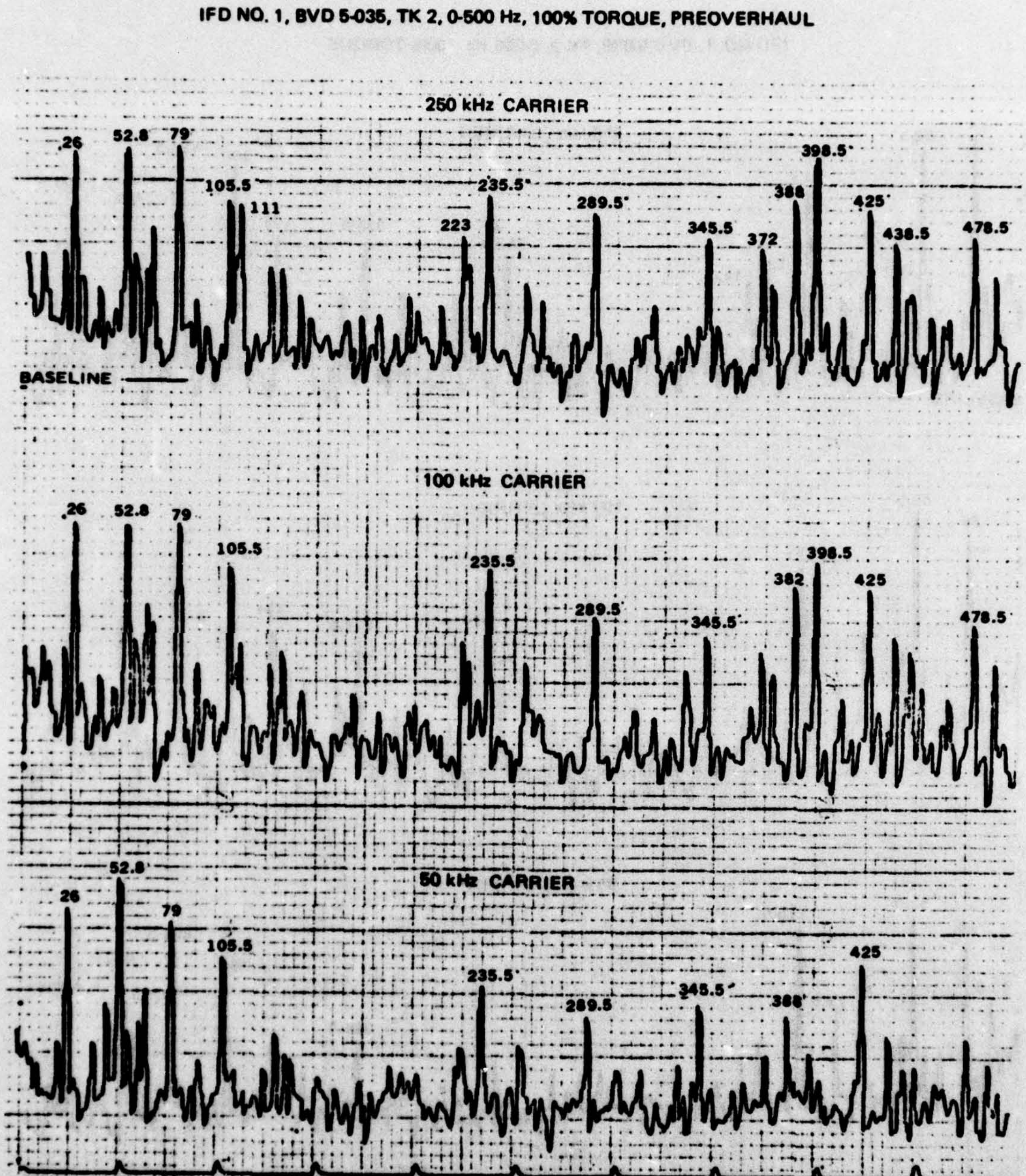

Figure 47. PSD Plot, No Defect, High Time Aft Transmission A9-971.

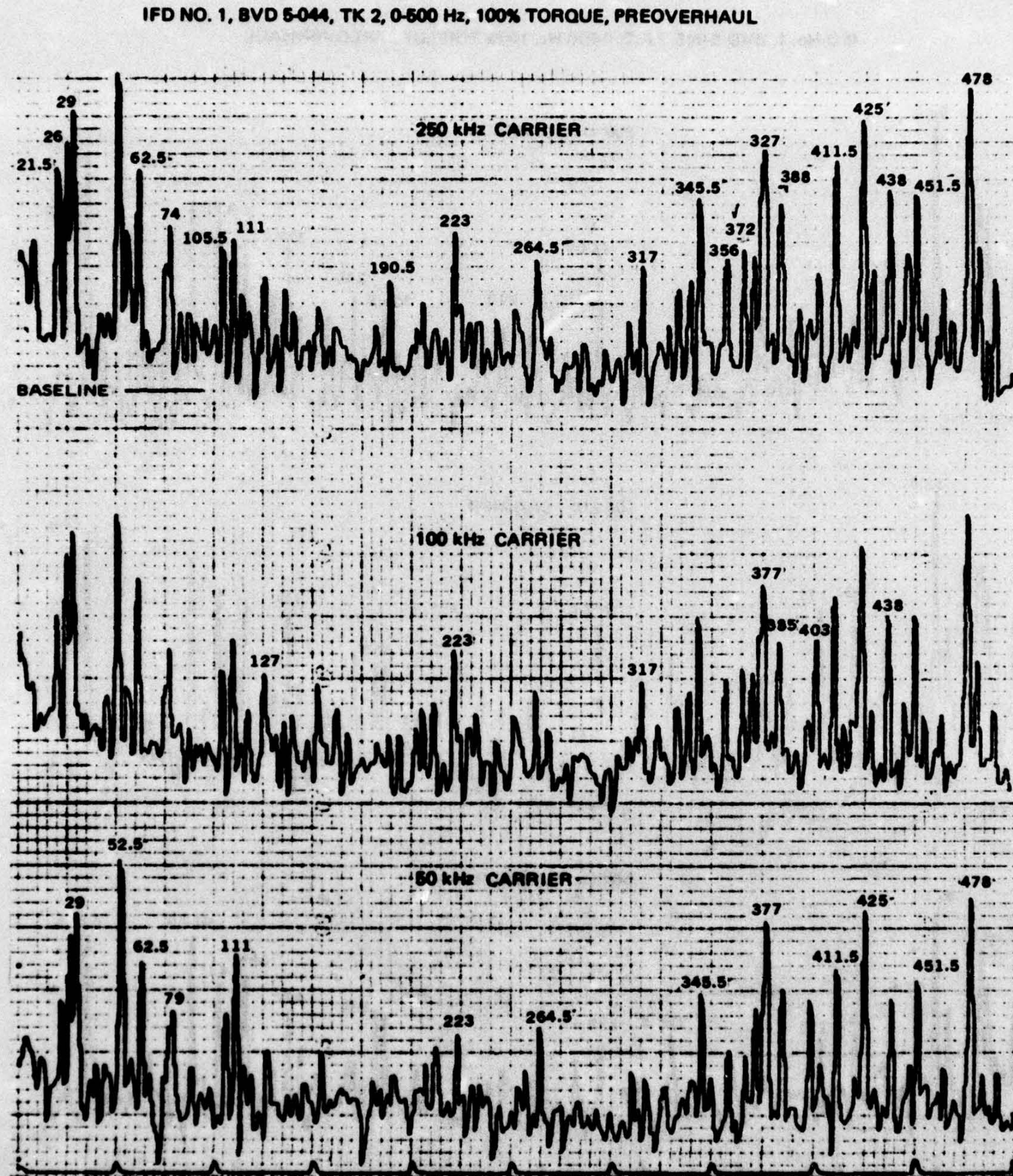

Figure 48. PSD Plot, No Defect, High Time Aft Transmission A9-1082.

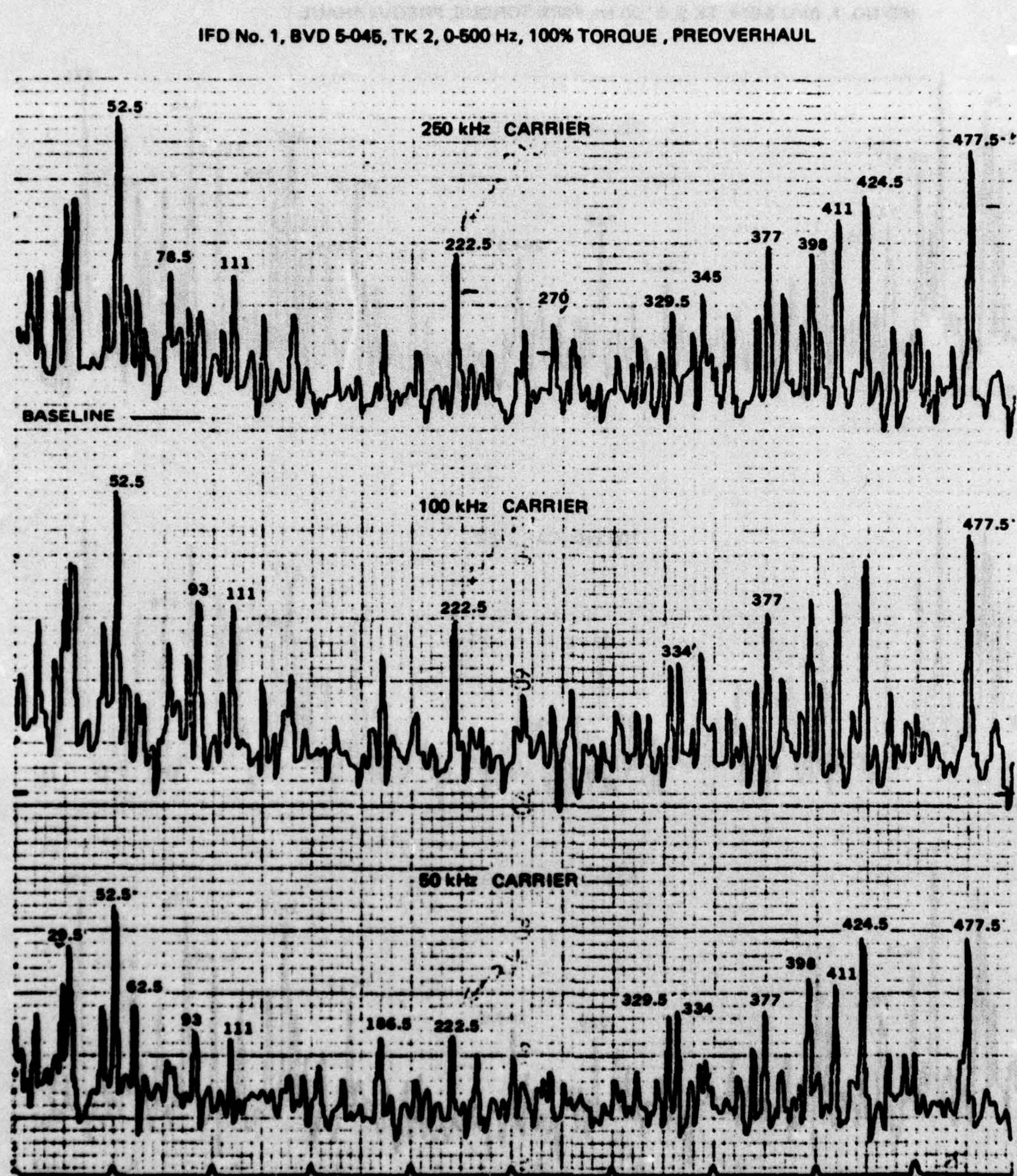

Figure 49. PSD Plot, No Defect, High Time Aft Transmission A9-1083.

The answer starts with the fact that the first-stage CH-47C planetary system has four gears in two directly opposed pairs as shown in Figure 50. Due to a design anomoly of the first-stage planetary gear system, there is an angular offset in the relative position of the two opposed planet gear pairs. This results in unequal loading of the two planet gear pairs. Thus, the two planet gears of the heavily loaded pair generate a high signal level at a twice-per-planet-carrier-revolution rate, relative to a stationary transducer on the external surface of the transmission. Although this type of design anomoly is also present in the CH-47C second-stage planetary system, the planet gear loading disparity is far less due to (1) an offset angle that is only 60% as large as that of the first stage, and (2) three planet gear pairs (six gears total) to share the load disparity. In the YUH-61A UTTAS planetary gear system there is no offset angle, and all gears are sequentially loaded. (No two gear pairs enter mesh at the same point in time.) Loads are shared equally by all planet gears and no large planet carrier peaks are generated.

Fault Detection Capability

To evaluate the fault detection capability of the high frequency vibration technique, seven defect cases were selected from the CH-47C aft rotor transmissions that were returned for overhaul and subsequently, during teardown inspection, were found to have defects which rendered them unacceptable for continued use. The defect cases considered included the two gear pairs and five bearings (two of which were planet bearings) listed in Table 17. The discrepant parts involved in each defect case can be located within the transmission by referring to the CH-47C aft rotor transmission drawing of Figure 51. In order to determine the detectability of the individual defect cases, the following analytical procedure was employed.

1. The 0- to 500-Hz PSD from the defect case input pinion IFD sensor at a 250-kHz carrier frequency was overlaid with the generic baseline envelope of the ten new transmissions (Figure 42). Any exceedances that were more than 10 db above this baseline envelope were tabulated to display their amplitude and the machine frequency.

2. Additional special case PSDs were generated from the defect case data over the spectral ranges which gave the best resolution of the machine frequencies characteristic of the discrepant conditions and from the IFD sensors that were closest to the discrepant parts. Special case generic baseline envelopes were then generated from each additional sensor location and spectral range using four of the new transmissions

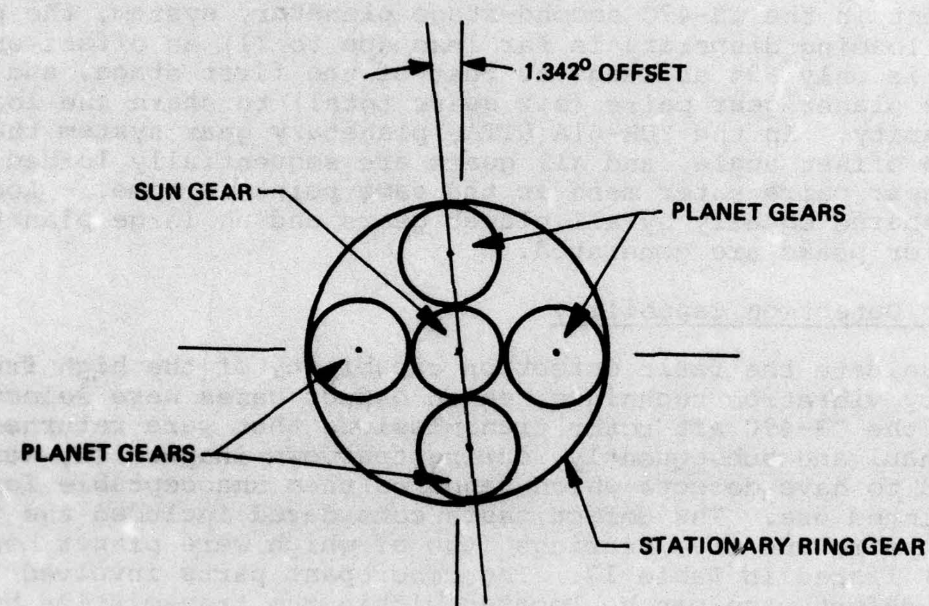

Figure 50. CH-47C Aft Transmission First-Stage Planetary Gear System.

TABLE 17. HIGH FREQUENCY VIBRATION ANALYSIS DEFECT CASES

CASE	XMSN S/N	PART	DISCREPANT CONDITION	CAUSE FOR REMOVAL	TSO (Hrs.)
1	A9-734	114DS274, 2ND-STAGE CARRIER THRUST BRG.	INNER & OUTER RACES SEVERELY SPALLED, CAGE & BALLS OK (FIGURE 15)	HIGH METAL CONTENT IN OIL	377
2	A9-856	114DS251, INPUT PINION OTBD. THRUST BRG. (BLOWER DRIVE ATTACHMENT)	CAGE SEVERELY DISTORTED & WORN, ALL BALLS SEVERELY SPALLED, RACES MODERATELY SPALLED ALL AROUND (FIGURE 20)	INTERNAL FAILURE (FILTER INSP.)	272
3	A9-748	114DS256, ACCESSORY DRIVE BEARING	CAGE SEVERELY WORN & DISTORTED, BROKEN BALLS, INNER & OUTER RACES LIGHTLY SPALLED (FIGURE 16)	INTERNAL FAILURE (FILTER INSP.)	133
4	A9-728	114D2063 & 114D2091 ACCESSORY GEARBOX DRIVE GEARS	DEEP IMPRESSIONS (.025") ON ALL TEETH (FIGURES 21 & 22)	METAL ON MAG. PLUG	299
5	A9-1245	114D2056 & 114D2169 OIL COOLER BLOWER DRIVE GEARS	ALL TEETH OF BOTH GEARS SPALLED ON BOTH THE DRIVE AND COAST SIDES (FIGURES 23 & 24)	LOOSE "PLUG" ON INPUT PINION (MAY BE RELATED TO MODE)	447
6	A9-962	114DS281 FIRST-STAGE PLANET BRG.	EXCESSIVE SPALLING (≈180°) ON INNER RACE (FIGURE 14)	METAL ON FILTER	204
7	A9-724	114DS282 SECOND-STAGE PLANET BRG.	EXCESSIVE SPALLING (≈ 180°/45°) OF INNER RACE. (FIGURE 12)	METAL CONTAM. (FILTER INSP.)	949

AD-A035 215 BOEING VERTOL CO PHILADELPHIA PA F/G 13/9

TRANSMISSION CONDITION ASSESSMENT.(U)

DEC 76 O L SANDORA DAAJ02-75-C-0021

UNCLASSIFIED D210-11067-1 USAAMRDL-TR-76-36 NL

2 OF 2

AD A035215

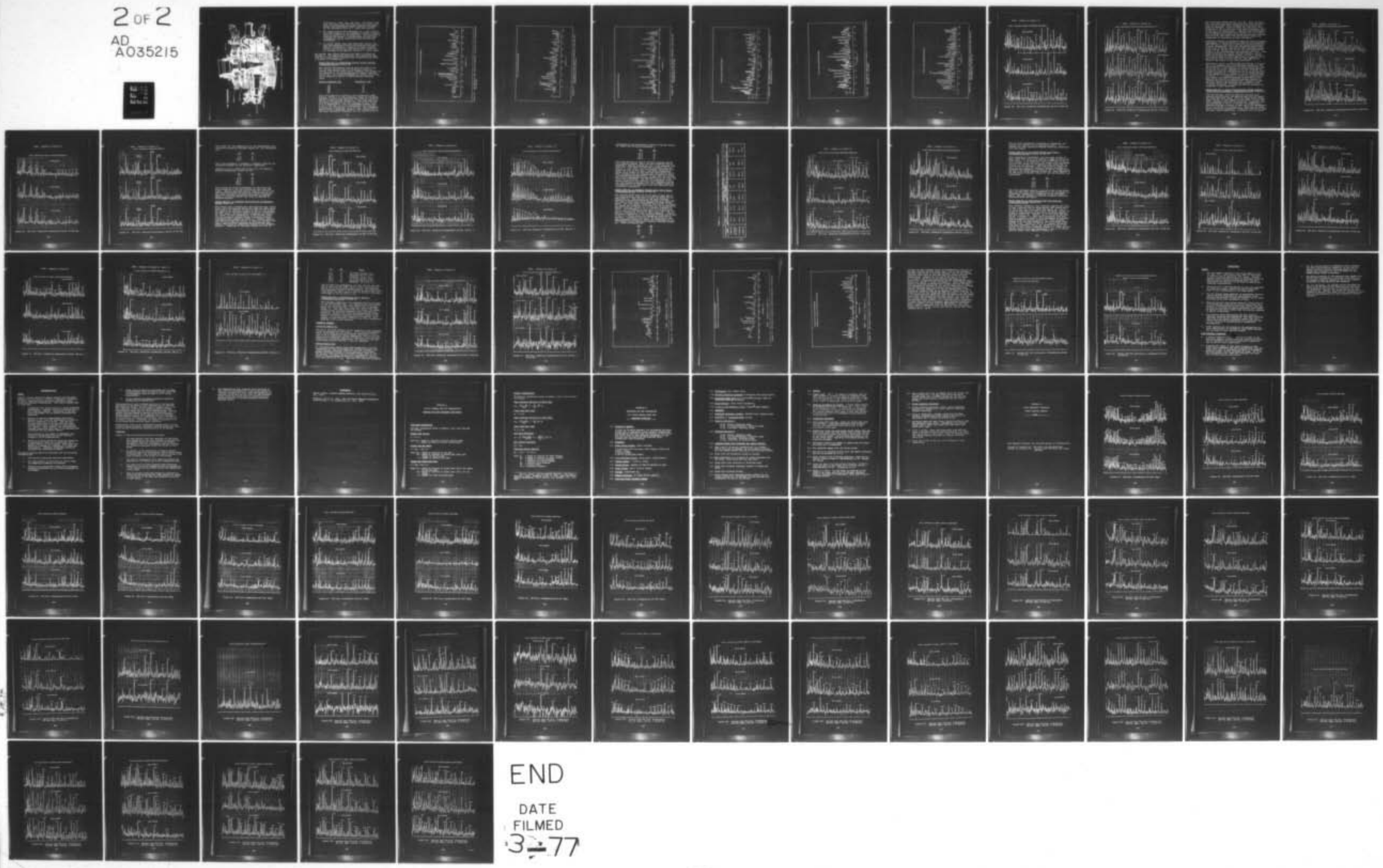

END

DATE FILMED 3-77

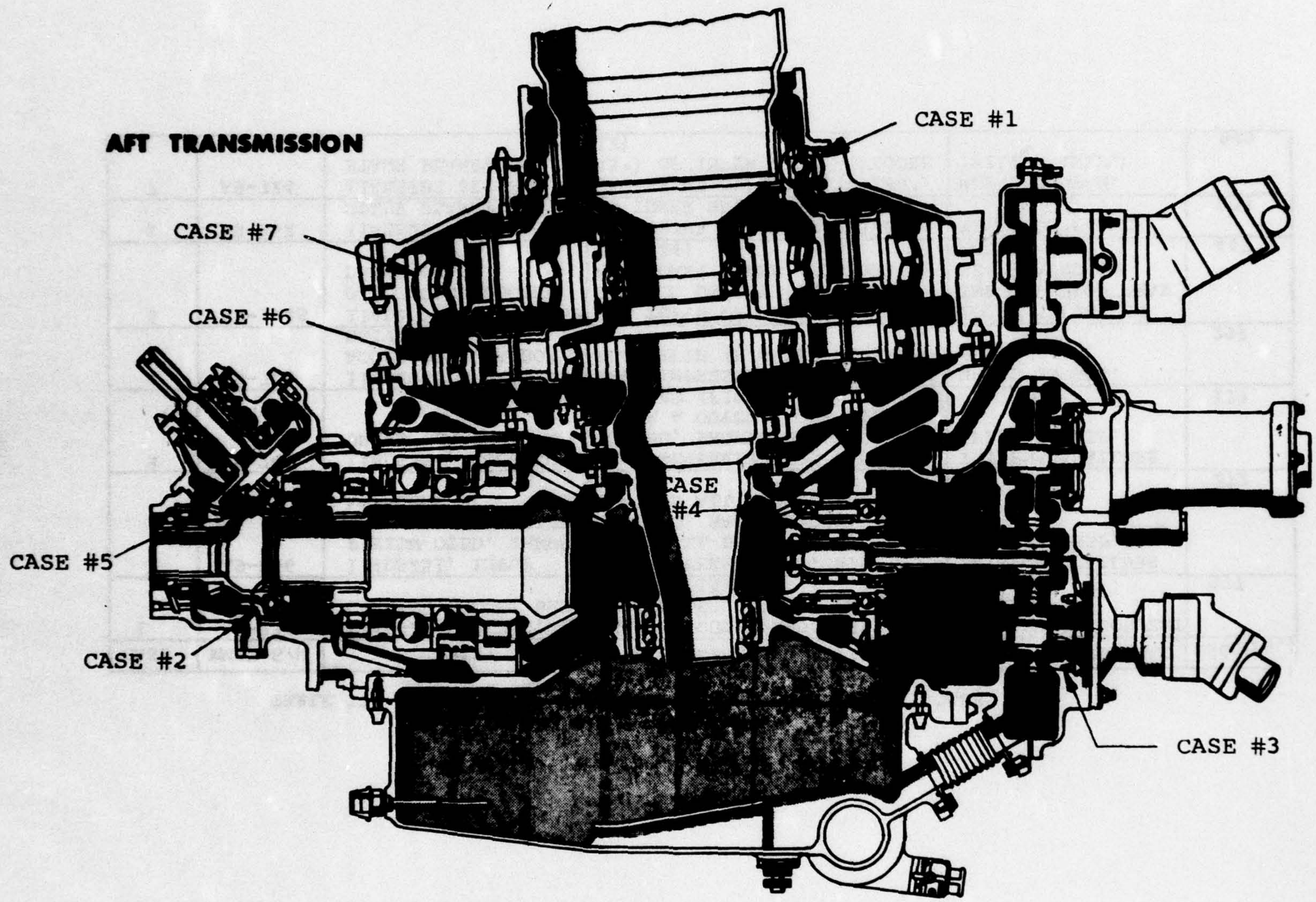

Figure 51. CH-47C Aft Transmission.

(S/N A9-1337, 1339, 1341, and 1342). The special case PSDs from defect data were then overlaid by the appropriate four-transmission generic baseline envelopes, and the exceedance tests of 1. above were applied.

3. The greater-than-10-db exceedances of 1. and 2. above were then compared to the fundamental machine frequency characteristics of the discrepancies. This was done to establish the degree of correspondence between these fundamentals and the significant baseline envelope exceedances.

4. In certain defect cases some additional special case PSDs were generated without corresponding baselines to identify the presence or absence of higher harmonic content or certain gear mesh and bearing frequencies not included in the spectral ranges of 1. and 2. above.

The special case generic baselines are shown in Figures 52 through 57. The associated individual new transmission PSDs from which these generic baselines were constructed are shown in Figures C11 through C36.

Defect Case No. 1, Second-Stage Carrier Thrust Bearing, Transmission A9-734 (Figure 20)

This bearing had severely spalled inner and outer races, but the cage and balls were in acceptable condition. Looking first at the input pinion transducer PSD (Figure 58) and comparing it to the appropriate PSD generic baseline (Figure 42), the following exceedances (greater than 10 db) can be observed in the 0- to 500-Hz Machine Frequency Range:

Machine Frequency (Hz)	Exceedance (-db)
47	11
256	10
289	10
303	15
350	15

Since this bearing is located in the transmission upper housing, IFD No. 5 is the transducer closest to the defect. Therefore, special case PSDs were made with the output of IFD No. 5 from 0-100 Hz (Figure 59). The inner and outer race defect frequencies for this bearing are 59.2 Hz and 53.3 Hz respectively. The only exceedance greater than 10 db in this PSD, with its corresponding four-transmission baseline (Figure 56), is at 66.4 Hz. This exceedance appears to be a "sideband" formed in this transmission by the outer-race-defect frequency, 53.1 Hz, and the 1/rev of

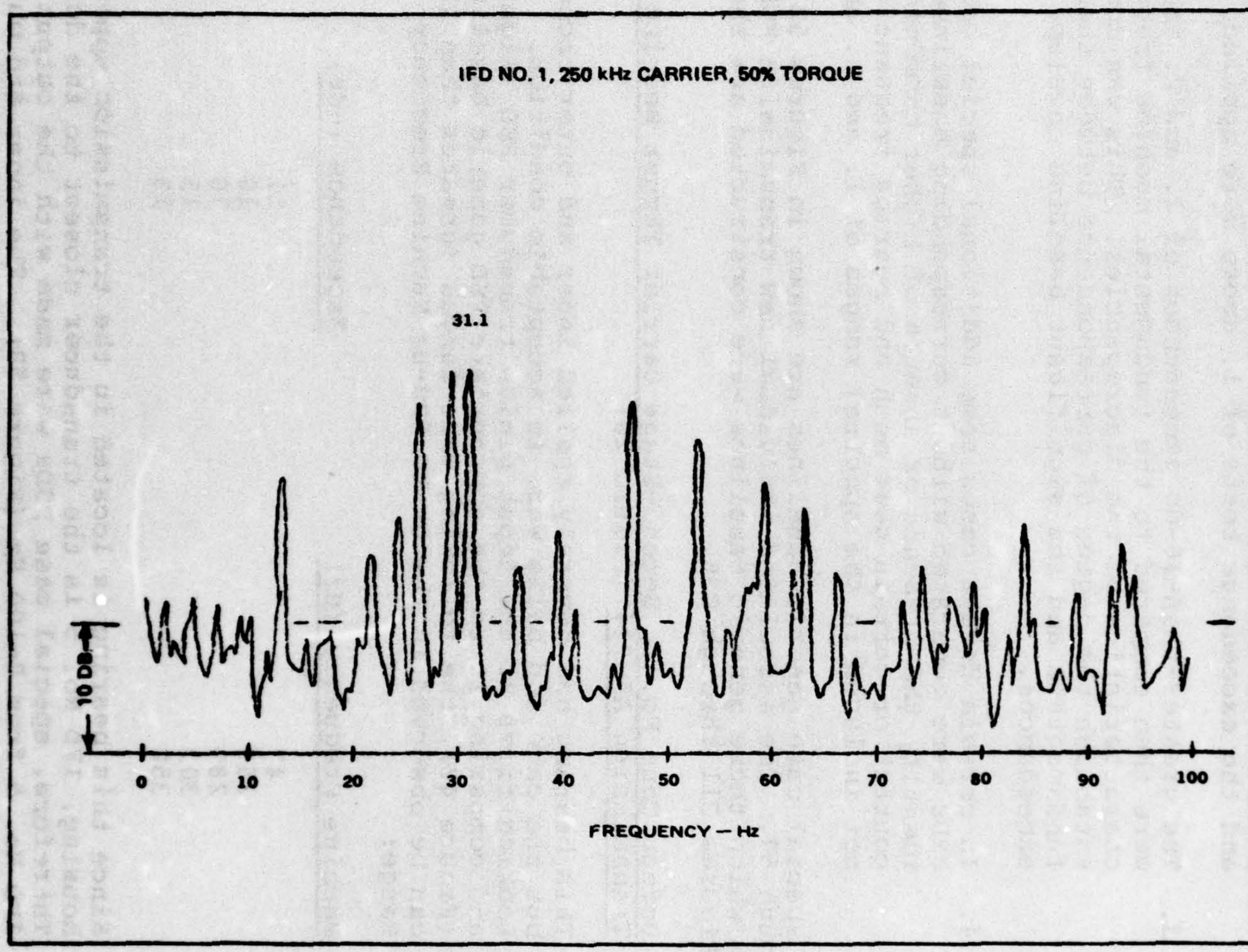

Figure 52. PSD Special Case Generic Baseline, Four New Aft Transmissions (0-100 Hz).

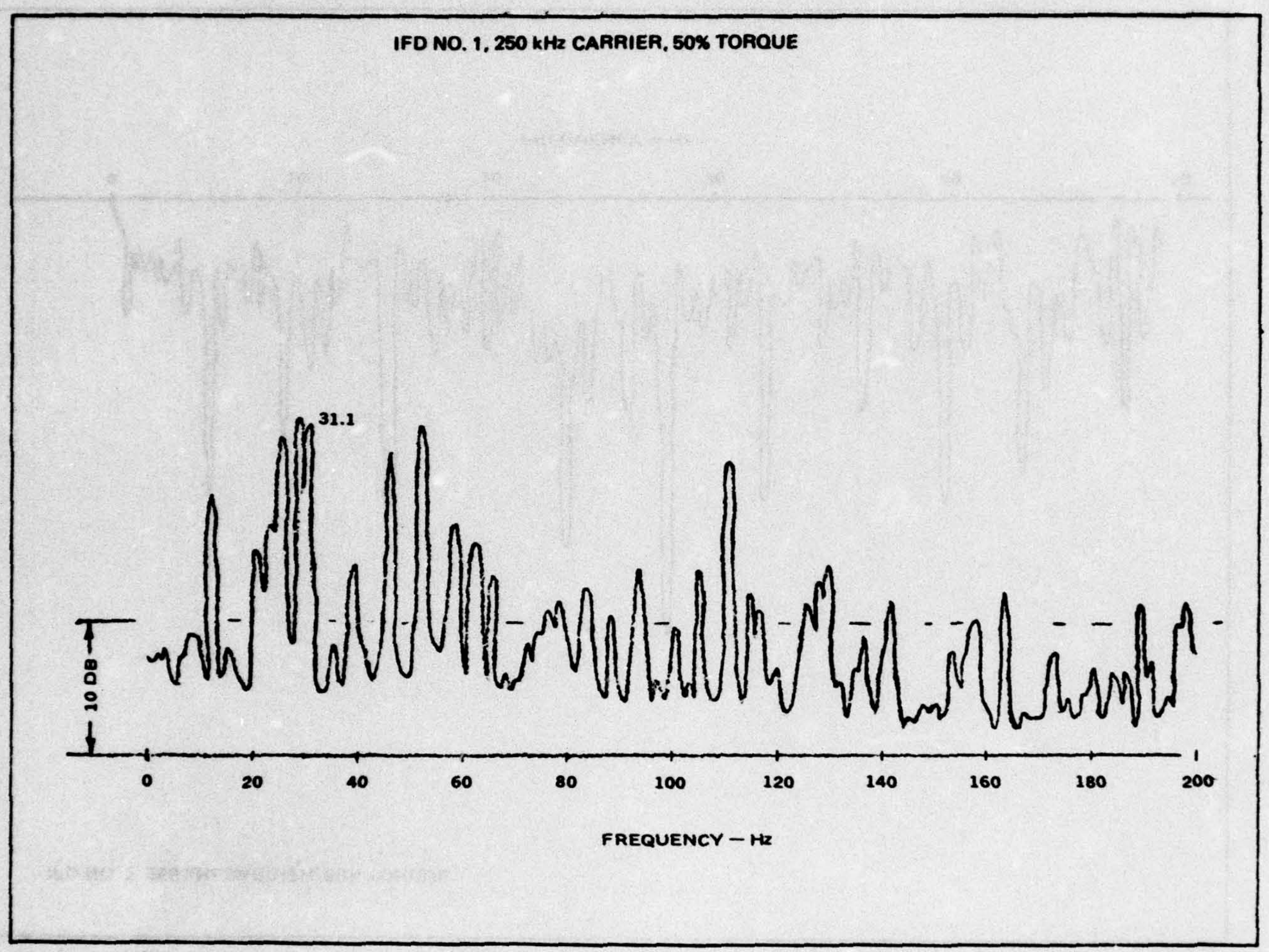

Figure 53. PSD Special Case Generic Baseline, Four New Aft Transmissions (0-200 Hz).

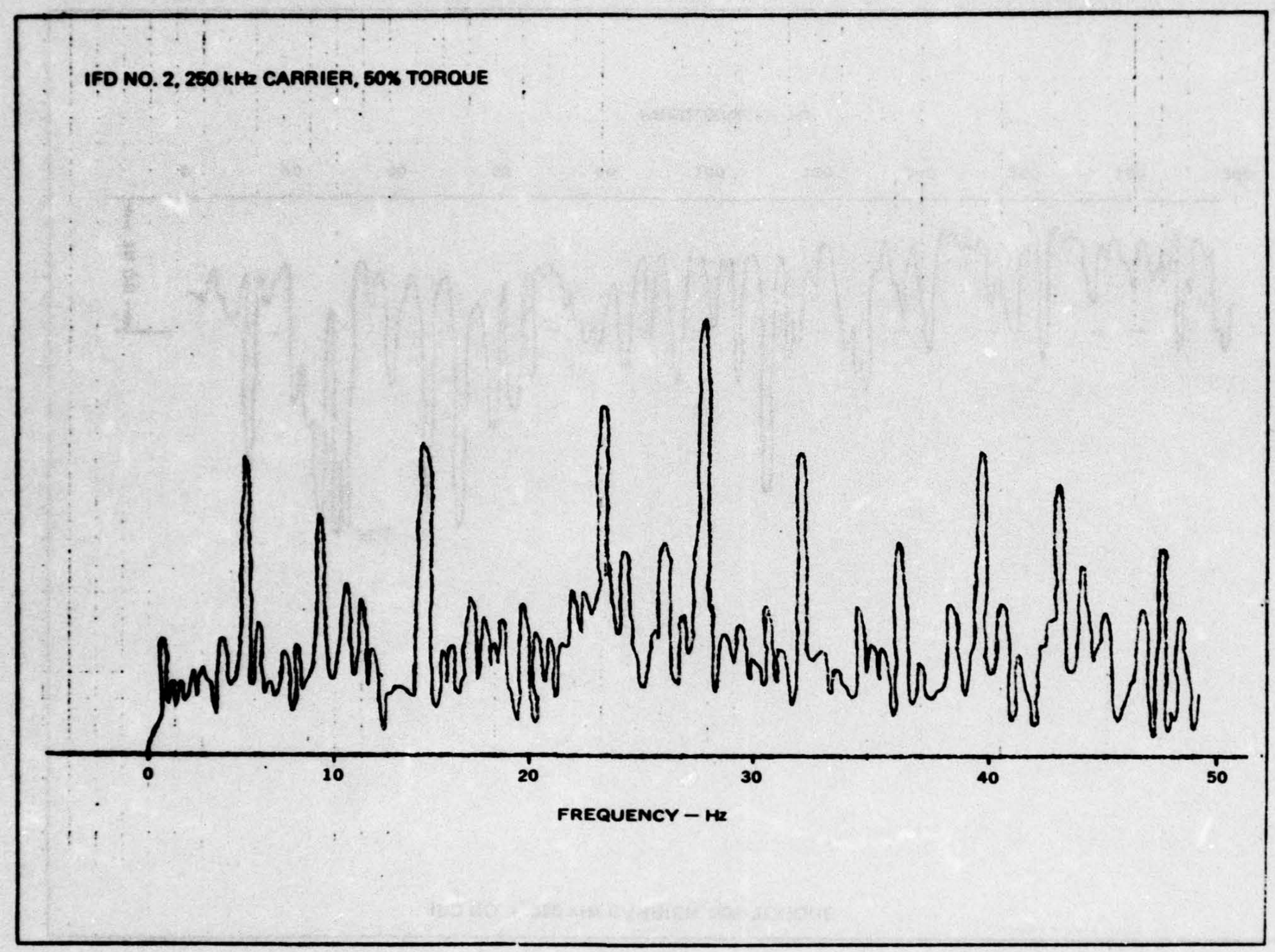

Figure 54. PSD Special Case Generic Baseline, Four New Aft Transmissions (0-50 Hz).

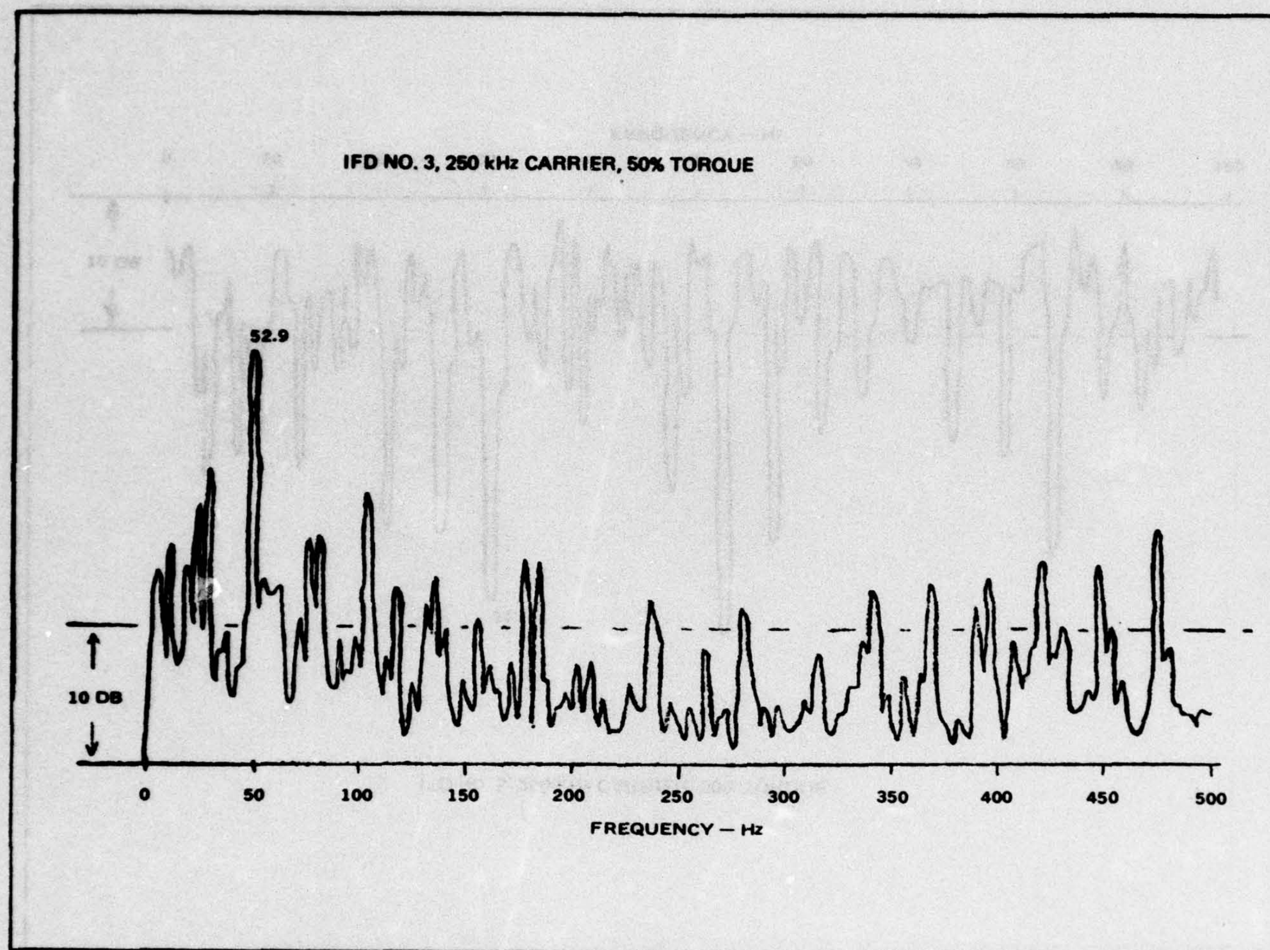

Figure 55. PSD Special Case Generic Baseline, Four New Aft Transmissions, (0-500 Hz).

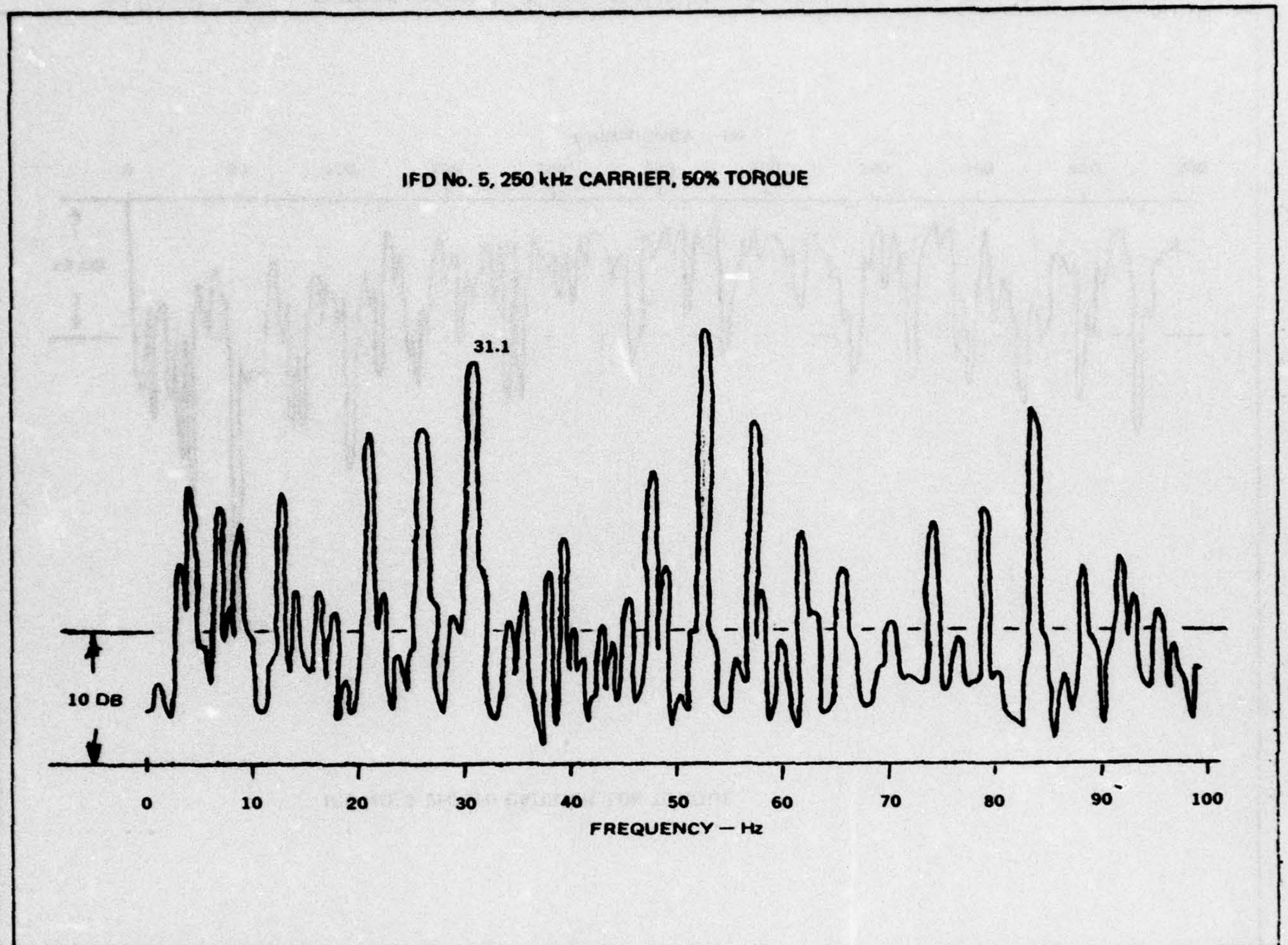

Figure 56. PSD Special Case Generic Baseline, Four New Aft Transmissions IFD No. 5, (0-100Hz).

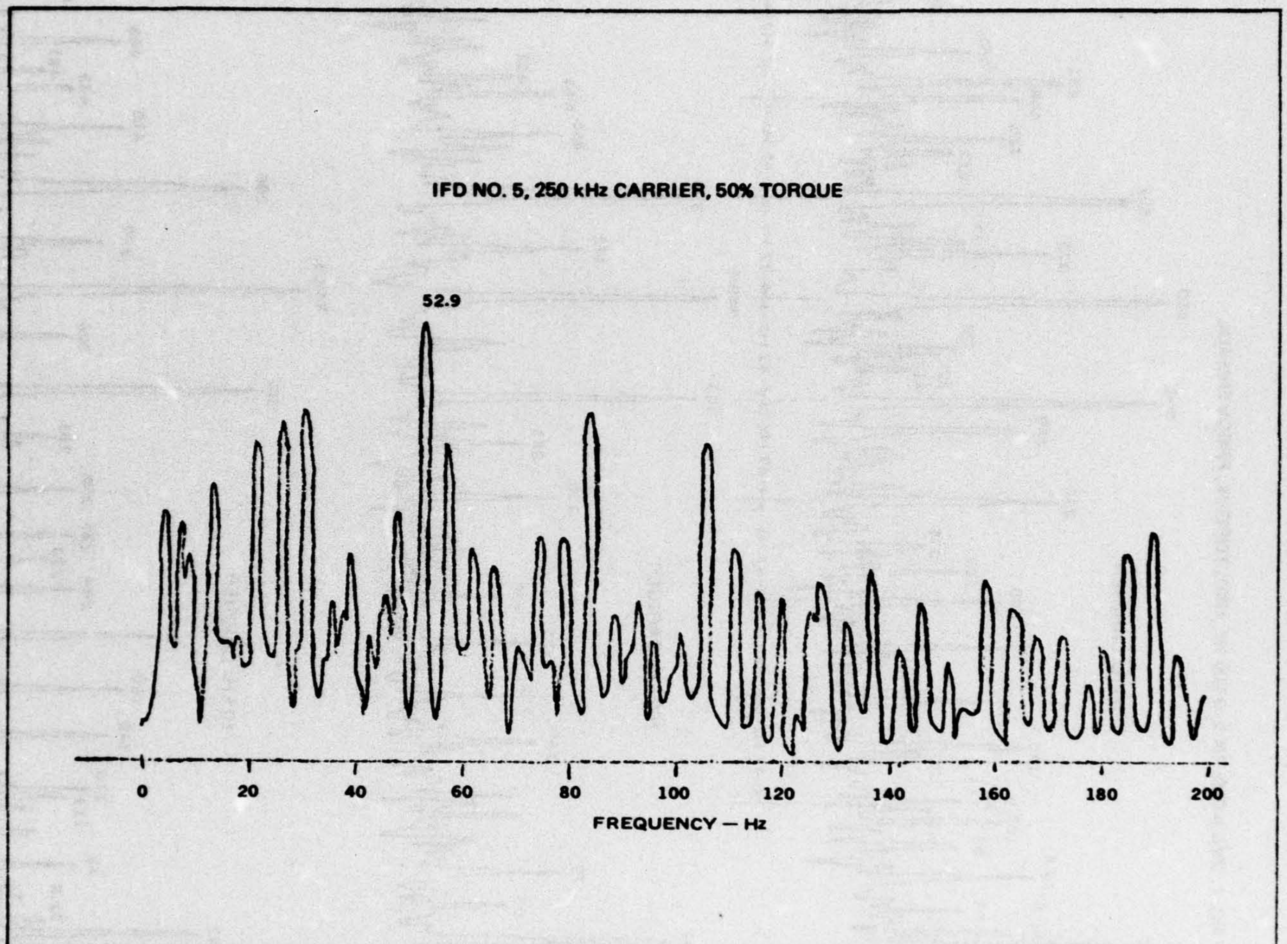

Figure 57. PSD Special Case Generic Baseline, Four New Aft Transmissions, (0-200 Hz).

NOTE: Compare to Figure 42

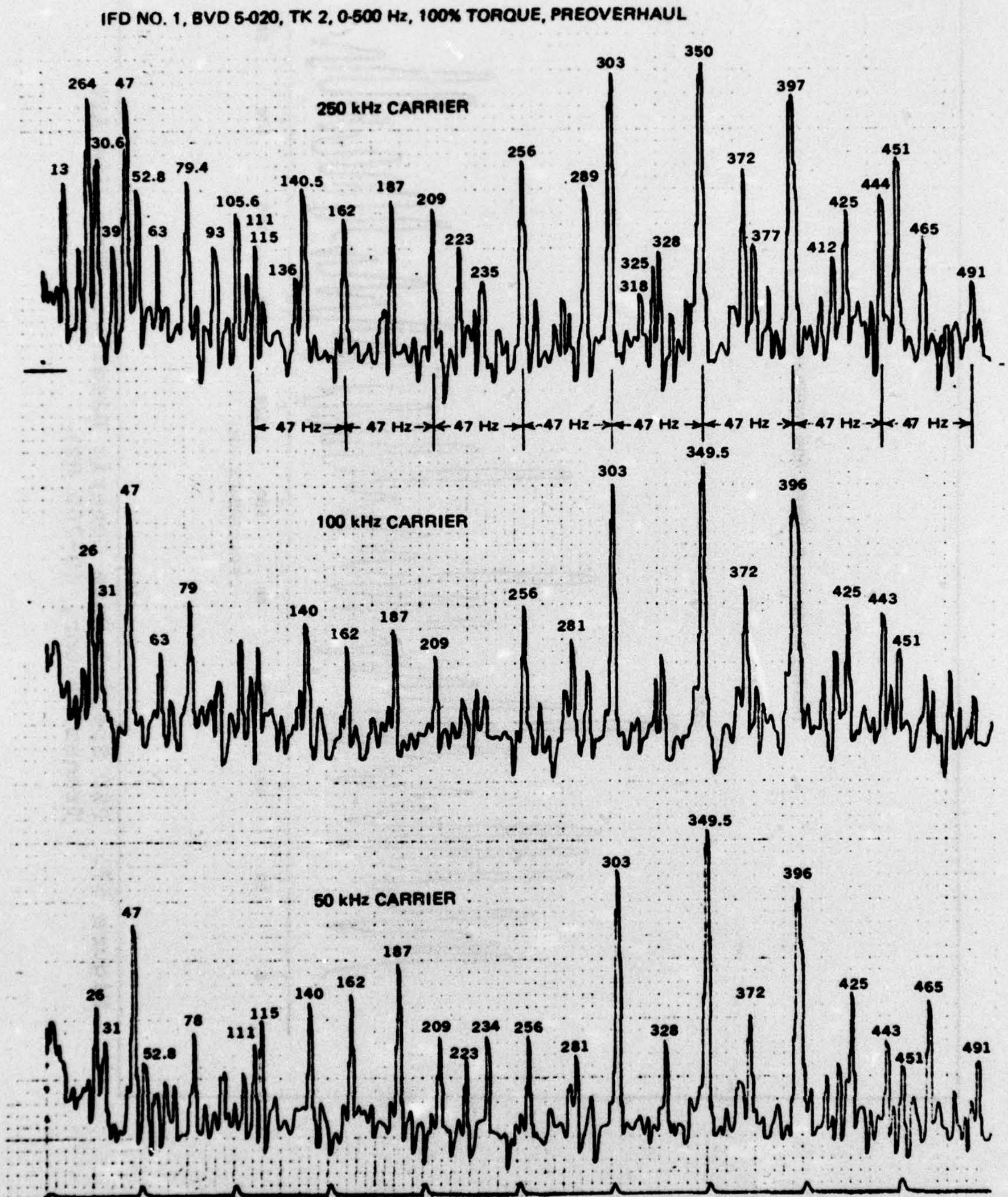

Figure 58. PSD Plot, Defective Transmission A9-734 (0-500 Hz).

NOTE: Compare to Figure 56

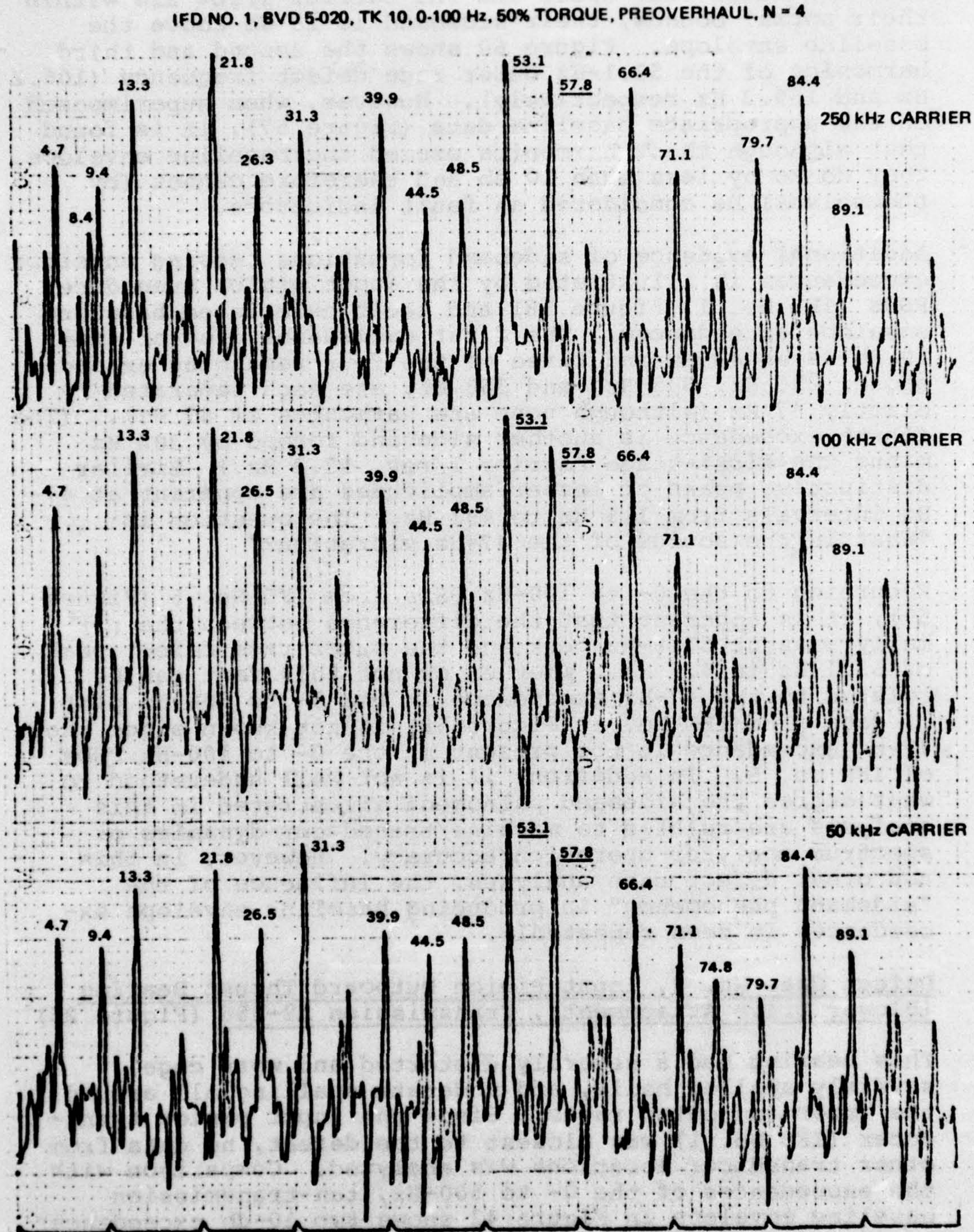

Figure 59. *PSD Plot,* Defective Transmission A9-734 (0-100 Hz).

the first-stage planet carrier, 13.3 Hz. Thus, although both the outer race spall and the carrier 1/rev are within their normal bounds, their sideband is 10 db above the baseline envelope. Figure 60 shows the second and third harmonics of the 53.1-Hz outer race defect frequency (106.2 Hz and 159.3 Hz respectively). However, when superimposed on the appropriate baseline data (Figure 57), it is found that although these harmonics exceed the baseline envelope, they do so by less than 10 db and therefore cannot (by themselves) be considered as fault indicators.

Additional evidence of sideband formations causing envelope exceedances is illustrated by the input pinion transducer PSDs (IFD No. 1, Figure 58) and their associated baseline envelope exceedances. The first exceedance greater than 10 db is at 47 Hz and three of the four remaining exceedances, 256 Hz, 303 Hz, and 350 Hz, are each separated by exactly 47 Hz (although none are harmonics of 47 Hz). (The fourth exceedance is another sideband formed by 303 Hz minus the first-stage carrier 1/rev, 13.3 Hz.) Similar distinctive peaks of lesser amplitudes are apparent at 47-Hz intervals from 115 Hz to 491 Hz. The question is: "What is the source of the 47-Hz vibration?"

Returning to the 0- to 100-Hz PSDs from IFD No. 5 (Figure 59), it is apparent that the difference between the normally present 57.8-Hz peak and the outer race defect peak of 53.1 Hz is 4.7 Hz. Whether or not this fact can be related to the 47-Hz exceedance in the 0- to 500-Hz plot of data from IFD No. 1 (Figure 58) is not known since the 47-Hz exceedance is not present in the 0- to 100-Hz PSDs of IFD No. 5. In addition, it is not well understood to what degree the sideband phenomena illustrated in this analysis are related to machine/transducer dynamics or spectrum analyzer operation/accuracy. However, in this and other defect case analyses, the influence of the "sideband phenomenon" in producing baseline envelope exceedances is seen repeatedly.

<u>Defect Case No. 2, Input Pinion Outboard Thrust Bearing (Blower Drive Attachment), Transmission A9-856</u> (Figure 25)

This bearing had a severely distorted and worn cage, severely spalled balls, and moderate spalling all around the inner and outer races. Since the input pinion transducer (IFD No. 1) was closest to the defect, no data from other transducer locations was analyzed. Comparison with the exceedances of the 0- to 500-Hz, ten-transmission baseline envelope in Figure 42 shows two 10-db exceedances at 51.1 Hz and 60.6 Hz (Figure 61). These are the fundamental rotational frequencies of the cage relative to outer and inner races respectively. Looking at a 0- to 100-Hz

NOTE: Compare to Figure 57

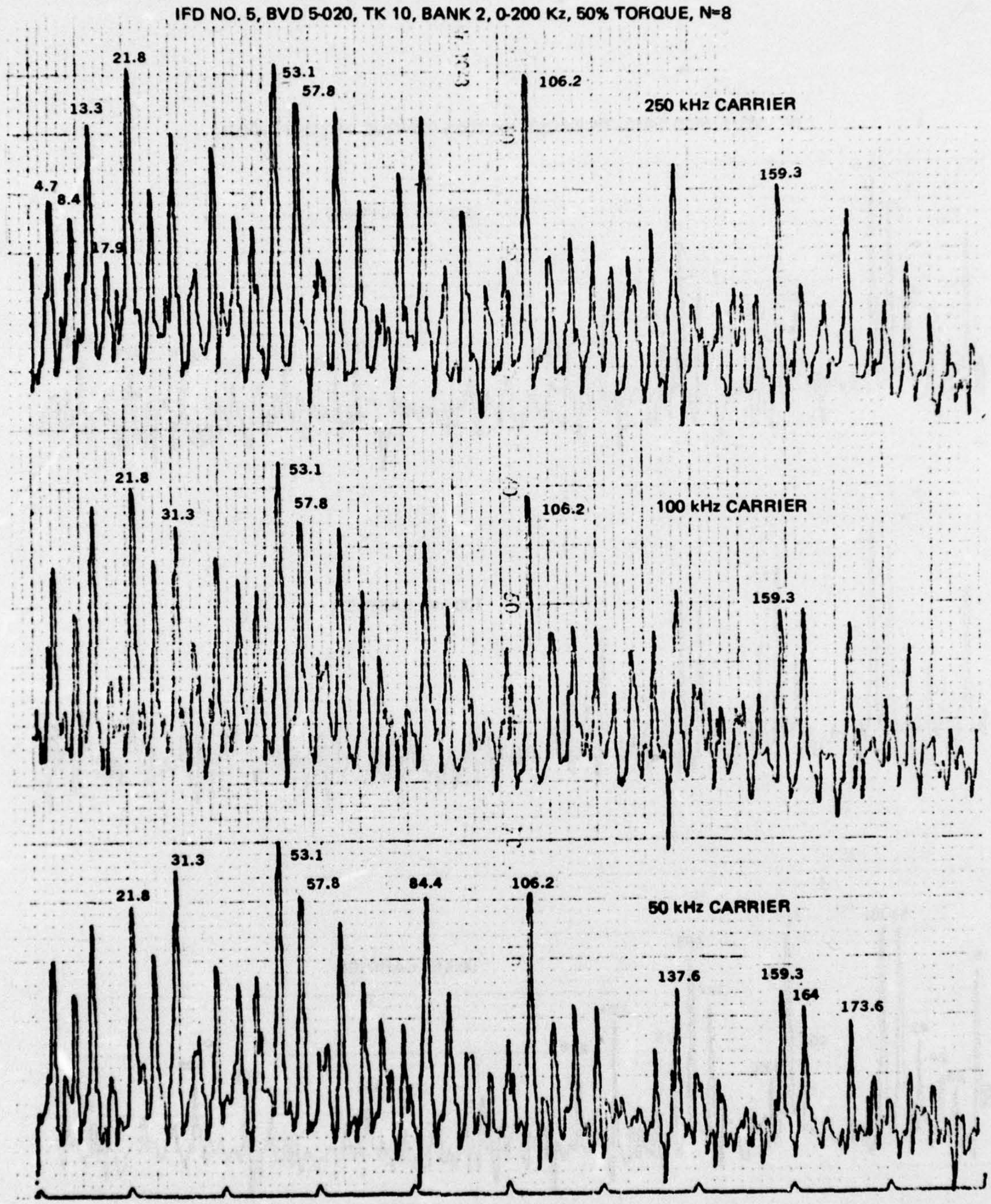

Figure 60. PSD Plot, Defective Transmission A9-734 (0-200 Hz).

NOTE: Compare to Figure 42

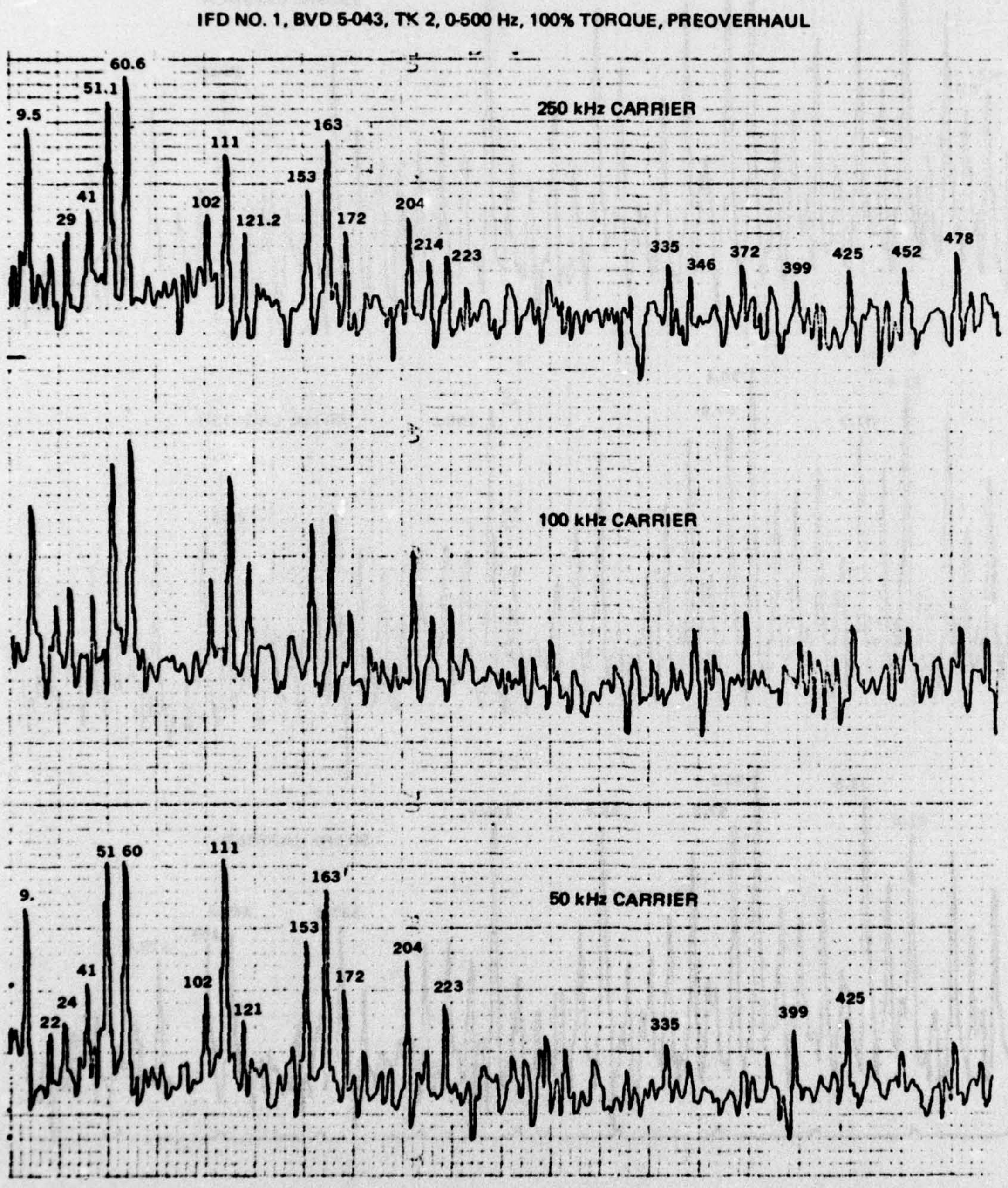

Figure 61. PSD Plot, Defective Transmission A9-856 (0-500 Hz).

NOTE: Compare to Figure 52

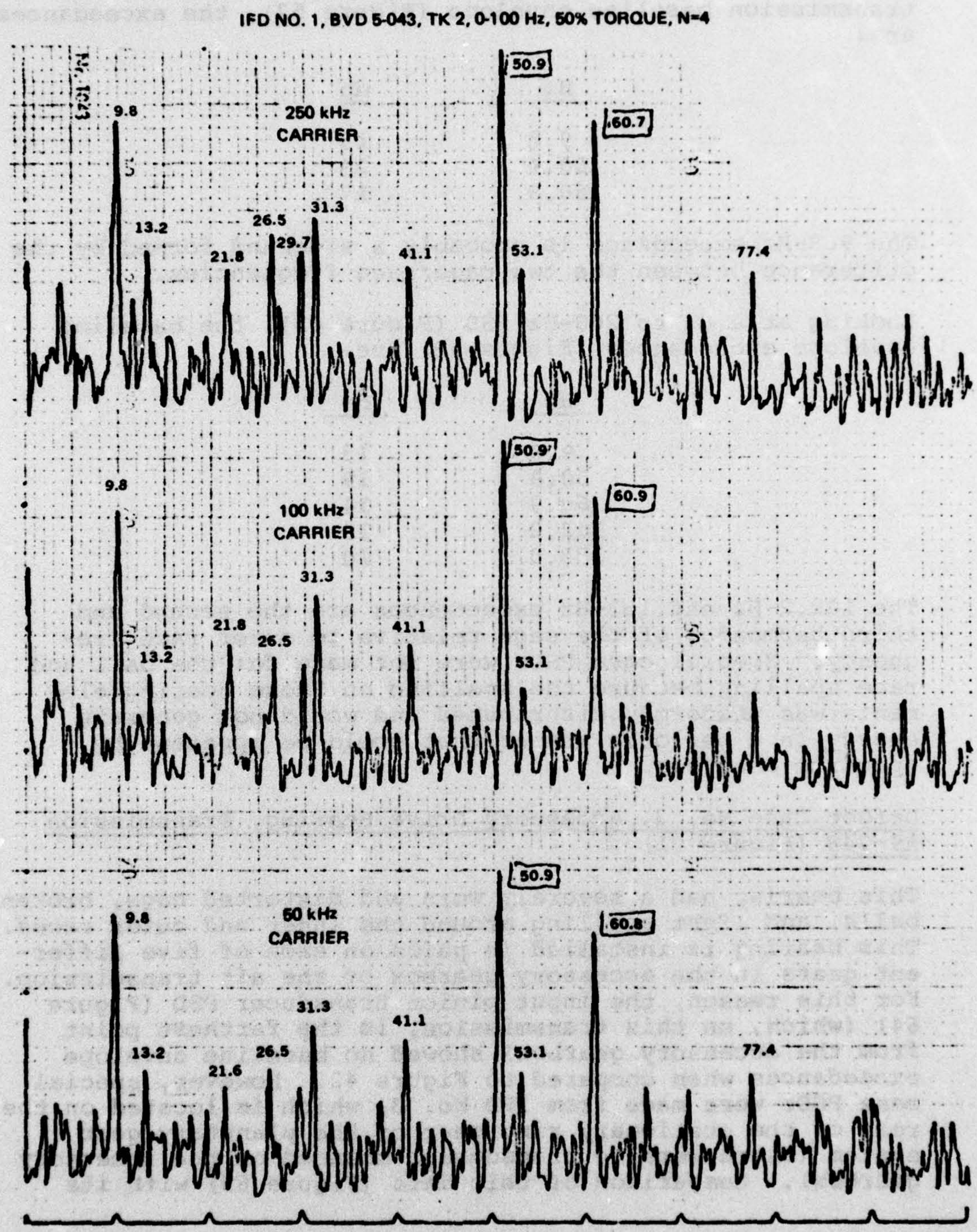

Figure 62. PSD Plot, Defective Transmission A9-856 (0-100 Hz).

PSD (Figure 62) and comparing it to its corresponding four-transmission baseline envelope (Figure 52), the exceedances are:

Hz	db
9.8	13
50.9	23
60.9	17

The 9.8-Hz exceedance is probably a sideband formed by the difference between the two cage/race frequencies.

Looking at a 0- to 200-Hz PSD (Figure 63), the baseline envelope exceedances (Figure 53) are:

Hz	db
9.8	13
50.9	19
60.9	14
102.2	10
153.0	10

The 102.2-Hz and 153-Hz exceedances are the second and third harmonics of the cage relative to outer race frequency. Special case PSDs were not made for the ball and race spalling because the spalling on these bearing elements was uniformly distributed and would not generate energy in a periodic manner that would be apparent by spectrum analysis.

Defect Case No. 3, Accessory Drive Bearing, Transmission A9-748 (Figure 21)

This bearing had a severely worn and distorted cage, broken balls, and light spalling around the inner and outer races. This bearing is installed in pairs on each of five different gears in the accessory gearbox of the aft transmission. For this reason, the input pinion transducer PSD (Figure 64) (which, on this transmission, is the farthest point from the accessory gearbox) showed no baseline envelope exceedances when compared to Figure 42. However, special case PSDs were made from IFD No. 3, which is located on the rear of the stationary ring gear of the planetary gear system (there were no transducers mounted on the accessory gearbox). Comparison of this data (Figure 65) with its

NOTE: Compare to Figure 53

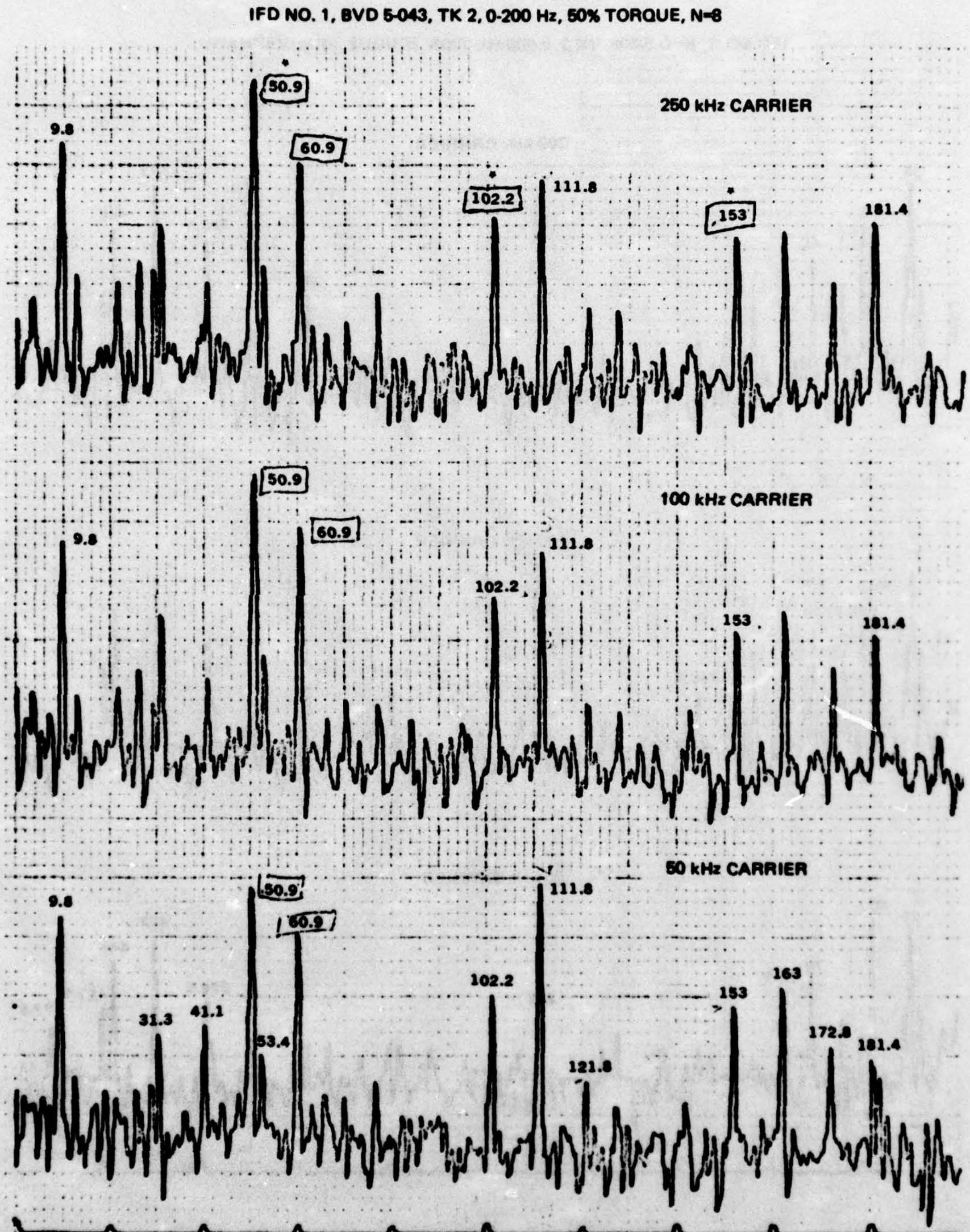

Figure 63. PSD Plot, Defective Transmission A9-856 (0-200 Hz).

NOTE: Compare to Figure 42

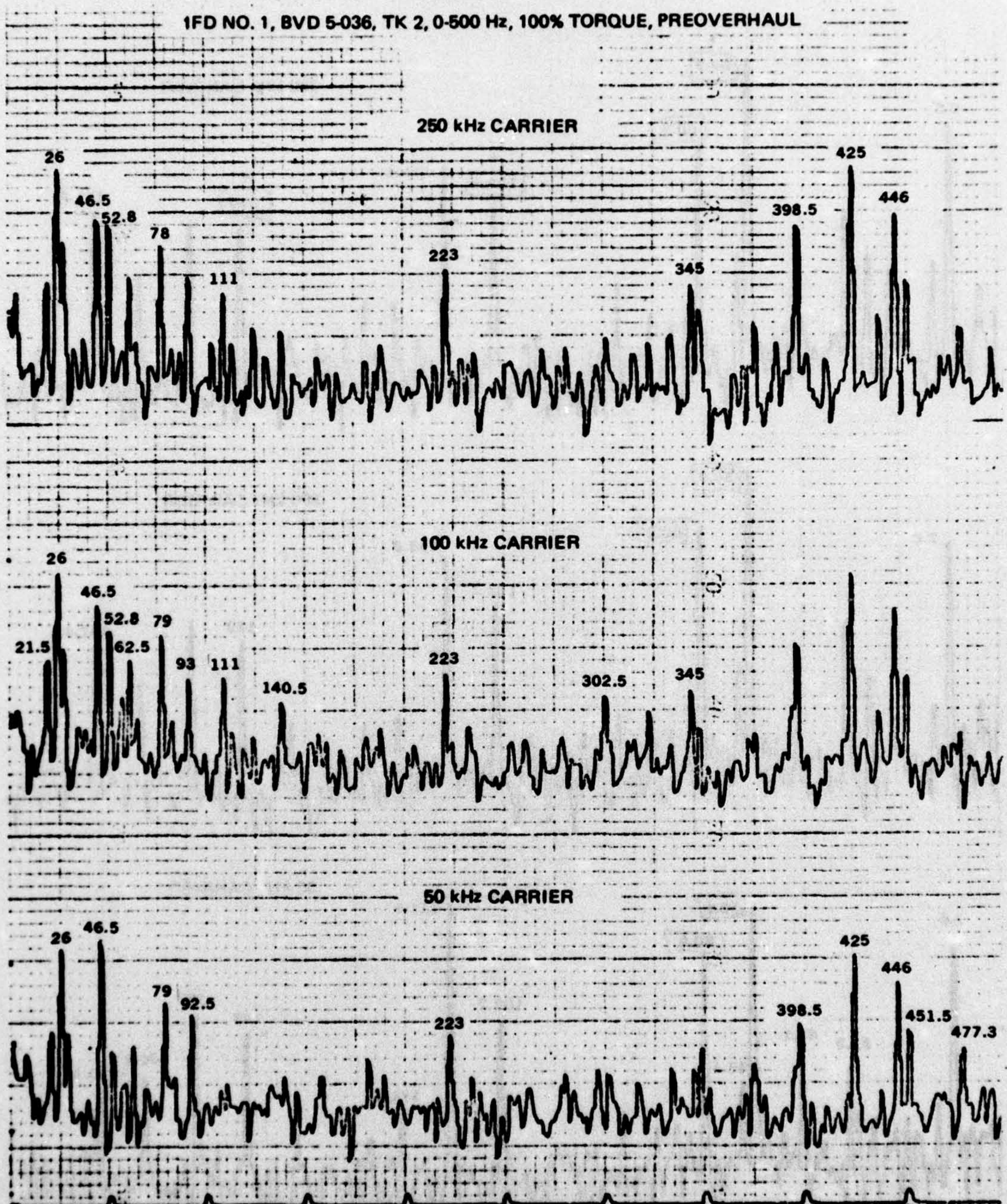

Figure 64. PSD Plot, Defective Transmission A9-748, IFD No. 1.

NOTE: Compare to Figure 55

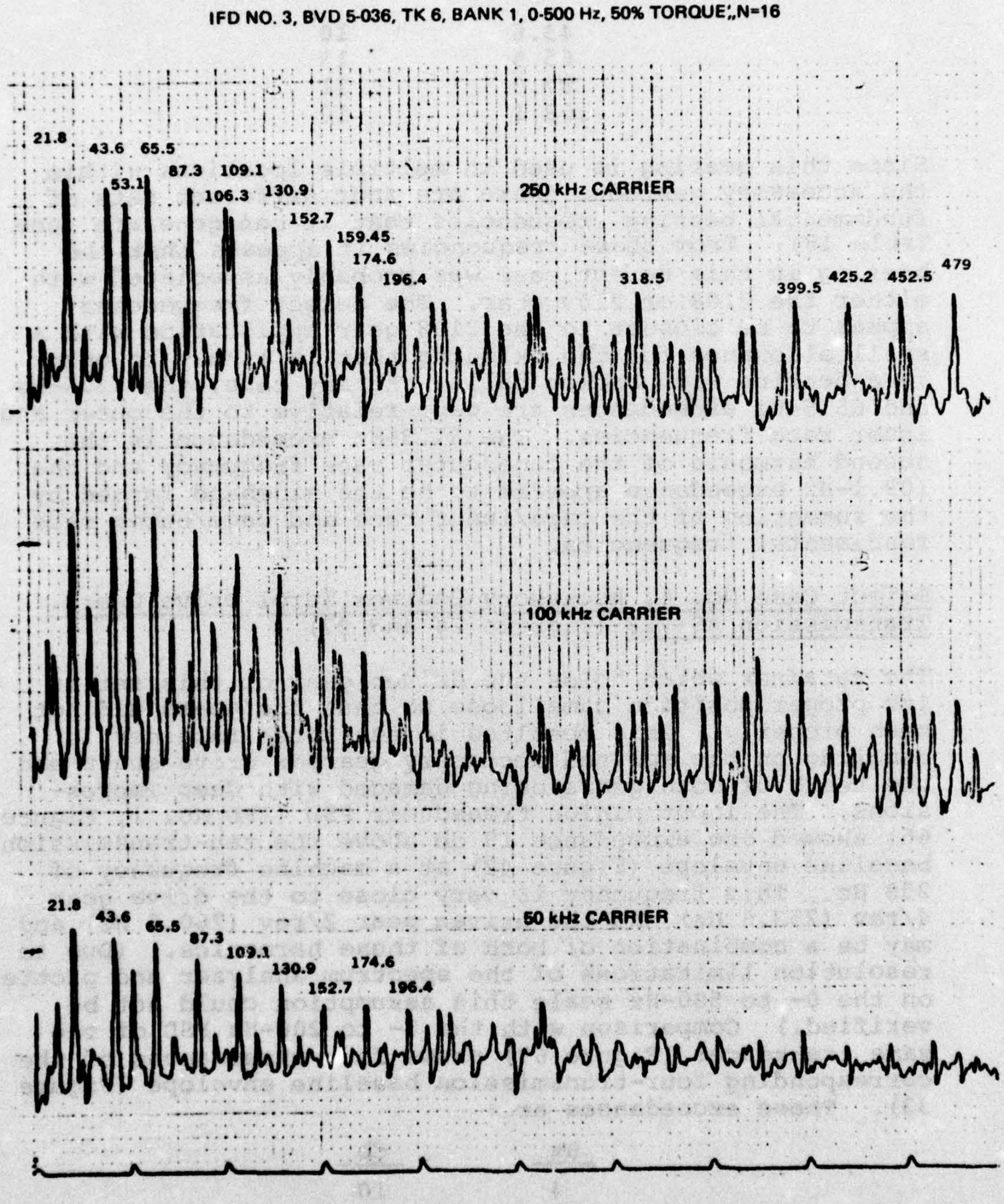

Figure 65. PSD Plot, Defective Transmission A9-748, IFD No. 3.

corresponding four-transmission baseline envelope (Figure 55) showed the following exceedances:

Hz	db
43.6	10
65.5	13
87.3	11
109.1	10

Since this bearing is used in multiple locations within the accessory gearbox, there are four different sets of fundamental bearing frequencies that it can generate (see Table 18). From these frequencies it appears that the bearing in this defect case was probably associated with either the 2108 or 2109 gear. The defect frequencies appear to be closest to the 2108 gear application with a small allowance for the skidding that is likely to occur in a bearing with broken balls. At any rate, the 43.6-Hz and 65.5-Hz exceedances are cage-relative to the outer and inner race frequencies. The 87.3-Hz exceedance is the second harmonic of the cage/outer race frequency and the 109.1-Hz exceedance appears to be the sideband formed by the summation of the cage/inner race and cage/outer race fundamental frequencies.

Defect Case No. 4, Accessory Gearbox Zerol Drive Gears, Transmission A9-728 (Figures 26 and 27)

The retainer which holds the driven gear of this set in its proper position came loose so that the gears did not mesh properly. This resulted in the loose retainer dangling on the splined accessory gearbox drive shaft and the teeth of both gears being damaged with deep impressions. The input pinion transducer PSD (IFD No. 1, Figure 66) showed one exceedance 10 db above the ten-transmission baseline envelope (Figure 42) at a machine frequency of 258 Hz. This frequency is very close to the drive gear 4/rev (253.6 Hz) and the driven gear 2/rev (260.6 Hz) and may be a combination of both of these harmonics. (Due to resolution limitations of the spectrum analyzer and plotter on the 0- to 500-Hz scale this assumption could not be verified.) Comparison with the 0- to 200-Hz PSD of the same transducer (Figure 67) shows four exceedances of the corresponding four-transmission baseline envelope (Figure 53). These exceedances are:

Hz	db
4	10
53	10
79	11
84	11

TABLE 18. 114DS256 ACCESSORY DRIVE BEARING FUNDAMENTAL FREQUENCIES

ASSOCIATED GEAR	FUNDAMENTAL FREQUENCIES - Hz						
	CAGE/ INNER RACE	CAGE/ OUTER RACE	BALL PASSAGE INNER RACE	BALL PASSAGE OUTER RACE	BALL SPIN	BALL DEFECT	SHAFT 1/REV
114D2109	69.6	47.7	695.8	477	303.5	607	117.3
114D2178 or 2110	40.7	27.9	407	279	177.5	355	68.6
114D2108	60.0	41.1	599.2	410.8	261.4	522.7	101
114D2132	34.8	23.9	347.9	238.6	151.8	303.6	58.7

NOTE: Compare to Figure 42

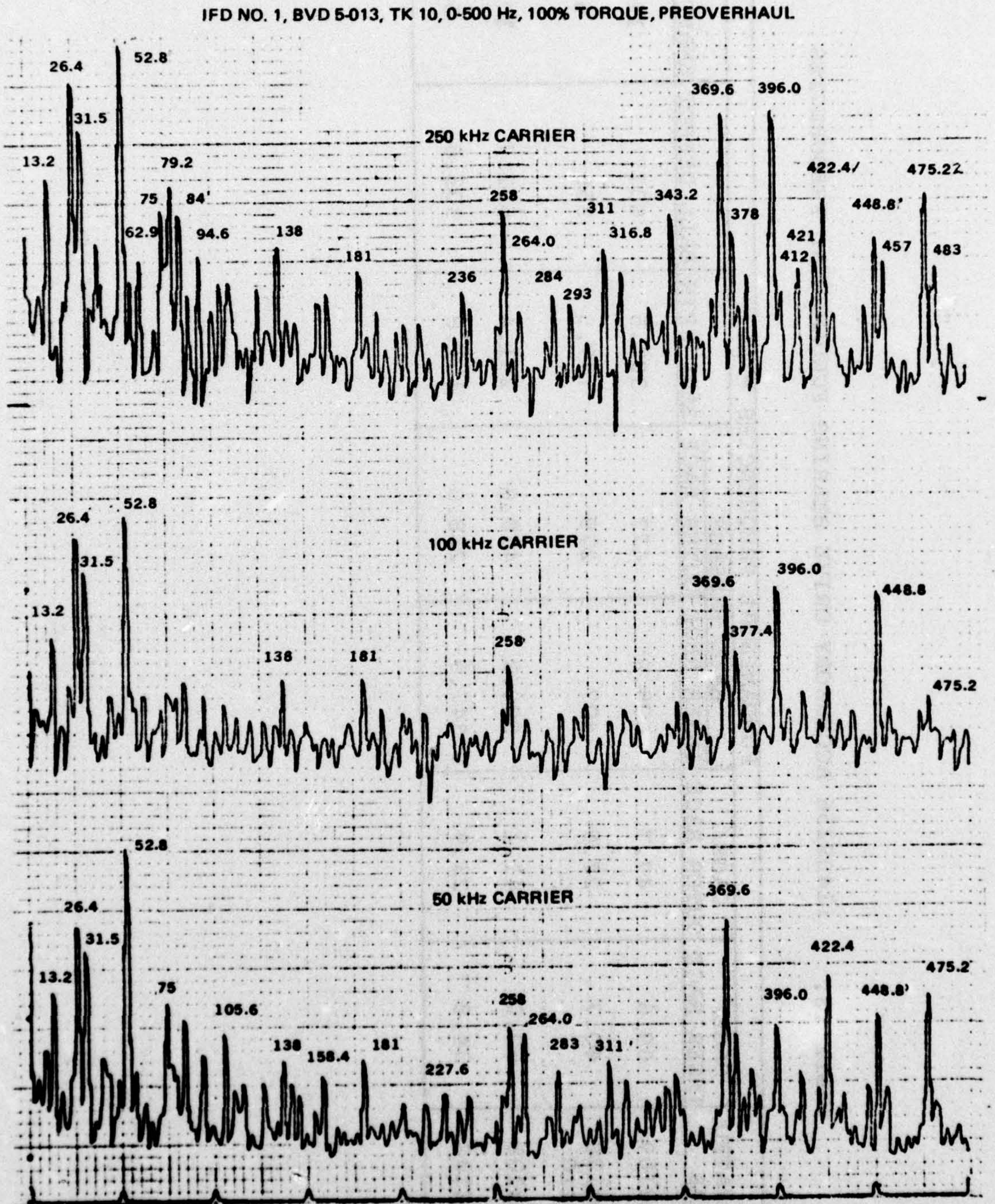

Figure 66. PSD Plot, Defective Transmission A9-728 (0-500 Hz).

NOTE: Compare to Figure 53

IFD NO. 1, BVD 5-013, TK 10, BANK 1, 0-200 Hz, 50% TORQUE, N=8

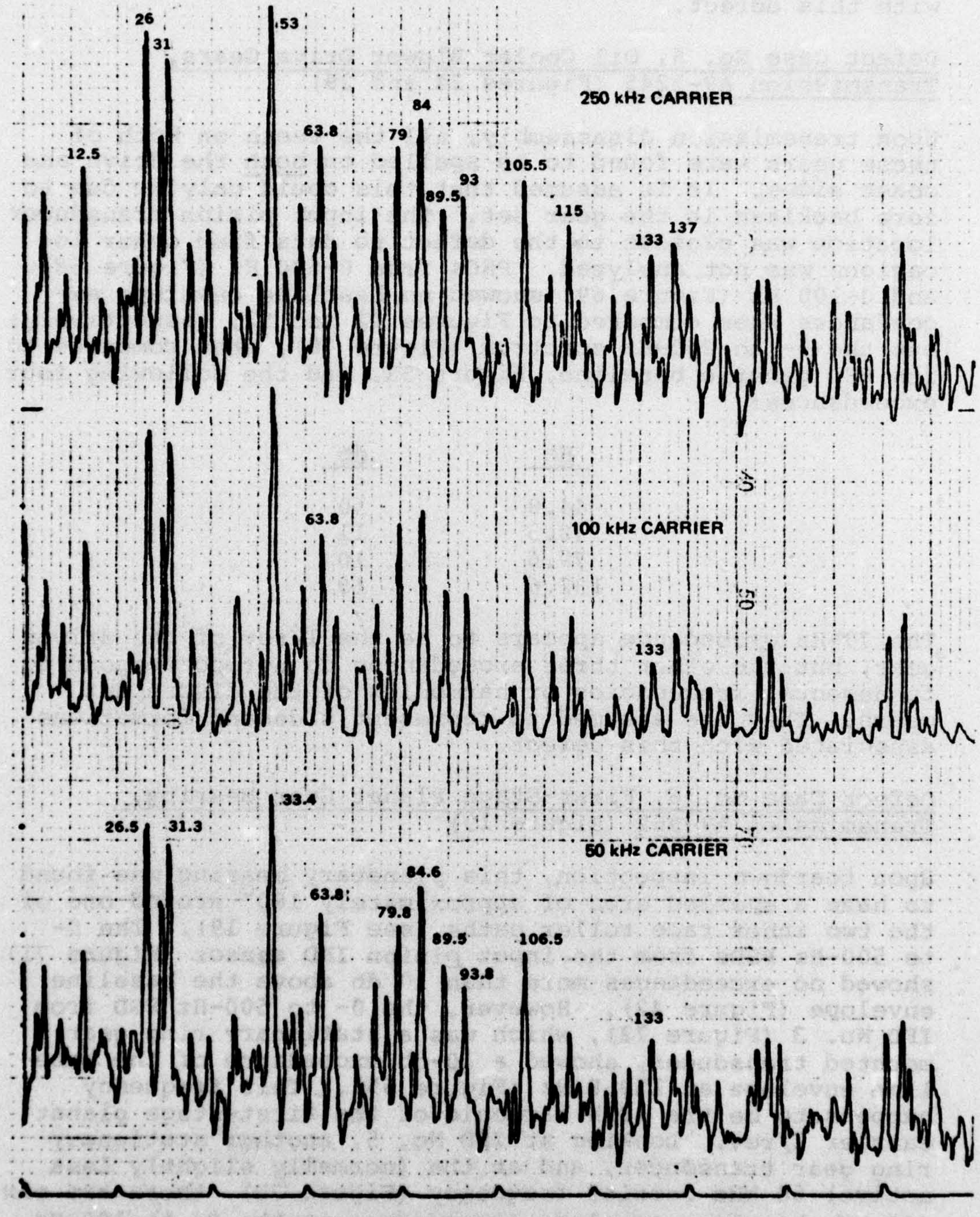

Figure 67. PSD Plot, Defective Transmission A9-728 (0-200 Hz).

None of these frequencies correspond to fundamental frequencies or harmonics of the discrepant gears. It is assumed that they represent sideband formations associated with this defect.

Defect Case No. 5, Oil Cooler Blower Drive Gears, Transmission A9-1245 (Figures 28 and 29)

Upon transmission disassembly, all the teeth on both of these gears were found to be spalled on both the drive and coast sides. It is assumed that this could only be due to zero backlash in the gear set. The input pinion transducer location was closest to the defect so data from other locations was not analyzed. PSDs from 0-500 Hz (Figure 68) and 0-100 Hz (Figure 69) showed no baseline envelope exceedances when compared to Figures 42 and 52, respectively; but the 0- to 200-Hz spectrum (Figure 70), when compared to its PSD generic baseline, Figure 53, had the following four exceedances:

Hz	db
44.0	10
48.5	11
79.6	10
132.6	10

The 79-Hz exceedance appears to be the 1/rev of the driven gear, but the other three exceedances do not correspond to fundamental frequencies or harmonics of the discrepant gears. They are assumed to represent sideband formations associated with this defect.

Defect Case No. 6, First-Stage Planet Gear Bearing, Transmission A9-962 (Figure 19)

Upon teardown inspection, this planetary bearing was found to have a spalled area of approximately 180° around one of the two inner race roller paths (see Figure 19). The 0- to 500-Hz PSDs from the input pinion IFD sensor (Figure 71) showed no exceedances more than 10 db above the baseline envelope (Figure 42). However, the 0- to 500-Hz PSD from IFD No. 3 (Figure 72), which was a stationary ring gear mounted transducer, showed a 10-db exceedance of the baseline envelope at 159.8 Hz (Figure 55). This frequency happens to be the 12th harmonic of the first-stage planet carrier 1/rev. Looking at IFD No. 5, another stationary ring gear transducer, and at the (normally slightly less active) 50 kHz carrier frequency (Figure 73), there are six 250-kHz baseline envelope exceedances in the 0- to 100-Hz spectral range, when compared to Figure 56.

NOTE: Compare to Figure 42

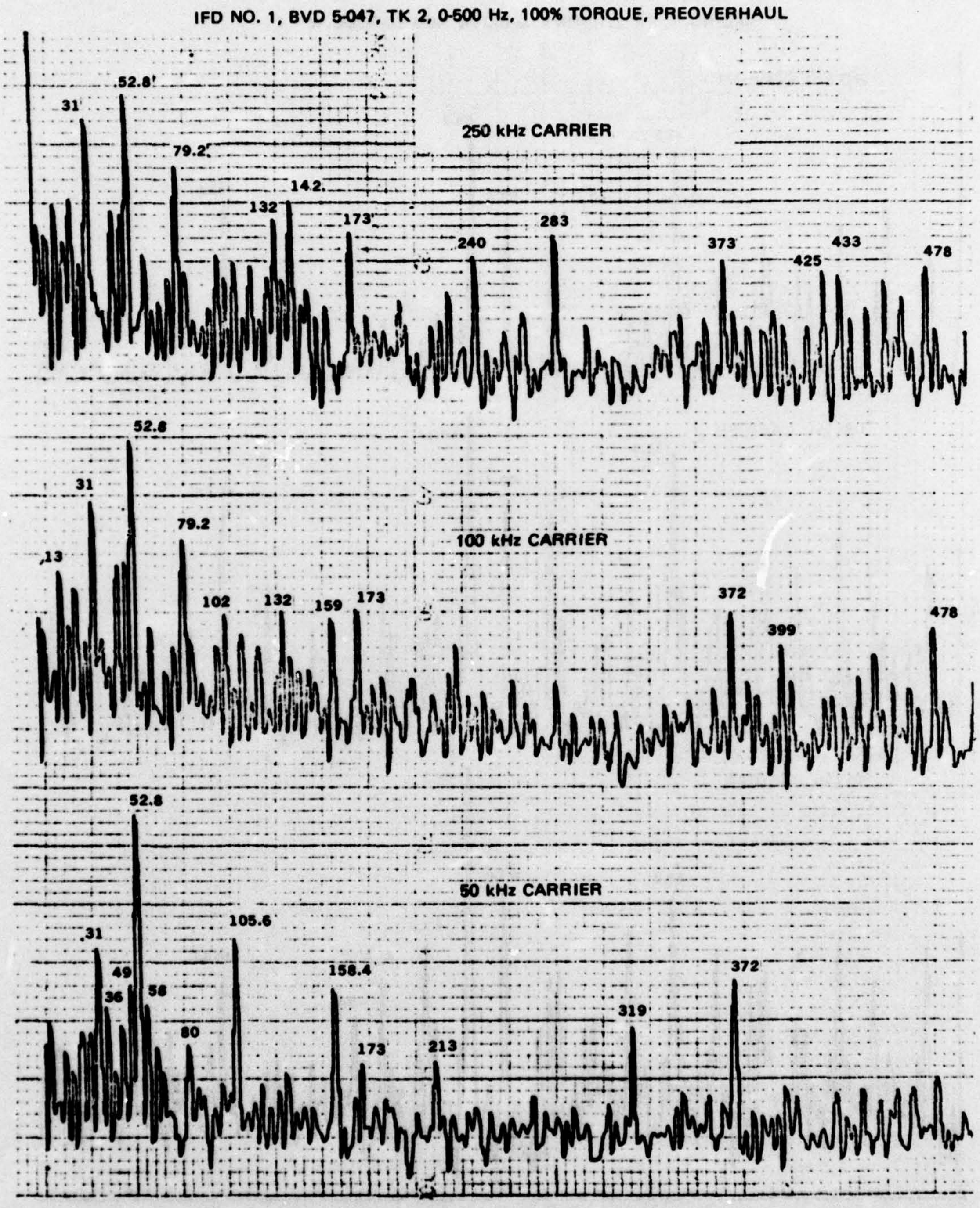

Figure 68. PSD Plot, Defective Transmission A9-1245 (0-500 Hz).

NOTE: Compare to Figure 52

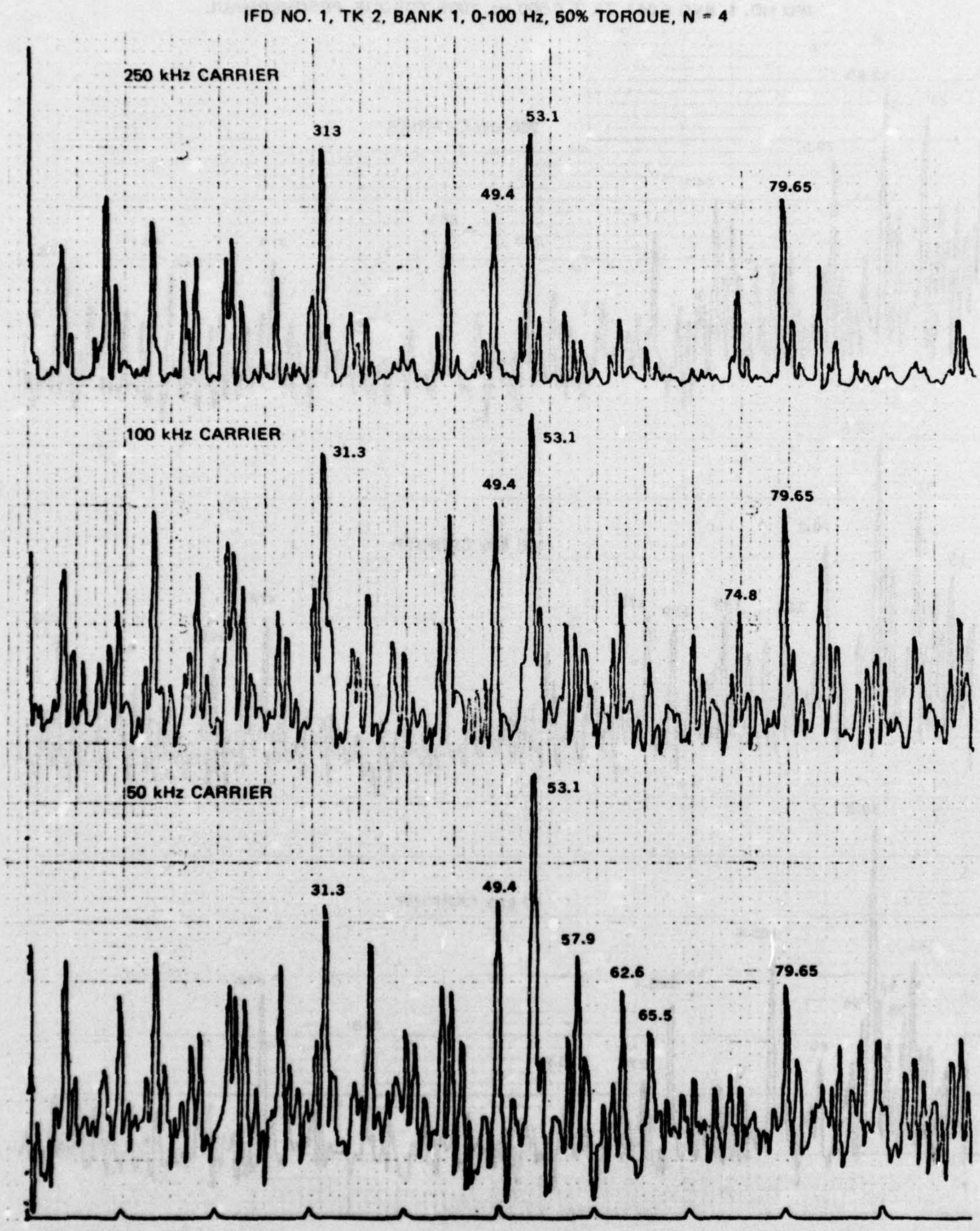

Figure 69. PSD Plot, Defective Transmission A9-1245 (0-100 Hz).

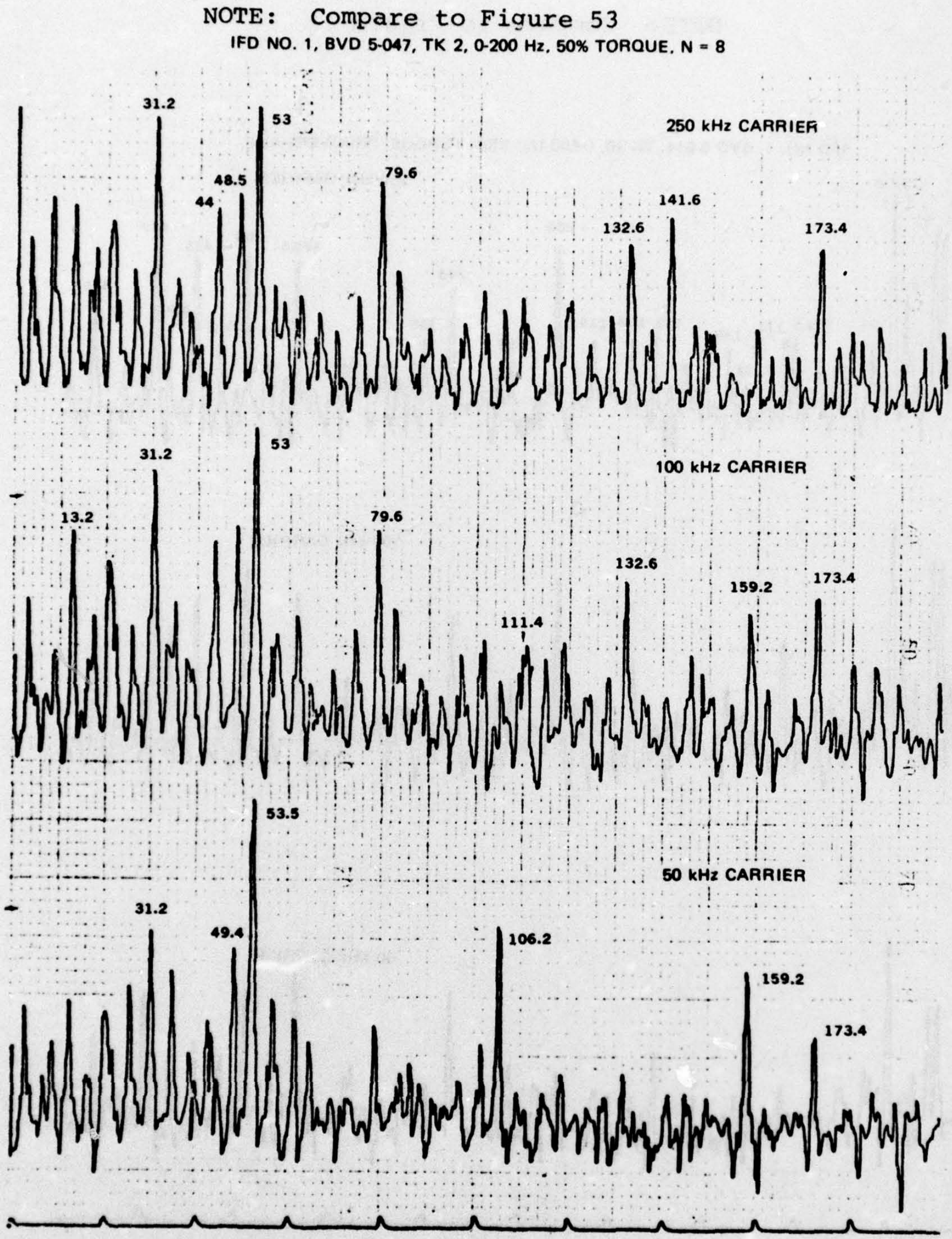

Figure 70. PSD Plot, Defective Transmission A9-1245 (0-200 Hz).

NOTE: Compare to Figure 42

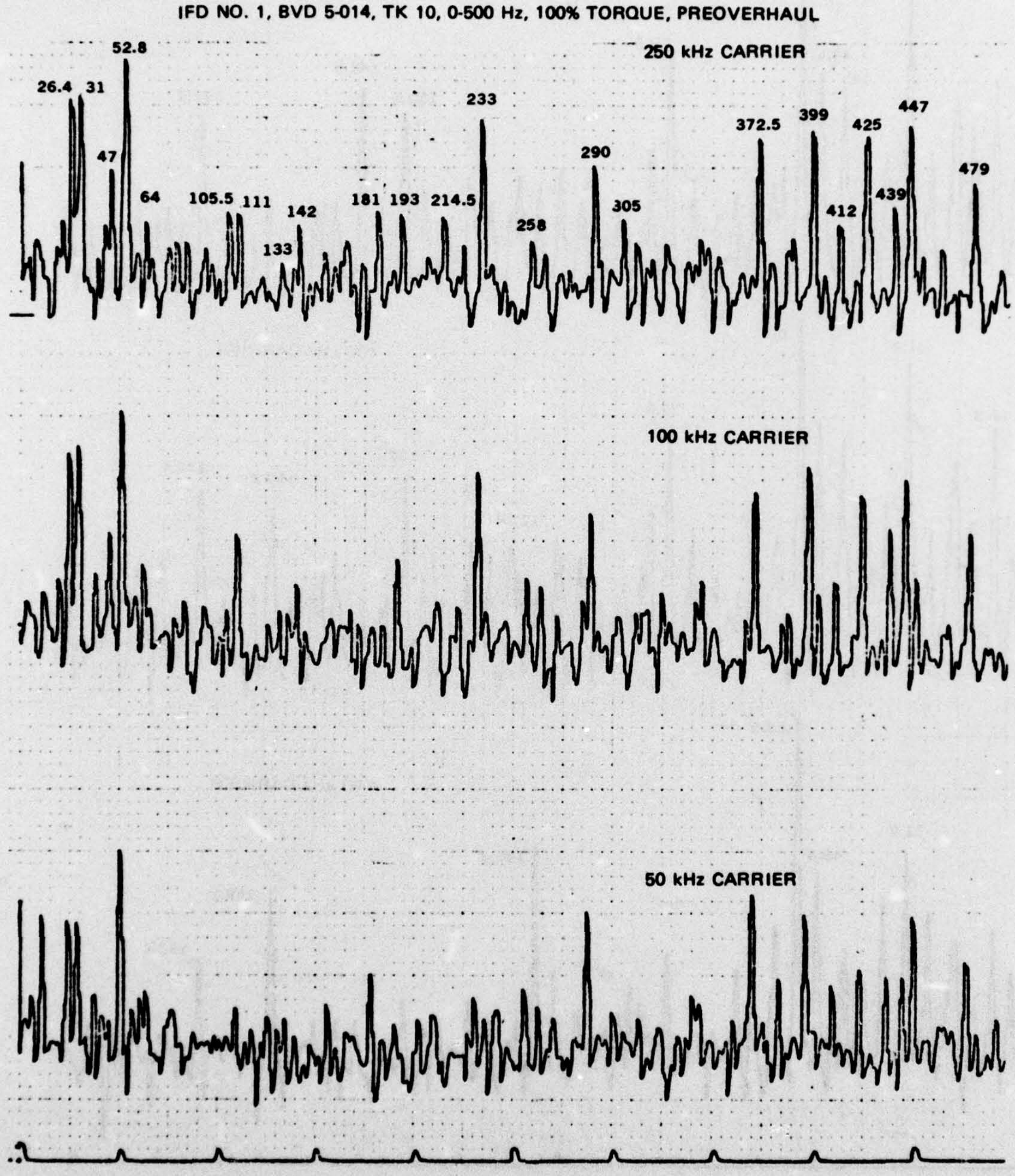

Figure 71. PSD Plot, Defective Transmission A9-962, IFD No. 1.

NOTE: Compare to Figure 55, page 101

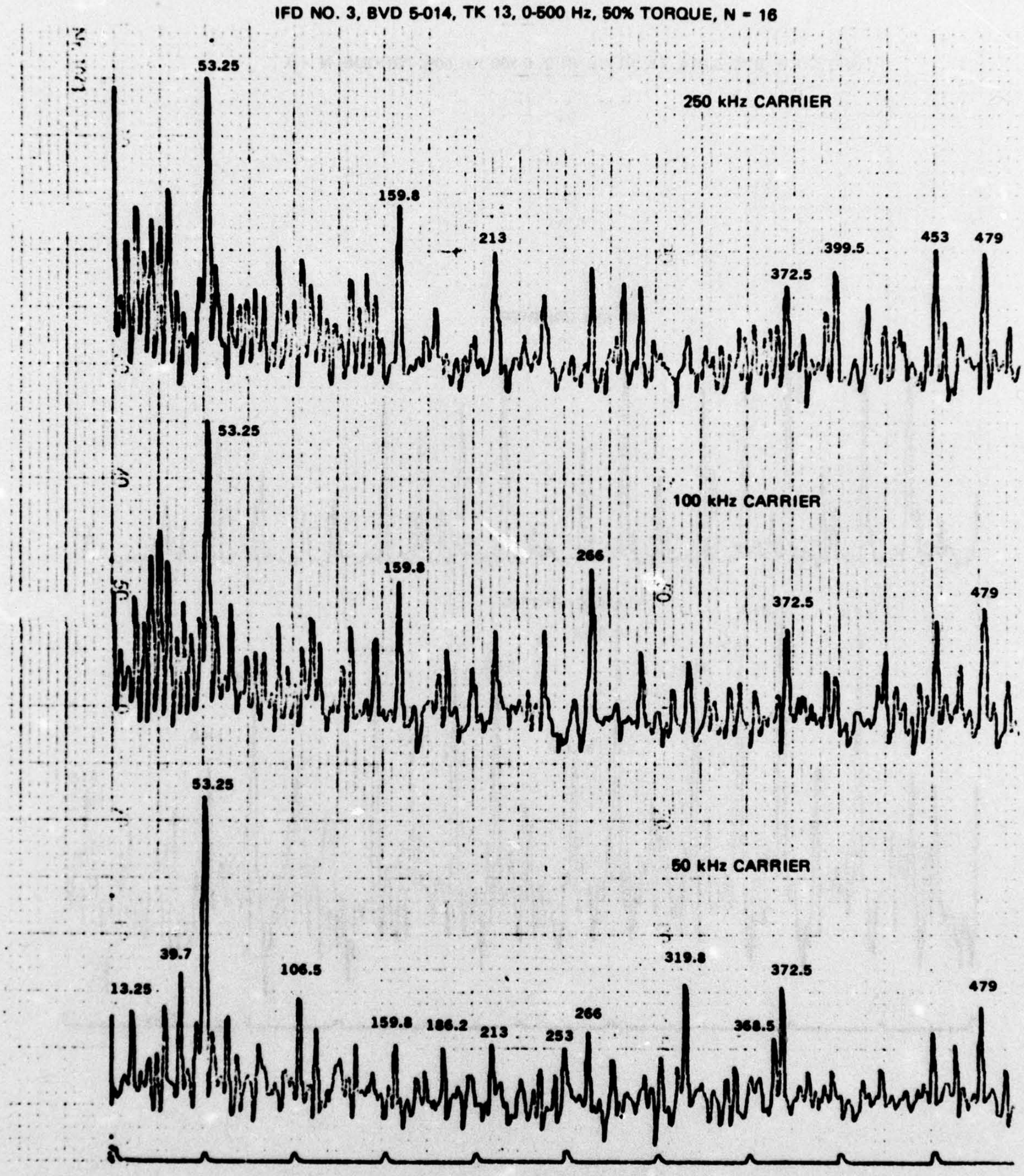

Figure 72. PSD Plot, Defective Transmission A9-962, IFD No. 3.

NOTE: Compare to Figure 56

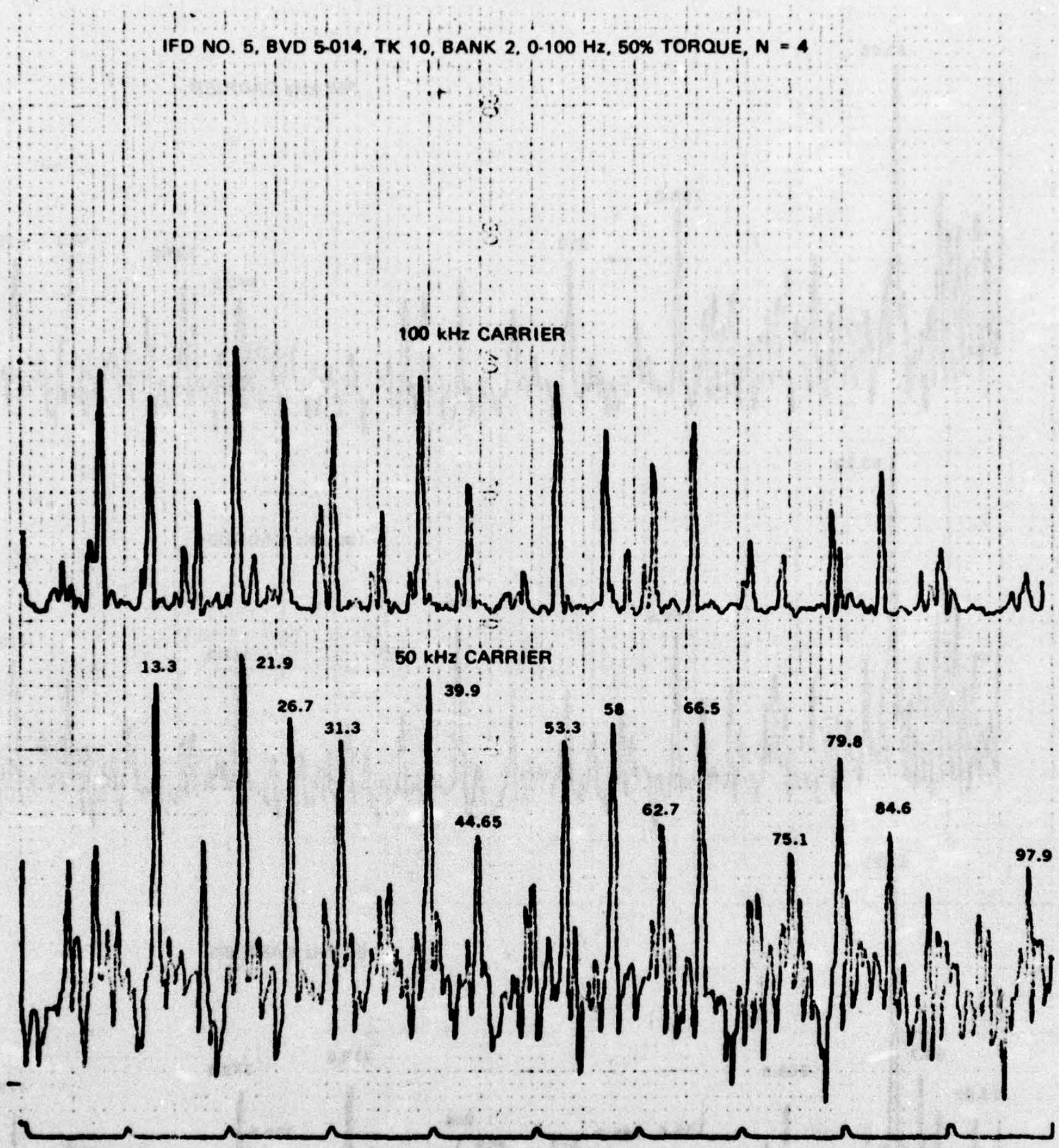

Figure 73. PSD Plot, Defective Transmission A9-962, IFD No. 5.

Hz	db	Cause
13.3	10	1st-Stage Carrier 1/rev
39.9	13	1st-Stage Carrier 3/rev
44.7	13	Sideband: 66.5 - 21.9
66.5	17	1st-Stage Carrier 5/rev
79.8	17	1st-Stage Carrier 6/rev
97.9	10	Sideband: 66.5 and 31.3

Four of these six exceedances, 13.3 Hz, 39.9 Hz, 66.5 Hz, and 79.8 Hz, are the first, third, fifth, and sixth harmonics of the first-stage planet carrier. The remaining two exceedances appear to be sidebands formed by the first-stage planet carrier harmonics and the normally high amplitude peaks at 21.9 Hz and 31.3 Hz.

Defect Case No. 7, Second-Stage Planet Bearing, Transmission S/N A9-724 (Figure 17)

Upon teardown inspection, this planetary bearing was found to have two spalled areas: one approximately 180° around one of the two inner race roller paths, and one approximately 45° around the other inner race roller path (see Figure 17). The input pinion IFD data (Figure 74) showed no significant baseline exceedances when compared with Figure 42. Neither were there any abnormalities in data from the stationary ring gear transducers (Figure 75 for IFD No. 2 is typical) when compared to Figure 54. With respect to high frequency vibration data, this transmission appeared to be in good condition.

VIBRATION SUMMARY

Detection Capability

Six out of the seven defects (85.7%) examined by high frequency vibration analysis were detectable. Of the six detectable defects, three produced baseline envelope exceedances of more than 10 db at fundamental defect frequencies, and all six produced similar amplitude baseline exceedances at what have been referred to as sideband frequencies. The failure of the 2nd-stage planet bearing (Case No. 7) was not detected.

Endevco Sensor Data

To illustrate that signals from other commercially available transducers can also be processed by the high frequency vibration analysis technique, data was obtained from Endevco 6230M8 transducers mounted in the same general areas as the IFD sensors. The data from the Endevco transducers was recorded (without bandpass-filtering or demodulation) directly onto tape running at 15 ips. This data was then post-processed

NOTE: Compare to Figure 42

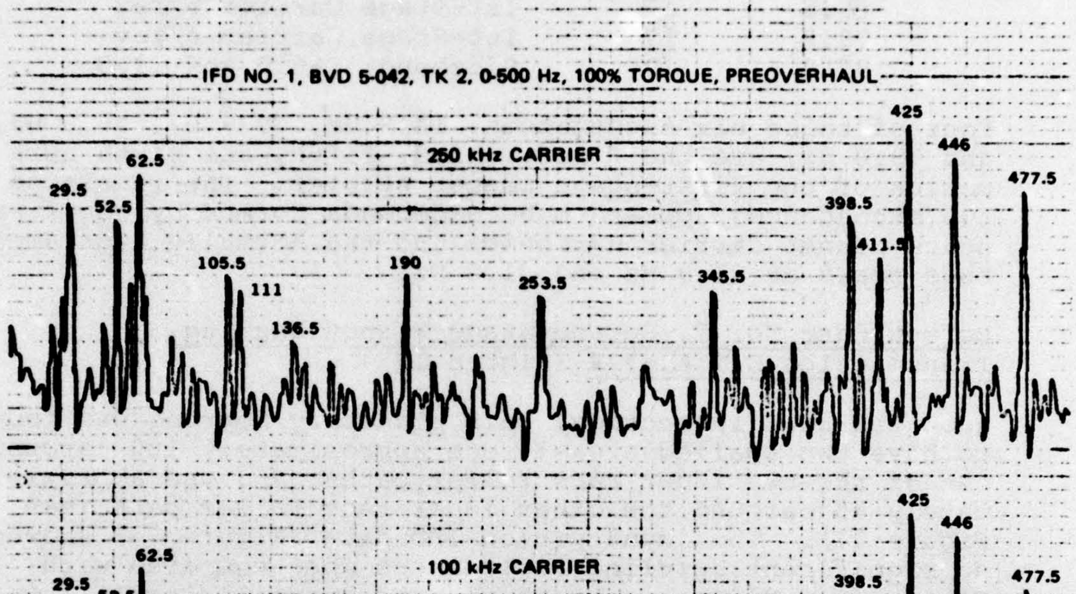

Figure 74. PSD Plot, Defective Transmission A9-724 (0-500 Hz).

NOTE: Compare to Figure 54

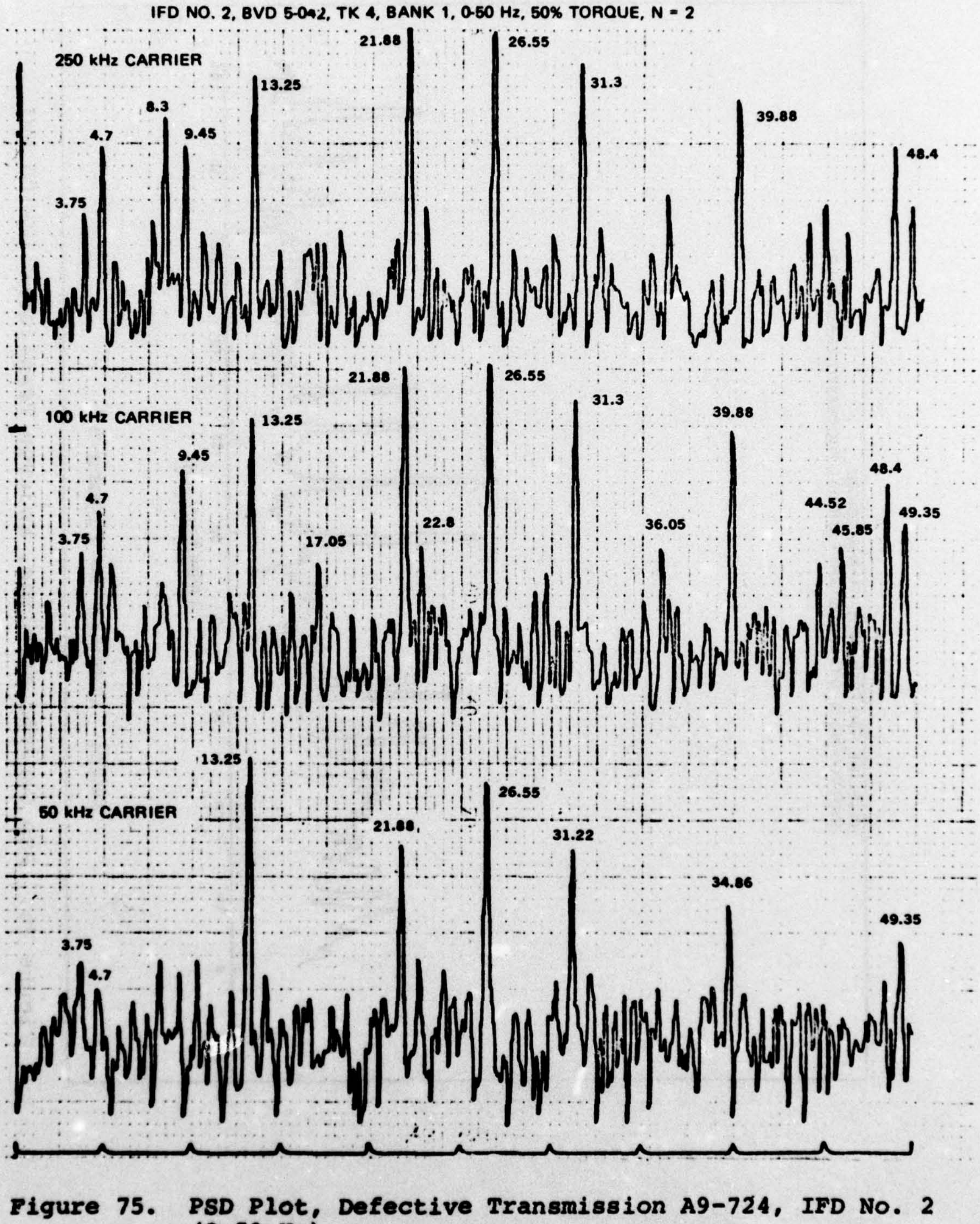

Figure 75. PSD Plot, Defective Transmission A9-724, IFD No. 2 (0-50 Hz).

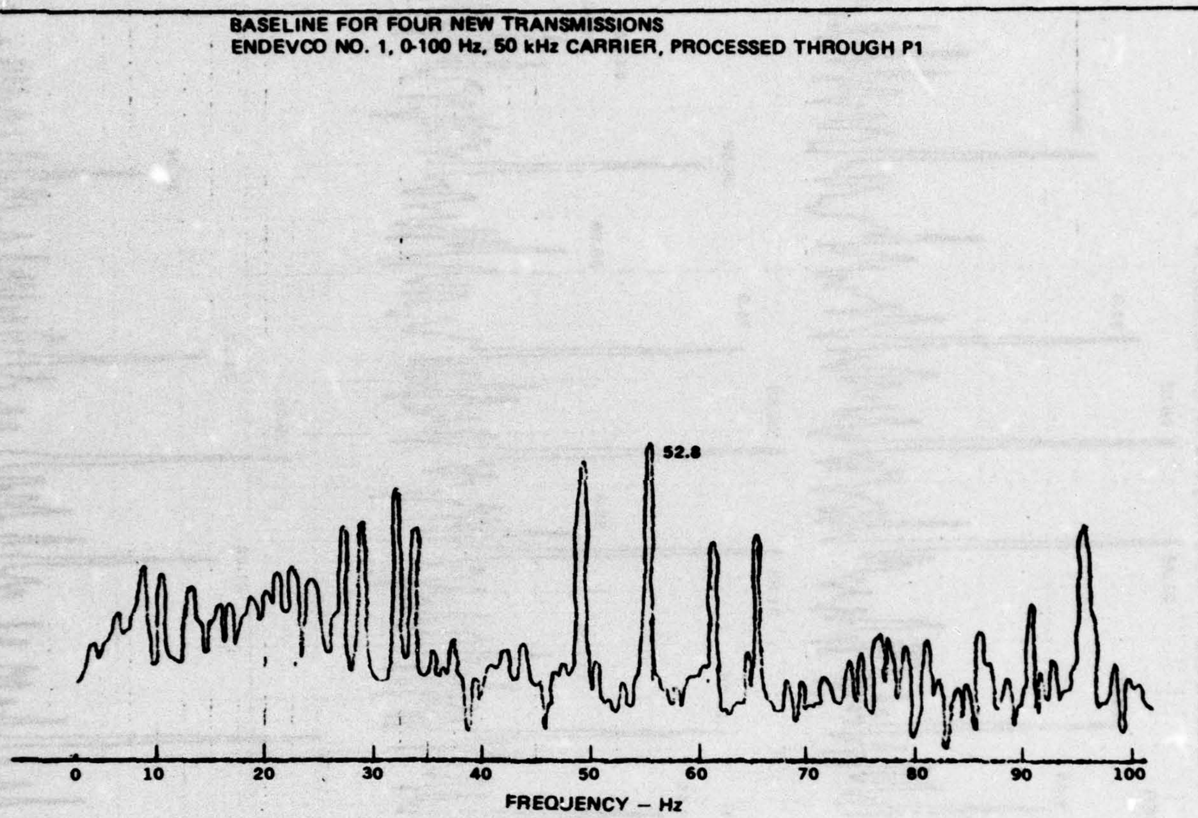

NOTE: Compare to Figure 52

Figure 76. PSD Generic Baseline, Endevco Transducer (0-100 Hz).

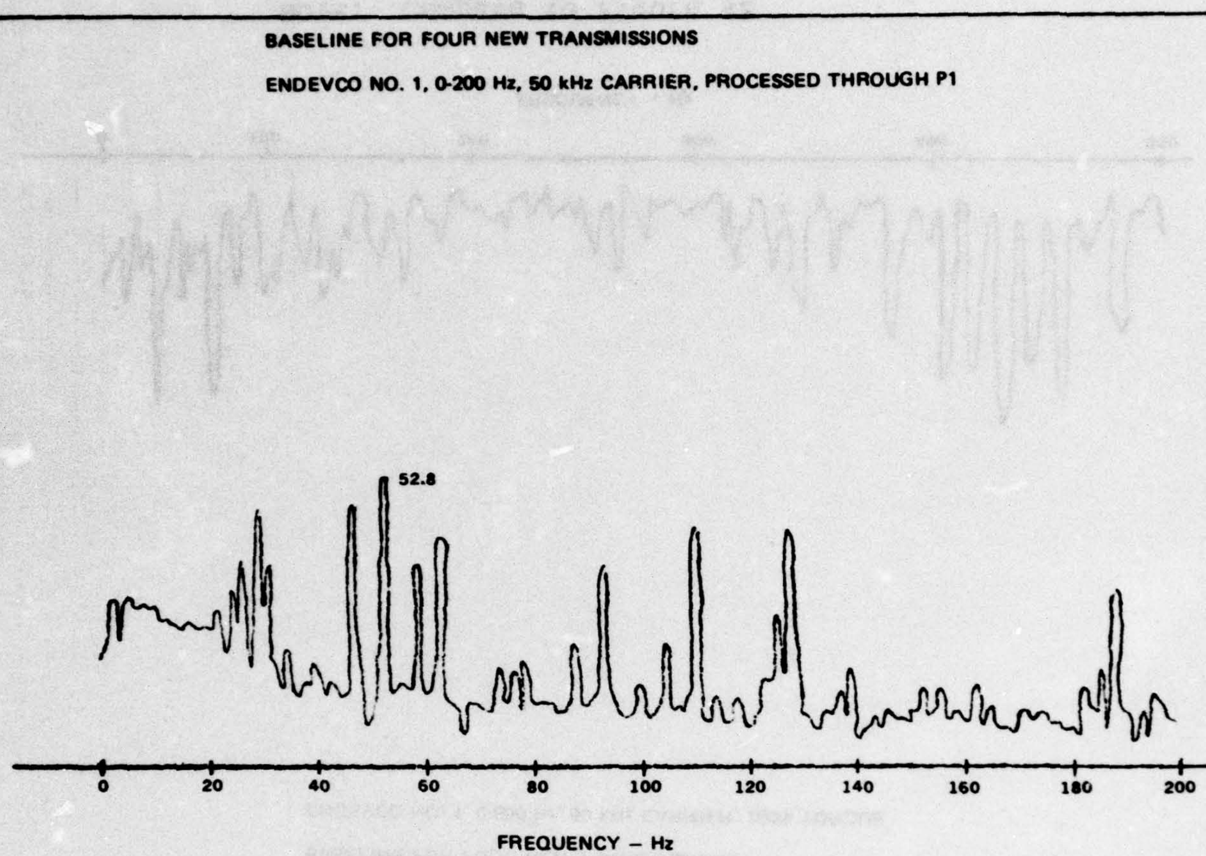

NOTE: Compare to Figure 53

Figure 77. PSD Generic Baseline, Endevco Transducer (0-200 Hz).

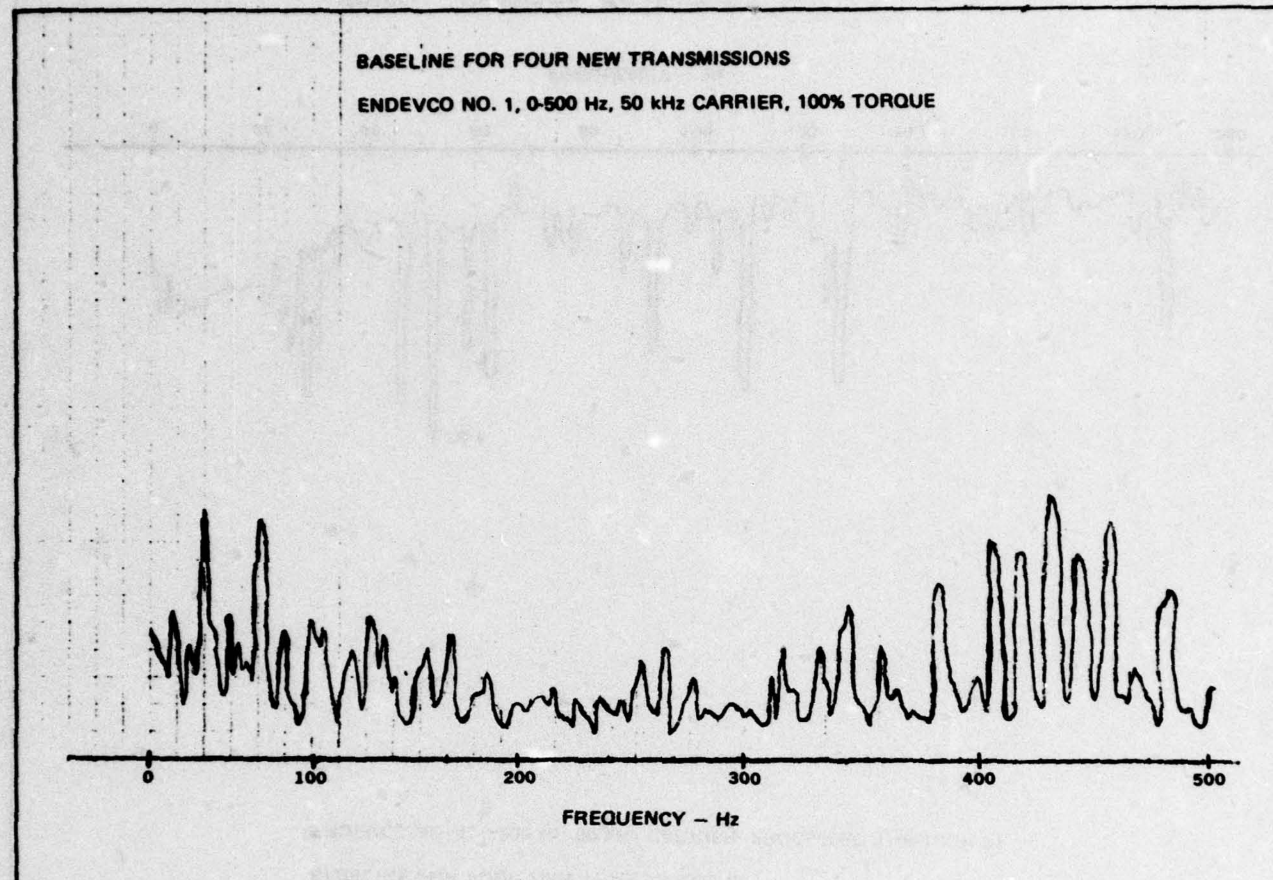

NOTE: Compare to Figure 42

Figure 78. PSD Generic Baseline, Endevco Transducer (0-500 Hz).

through the same bandpass filter and demodulation circuitry as had been used for the IFD sensor data. Due to the frequency response limitations of the tape recorder, only 50 kHz carrier frequency data could be obtained from the direct-recorded Endevco data. Figures 76, 77, and 78 are the 0- to 100-Hz, 0- to 200-Hz, and 0- to 500-Hz baseline envelopes of the Endevco No. 1 transducer located on the aft transmission input pinion near IFD No. 1 (refer to Figure 5). Thus, these Endevco baseline envelopes correspond most closely with the IFD baseline envelopes of Figures 52, 53, and 42 respectively, although the IFD envelopes were for 250-kHz carrier frequency data. However, the best comparison of IFD and Endevco data is for a discrepant condition such as the bearing in defect case No. 2. Figures 79 and 80 are comparison PSDs over the 0- to 100-Hz and 0- to 200-Hz spectral ranges for both the Endevco and IFD transducers that were located on the input pinion. All this data is at a 50-kHz carrier frequency and 50% torque level with the same bearing defect present. It is obvious from an inspection of these PSDs that both transducer types produced significant peaks of roughly the same relative amplitudes at the fundamental defect frequencies (50.9 Hz and 60.9 Hz), their harmonics (102 Hz, 122 Hz, 153 Hz, and 182 Hz), and at the 9.8-Hz sideband (60.9 - 50.9).

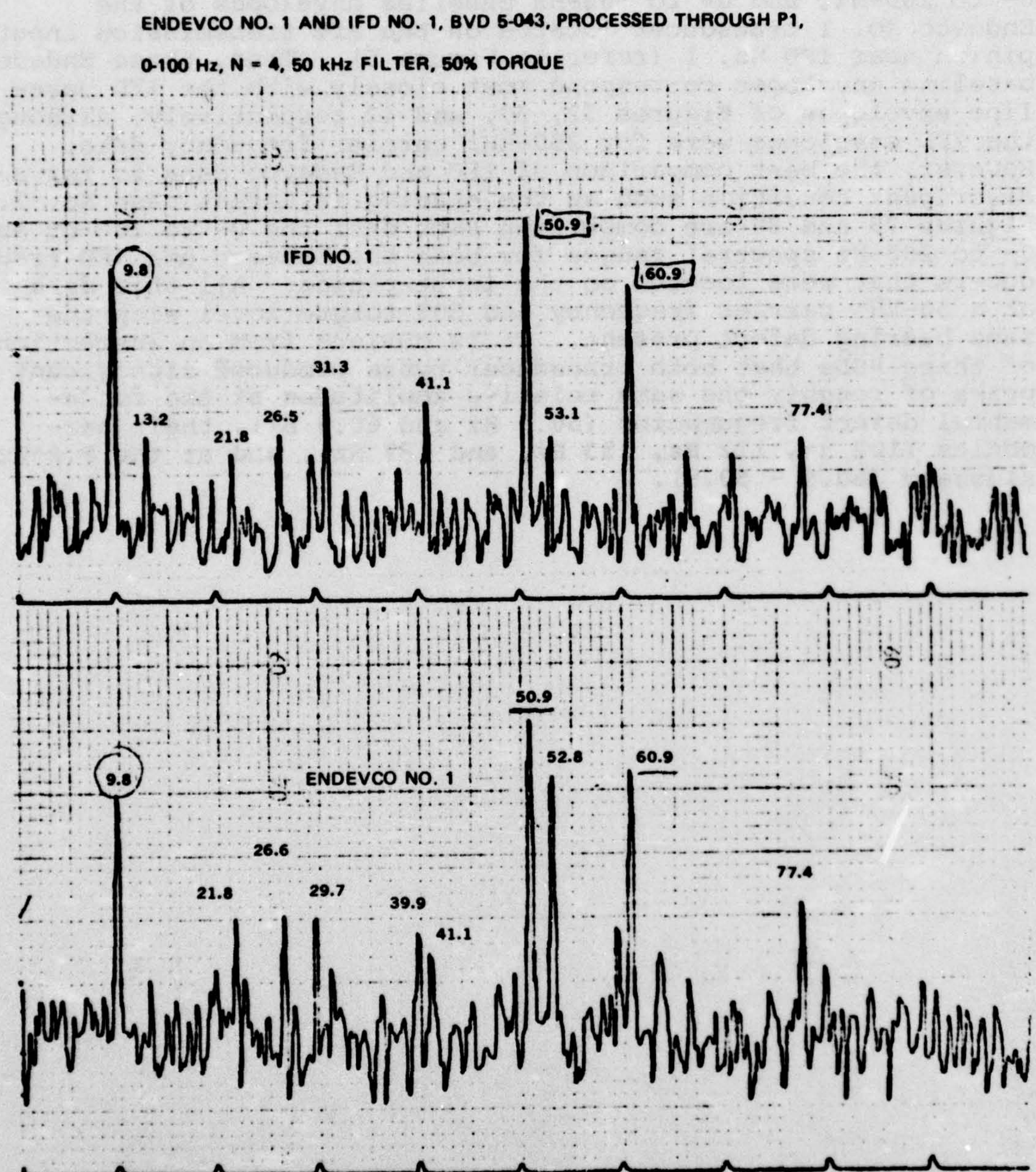

Figure 79. Endevco/IFD PSD Correlation, Transmission A9-856 (0-100 Hz).

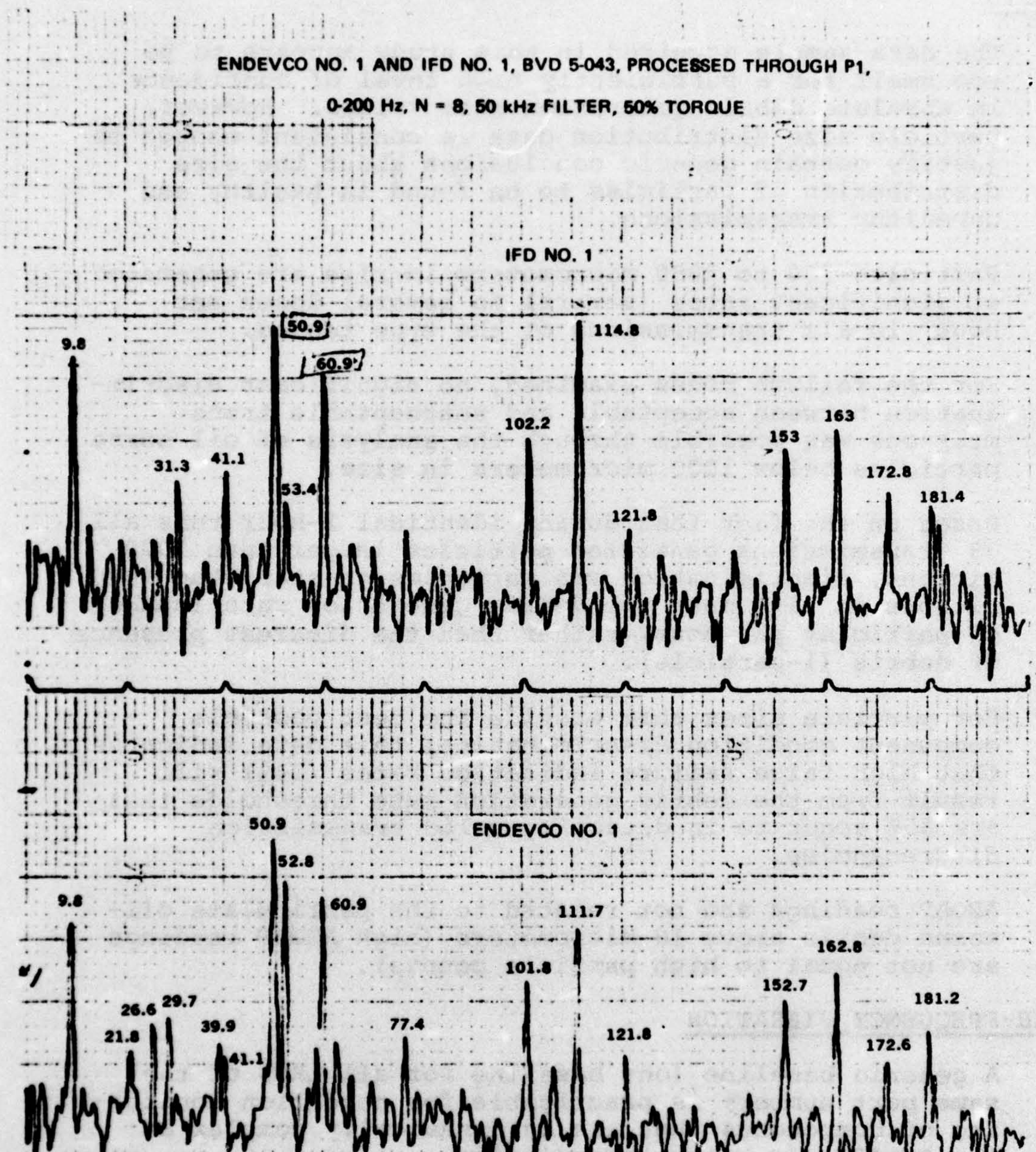

Figure 80. Endevco/IFD PSD Correlation, Transmission A9-856 (0-200 Hz).

CONCLUSIONS

DEBRIS

1. The data sample acquired in this study appears to be too small for a sufficiently high level of confidence in absolute debris generation rate values. However, particle size distribution data is consistent enough to justify certain generic conclusions about the size distribution of particles to be found in healthy and unhealthy transmissions.

2. Particles 750 to 2000 micrometers in size are generated at significant rates (several to several dozen per hour) in all transmissions of the type tested.

3. For the failure modes examined, no significant discrimination between acceptable and unacceptable transmissions was possible through the analysis of oil borne particles below 1000 micrometers in size.

4. Based on the fact that during identical 2-hour runs all 38 transmissions generated particles larger than 1000 microns, discrimination via particles greater than 1000 microns in size must use debris generation rate (number of particles per hour) rather than the discreet presence of debris (1-particle).

5. For particle sizes that provide the best possible component condition discrimination, this data indicates that high false failure indication rates (54%) will result from the debris generation rate thresholds that are 85% accurate in detecting valid transmission discrepancies.

6. ASOAP readings are not related to the particulate oil-borne debris above 10 micrometers (high ASOAP readings are not equal to high particle counts).

HIGH-FREQUENCY VIBRATION

1. A generic baseline (one baseline for all LRUs of the same part number) is practicable for condition monitoring of components that are as dynamically complex as the CH-47C aft rotor transmission.

2. Although the number of test cases analyzed in this study (four acceptable and seven unacceptable) does not allow high level of confidence estimates of diagnostic accuracy values, initial estimates are good: 85.7% of the unacceptable test cases were detected, and there were no false failure indications.

3. For the limited amount of comparative data analyzed, the fault discrimination capability of the high frequency vibration analysis technique appears to be essentially equivalent for both IFD Model 253 and Endevco Model 6230M8 transducers.

4. The design anomolies of the planetary gear system in a CH-47C rotor transmission contribute significantly to the dynamic signature complexity and to the frequent occurrence of high amplitude PSD sidebands.

5. For the IFD sensor, the 250-kHz carrier frequency appears to be the best of the three carriers evaluated for diagnosing the condition of the CH-47C aft rotor transmissions. However, the 50-kHz and 100-kHz data appears to indicate that these carrier frequencies could also be used effectively for high frequency vibration analysis.

RECOMMENDATIONS

DEBRIS

Conduct a filter collection debris analysis program using filters with a minimum of 10 hours of operation, preferably 50 hours. Debris analysis should be performed on both failed and unfailed transmissions. This can be accomplished in three ways.

1. A dedicated test stand utilizing a known acceptable transmission. Implants could be installed and run for a desired interval. Conditions in the test stand environment can be closely controlled and monitored.

2. Monitor in-service transmissions with filter removals at the time the transmission's filter is due for inspection (50 hours). The activity selected would have to be one which has close aircraft monitoring, preferably a test activity (Ft. Rucker). After removal, the transmission's teardown evaluation would have to be monitored and correlated with the debris results.

   The selection of the number of components monitored is discretionary but should include a minimum of 10-20 transmissions.

3. Select an activity which will have the capability of providing at least 100 transmissions for a program similar to this program. Test stand time should be increased to a minimum of 10 hours per transmission. Component disassembly should be monitored and correlated as above.

The debris analysis should be performed with the following considerations.

1. Only metallic particles should be quantified.

2. All debris should be recovered for future shape and composition analysis as required.

3. Particle size distribution above 2500 micrometers should be quantified (up to 10,000 micrometers at a minimum).

4. ASOAP analysis should be performed only on those aircraft where finer filtration levels (less than 10 micrometers) have not been or will not be incorporated.

5. Filter cleaning procedures should be carefully documented and standardized.

The objectives of such a program would be to continue the definition of the particle size distributions of "failed" and "unfailed" units. At this point it appears that it is more important to define the distributions of unfailed transmissions rather than of failed transmissions. This is because the high degree of scatter (wide distributions) of debris revealed by this study suggests that the ultimate effectiveness of debris as a diagnostic's tool lies more in controlling the erroneous signals rather than in its ability to detect failures. Therefore, the debris signatures of unfailed boxes should receive higher attention.

Nevertheless, most of the recommended programs would, in the course of their execution, encounter failures which would also allow failure distribution characteristics to be defined.

VIBRATION

Conduct a vibration analysis program as follows:

1. The same analysis that was conducted for the detection capability of the high frequency technique with IFD sensors should be conducted for the Endevco transducers (only one discrepancy case was analyzed for comparison purposes during the course of this study).

2. An analysis of the sensitivity of high frequency vibration results to transmission torque levels should be carried out. The raw data for such an analysis has been collected in the course of this program.

3. The forward transmission data should be reduced and analyzed for its similarity to aft transmission data.

4. The sensitivity of high frequency fault detection capability to carrier frequency should be assessed by a full analysis of the 50-kHz and 100 kHz demodulated carrier data.

5. Some on-aircraft field data should be collected inflight and during ground run, then analyzed to assess its similarity to the test cell baselines contained in this report.

6. **The undemodulated high frequency data contained on tape from the transmissions in this study should be analyzed to assess the fault detection capability of aperiodic spikes and the rms level of high frequency energy (which were eliminated by demodulation and spectrum analysis in the data-reduction procedure employed herein).**

REFERENCES

Harris, Tedric, ROLLING BEARING ANALYSIS, John Wiley and Son, Inc., 1966.

Palmgren, Arvid, Dr., Eng., BALL AND ROLLER BEARING ENGINEERING, Third Edition, S. H. Burbank and Co., Inc., 1959.

APPENDIX A

CH-47C FORWARD AND AFT TRANSMISSION

BEARING AND GEAR FREQUENCY DERIVATION

GEAR MESH FREQUENCIES

The gear frequencies noted in Tables 5 and 6 were derived as follows:

Simple Gear Trains

$F = N \times Z$

where N = speed of rotation of driver (driven gear)
Z = number of teeth of driver (driven gear)

Planet and Sun Gears

$f = (N_1 - N_2) \times Z$

where N_1 = speed of rotation of sun gear
N_2 = speed of rotation of planet gear about the center of the sun gear
Z = number of teeth of sun gear

Planet and Fixed Ring Gear

$f = (N_2 + N_3) \times Z$

where N_2 = speed of rotation of planet gear about the center of the sun gear
N_3 = speed of rotation of planet gear about its own center
Z = number of teeth of planet gear

BEARING FREQUENCIES[1]

The bearing frequencies noted in Tables 5 and 6 were derived as follows:

Cage Frequency Relative to Outer Race

$$Fco = \frac{Ni - Ne}{120} \left(1 - \frac{d}{Dp} \cos B\right)$$

Outer Race Ball Pass

$$Fo = Z\ Fco$$

Cage Frequency Relative to Inner Race

$$Fcs = \frac{Ni - Ne}{120} \left(1 + \frac{d}{Dp} \cos B\right)$$

Inner Race Ball Pass

$$Fi = Z\ Fcs$$

Ball Spin Frequency

$$Fs = Dp \frac{(Ni - Ne)}{120\ d} \left(1 - \frac{(d)^2}{(D_p)^2} \cos^2 B\right)$$

Ball Defect Frequency

$$F_B = 2F_s$$

Spherical Roller Bearing

$$D_p = (S.D. - d) \cos B$$

where N_i = speed of rotation of inner raceway
N_e = speed of rotation of outer raceway
Z = number of rolling elements
d = diameter of rolling element
D_p = bearing pitch diameter
B = contact angle
S.D. = spherical diameter

---

[1]Harris, Tedric, ROLLING BEARING ANALYSIS, John Wiley & Sons Inc., 1966. Palmgren, Arvid, Dr. Eng., BALL AND ROLLER BEARING ENGINEERING, Third Edition, S.H. Burbank & Co., Inc., 1959.

APPENDIX B

PROCEDURE FOR THE PREPARATION OF A FLUID SAMPLE USING THE MEMBRANE TECHNIQUE

1.0 OUTLINE OF METHOD:

A fluid is filtered through a 0.8 micrometer millipore filter disc or equivalent using vacuum to impinge the contamination particles upon the surface of the filter. The filter disc is then rendered transparent by dissolution and the particles are observed using transmitted light microscopy.

2.0 APPARATUS

2.1 Pyrex Filter Holder, which includes:

A glass base with stainless steel support screen and rubber stopper
A holding clamp
A 250 ml Pyrex glass funnel

2.2 0.8μm Membrane Filter, white plain, 47mm diameter

2.3 Vacuum Flasks, 1 liter or larger

2.4 Vacuum Source, capable of 66cm of mercury or more

2.5 Glass Slides, 5cm x 7.5cm or larger

2.6 Forceps, unserrated tip

2.7 Sample Container, at least 100 ml capacity.

2.8 Stainless Steel Pressure Vessel

2.9 Eyedroppers with rubber bulbs

2.10 Solvent Filtering Dispenser w/stainless cone spray nozzle

2.11 Stainless Steel Unit with Luer-Lok® fittings, 25mm for filtering clearing solution.

2.12 Glass Syringe, large volume hypodermic

2.13 0.5μm or less Membrane Filter, Teflon® 25mm diameter

3.0 REAGENTS:

3.1 Anhydrous Isopropyl Alcohol, acetone free, reagent grade

3.2 Freon® TF or Petroleum Ether Solvent

3.3 Clearing Solution A

33 ml Hexane, Technical grade
33 ml 1,2 Dichloroethane, Technical grade
33 ml P-Dioxane, Technical grade

3.4 Clearing Solution B

15 ml Hexane, Technical grade
15 ml 1.2 Dichloroethane, Technical grade
70 ml P-Dioxane, Technical grade
2.5 ml Distilled or dionized water

4.0 CLEANING METHOD FOR APPARATUS AND SAMPLE BOTTLES:

4.1 Each item of filtration apparatus will be cleaned before each run of samples, and each sample container will be cleaned before each use by the following method:

4.2 Rinse with two successive rinses of solvent.

4.3 Wash thoroughly in a solution of liquid detergent and hot water, rinse twice with hot tap water.

4.4 Rinse twice with distilled or deionized water.

4.5 Rinse with filtered isopropyl alcohol to remove all water.

4.6 Rinse with filtered solvent.

4.7 After rinsing with filtered solvent, hold in an inverted position for 30 seconds to allow drainage and evaporation of most of the solvent.

5.0 SAMPLES

5.1 Sample Size: 100 ± 1 ml sample is normally used for this procedure, although it must be remembered that the limiting factor of the membrane technique is the total contamination of the filter surface (e.g., 100 ml at 1 mg/l is equivalent to 10 ml at 10 mg/l).

5.2 Sampling Procedure for Blanks: A blank sample should be prepared before each run using 100 ± 1 ml of filtered suspension fluid. It should be run according to the following filtration and clearing procedure. The cleared membrane shall have no more than 300 particles greater than 10 micrometers on the effective filtering area.

6.0 FILTRATION PROCEDURE

6.1 Using unserrated forceps, remove one filter disc from its container. Rinse both surfaces, with filtered solvent, and immediately place the filter on the precleaned filter base.

6.2 Immediately lower the precleaned filter funnel onto the filter base which has been prewet with solvent, secure with the holding clamp, and place a clean cover on top of the filter funnel. Do not slide the funnel on top of the filter disc. Add 20 ml of filtered solvent to completed assembly.

6.3 Thoroughly agitate the sample to assure that all solid particles are in suspension.

6.4 Pour measured sample into the filter funnel

6.5 Add 100 ml of filtered solvent into the sample container; agitate and proceed as in 6.4.

6.6 Apply vacuum to the filtering apparatus. When the filtration volume is down to approximately 20 ml, release the vacuum.

6.7 Using the spray from the solvent dispenser, carefully wash the sides of the funnel with filtered solvent (approximately 50 ml). Proceed as in 6.6.

6.8 Repeat 6.7 twice. If free water is observed in the final 50 ml rinse, add 20 cc of filtered isopropyl alcohol, followed by an additional rinse with 50 ml of filtered solvent.

6.9 Apply vacuum and allow to operate until the filter disc is completely dry. Do not rinse the funnel walls further after the filter has become dry, as this may change the distribution of particles on the filter surface.

7.0 <u>Filter Clearing Procedure</u>:

7.1 Filter clearing solutions A and B, using apparatus specified in clauses 2.11, 2.12, and 2.13 into pre-cleaned containers.

7.2 Using an eyedropper, freshly rinsed with filtered solvent, dispense sufficient clearing Solution A to thoroughly wet a cleaned microscope slide.

7.3 Carefully place the test filter, particle side up, onto the prewetted glass slide. Immediately roll the wet filter onto a clean, dry glass slide and cover with glass petri dish.

7.4 After 1 minute, remove the glass petri dish and dispense sufficient filtered clearing Solution B to cover the top surface of the filter. After 10 seconds, drain the excess clearing solution and replace the glass petri dish.

7.5 Allow the filter to dry for 2 to 5 minutes at room temperature.

APPENDIX C

HIGH FREQUENCY VIBRATION

POWER SPECTRAL DENSITY

DATA

This Appendix contains the following groups of illustrations:

Figures C1 through C10. PSD plots, New Transmissions
Figures C11 through C36. Special Case PSD Plots, New Transmissions

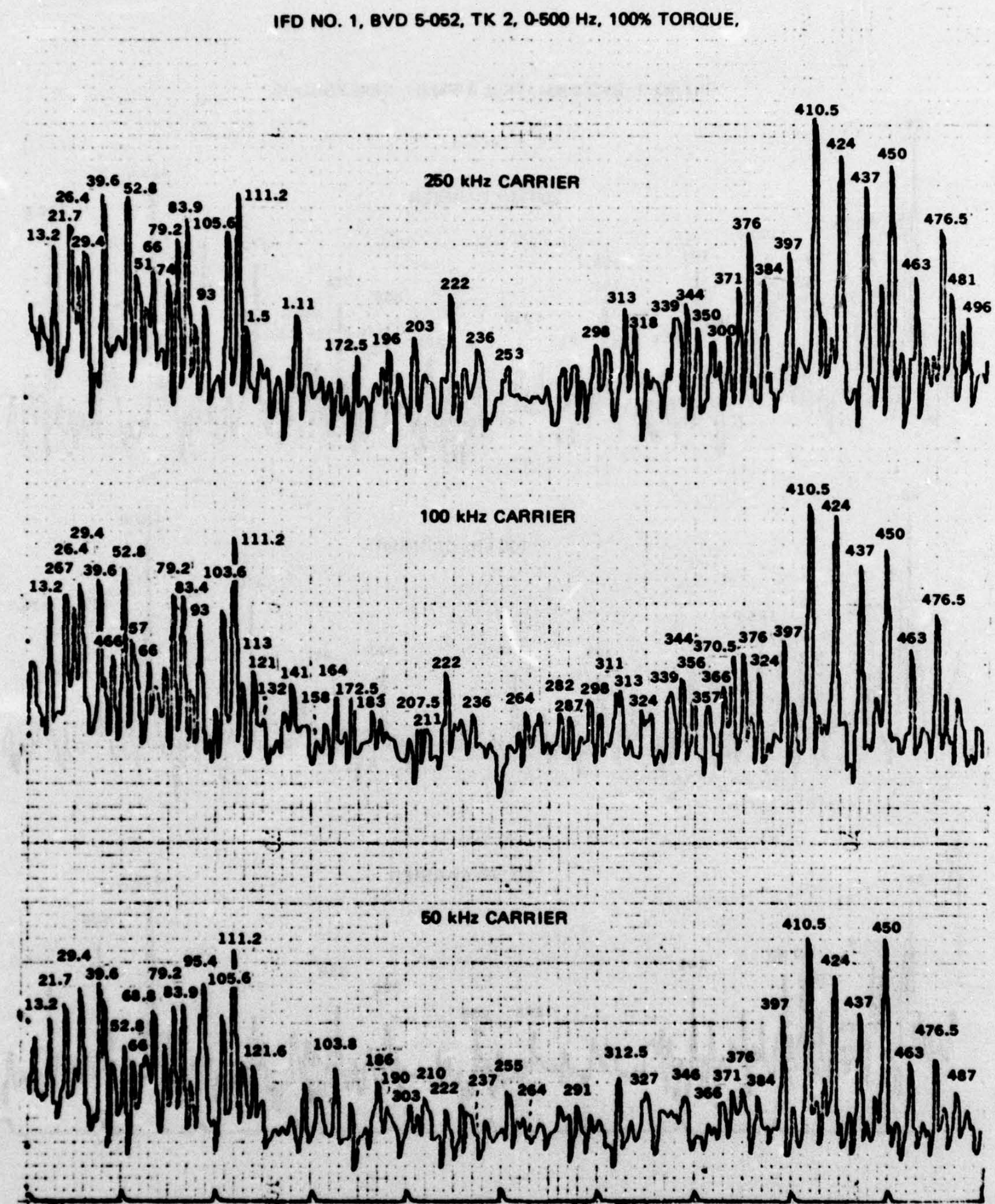

Figure C1. PSD Plot, Transmission A9-1368 (New).

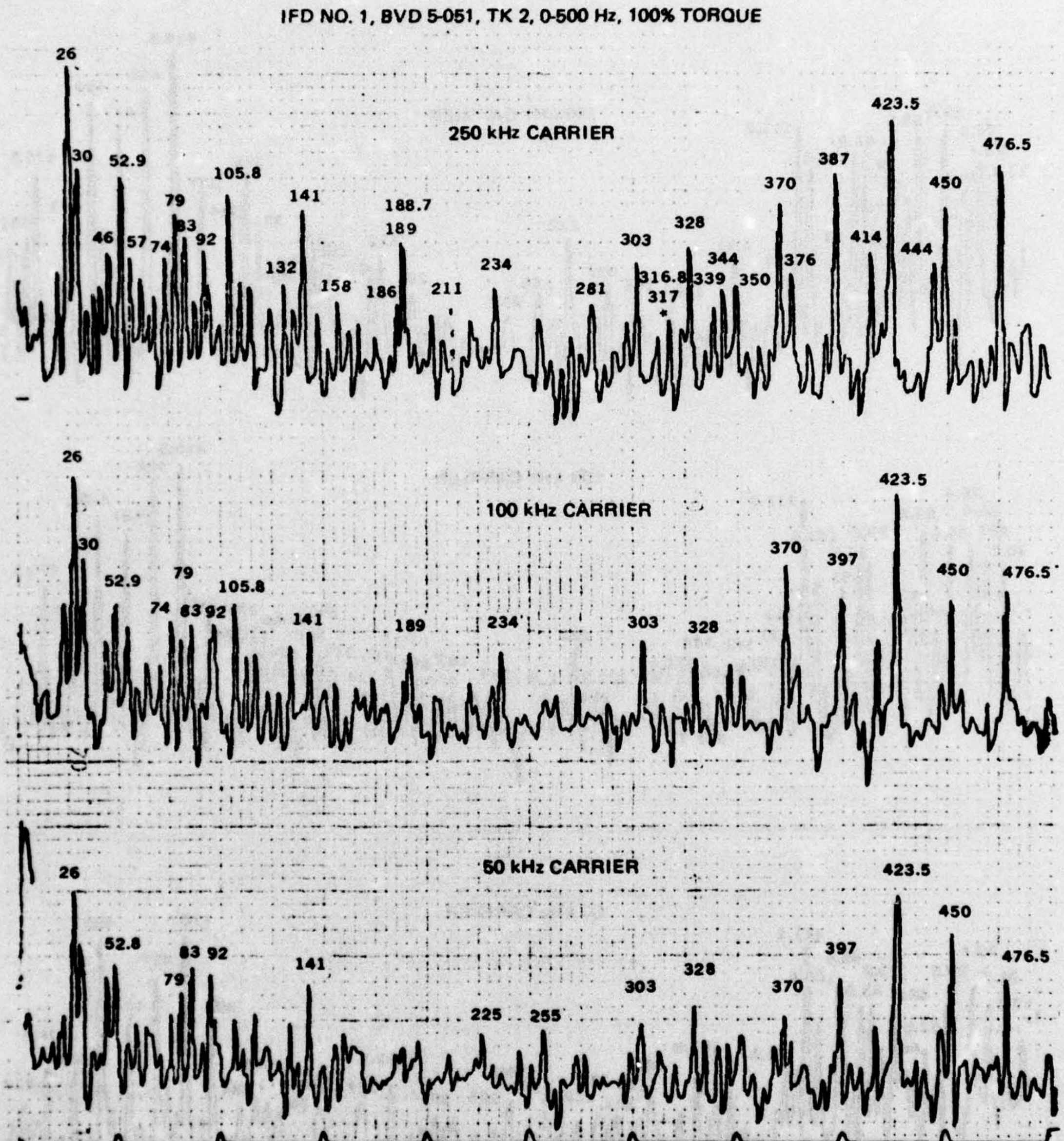

Figure C2. PSD Plot, Transmission A9-1367 (New).

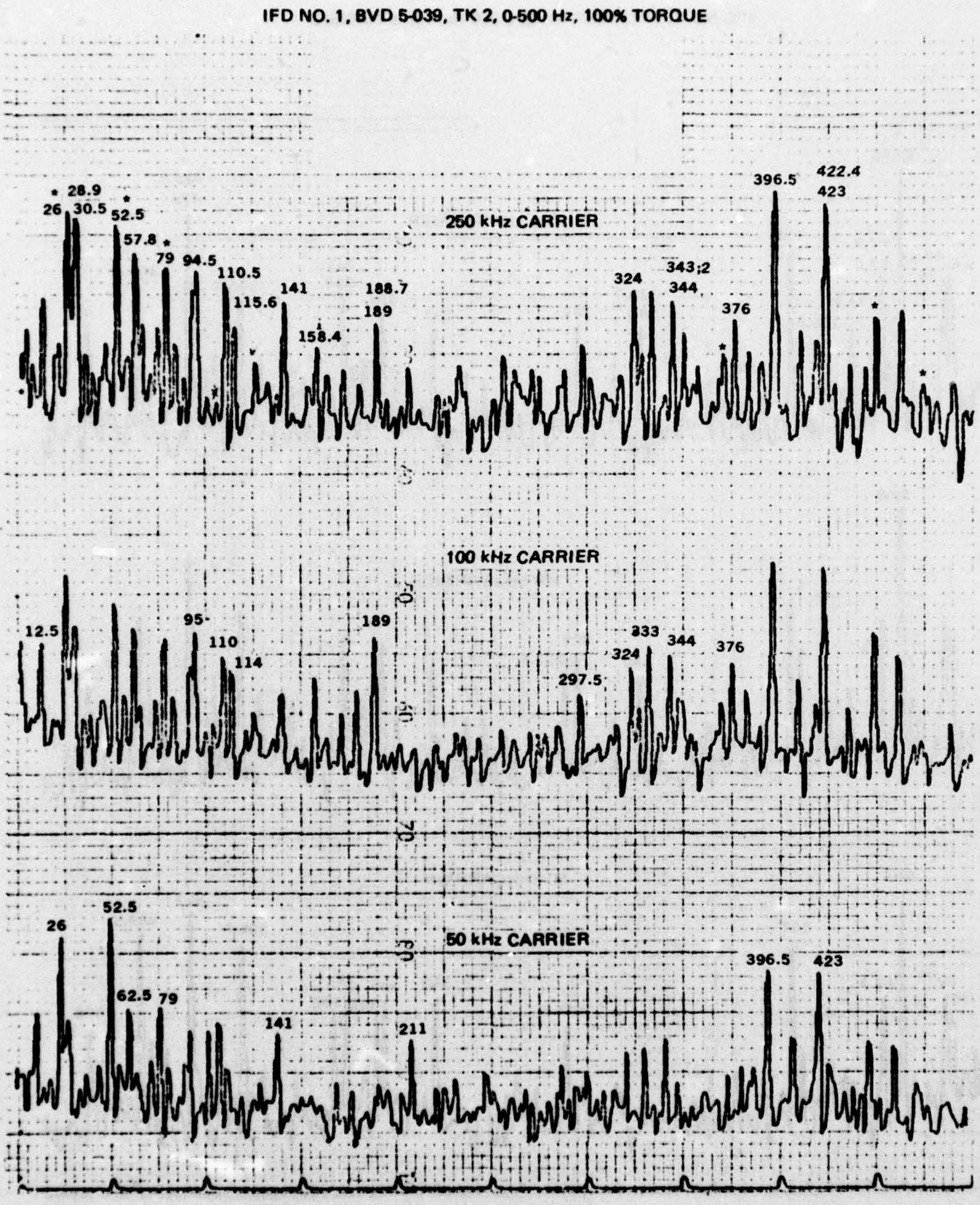

Figure C3. PSD Plot, Transmission A9-1355 (New).

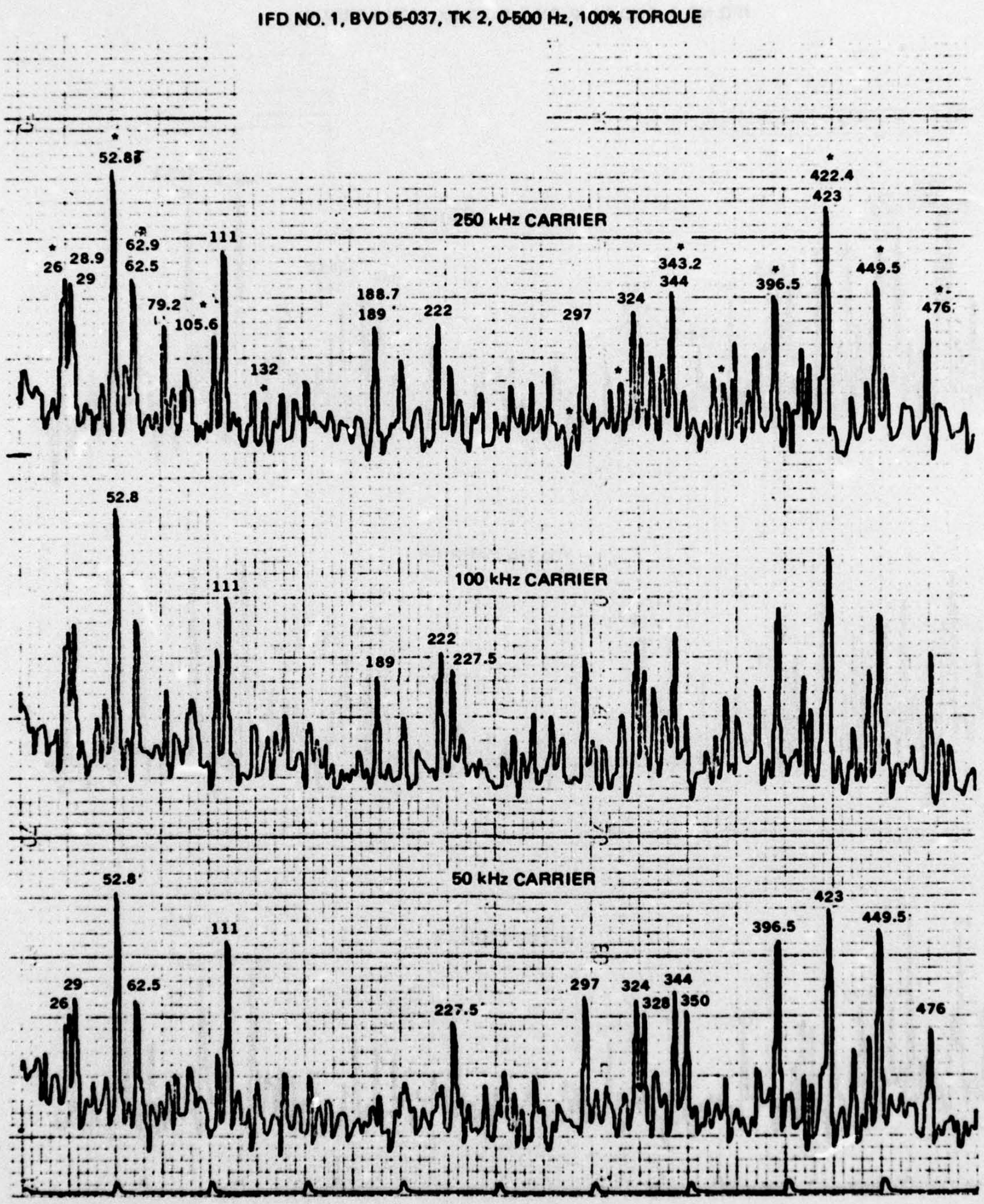

Figure C4. PSD Plot, Transmission A9-1349 (New).

IFD NO. 1, BVD 5-031, TK 2, 0-500 Hz, 100% TORQUE

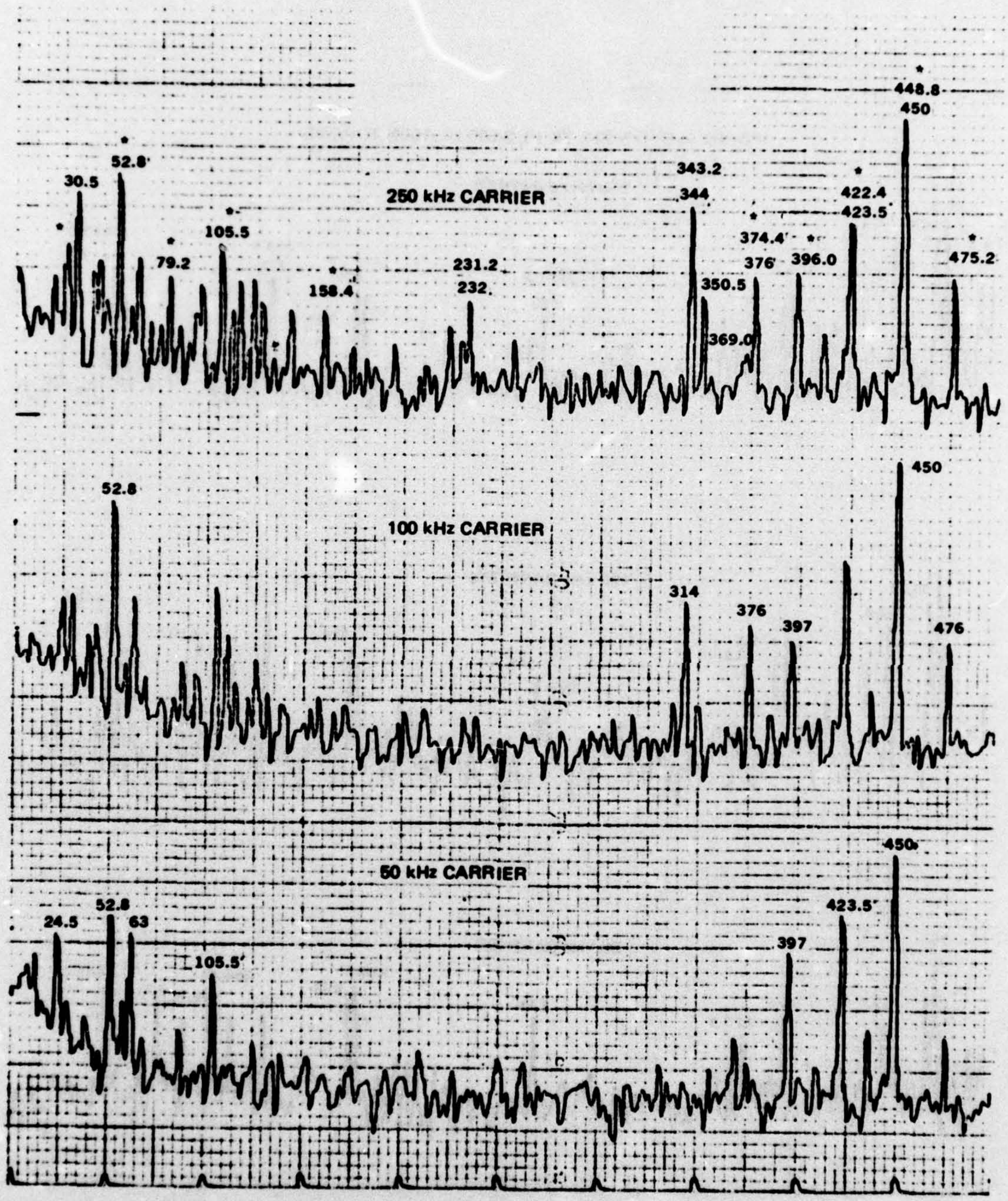

Figure C5. PSD Plot, Transmission A9-1348 (New).

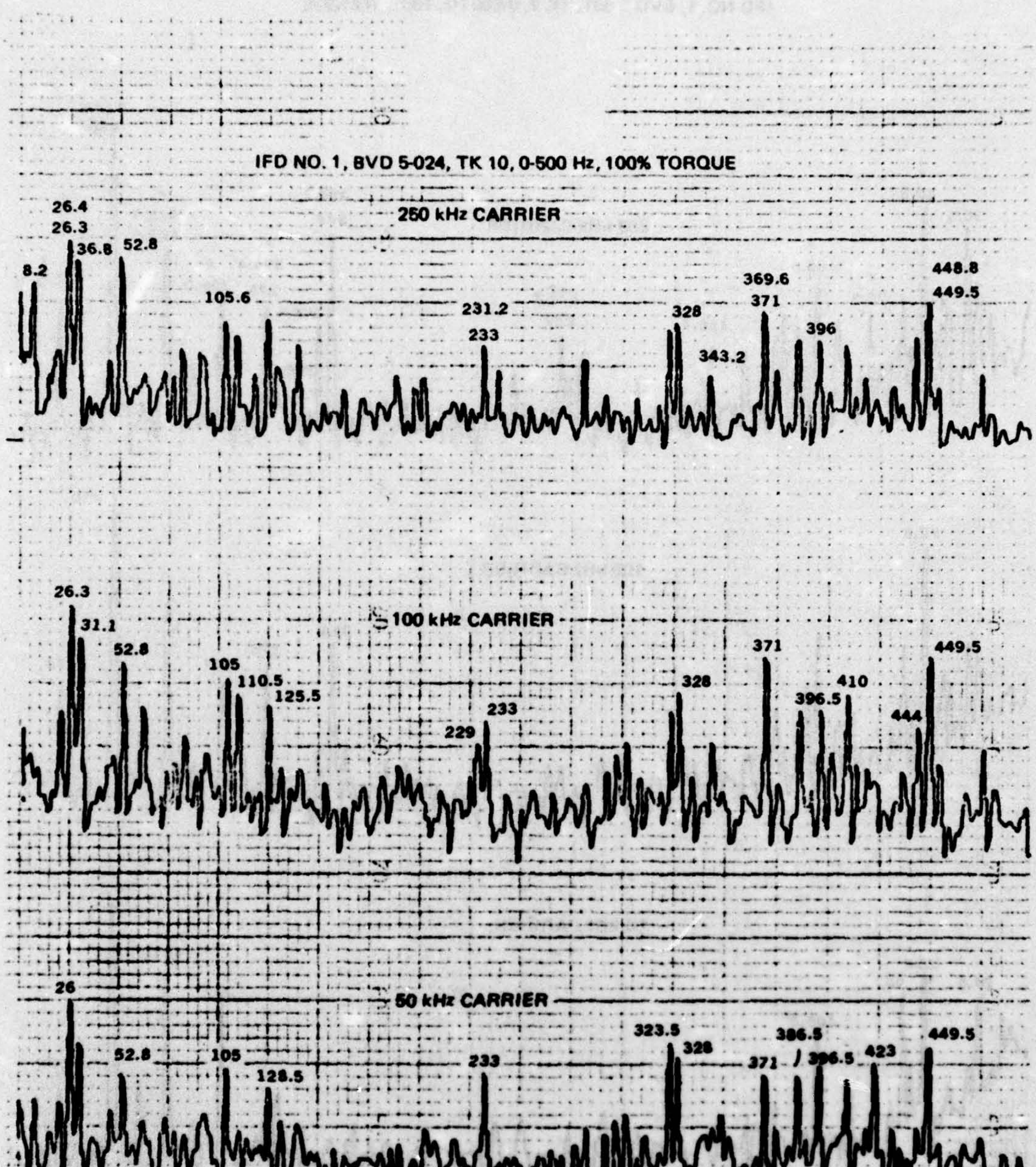

Figure C6. PSD Plot, Transmission A9-1342 (New)

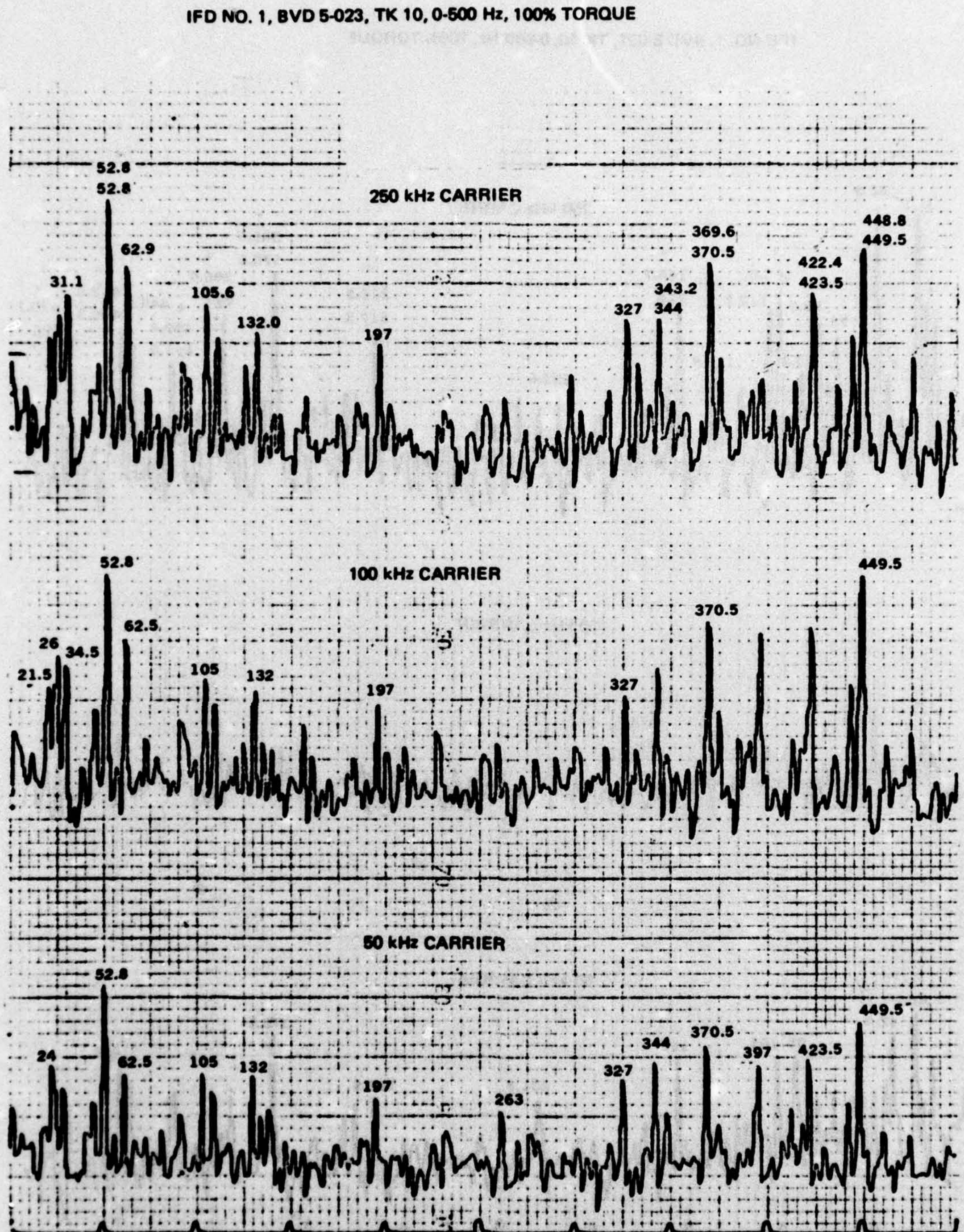

Figure C7. PSD Plot, Transmission A9-1341 (New).

IFD NO. 1, BVD 5-021, TK 10, 0-500 Hz, 100% TORQUE

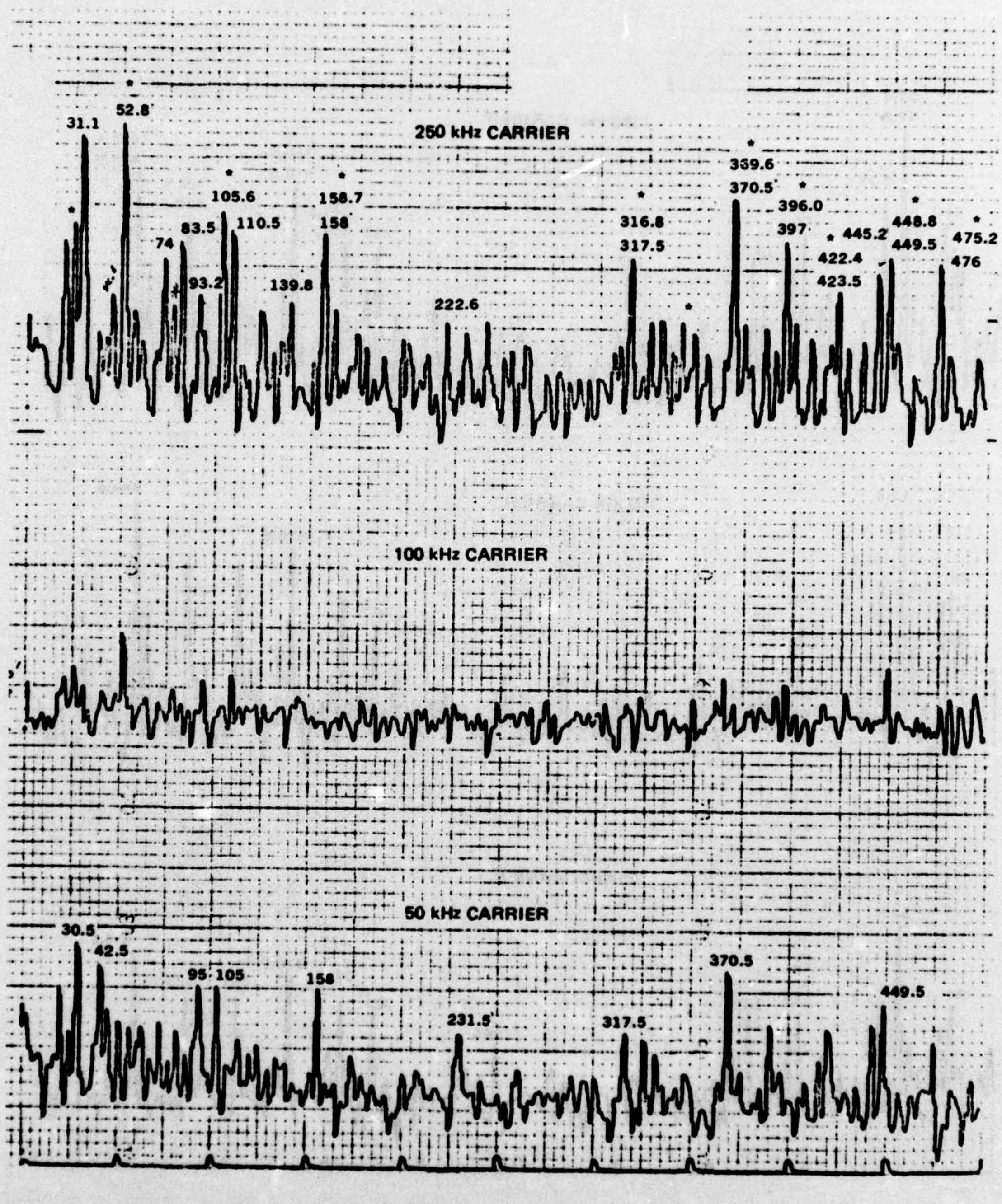

Figure C8. PSD Plot, Transmission A9-1339 (New).

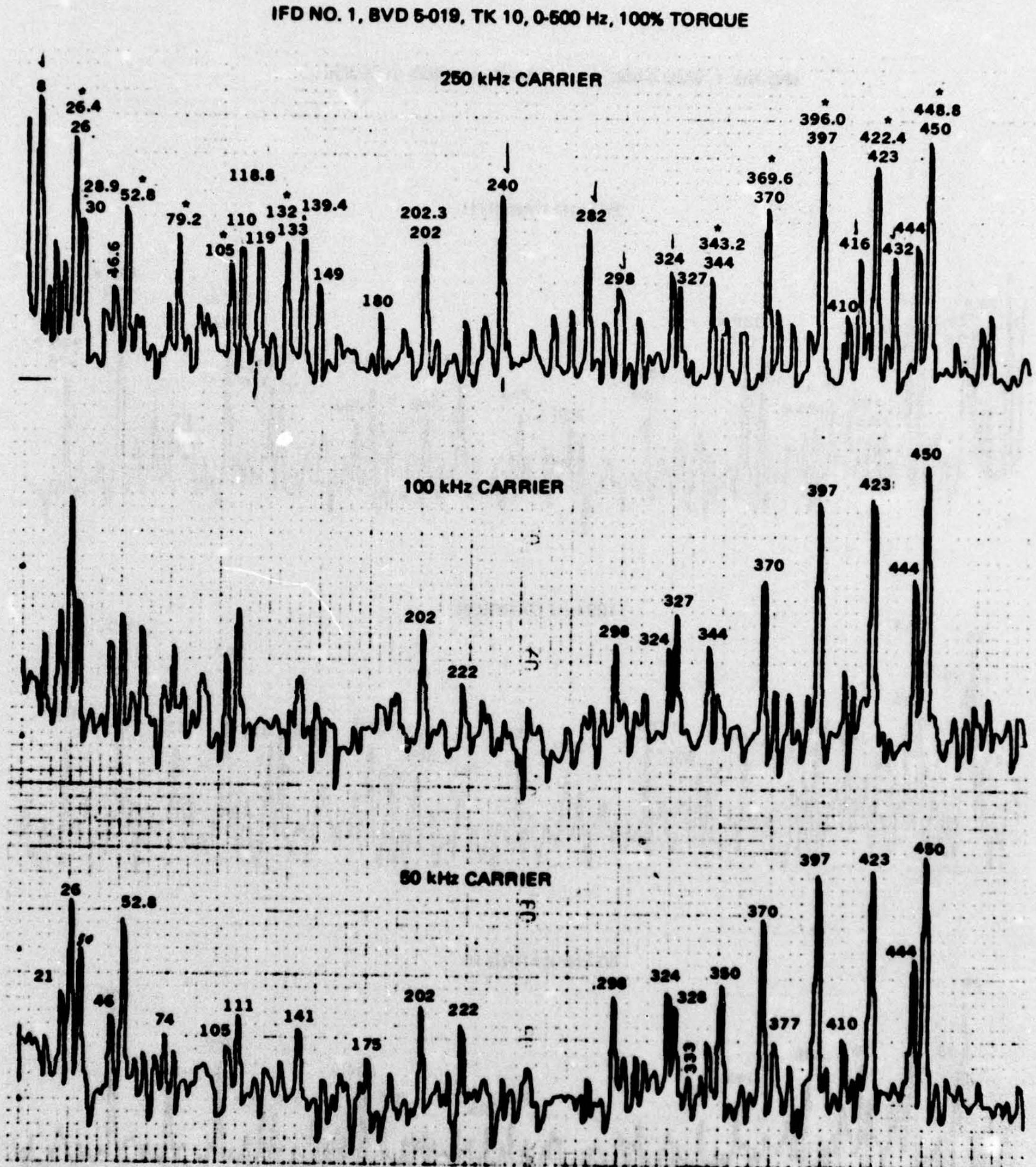

Figure C9. PSD Plot, Transmission A9-1337 (New).

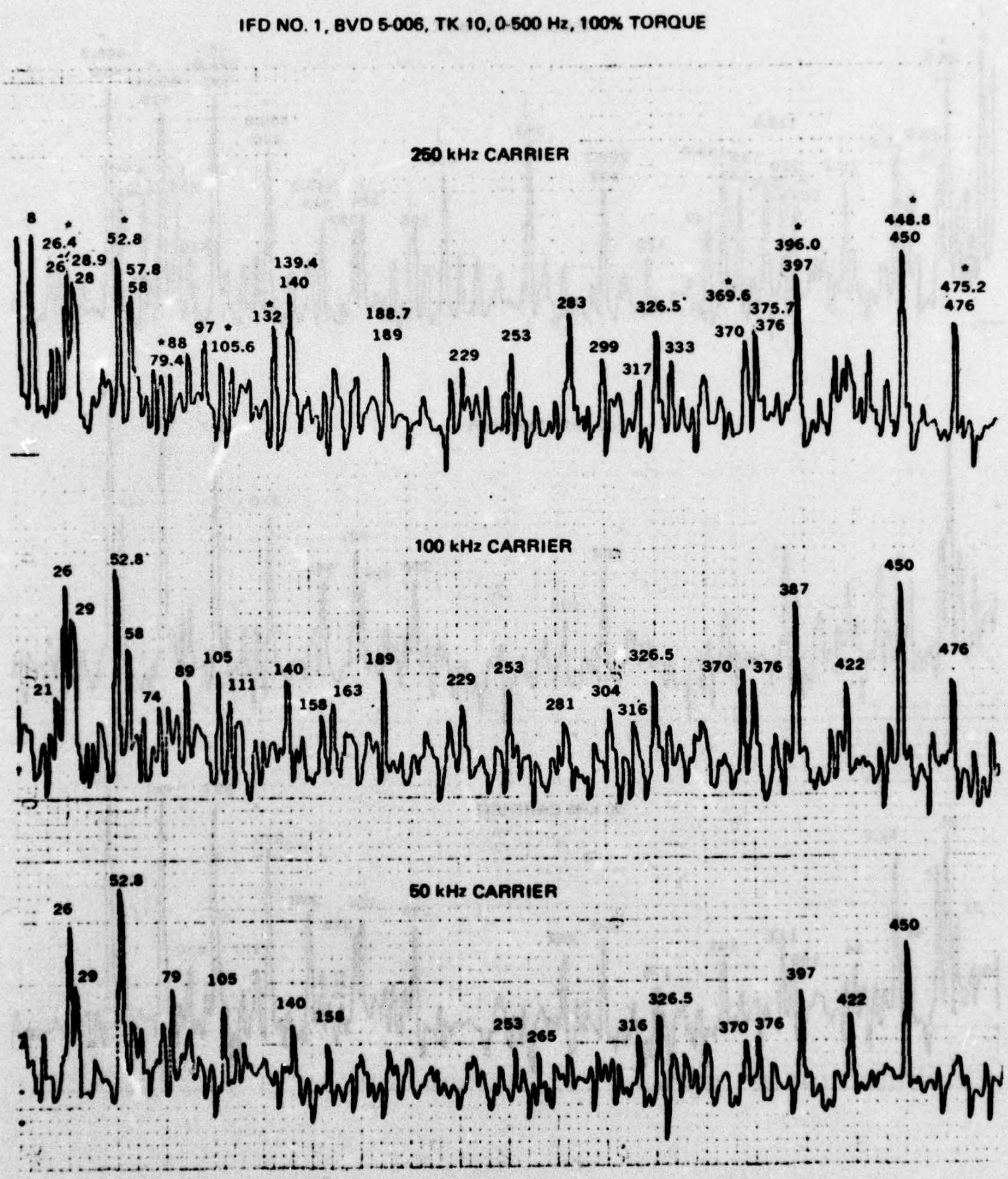

Figure C10. PSD Plot, Transmission A9-1330 (New).

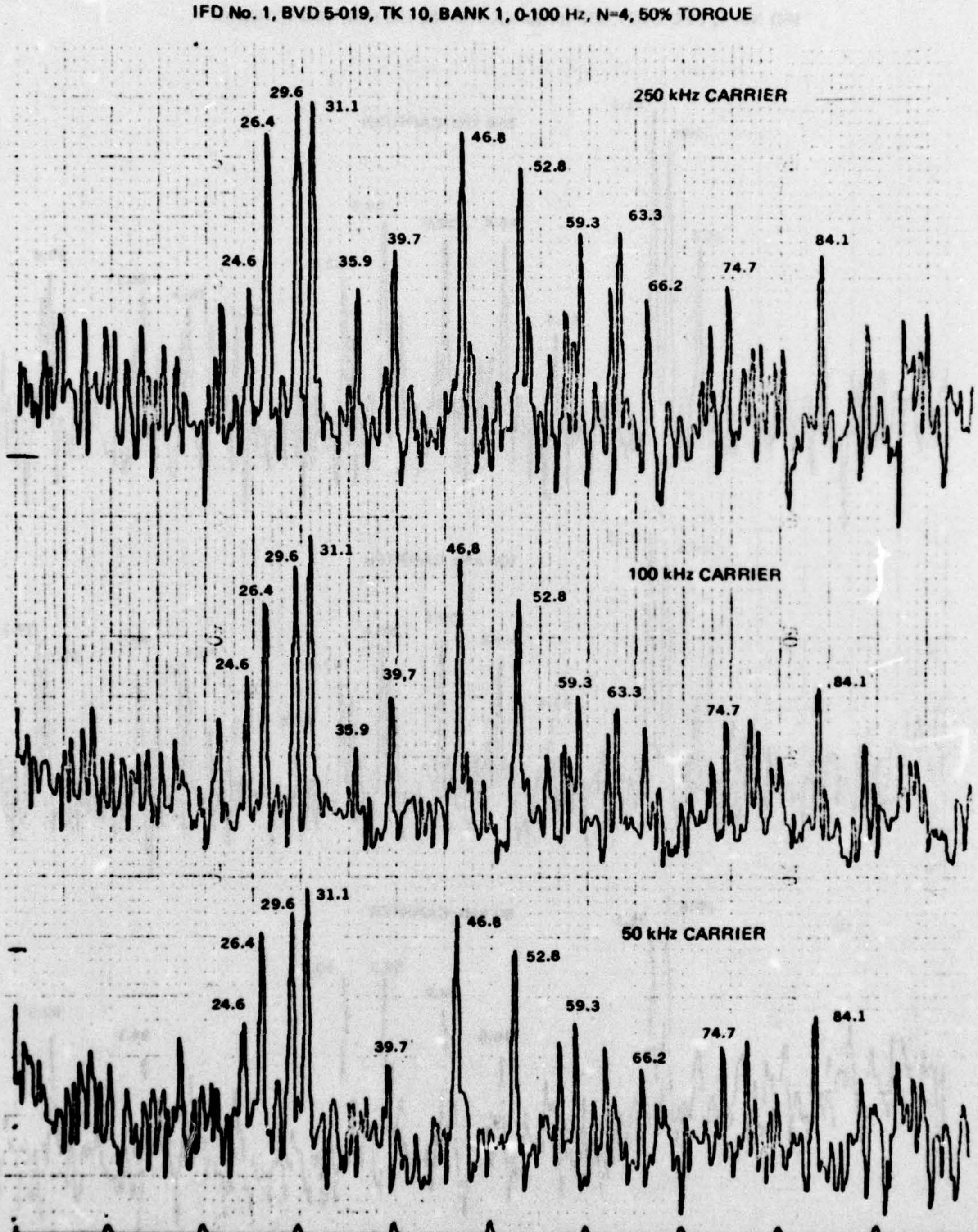

Figure C11. Special Case PSD Plot, Transmission A9-1337 (New) (0-100 Hz).

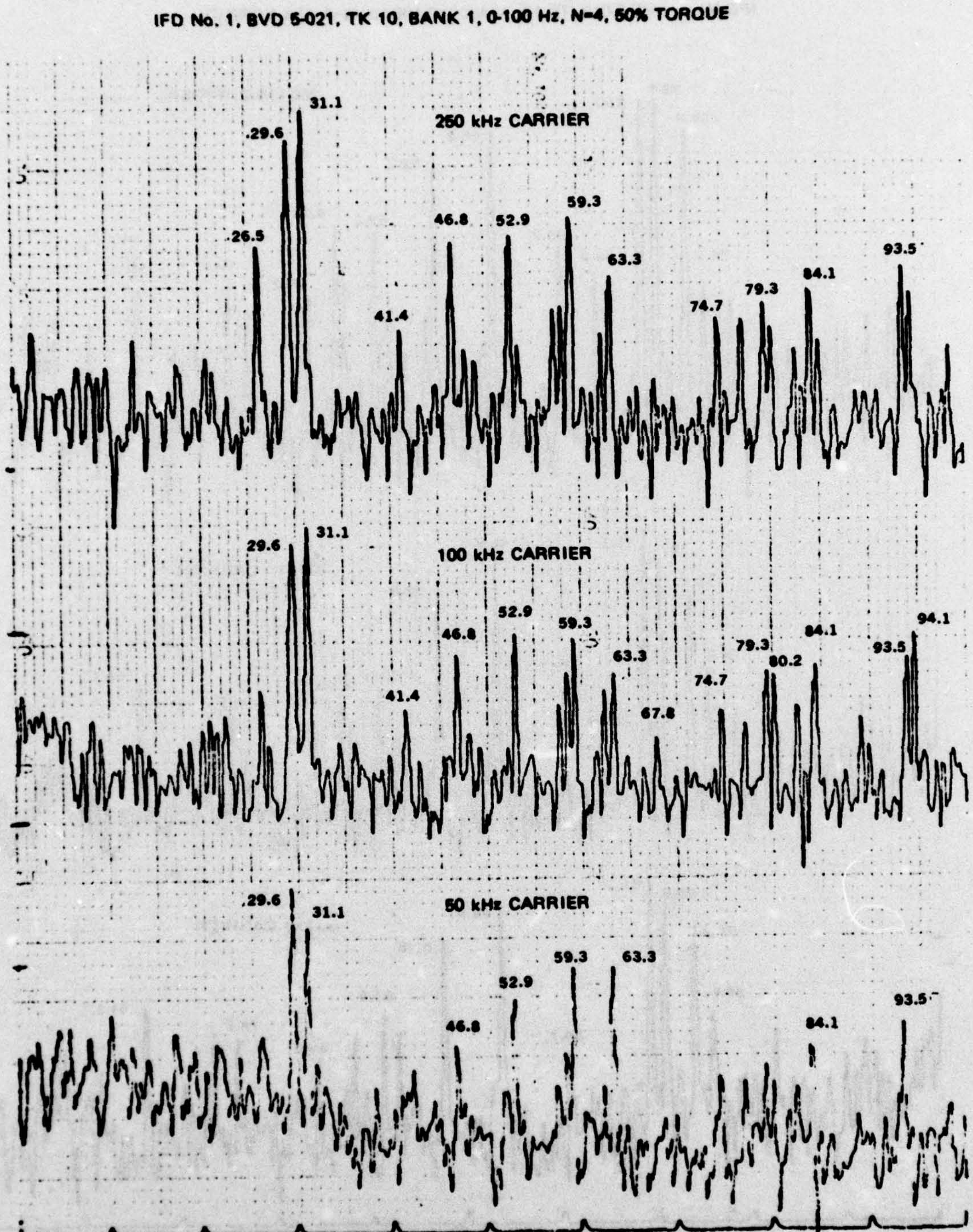

Figure C12. Special Case PSD Plot, Transmission A9-1339 (New) (0-100 Hz).

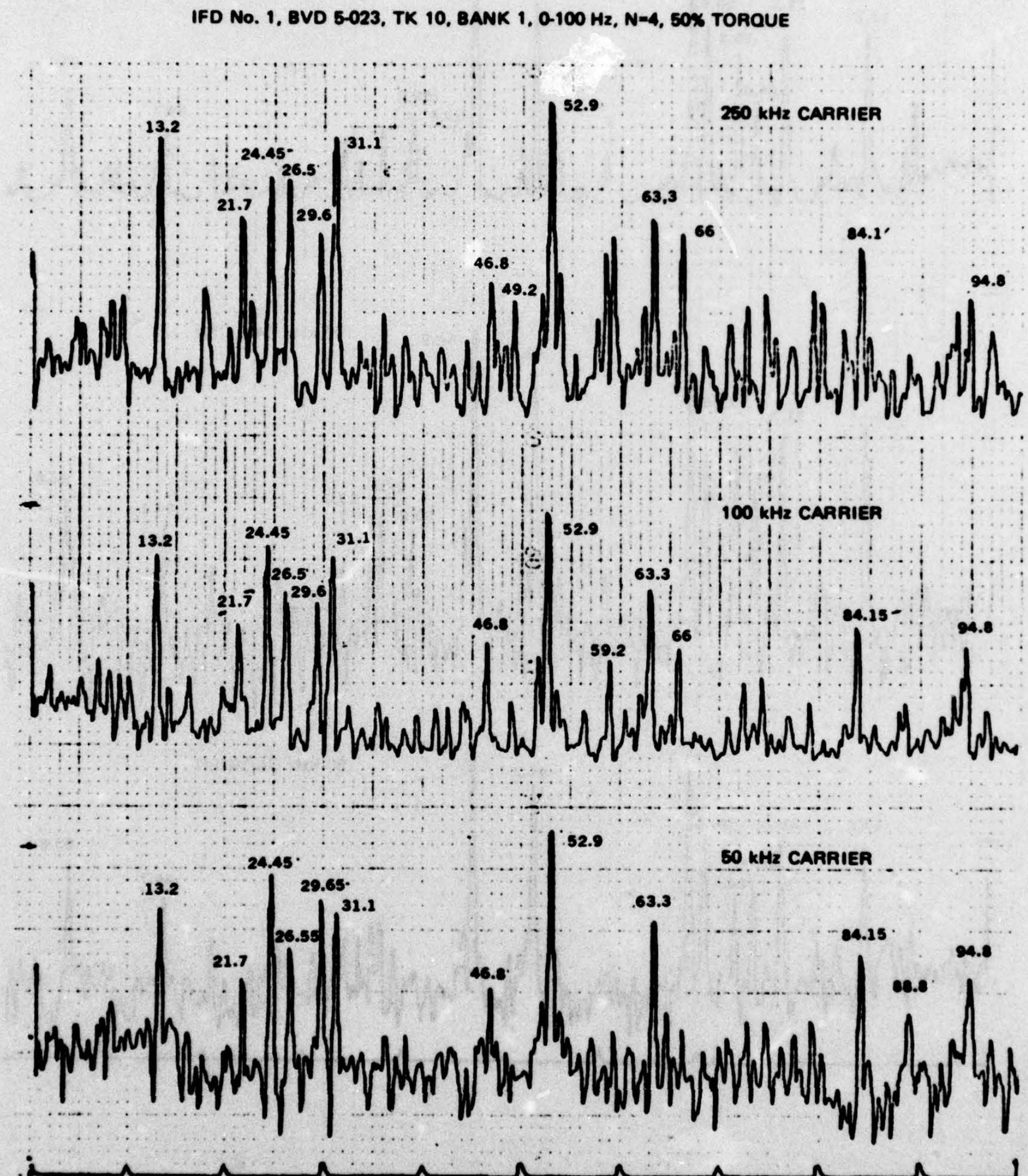

Figure C13. Special Case PSD Plot, Transmission A9-1341 (New) (0-100 Hz).

IFD NO. 1, BVD 5-024, TK 10, BANK 1, 0-100 Hz, N=4, 50% TORQUE

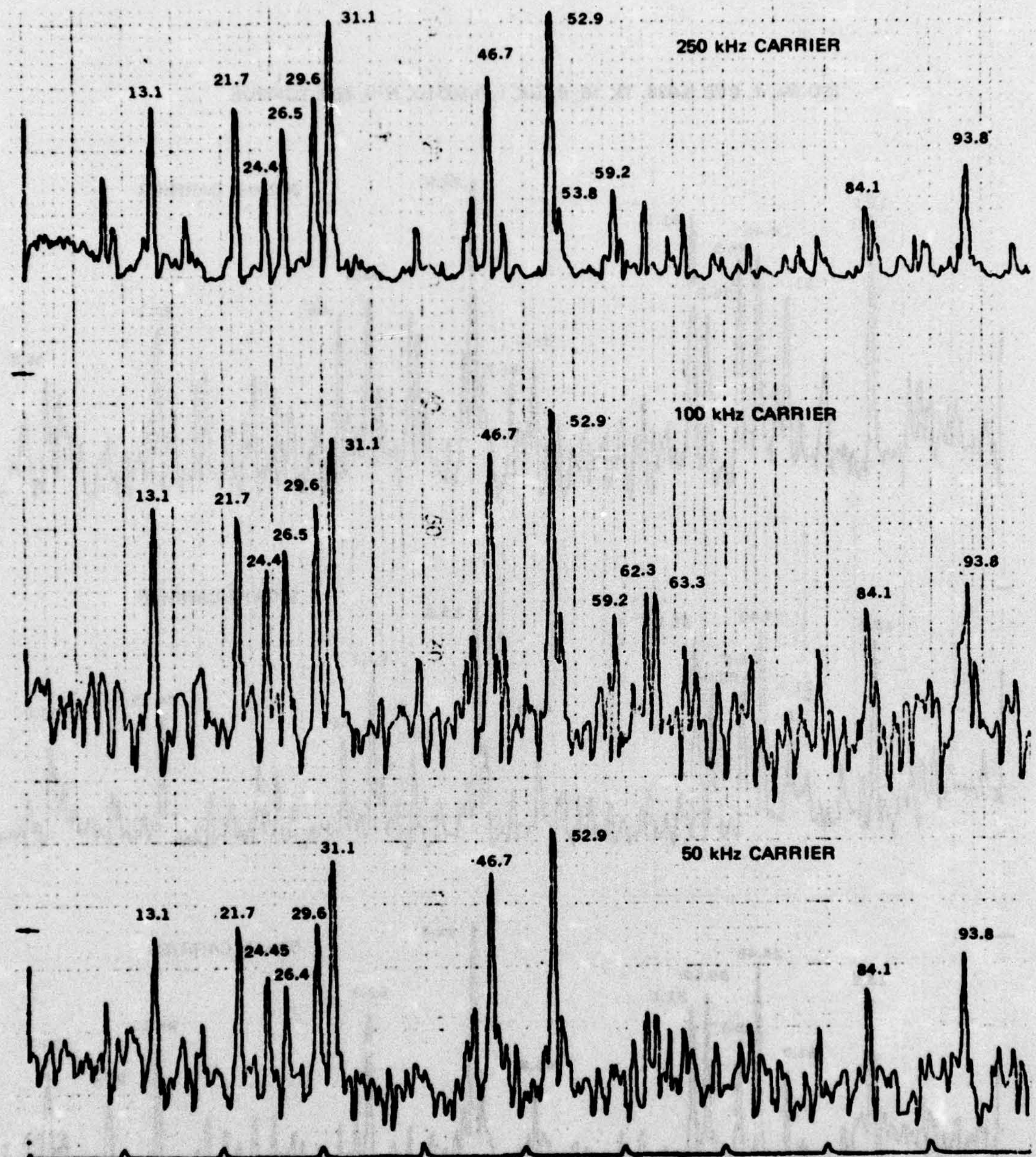

Figure C14. Special Case PSD Plot, Transmission A9-1342 (New) (0-100 Hz).

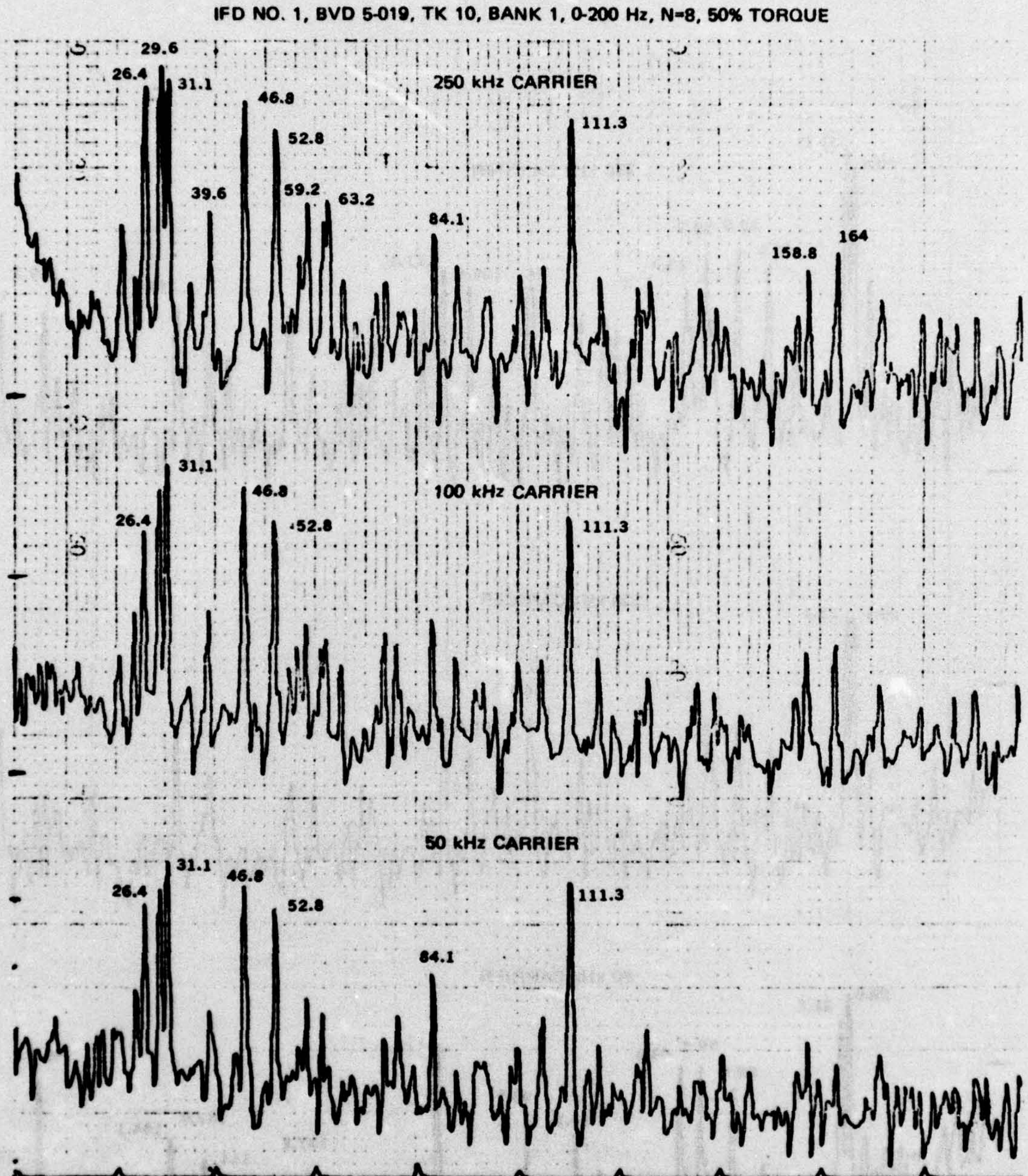

Figure C15. Special Case PSD Plot, Transmission A9-1337 (New) (0-200 Hz).

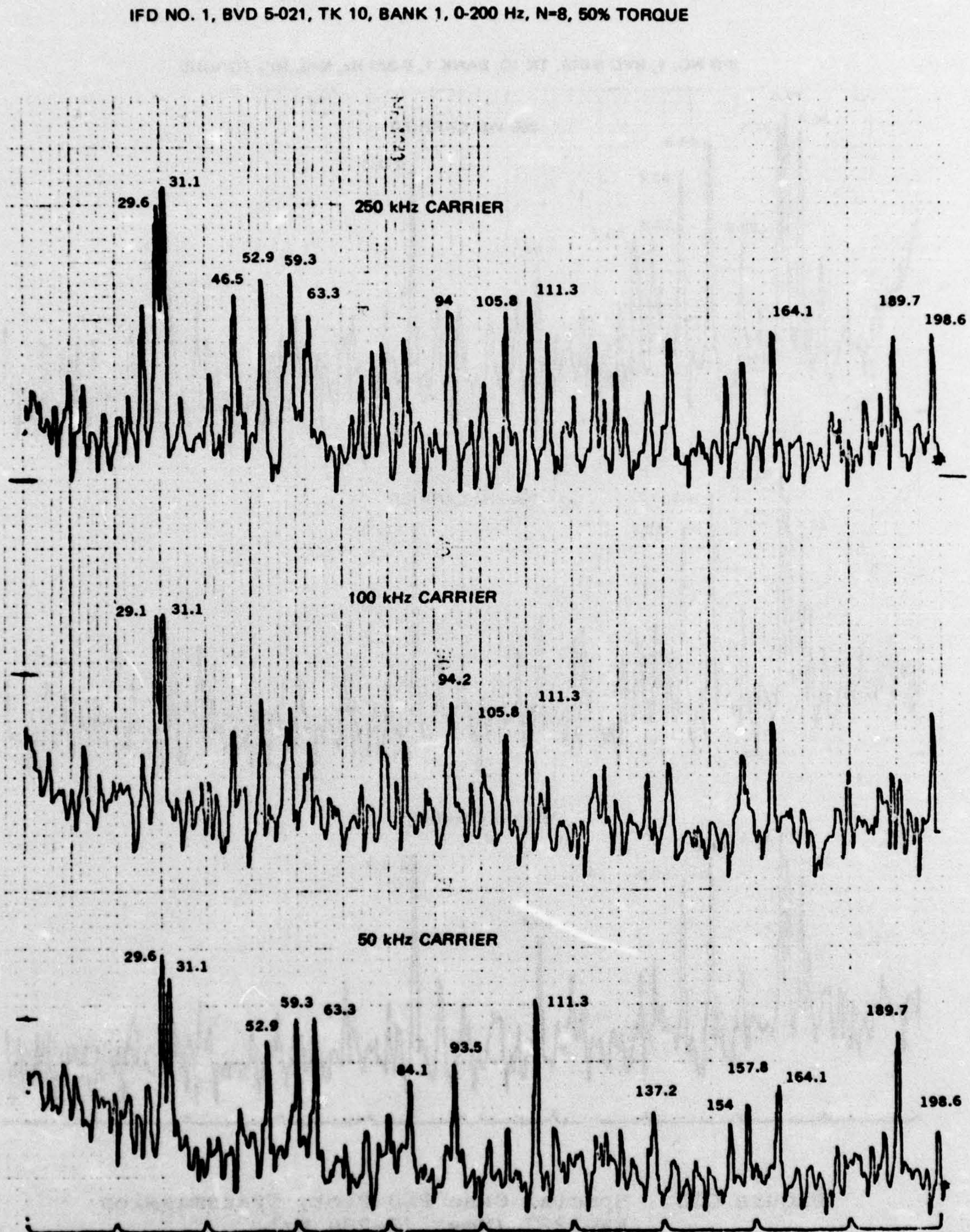

Figure C16. Special Case PSD Plot, Transmission A9-1339 (New) (0-200 Hz).

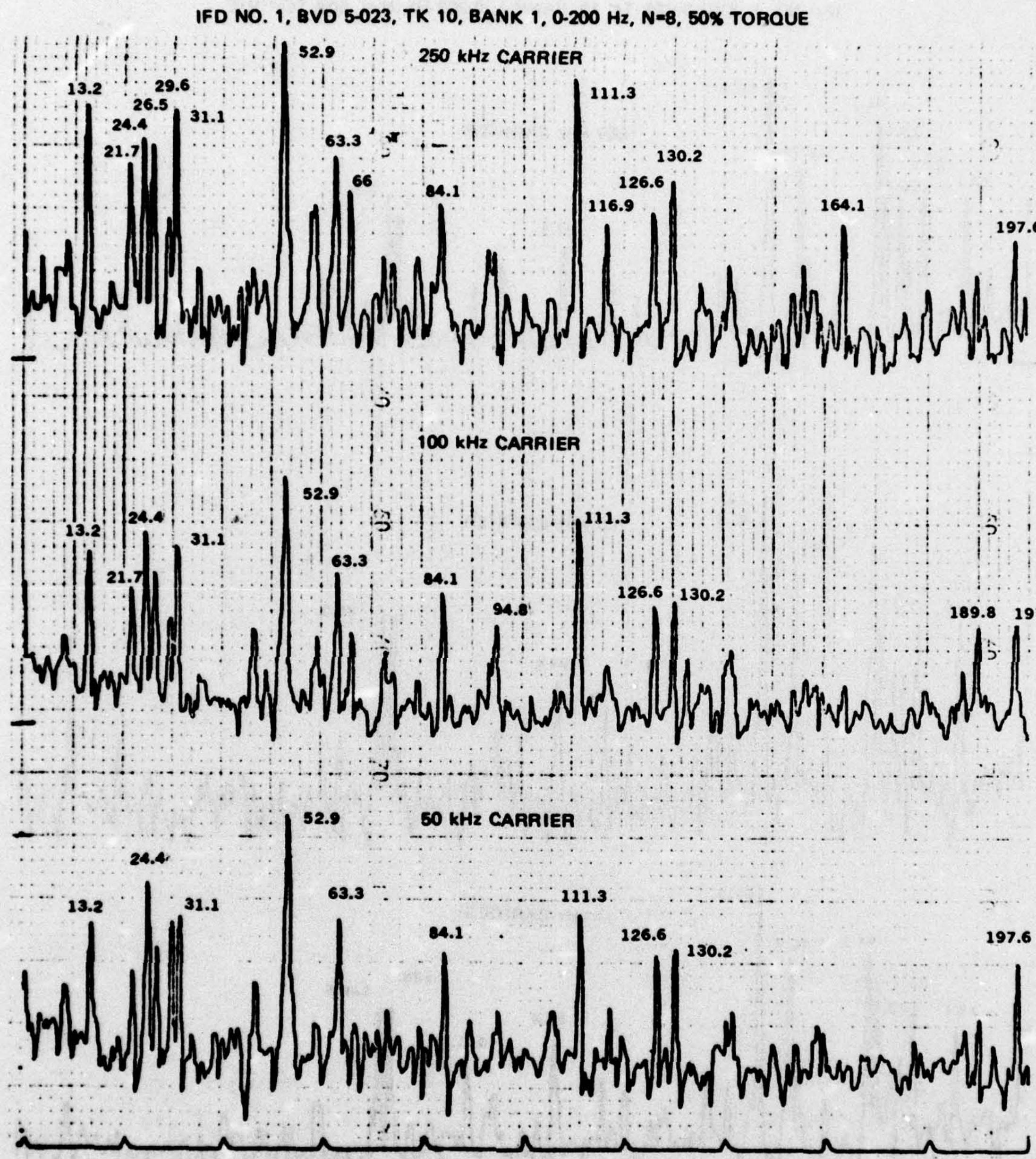

Figure C17. Special Case PSD Plot, Transmission A9-1341 (New) (0-200 Hz).

IFD NO. 1, BVD 5-024, TK 10, BANK 1, 0-200 Hz, N=4, 50% TORQUE

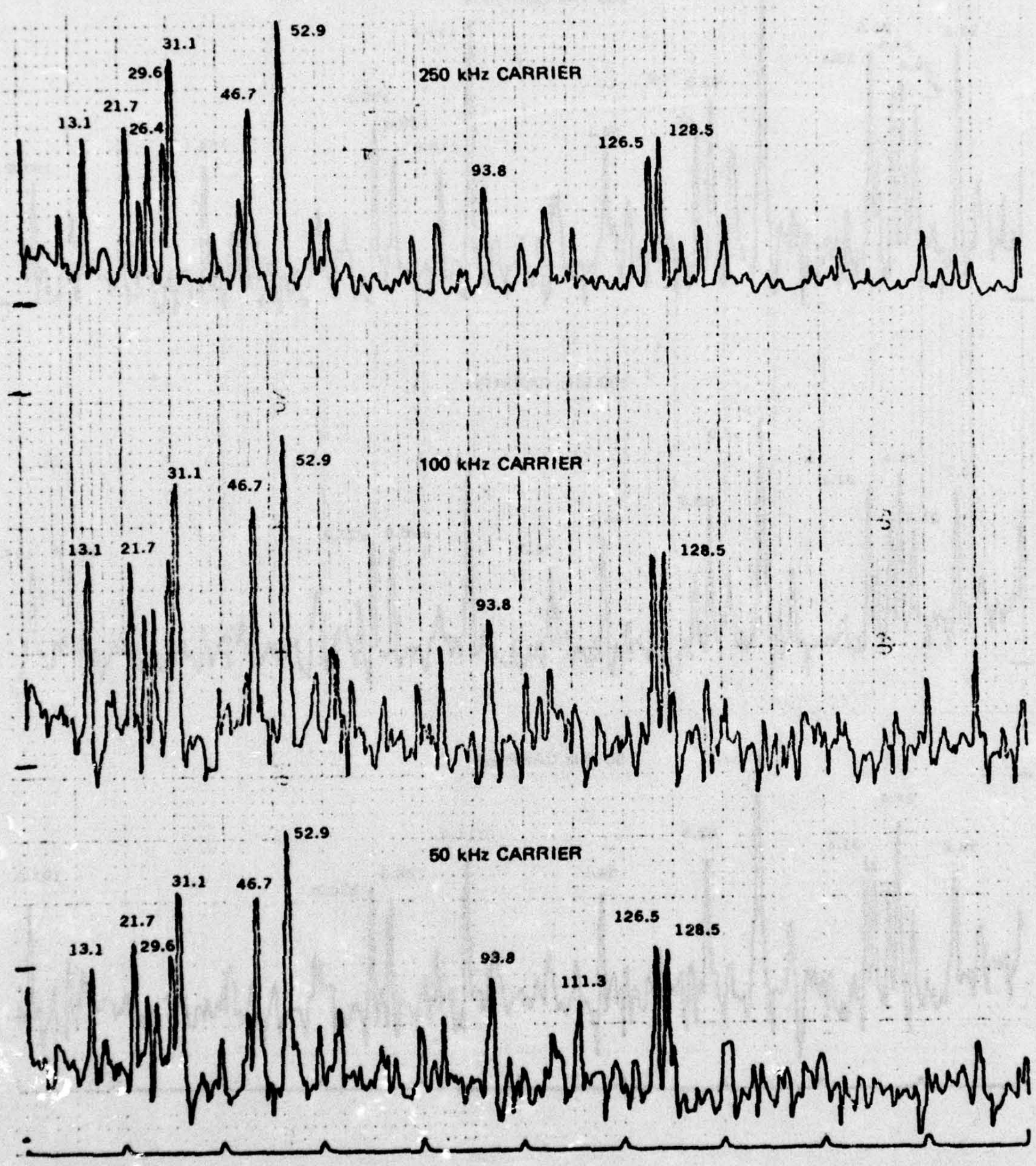

Figure C18. Special Case PSD Plot, Transmission A9-1342 (New) (0-200 Hz).

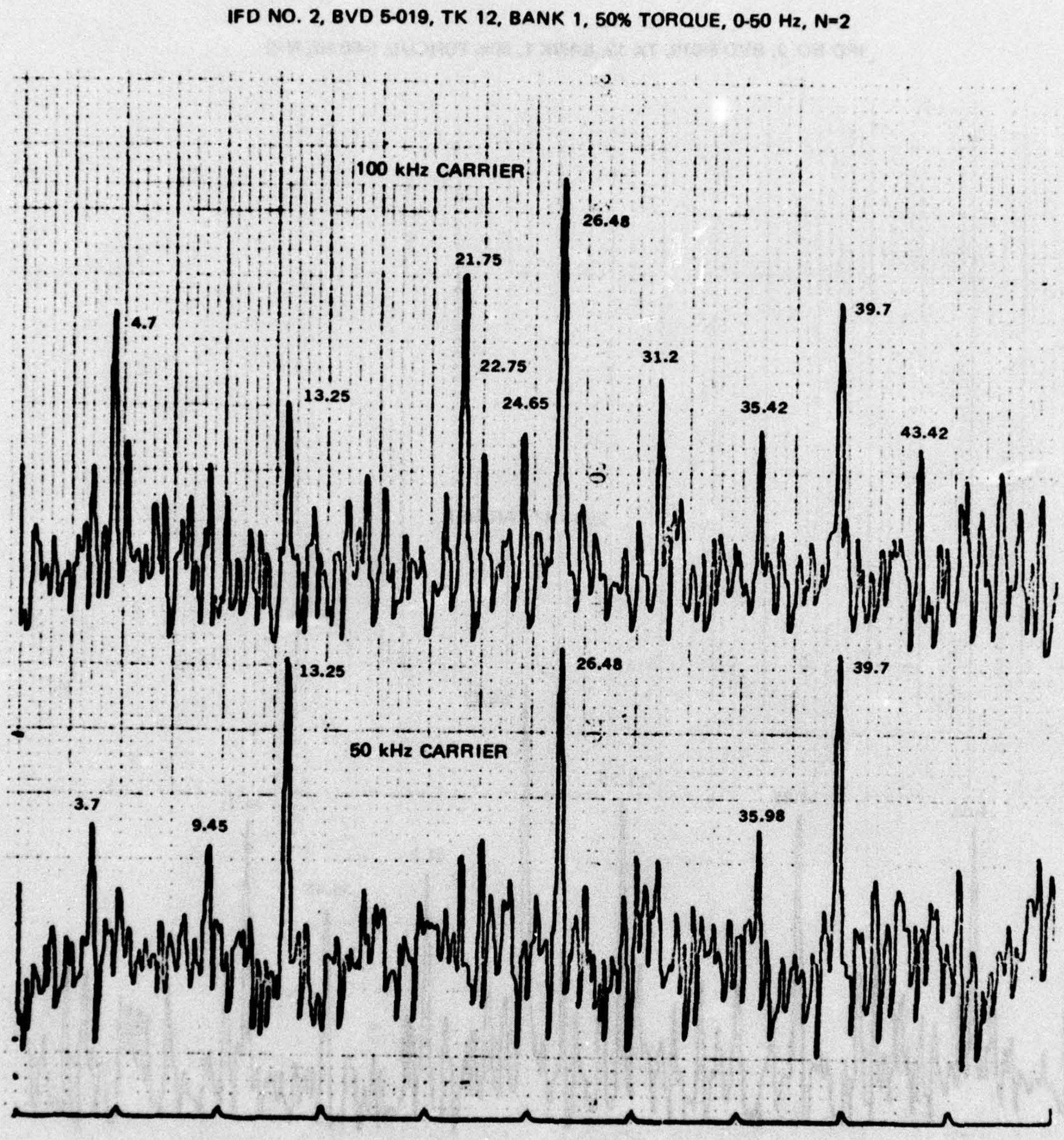

Figure C19. Special Case PSD Plot, Transmission A9-1337 (New), IFD No. 2 (0-50 Hz).

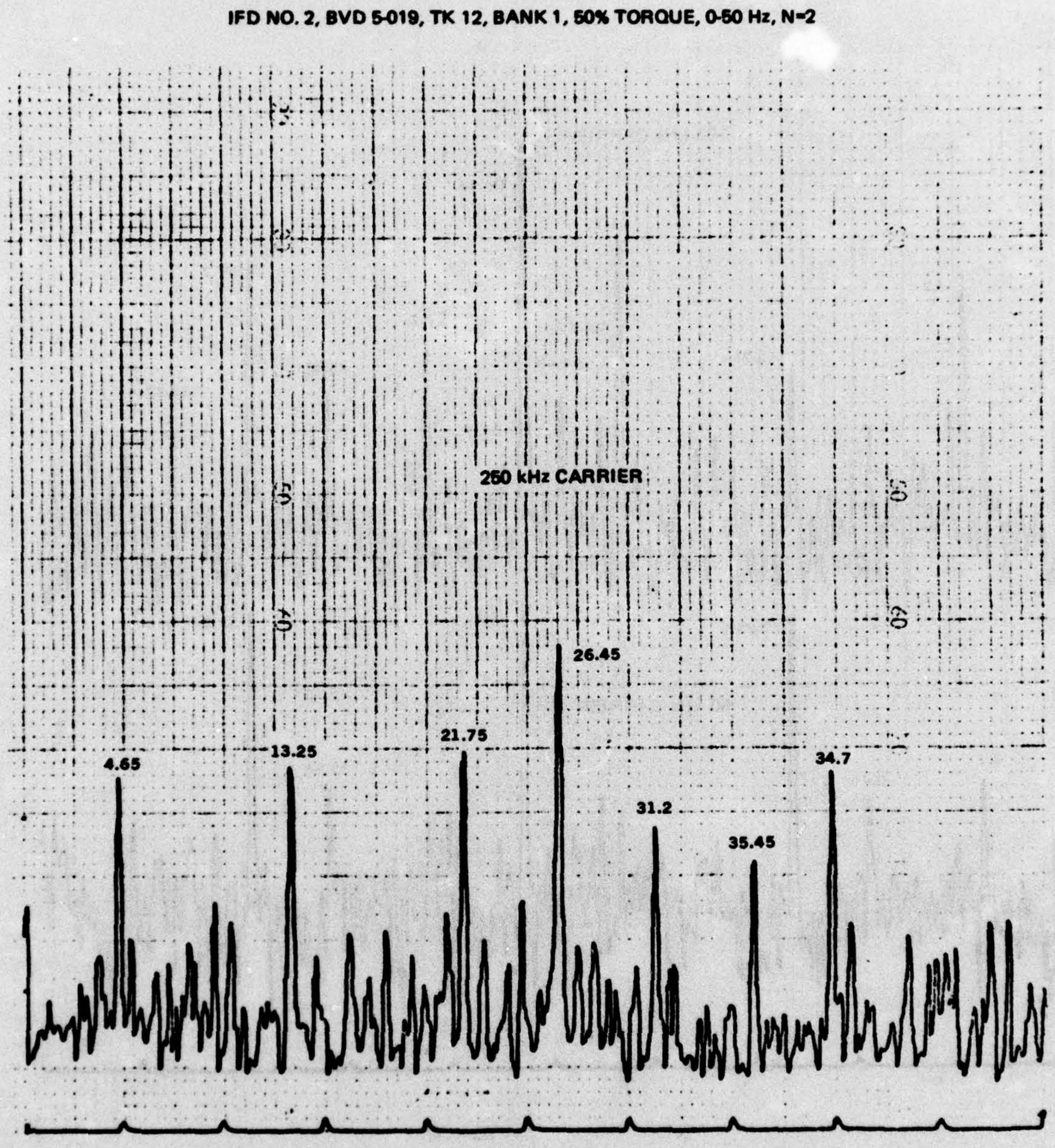

Figure C20. Special Case PSD Plot, Transmission A9-1337 (New), IFD No. 2 (0-50 Hz).

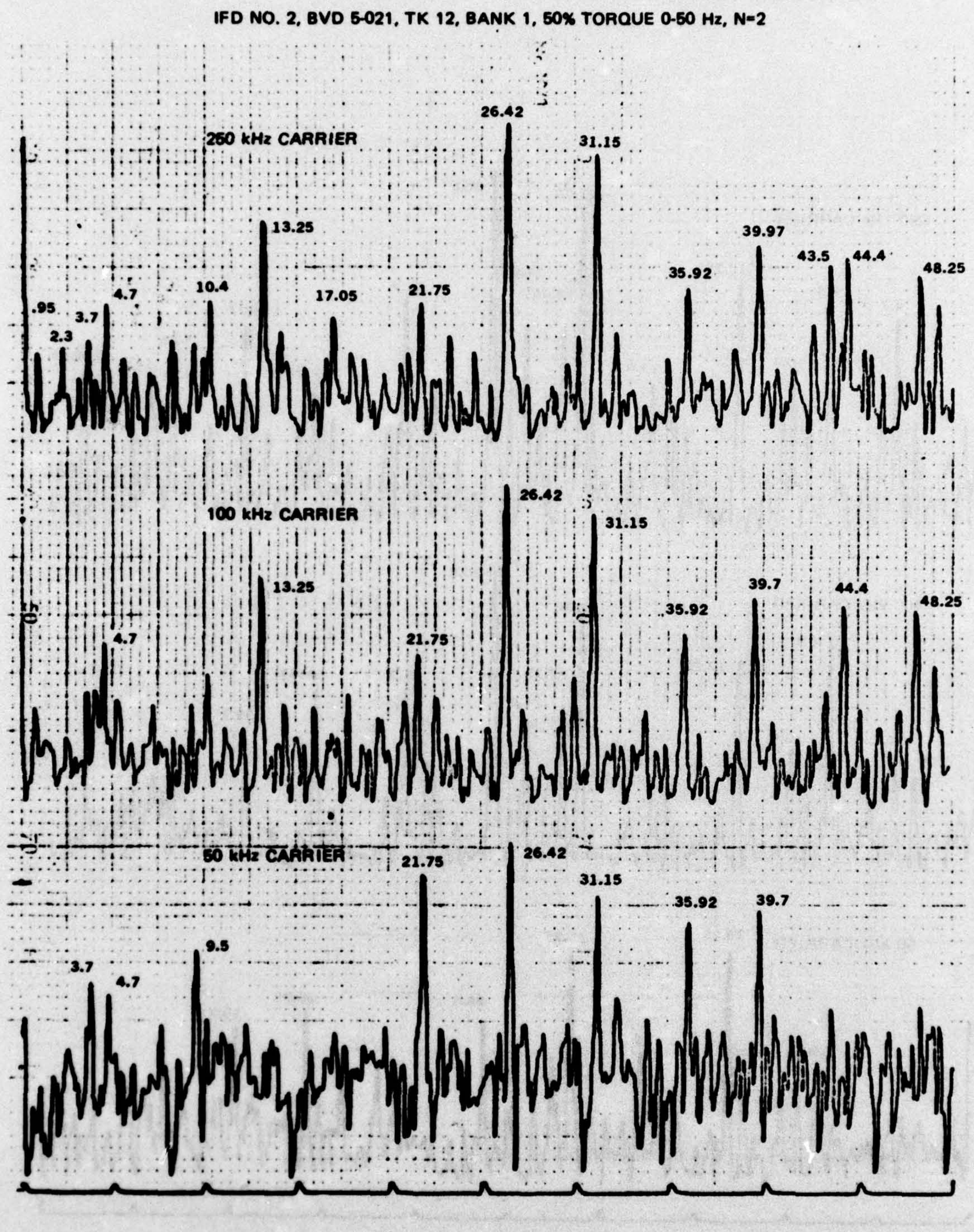

Figure C21. Special Case PSD Plot, Transmission A9-1339 (New), IFD No. 2 (0-50 Hz).

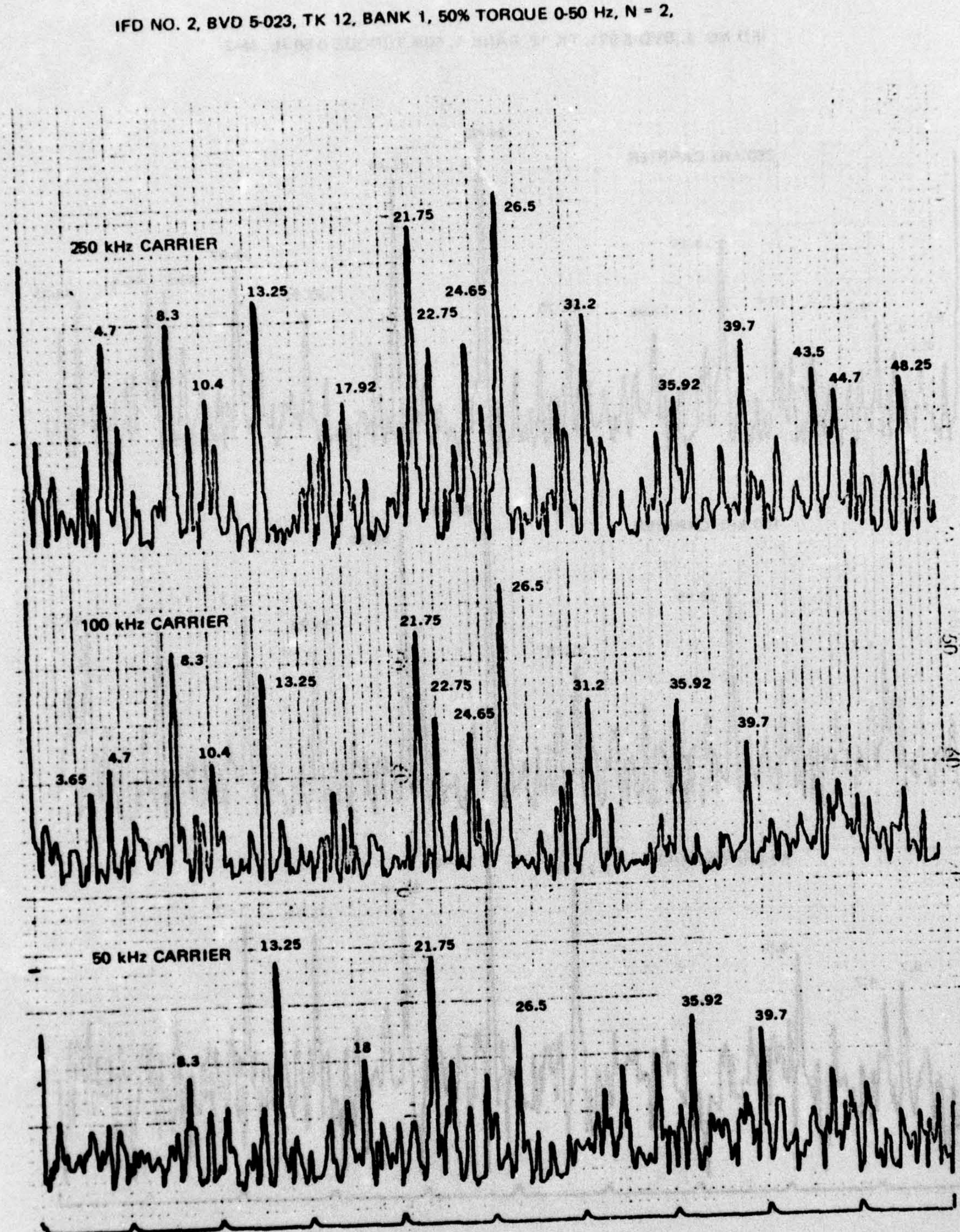

Figure C22. Special Case PSD Plot, Transmission A9-1341 (New), IFD No. 2 (0-50 Hz).

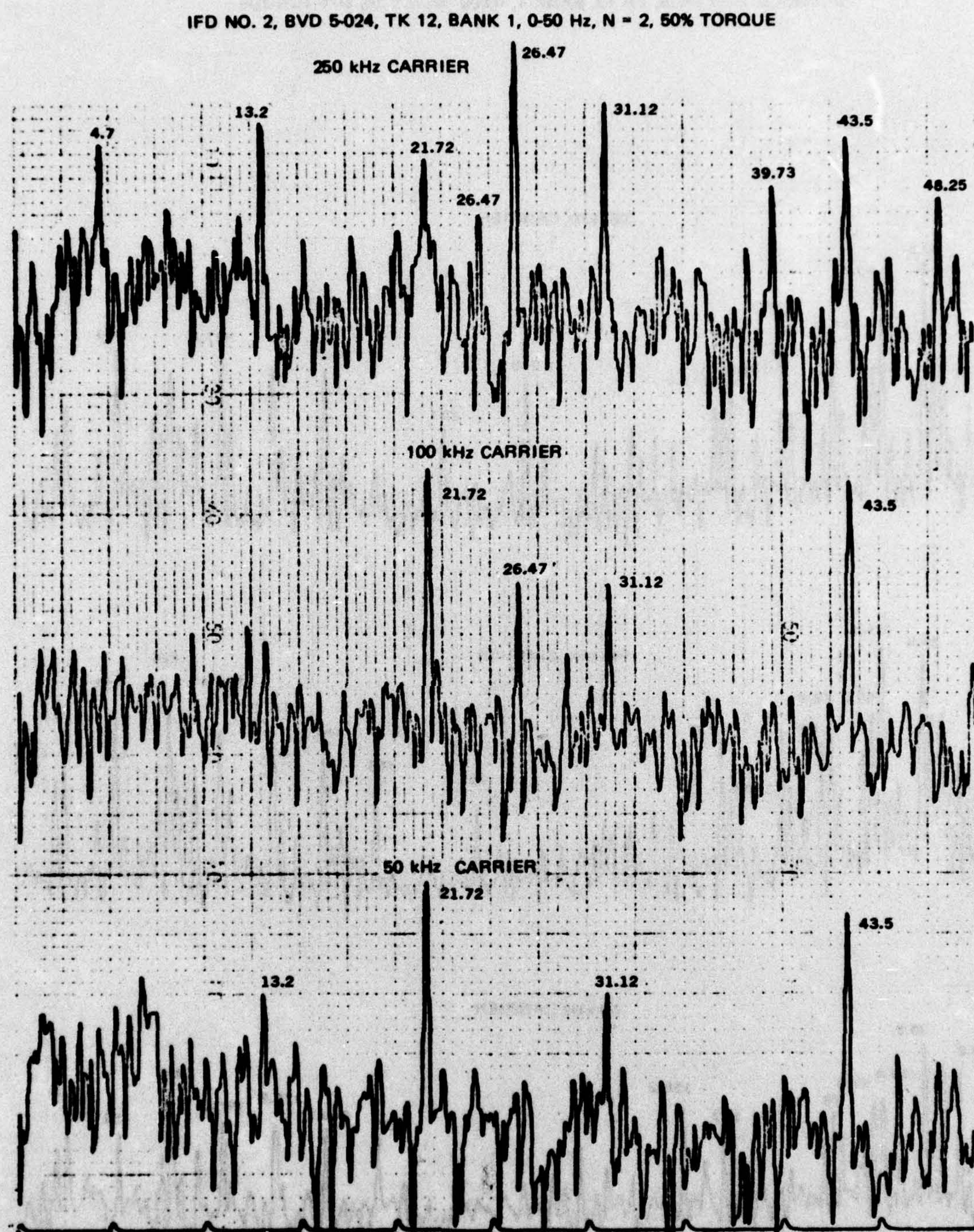

Figure C23. Special Case PSD Plot, Transmission A9-1342 (New), IFD No. 2 (0-50 Hz).

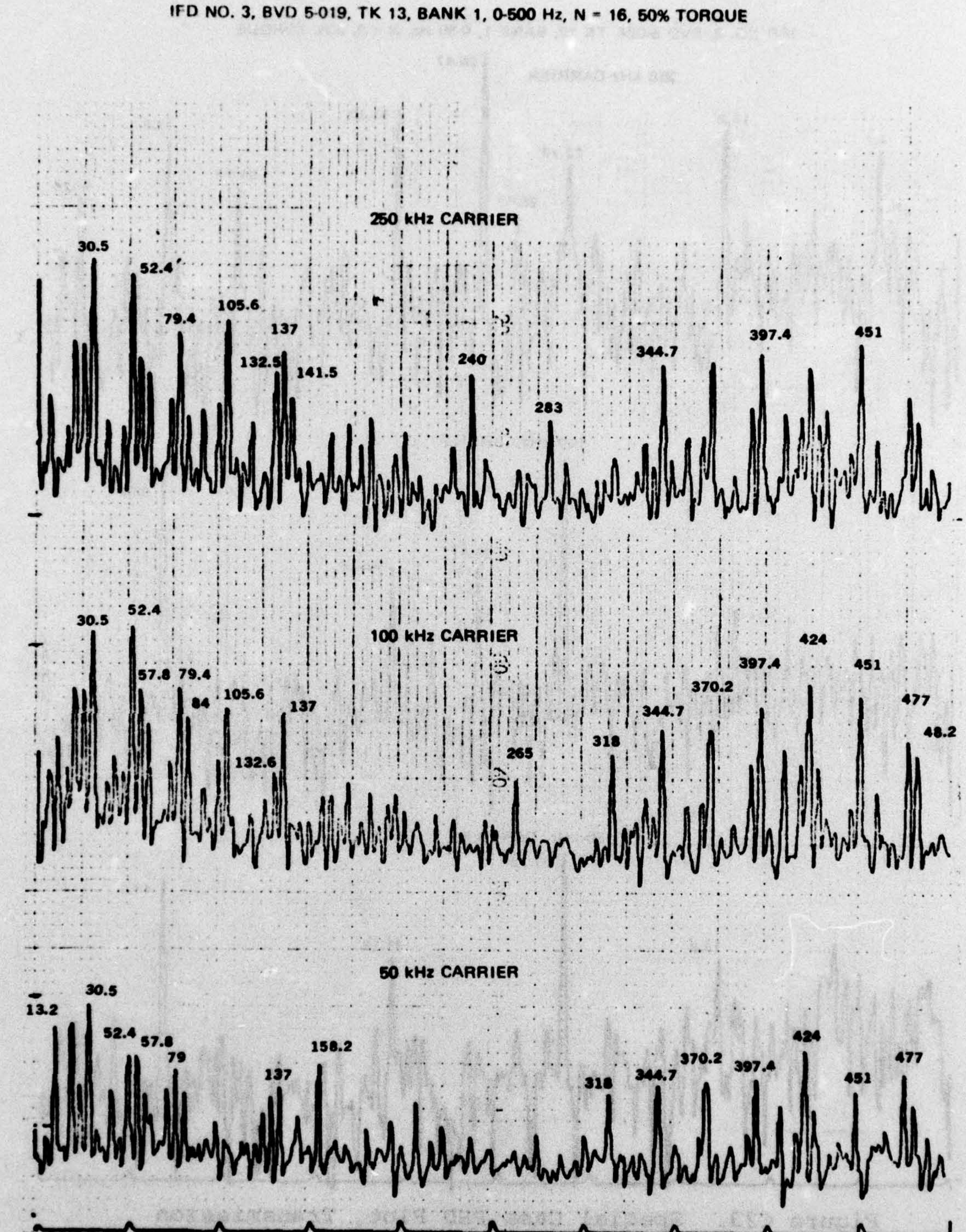

Figure C24. Special Case PSD Plot, Transmission A9-1337 (New), IFD No. 3 (0-500 Hz).

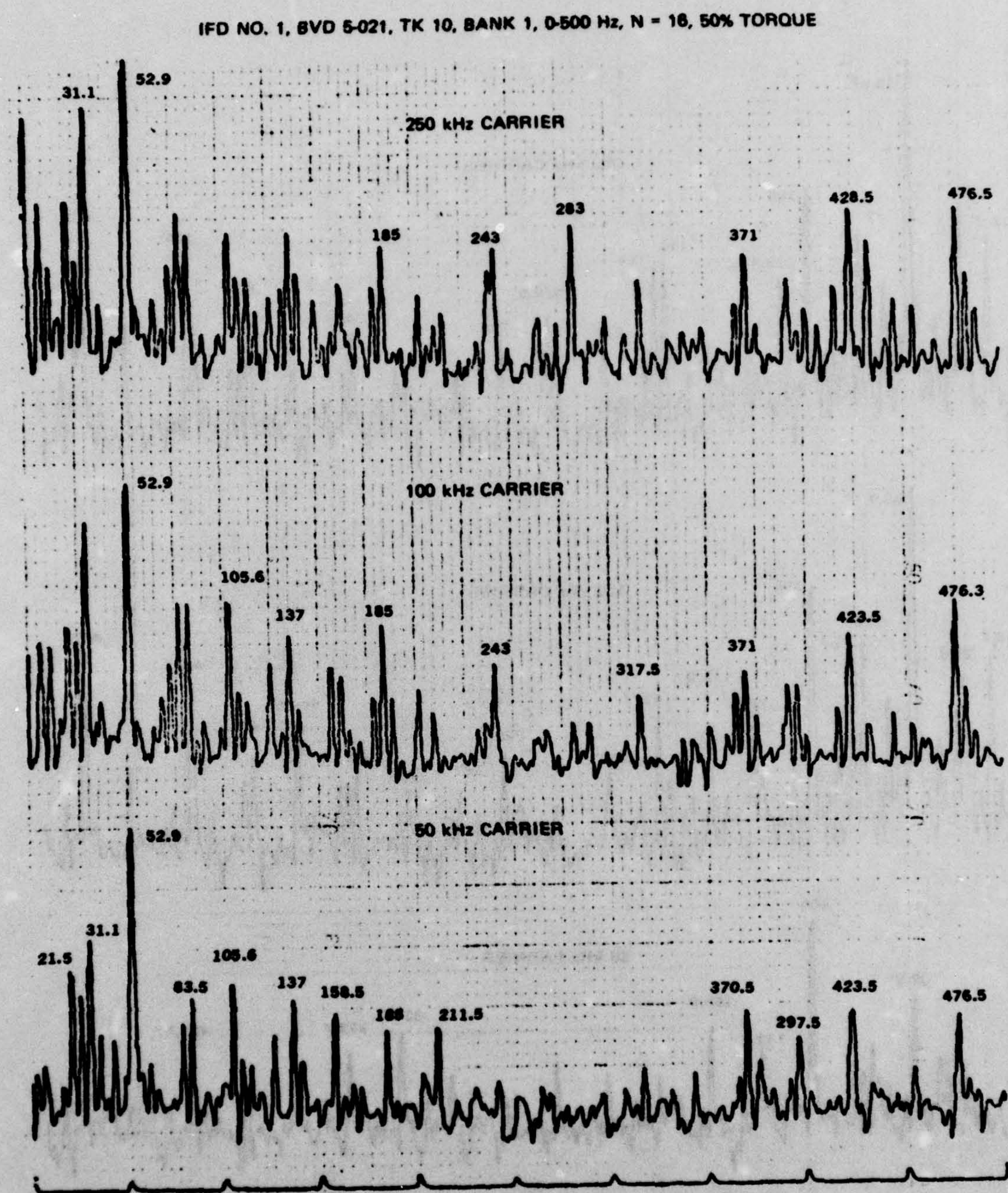

Figure C25. Special Case PSD Plot, Transmission A9-1339 (New), IFD No. 3 (0-500 Hz)

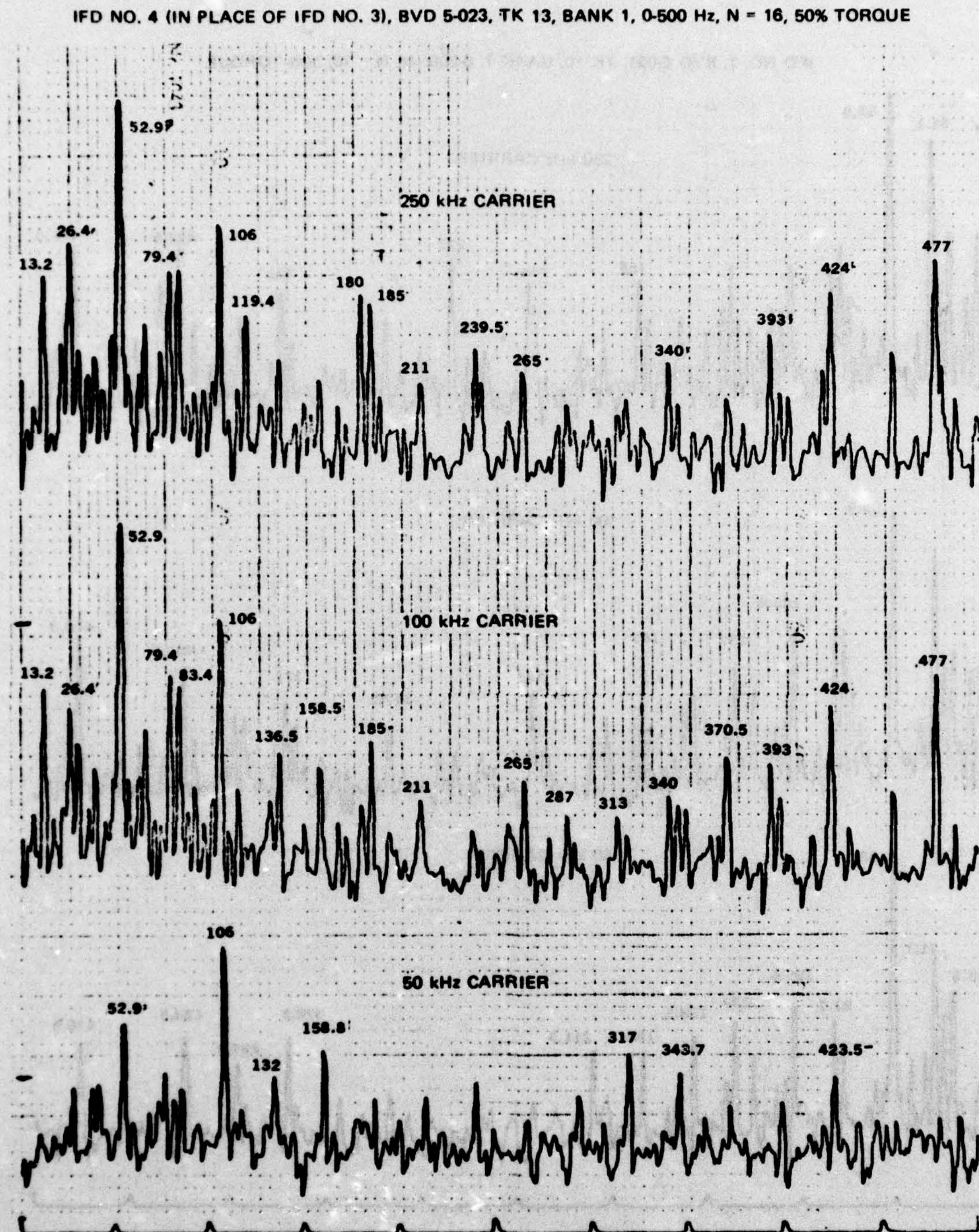

Figure C26. Special Case PSD Plot, Transmission A9-1341 (New), IFD No. 3 (0-500 Hz).

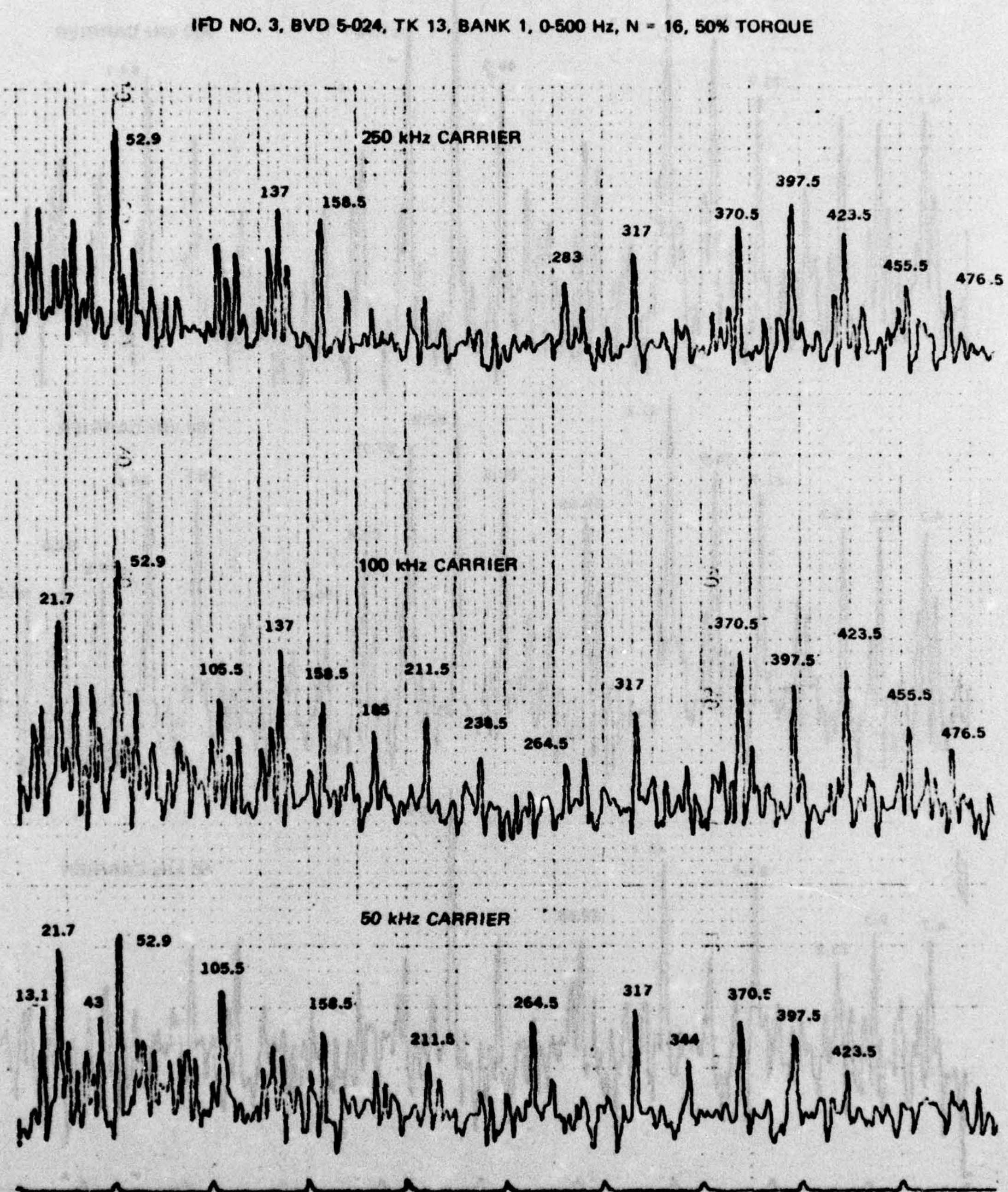

Figure C27. Special Case PSD Plot, Transmission A9-1342 (New), IFD No. 3 (0-500 Hz).

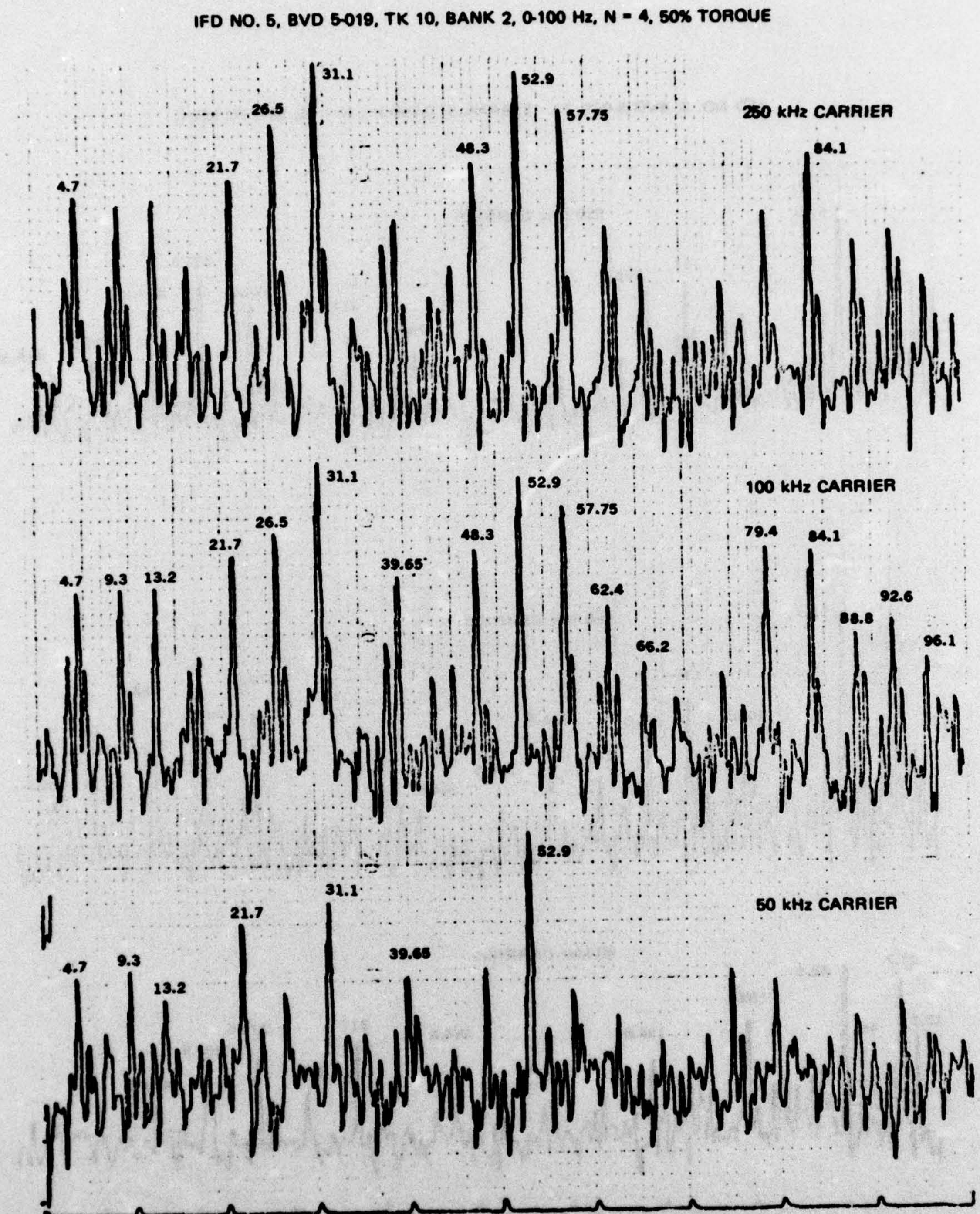

Figure C28. Special Case PSD Plot, Transmission A9-1337 (New), IFD No. 5 (0-100 Hz).

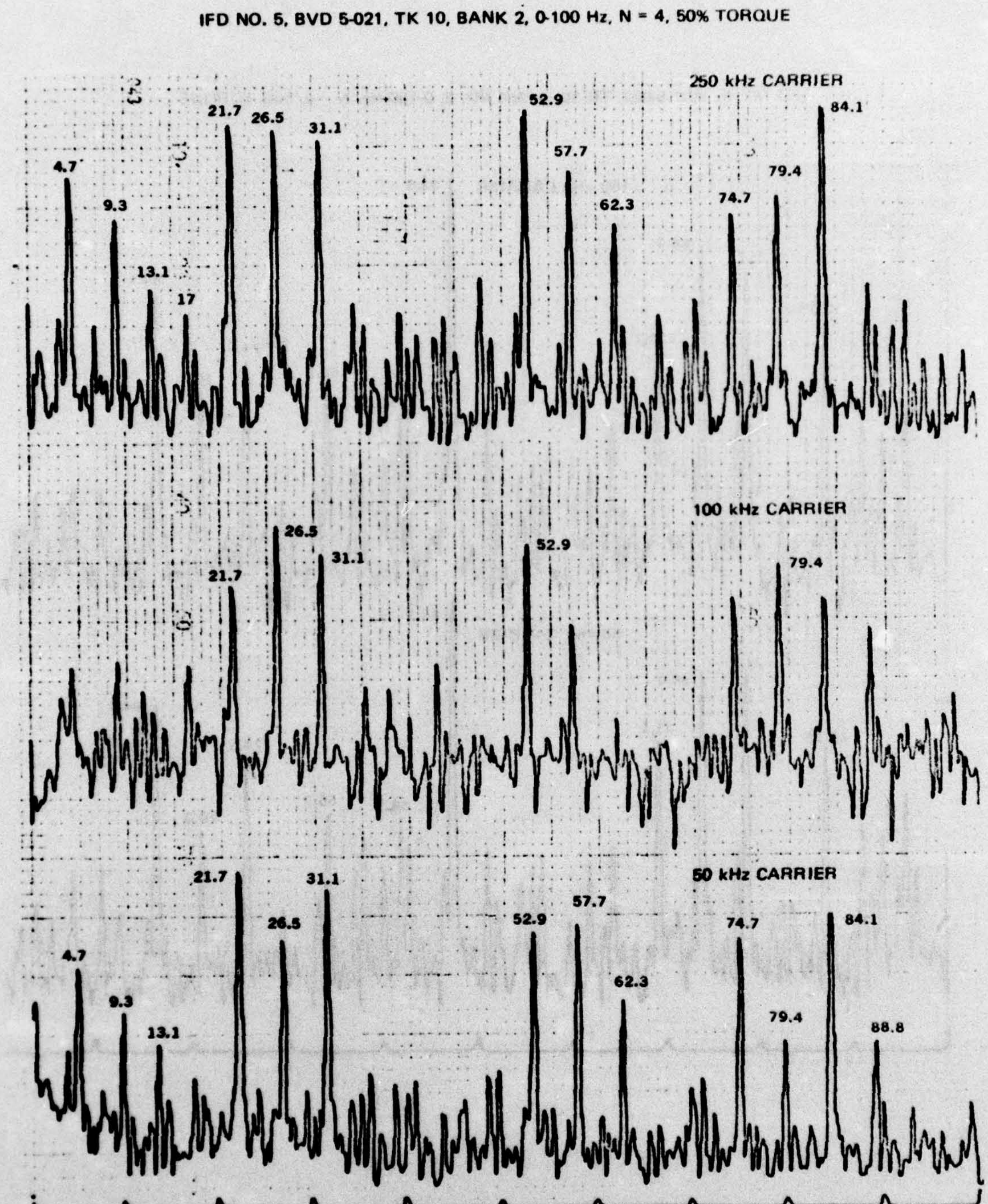

Figure C29. Special Case PSD Plot, Transmission A9-1339 (New), IFD No. 5 (0-100 Hz).

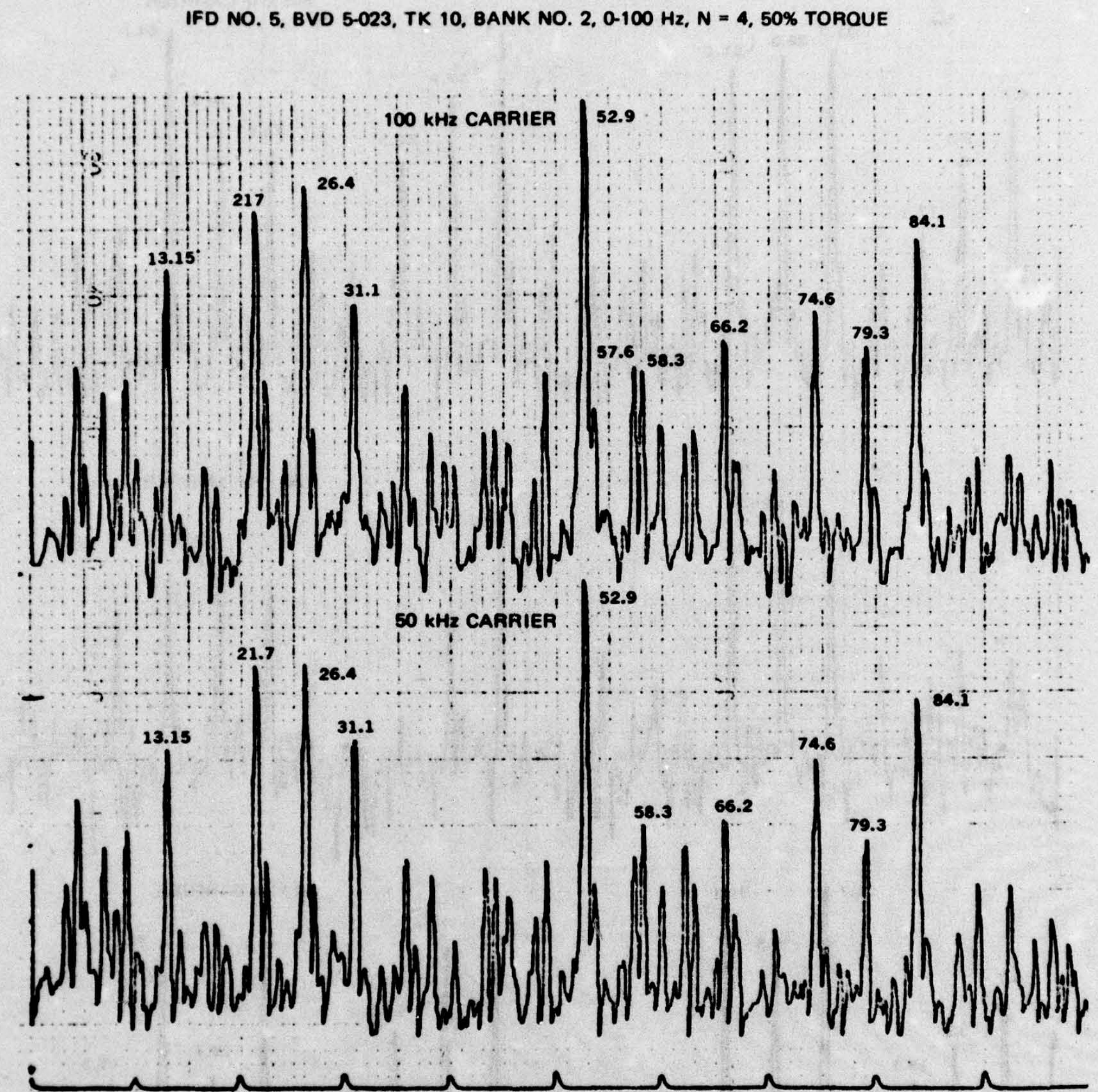

Figure C30. Special Case PSD Plot, Transmission A9-1341 (New), IFD No. 5 (0-100 Hz).

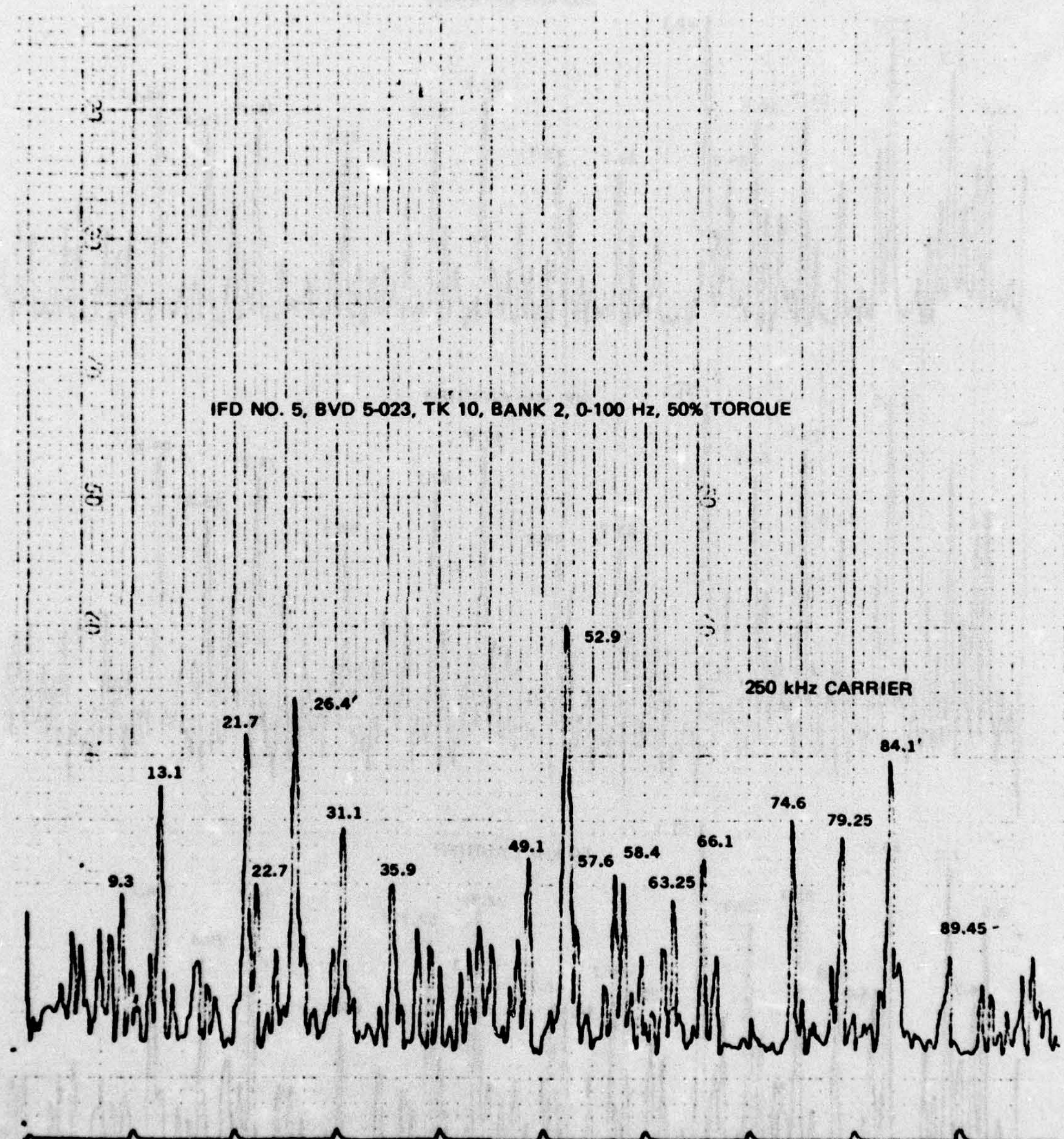

Figure C31. Special Case PSD Plot, Transmission A9-1341 (New), IFD No. 5 (0-100 Hz).

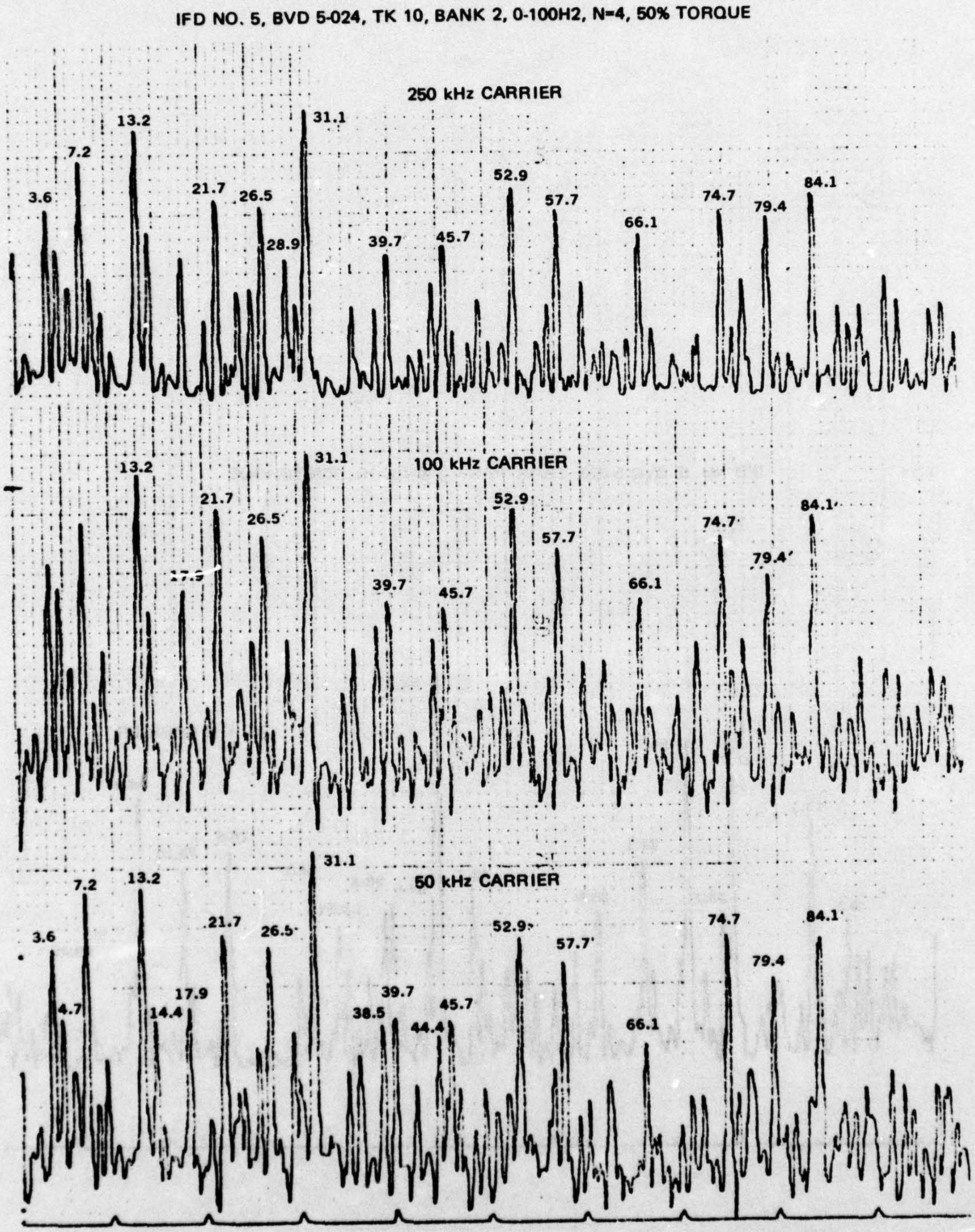

Figure C32. Special Case PSD Plot, Transmission A9-1342 (New), IFD No. 5 (0-100 Hz).

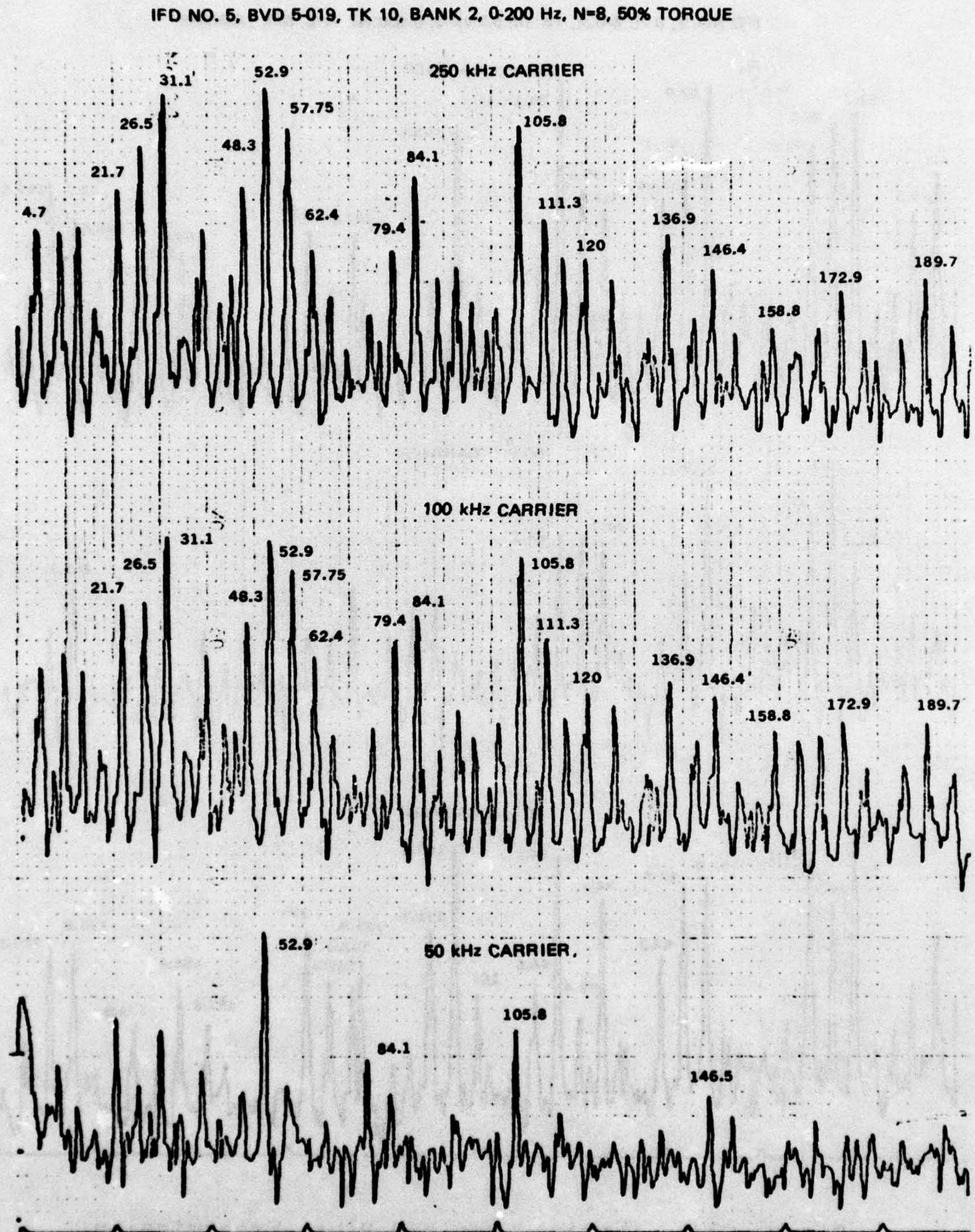

Figure C33. Special Case PSD Plot, Transmission A9-1337 (New), IFD No. 5 (0-200 Hz).

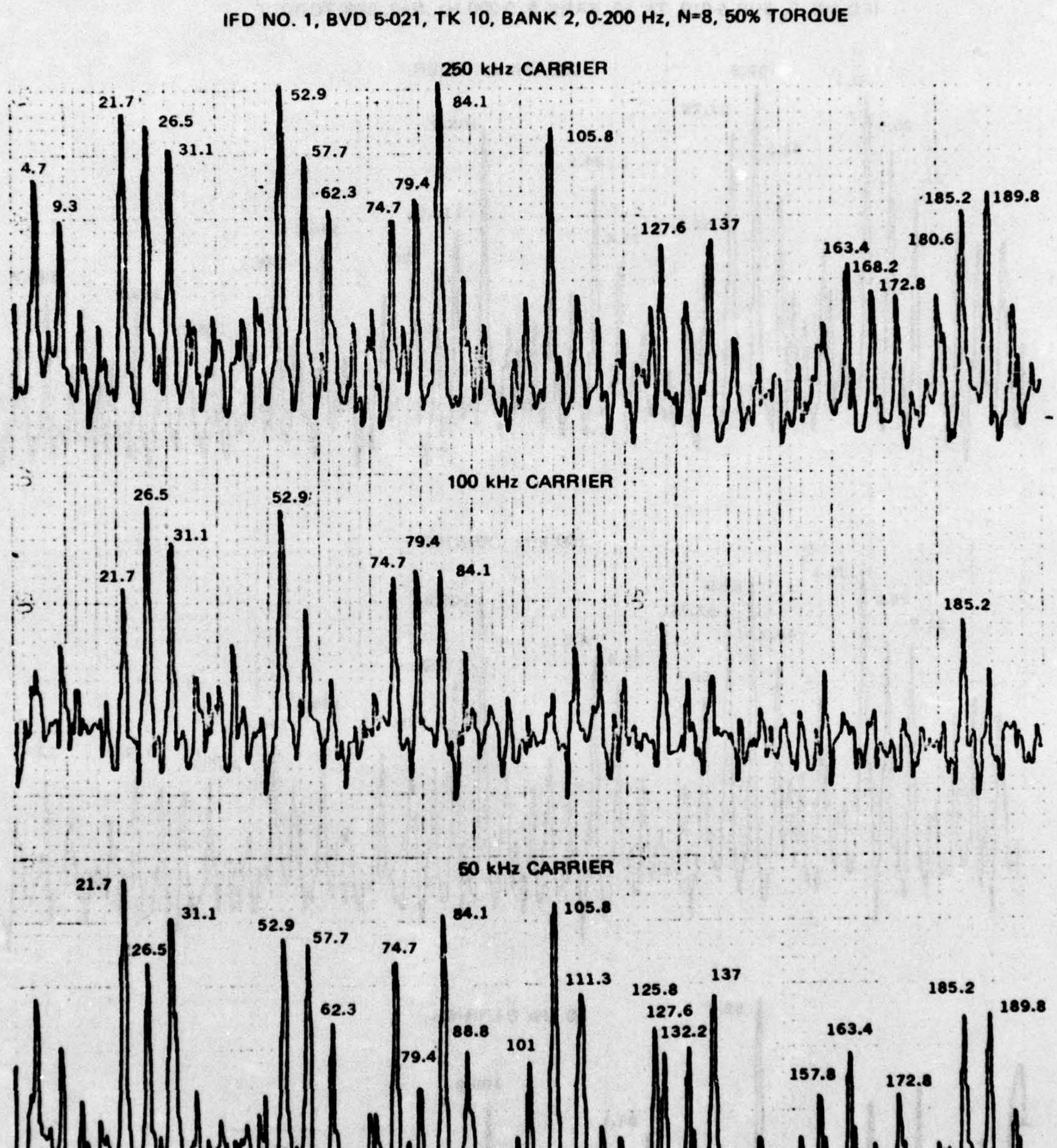

Figure C34. Special Case PSD Plot, Transmission A9-1339 (New), IFD No. 5 (0-200 Hz).

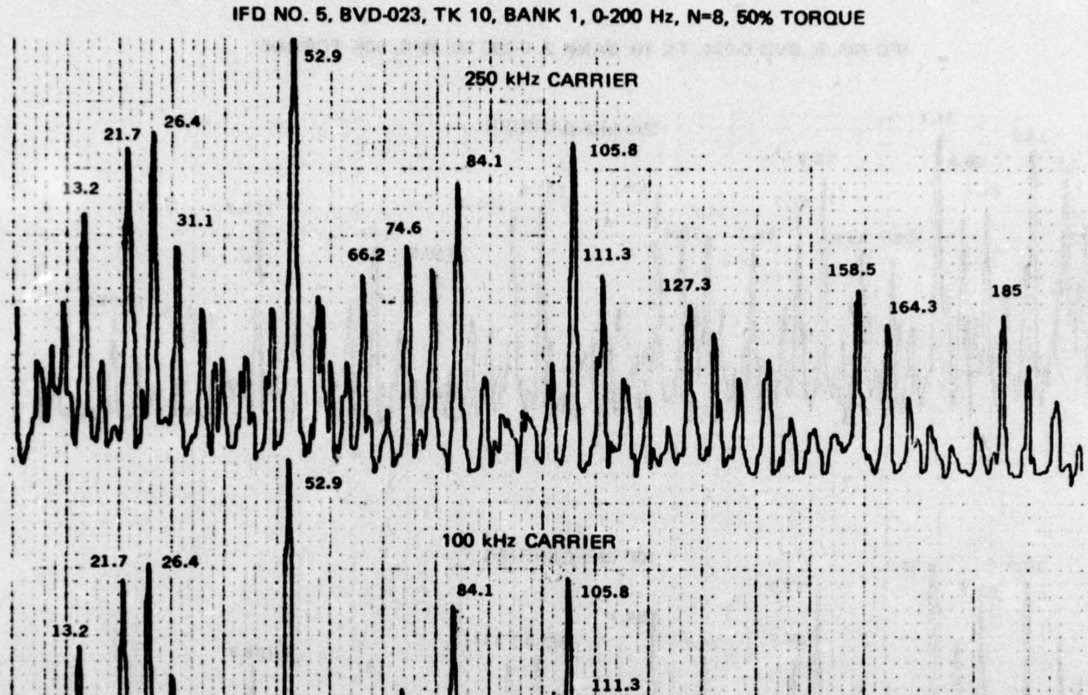

Figure C35. Special Case PSD Plot, Transmission A9-1341 (New), IFD No. 5 (0-200 Hz).

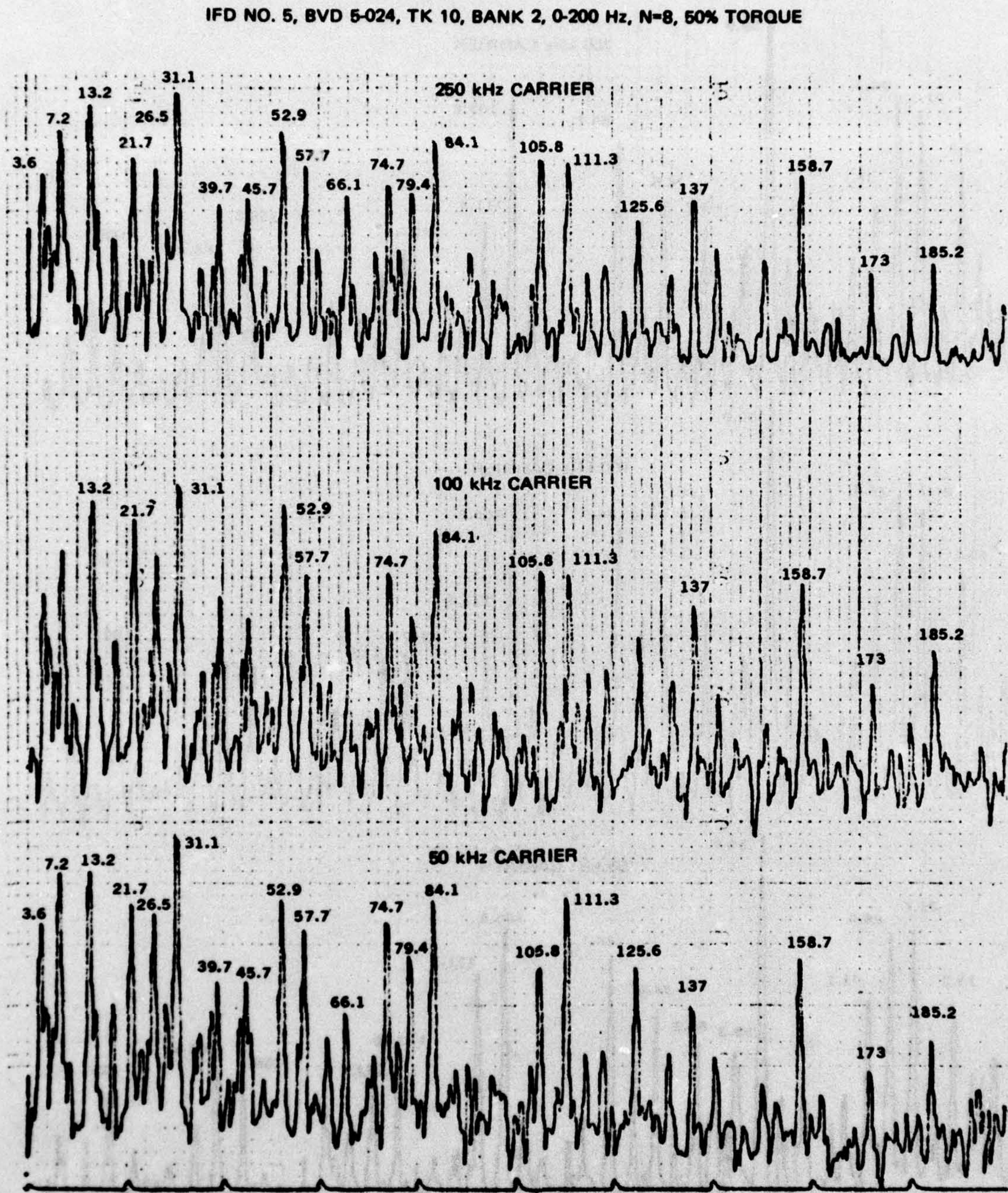

Figure C36. Special Case PSD Plot, Transmission A9-1342 (New), IFD No. 5 (0-200 Hz).